UNIVERSIDADE DE SÃO PAULO
FACULDADE DE MEDICINA

ALEXIS GERMAN MURILLO CARRASCO

Heterogeneidade relacionada ao câncer de mama representada em miRNAs circulantes e vesiculares: resultados de ensaios de alto rendimento e prova de conceito para seleção de vesículas extracelulares derivadas de tumor

Breast cancer-related heterogeneity reflected on circulating and vesicular miRNAs: high-throughput results and proof-of-concept for selecting tumor-derived extracellular vesicles

São Paulo
2023

ALEXIS GERMAN MURILLO CARRASCO

Heterogeneidade relacionada ao câncer de mama representada em miRNAs circulantes e vesiculares: resultados de ensaios de alto rendimento e prova de conceito para seleção de vesículas extracelulares derivadas de tumor

Versão Corrigida

(Versão original encontra-se na unidade
que aloja o Programa de Pós-graduação)

Tese apresentada à Faculdade de Medicina da Universidade de São Paulo para obtenção do título de Doutor em Ciências

Programa de Oncologia

Orientador: Prof. Dr. Roger Chammas

São Paulo
2023

ALEXIS GERMAN MURILLO CARRASCO

Breast cancer-related heterogeneity reflected on circulating and vesicular miRNAs: high-throughput results and proof-of-concept for selecting tumor-derived extracellular vesicles

Corrected Version

(The original version is found on the unit that hosts the Post-graduation Program)

Ph. D. Thesis presented the “Faculdade de Medicina da Universidade de São Paulo” to obtain the degree of Doctor of Science

Program of Oncology

Advisor: Prof. Dr. Roger Chammas

Sao Paulo
2023

Dados Internacionais de Catalogação na Publicação (CIP)

Preparada pela Biblioteca da
Faculdade de Medicina da Universidade de São Paulo

Murillo Carrasco, Alexis German
Heterogeneidade relacionada ao câncer de mama representada em miRNAs circulantes e vesiculares : resultados de ensaios de alto rendimento e prova de conceito para seleção de vesículas extracelulares derivadas de tumor / Alexis German Murillo Carrasco. -- São Paulo, 2023.
Tese(doutorado)--Faculdade de Medicina da Universidade de São Paulo.
Programa de Oncologia.
Orientador: Roger Chammas.

Descritores: 1.miRNA 2.Neoplasias da mama 3.Biópsia líquida 4.Vesículas extracelulares 5.Proteínas de ligação a glicanos 6.Ensaios de triagem em larga escala

USP/FM/DBD-396/23

Responsável: Erinalva da Conceição Batista, CRB-8 6755

To my grandfather, who always put his hope and support in my scientific career, especially at the beginning of my graduate research. He would be so proud to know that I finished my doctorate...

Agradecimentos

Esse doutorado foi o resultado de um longo caminho de aprendizado e crescimento, não apenas científico, mas também pessoal. Assim, gostaria de agradecer a todas as pessoas que contribuíram de diversas formas a conseguir essa realização.

Em princípio, agradecer ao Prof. Roger Chammas e a Luciana (Lu) Andrade pela grande oportunidade de participar no projeto “Retratos da Mama” e contribuir através do desenvolvimento desta tese. Obrigado por todos os conselhos, sessões de discussão, viagens, apresentações, oportunidades de colaboração e mensagens de apoio.

Gostaria também de agradecer a Tatiane (Tuty) Furuya e a Miyuki Uno por serem o meu primeiro contato no lab, por me acolherem e por me guiar na minha inserção ao Centro de Investigação Translacional em Oncologia (CTO). Um passo que logo se tornou uma série de colaborações, com excelentíssimas pessoas e grandes aprendizados. Muito obrigado!

Assim, aproveito a ocasião para mostrar a minha gratidão ao Curso em Oncologia Molecular (https://www.cursooncologia.com.br/), o evento que me abriu as portas, me permitiu conhecer o CTO e o Instituto do Câncer do Estado de São Paulo (ICESP), e saber da qualidade dos profissionais que trabalham neste local, que se transparece através de suas conquistas. Parte dessa gratidão foi retribuída na minha participação nas comissões que organizaram a V e VI edição desse curso. Especial agradecimento à Ana Carolina, Gláucia, Isabela, Jean, Lívia, Nadine, Nathália, Pedro e Vinícius (Vini), colegas da pós-graduação, que participaram na parceria para mover as engrenagens para organizar um curso, um simpósio, e delinear a escrita de um livro de conceitos em Oncologia (da molécula à clínica), no contexto da maior alteração mundial que nós fez trabalhar a distância, mas sempre juntos.

De fato, a produção do livro (https://lnkd.in/ejWKwKts), em companhia dos membros do CTO, e guiados pelos editores (Prof. Roger Chammas, Profa. Luisa Villa, e Profa. Maria Aparecida Koike), contribui enormemente à consolidação dos nossos conhecimentos e à canalização dessa informação para as novas gerações. Aproveito em agradecer aos membros do CTO e o nosso sistema de pós-graduação por todas as sugestões fornecidas ao projeto nas diferentes apresentações, bem como na jornada acadêmica em Oncologia.

Essa tese foi realizada com amostras de plasma e blocos de parafina de 54 pacientes diagnosticadas com câncer de mama e atendidas no ICESP, sem a generosa contribuição delas seria inviável a realização desta pesquisa. Muito obrigado. Também gostaria de agradecer às agências de fomento que outorgaram recursos financeiros para esta tese. O presente trabalho foi realizado com apoio da Coordenação de Aperfeiçoamento de Pessoal de Nível Superior – Brasil (CAPES) – Código de Financiamento 001; processo nº 2019/05583-0, Fundação de Amparo à Pesquisa do Estado de São Paulo (FAPESP); e projeto “Retratos da Mama”, Programa Nacional de Apoio à Atenção Oncológica (PRONON).

Já no ICESP, as amostras são coletadas, pré-processadas e armazenadas pelo time do Biobanco da Rede Acadêmica da Universidade de São Paulo (USP). Gostaria de agradecer à Miyuki, Maria José (Mazé), Diogo, Ana Paula (x2), Fabiola, Tais, Aline Celia e todos os que passaram no Biobanco nos últimos 5 anos e contribuíram a construir essa fonte de recursos.

Logo, organizar as informações necessárias para selecionar as pacientes é um processo que precisa de muita atenção e cuidado. Graças à Luciana Barros pelo esforço de facilitar o acesso aos bancos de dados através do REDCap, ferramenta utilizada nesta tese.

Gostaria também de agradecer aos “vesiculólogos”, Renata (Rê) Saito, Lu Andrade, Nathália Leal, Isabela Ferreira e Silvina (Sil) Bustos pelas discussões, lições em matéria de vesículas extracelulares, e troca de protocolos.

Especialmente, gostaria de agradecer à Sil por me ensinar a realizar ensaios proteicos usados nesta tese: western blot, quantificação por quimiluminescência, outros. Também, por estabelecer a colaboração com a Profa. Cristiane Damas Gil (UNIFESP) que nos permitiu realizar a caracterização das vesículas por microscopia eletrônica de transmissão.

Adicionalmente, gostaria de agradecer à Allane dos Santos, quem me mostrou o processo de histoquímica com lectinas, um passo importante na confirmação da marcação de tecidos FFPE com Jacalina.

Em aspectos associados aos miRNAs e seu estudo, gostaria de agradecer novamente à Tuty, Miyuki, Lu Andrade, e o Prof. Roger pelas orientações sobre o manejo destas amostras e por me ensinar o fluxo de trabalho com esse material no Instituto. Através da Tuty e Miyuki conheci a Vanessa Ota (UNIFESP) e a Sueli Oba (USP), que me permitiram realizar os ensaios de avaliação de qualidade dos

miRNAs na plataforma Bioanalyzer. Já a Lu Andrade e o Prof. Roger estabeleceram uma parceria com a Profa. Patricia Pintor, quem junto com a Tainara Felix e o Marcio de Carvalho, nos permitiram realizar os ensaios de quantificação por barcoding no equipamento nCounter. Obrigado também aos nossos colaboradores neste processo.

Também gostaria de agradecer à Andreia Otake e a Cristina (Cris) Rangel por me orientarem sobre os processos de crescimento celular, ceder linhagens de câncer de mama para seu estudo, e me brindar informações sobre o processo de glicosilação aberrante decorrente das células tumorais e estratégias para selecionar partículas com estas ferramentas.

Esta tese é composta por diversos métodos de análise de dados, cujo aprendizado fez parte importante deste doutorado. Assim, gostaria de destacar a geração da plataforma (dXpress, https://alexismurillo.shinyapps.io/dXpress/) para avaliação comparativas de níveis de expressão gênica em grande escala. Essa plataforma está atualmente em revisão, mas será utilizada em futuras fases deste projeto. Assim, gostaria de agradecer ao Tharcisio (Tharci), Tuty, Miyuki e Prof. Roger que guiaram e conferiram os métodos de análise que fizeram isto possível.

Assim, falando de dados, também gostaria de agradecer à Rossana Mendoza, quem junto à Tuty contribuíram a minha compreensão dos modelos estatísticos e a sua aplicação na análise de dados. Adicionalmente, a Rossana tem contribuído a não me sentir tão longe de casa, especialmente nos momentos que o contexto mundial tornou uma viagem de avião em uma questão de saúde pública.

Por falar em proximidade de conterrâneos, gostaria de agradecer à minha pequena comunidade de peruanos no HCFMUSP, liderados pela Ruth (Tamara) Valencia, quem tem contribuído a discutir aspectos de pesquisa, mas também a conhecer visões diferentes do nosso país, atualizá-las e pensar novas formas de contribuir apesar da distância. No fim, a ciência não conhece fronteiras...

Finalmente, mas não em último lugar, gostaria de agradecer à minha família em Peru. Passaram-se sete anos desde a primeira vez que sai do país e cinco anos desde que decidi apostar por um câmbio de rumo e eles aceitaram e apoiaram os meus sonhos apesar da grande nostalgia que veio com essa decisão. Desde então, tomo essa saudade para dar o meu melhor e acredito que todo o nosso esforço está valendo a pena. Que Deus nos cuide e guie para seguir em frente nos próximos passos. Obrigado!

“Science knows no country, because knowledge belongs to humanity,

and is the torch which illuminates the world.”

Louis Pasteur

"The more I learn, the more I realize how much I don't know."
Isaac Newton

Resumo

Murillo Carrasco AG. Heterogeneidade relacionada ao câncer de mama representada em miRNAs circulantes e vesiculares: resultados de ensaios de alto rendimento e prova de conceito para seleção de vesículas extracelulares derivadas de tumor [tese]. São Paulo: Faculdade de Medicina da Universidade de São Paulo; 2023.

O câncer de mama conquistou recentemente o título de tipo de câncer mais diagnosticado em todo o mundo, com destaque para as mulheres diagnosticadas antes dos 40 anos (câncer de mama jovem). Independentemente da idade, embora a classificação baseada em perfis imunohistoquímicos seja um amplo sistema de triagem, prognóstico e predição de tratamento, os pacientes com CM necessitam de informações adicionais para receber tratamento mais adequado. Então, foi proposto que as características do tumor pudessem ser coletadas a partir de amostras de sangue (biópsias líquidas sistêmicas). No plasma sanguíneo, os microRNAs (miRNAs) são ferramentas reguladoras que podem ser coletadas e medidas como material circulante livre de células ou em vesículas extracelulares (VEs). Nesta tese, exploramos o miRNoma do conteúdo circulante (cf-miRNA) e vesicular (EV-miRNA) de pacientes com CM classificados nos principais grupos imuno-histoquímicos (Luminal A, Luminal B, Luminal HER2, HER2+ e Triplo-negativo). Investigamos duas coortes diferentes de amostras de CM em experimentos de EV-miRNA para avaliar protocolos técnicos e descobertas consistentes. Percebemos que o cf-miRNA é suscetível à contaminação com outras fontes circulantes, como a hemólise. No entanto, tanto o cf-miRNA quanto o EV-miRNA, são fontes informativas para determinar diferenças de expressão de miRNA entre os subtipos de BC. Os níveis circulante e vesicular dos microRNAs hsa-miR-197-3p e hsa-miR-5001-5p diferenciam pacientes Triplo-negativo e Luminal HER2, respetivamente. Somente na carga vesicular, hsa-miR-411-5p caracteriza pacientes Luminal HER2, enquanto hsa-miR-1266-5p, hsa-miR-584-5p, hsa-miR-2053, hsa-miR-525-5p e hsa-miR-642a-5p distinguem pacientes jovens com câncer de mama Triplo-negativo. Junto com esses experimentos, encontramos diversos miRNAs desregulados, alguns associados a vias associadas a tumores, mas outros relacionados a processos antitumorais. Então, realizamos também experimentos com uma proteína ligante de

glicanos produzida em jaca (*Artocarpus integrifolia*) para demonstrar que esta lectina pode marcar seus alvos, o antígeno Tn relacionado ao tumor e seus derivados, em tecidos fixados em formalina e embebidos em parafina (FFPE) e linhagens celulares de CM, bem como VEs isoladas de pacientes com CM. Observamos que 10% do total de VEs circulantes são Tn+, demonstrando assim ser possível selecionar frações de VEs plasmáticas por proteínas em sua superfície usando estratégias de afinidade.

Palavras-chave: miRNA, câncer de mama, biópsia líquida, vesículas extracelulares, proteínas de ligação a glicanos, ensaios de triagem em larga escala.

Abstract

Murillo Carrasco AG. Breast cancer-related heterogeneity reflected on circulating and vesicular miRNAs: high-throughput results and proof-of-concept for selecting tumor-derived extracellular vesicles [thesis]. Sao Paulo: Faculdade de Medicina, Universidade de São Paulo; 2023.

Breast cancer has recently become the most frequently diagnosed cancer type worldwide, with a particular emphasis on women diagnosed before age 40, known as early-onset (young diagnosed) breast cancer. While classification based on immunohistochemical profiles serves as a broad screening, prognosis, and treatment prediction system, BC patients often require additional information for precise treatment. Clinical routines also demand minimally invasive methods to obtain patients' data and monitor their treatment response. In light of these challenges, this study proposed the collection of tumor characteristics from blood samples (liquid biopsies), with emphasis on the accumulation of microRNAs (miRNAs) – regulatory molecules that are found in the cell-free circulating material, such as extracellular vesicles (EVs). In this thesis, we explored the miRNome of both circulating (cf-miRNA) and vesicular (EV-miRNA) content of BC patients classified into main immunohistochemical groups (Luminal A, Luminal B, Luminal HER2, HER2+, and TNBC). Two separate cohorts of BC samples were run in EV-miRNA experiments to assess technical protocols to ensure consistent results.

Upon analyzing miRNA expression data, it became evident that cf-miRNA is susceptible to contamination from other circulating sources, such as hemolysis. However, both cf-miRNA and EV-miRNA proved to be informative sources for discerning miRNA expression differences between BC subtypes. For instance, hsa-miR-197-3p distinguished TNBC patients, and hsa-miR-5001-5p differentiated Luminal HER2 patients, as observed in both cf-miRNA and EV-miRNA datasets. Among vesicular cargo, hsa-miR-411-5p characterizes Luminal HER2 patients, whereas hsa-miR-1266-5p, hsa-miR-584-5p, hsa-miR-2053, hsa-miR-525-5p, and hsa-miR-642a-5p were indicative of young TNBC patients. In addition to these specific markers, various deregulated miRNAs were identified, some associated with tumor-related pathways and others linked to anti-tumor processes. This discovery led to the hypothesis that different EV subpopulations might exist in the bloodstream. We

then performed experiments using a glycan-binding protein derived from jackfruit (*Artocarpus integrifolia*) to identify specific targets (tumor-related Tn antigen and its derivatives) in formalin-fixed paraffin-embedded tissues and in plasma. BC cell lines, and EVs isolated from BC tumors were tested using Jacalin and recovered through incubation with D-galactose (the monosaccharide which binds in the carbohydrate recognition domain of Jacalin). This approach successfully separated 10% of total EVs, demonstrating the feasibility of selecting plasma EV fractions using surface glycoproteins and affinity strategies.

Keywords: miRNA, breast cancer, liquid biopsy, extracellular vesicles, glycan-binding proteins, high-throughput screening assays.

Figures List

Tables List

Appendices List

Attachments List

Summary

1. INTRODUCTION

1.1 Breast cancer: incidence and mortality

Breast cancer has recently conquered the title of the most commonly diagnosed cancer type around the world. In 2020, this disease recorded an incidence of 25.5% and a mortality rate of 15.5% among all women diagnosed with cancer [1]. According to information provided by the Global Cancer Observatory (GCO) from the International Agency for Research on Cancer (IARC) through the Cancer Today website [2], breast cancer is the top malignancy diagnosed in 2020 (last update), even when including males and females in the analysis (Figure 1A), despite only 0.5-1% of breast cancer cases are reported in men [3].

In this cohort, breast cancer is the first diagnosed cancer in 141 countries, accounting for 685 000 deaths globally [3]. It represents more age-standardized cases than prostate in many countries. Indeed, prostate cancer ranks first in some Latin American, Caribbean, and Central-Southern African countries, including Brazil. However, if we focus only on women, we observe that breast cancer is the first cancer-related health concern in 160 countries (Figure 1B), followed by cervix uterine cancer (top in 23 countries).

In women diagnosed with cancer before 40 years old (young diagnosed or early onset), the world map shows a similar pattern (Figure 1C). Breast cancer ranks first in 141 countries despite a higher incidence of thyroid and cervix uteri tumors in countries such as China, Italy, Kazakhstan, Papua New Guinea, Paraguay, Costa Rica, and others. Nevertheless, malignancies of the thyroid and cervix showed lower mortality rates, different from breast cancer and leukemia, which represent the first cancer-related death caused for patients diagnosed before 40 years old (elderly diagnosed or late onset) in 80 and 38 countries, respectively. Previous research identified that patients diagnosed with breast cancer before 40 years old used to show more aggressive tumors leading to lymph node invasion and metastasis, which gives them a poor prognosis [4–6]. Recently, Silva et al. (2021) demonstrated that mortality rates of young Brazilian women diagnosed with breast cancer have increased by 2.2-4.6% a year between 1996-2017 [7].

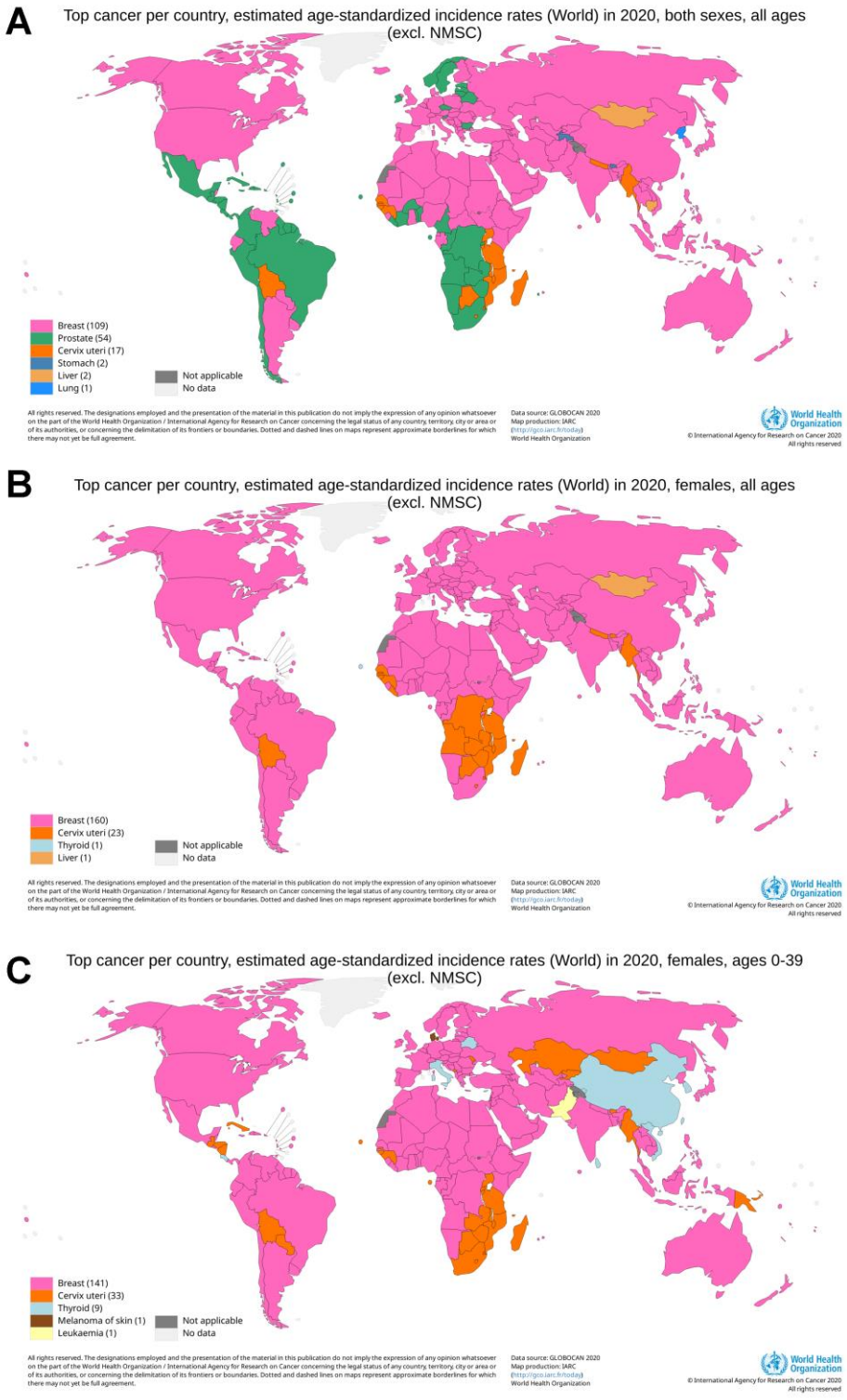

Figure 1. Top diagnosed cancer per country according to the Global Cancer Observatory. (A) World map showing the top diagnosed tumors in males and females (all ages) in 2020. (B) World map showing the top diagnosed tumors in females (all ages) in 2020. (C) World map showing the top diagnosed tumors in females (with 0-39 years old at diagnosis) in 2020. Information from the Global Cancer Observatory (GCO) through the Cancer Today tool (accessed on August 11, 2023). NMSC: Non-melanoma Skin Cancer.

In addition, it was found that age-related groups of breast cancer (BC) patients with specific expression of markers can give poor prognoses. For example, elderly BC patients (diagnosed after 40 years old) with higher expression of the HER2 receptor in their tumors, young BC patients (diagnosed before 40 years old) with lower expression of the estrogen receptor (ER) in their tumors, young BC patients with a high TNM stage [4], or young BC patients with a positive lymph-node [6].

As shown in Figure 2, records of our biobank institutional cohort (Academic Biobank of Research on Cancer from the University of São Paulo) allow us to check the potential association between the estrogen receptor status in young diagnosed BC patients and poor prognosis. Furthermore, these findings suggest that the expression of immunohistochemical biomarkers (p.e. ER or HER2) could be biomarkers of the modulation of aggressiveness of BC tumors. However, breast cancer still accounts for a highly spatiotemporal heterogeneous tumor [8].

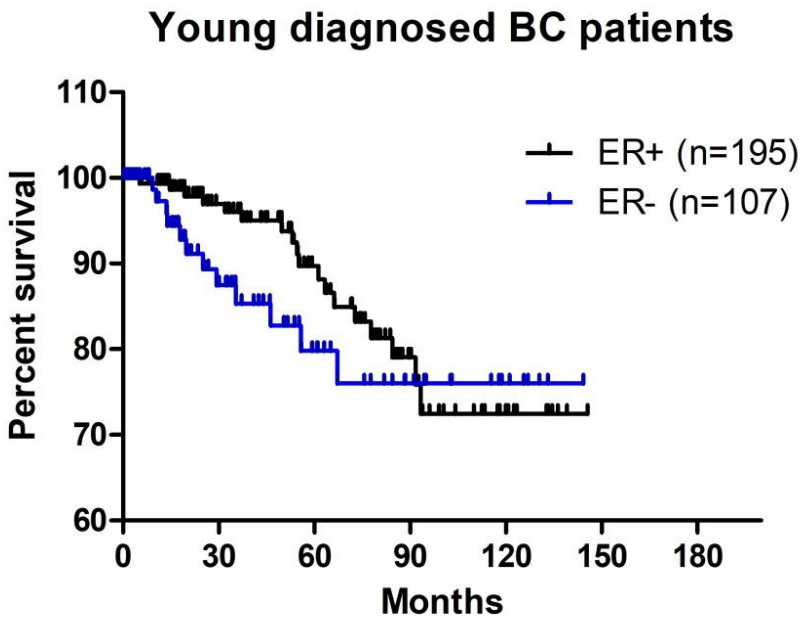

Figure 2. Overall Survival in Young diagnosed BC patients. This Kaplan-Meier plot shows the percent survival of BC patients diagnosed before 40 years old using data from the institutional record of the Academic Biobank of Research on Cancer from the University of São Paulo located at Instituto do Cancer do Estado de São Paulo (ICESP). Data was retrieved using the Research Electronic Data Capture (REDCap) application and plotted using GraphPad Prism v8 for Windows. ER: Estrogen Receptor, BC: Breast Cancer.

1.2 Traditional Classification Systems and Prognosis Assessment

Along with the research in breast cancer, some classification systems were proposed to improve the prognosis assessment of these patients. Traditionally, 70-80% of breast malignancies are classified as invasive breast cancer because these tumors originate in ducts or lobules but spread in surrounding breast regions [9–11]. The remaining cases include in situ lobular or duct carcinomas. Due to the low incidence of in situ and special-type invasive tumors, such as inflammatory breast cancer and Paget's disease [11], many classification systems are based on the expression of specific biomarkers beyond the anatomic localization.

Considering the prognosis features of ER and HER2 expression, these biomarkers, in combination with the progesterone receptor (PR), were used to classify breast cancer patients into main subtypes based on their immunohistochemistry-detected expression [8–10,12–16], directly evaluated on biopsy or surgery pieces. Interestingly, these three biomarkers (ER, PR, and HER2) are informative and support decisions to administrate hormonal or targeted therapy. Then, cancer biology research allows us to understand how they participate in tumor growth.

Initially, breast tumors were categorized according to their ER expression. Subsequently, further research found a differential molecular profile (gene expression dysregulation) in breast luminal cells, which coined the "Luminal" term for these patients [17]. Regarding that PR is partially regulated by ER, the expression of at least one of these biomarkers signs the luminal subtype [10,14]. Then, this group of patients is suggested to be treated with tamoxifen or aromatase inhibitors [10]. Nevertheless, it is known that not all Luminal patients get a complete response to these therapies [18–20]. Some resistance factors to this treatment are because ER levels do not necessarily correlate to PR levels, which suggests novel tumor-leading pathways involving ER [10] or the confluence of many clonal types in the same tumor [8].

Besides Luminal groups, currently sub-classified in Luminal A, Luminal B, and Luminal HER2 [13,21], breast cancer tumors can be classified as overexpressing HER2 receptor (or just HER2+, 13–20 % of all cases) or Triple-

negative tumors (TNBC, 10-15% of all cases). Remarkably, the two latter groups show lower survival times in breast cancer patients [12]. It opens new research questions about the putative biomarkers to anticipate these tumors and the biology behind these more aggressive malignancies.

For HER2+ patients, research-based initiatives have studied, produced, and distributed Trastuzumab (Herceptin), a humanized monoclonal antibody able to block HER2 receptors (binding to the subdomain IV, located extracellularly) affecting their function and reducing growth rates [8,10,14,16]. Although Trastuzumab is the gold-standard treatment for HER2+ patients, a review published in 2022 commented that 23% to 40% of patients get a complete response to this treatment [14]. These values stimulated the research in targeted alternatives, such as Pertuzumab [8,16], but not limited to. Recent studies also aimed to evaluate potential concerns surrounding patient classification. The overexpression of HER2 receptors is routinely determined by immunohistochemistry or fluorescence hybridization in situ (FISH) procedures, which evaluate the protein accumulation or gene amplification, respectively [15]. Nevertheless, each method technically has different detection limits able to alter the classification of breast cancer patients [22]. Further, in a biological aspect, the amplification of HER2 is not conclusive to induce overexpression of the protein in 100% of cases [23], especially in a tumor context with aberrant patterns.

Despite the above-described considerations, the expression of ER, PR, or HER2 receptors can be used to determine the treatment scheme and predict the overall survival of patients. Patients whose tumors do not express these markers usually show poor prognosis. For example, the Gruvberger-Saal cohort (n=3207) represents one large-population study involving breast cancer patients [24]. Herein patients not expressing ER nor HER2 receptors showed a worse survival prognosis (Figure 3A). Though this cohort includes a low percentage of patients diagnosed before 40 years old (3.13%), it is possible to observe the same trend (Figure 3B). Moreover, it is possible to differentiate the survival of BC patients not expressing any of these three biomarkers. According to our biobank cohort, we observed differences between TNBC patients and non-TNBC for the entire cohort (n=589, Figure 3C) and a similar pattern in the

young diagnosed group (n=302, Figure 3D). For this thesis, we will consider the Cirqueira et al. (2011) classification [21] as it is considered in the hospital systems. This system classifies patients into five categories as it follows: Luminal A (expression of estrogen and/or progesterone receptors, absence of HER2 receptors, and Ki-67 <14%), Luminal B (expression of estrogen and/or progesterone receptors, absence of HER2 receptors, and Ki-67 ≥14%), Luminal HER2 (expression of HER2 and estrogen or progesterone receptors), HER2+ (expression of HER2 with absence of estrogen or progesterone receptors), and TNBC (no expression of HER2, estrogen, or progesterone receptors).

Then, the TNBC subtype is confirmed as the BC group with poor survival [25,26]. Gonçalves et al. (2021) have evidenced a reduced 5-year overall survival percentage in TNBC from Southeastern Brazil compared with non-TNBC individuals (62.1% vs. 80.8%, p<0.001) [25], while the large-scale study of Li et al. (2017) evaluated over 150 000 individuals demonstrating the same outcome in every stage and sub-stage including univariate and multivariate analyses [26].

In addition, the TNBC cohort was proven to be a heterogeneous group [27]. It demonstrates that the classification based on immunohistochemical profiles is a broad screening, prognostic, and treatment prediction system, but it could require additional information for giving proper treatments. By analyzing over 500 TNBC cases from 21 different datasets, Lehman et al. (2011) proposed a classification of TNBC patients into six groups that includes: two basal-like (BL1 and BL2), an immunomodulatory (IM), a mesenchymal (M), a mesenchymal stem-like (MSL), and a luminal androgen receptor (LAR) groups [27].

Since then, molecular tests to characterize TNBC tumors have been proposed [28–30]. However, there is a need to balance the number of markers required to classify patients and the number of groups that could be determined for suggesting therapies and prognostic evaluation in the context of precision medicine [29]. Therefore, these concepts could also be applied to all BC patients beyond TNBC. It stimulated the research of scores based on gene expression and gene mutational profiles in large-scale cohorts.

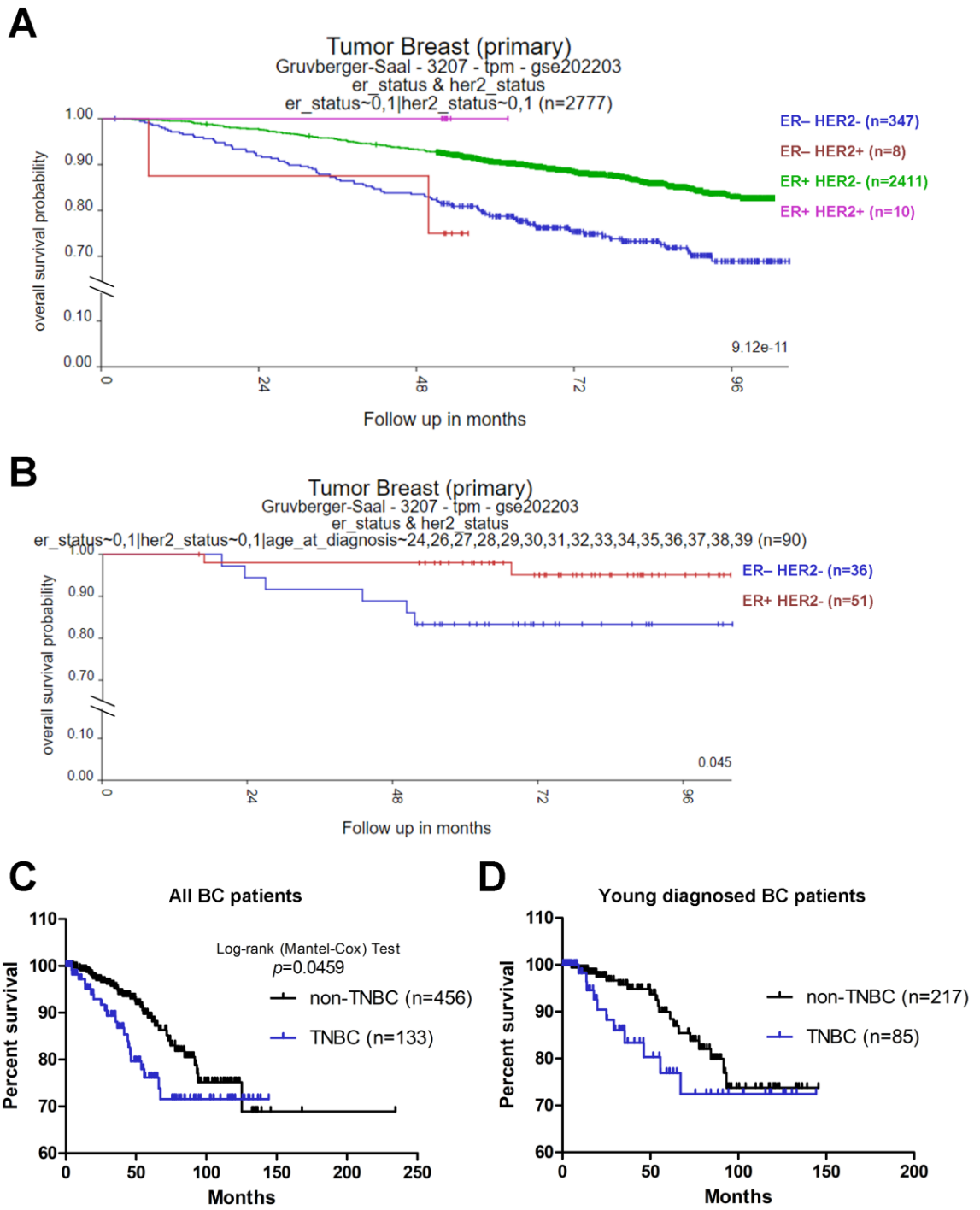

Figure 3. Overall survival of BC patients according to immunohistochemical subtypes. (A-B) Kaplan-Meier curves for BC patients of the Gruvberger-Saal cohort according to the expression of ER and HER2 receptors. Plot obtained using the R2 tool. Accessed on August 10, 2023. (A) Includes all BC patients, while (B) includes only BC patients diagnosed before 40 years old. (C-D) Kaplan-Meier curves for BC patients of the biobank cohort were dichotomized as Triple-negative BC (TNBC) subtype or non-TNBC patients. Data was retrieved using the Research Electronic Data Capture (REDCap) application and plotted using GraphPad Prism v8 for Windows. (C) Includes all BC patients, while (D) includes only BC patients diagnosed before 40 years old.

Among them, we found (i) the Oncotype DX 21-gene score to predict distant recurrence in tamoxifen-treated BC patients [31], (ii) the Prediction Analysis of Microarray data using 50 genes (PAM50) to add prognostic and predictive value to traditional pathologic, histologic, and clinical staging of BC patients [32], (iii) the MammaPrint test that requires expression levels of 70 genes to estimate the prognosis of node-negative BC patients [33], and (iv) the BluePrint test to determine BC molecular subtypes (Luminal-type, HER2-type, Basal-type) based on the expression of 80 genes with high accuracy [34].

Therefore, with the advent of high-throughput technologies, some datasets have published their multi-omics data for interested researchers to focus on specific gene sets and evaluate new molecular combinations. Between the most popular cancer-related omic datasets, we found The Cancer Genome Atlas for Breast Cancer (TCGA-BRCA) cohort [35] and the Molecular Taxonomy of Breast Cancer International Consortium (METABRIC) project [36].

In parallel to these research questions arose the need to improve the screening of candidates for patients before image evaluations such as mammography.

1.3 Circulating biomarkers of Breast Cancer

With all the knowledge accumulated (and still growing) about breast cancer tumors, the idea was proposed that it would be possible to collect tumor characteristics from blood samples (later known as systemic liquid biopsies) or other types of local fluids, for example, milk (in the case of breast cancer) [37].

Thus, liquid biopsies are a new tool for cancer detection and aid in treatment decisions [38]. The concept has been applied for the detection of different cancer-derived targets (cell-free DNA, cell-free miRNA, circulating tumor cells, platelet RNA, extracellular vesicles, etc.) in a variety of body fluids (plasma, pleura liquid, urine, etc.) [37,39–41]. Some potential liquid biopsy sources of biomarkers are presented in Figure 4.

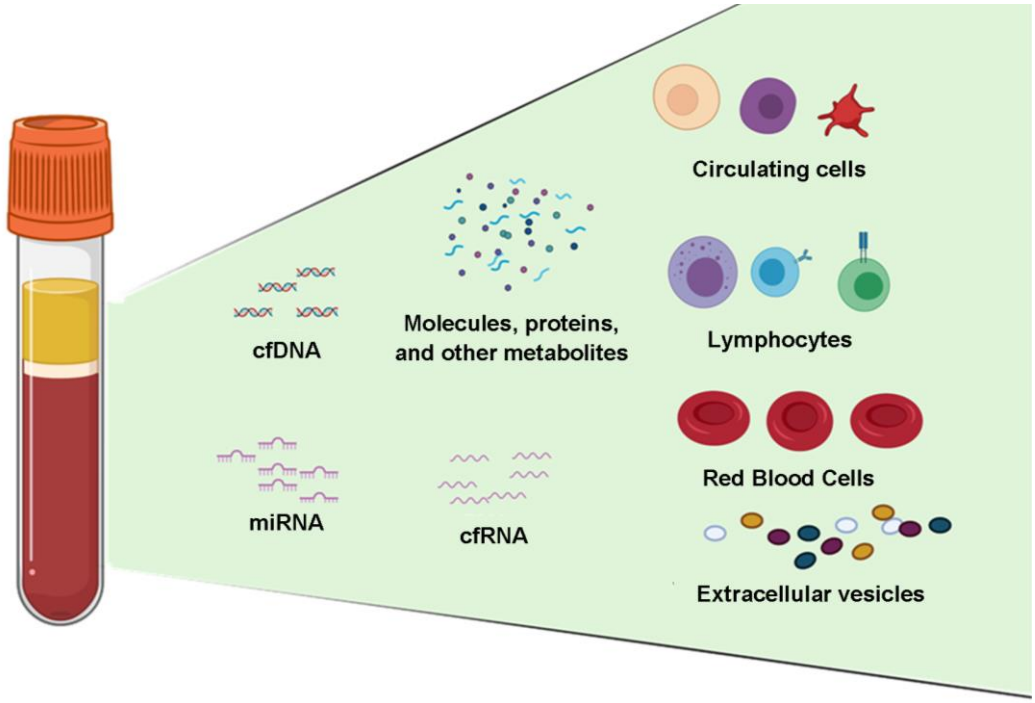

Figure 4. Sources of biomarkers in liquid biopsies. Representative image showing known sources of biomarker in an example of liquid biopsy (blood tube). Image created on BioRender.com. cfDNA: cell-free DNA; cfRNA: cell-free RNA.

1.3.1 cell-free DNA (cfDNA)

Circulating material was target of different studies in the context of BC. The DNA was the first molecule analyzed in circulating sources (cell-free DNA, cfDNA) of patients with cancer. Originally, cfDNA was measured by length to differentiate patients with pancreatic cancer [42]. Regarding BC specimens, cfDNA was used to classify patients and determine their prognosis based on the expression of specific markers [43,44], epigenetic modifications such as methylation [45–47], or the presence of somatic mutations derived from the tumor (coined as circulating tumor DNA, ctDNA) [48,49]. Nevertheless, the study of cfDNA presented some concerns mainly related to the integrity of this material. As cfDNA is usually found as fragments, it becomes a challenge to determine whether their degradation is associated with a biological or technical condition [50]. Then, the scientific community has not determined the proper length of these fragments. In addition, the presence of copy number alterations in cancer samples and the limited lifetime of cfDNA complicated the detection of specific probes, which suggests a paired test between tumor and circulating samples to improve the utility of this liquid biopsy source [50,51].

1.3.2 cell-free RNA (cfRNA) and miRNA (cf-miRNA)

Regarding molecular stability of nucleic acids, RNA based are more unstable than DNA, and it is reflected on circulating material [52]. Then, some reports realized that RNA carried by apoptotic bodies, more present in cancer patients [53], was more stable [52]. It suggests that protected RNAs could be considered good sources of information as they can provide unequivocal information on specific transcripts, overcoming technical challenges of analyzing methylation profiles in DNA-based analytes.

Among all types of RNA, we know two main groups: coding (messenger, mRNA) and non-coding RNA (ncRNA) [54,55]. In this sense, the relevance of RNA-based biomarkers relies on their ability to get a functional status related to tumor growth. In addition, RNA in circulation is sensitive to nucleases [56], which limits their effect in potential receipt cells. However, microRNAs (miRNAs) are a group of well-described non-coding RNAs with small lengths (18-24 nucleotides) that account for several regulatory processes by complementarity with mRNA (coding regions) to induce their repression [57–59].

miRNAs are produced in the cell nucleus by transcription from DNA regions by RNA polymerase II to generate primary microRNAs (pri-miRNAs) that are then processed to become small sequences ranging from 60-110 nucleotides called miRNA precursors (pre-miRNAs). In the cytoplasm, pre-miRNAs are cleaved by the enzyme DICER RNAse III to produce a double-strand mature miRNA. Then, the RNA-induced silencing complex (RISC) will select one strand to exert its regulatory effect in complementary sequences [60].

More interestingly, Letelier et al. (2016) have described different ways for miRNA exporting to the extracellular media [61]. Among them, we recognize two main groups: circulating (cell-free) miRNAs and vesicular miRNAs. Canonically, cell-free miRNA (cf-miRNA) will include all miRNA outside cells, including soluble miRNAs, miRNAs bound to protein or lipoprotein complexes, and miRNAs encapsulated in microvesicles, exosomes, and other membranous nanocompartments (extracellular vesicles) [61]. In addition, researchers are refining this source to explore only vesicular miRNA (EV-miRNA), miRNAs found inside these membranous partitions (extracellular vesicles) secreted by all human cells with no regard for their biogenesis.

The latest version of the most accurated miRNA database (miRBase v.22) reported 2654 mature miRNA sequences for the human [62], which supports a large dataset of possibilities for gene regulation. Then, miRNAs have been demonstrated to be deregulated in tumors, especially in carcinogenesis processes [59,63,64]. Therefore, it reinforces their evaluation as a relevant target in liquid biopsies.

Nevertheless, cf-miRNA and EV-miRNA are known to be low-concentrated sources. Then, their analysis requires high-throughput, high-resolution, and high-fidelity technologies such as quantification by digital barcoding hybridization.

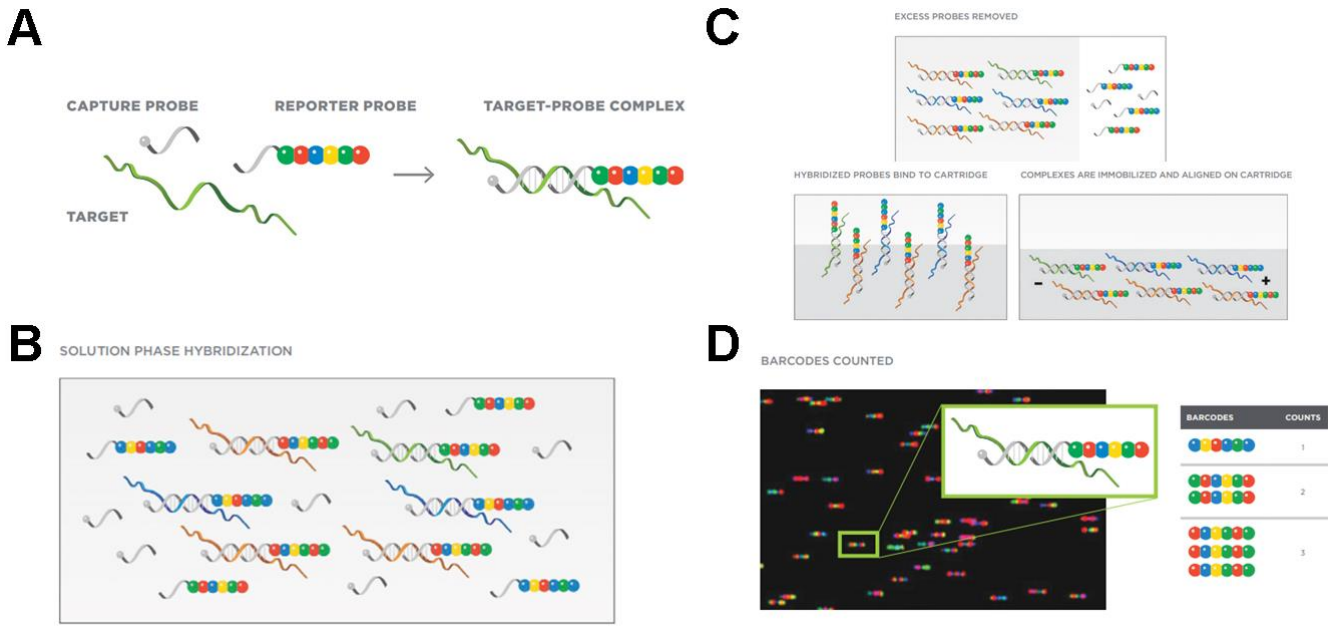

Figure 5. Mechanism of miRNA detection by digital barcoding hybridization using nCounter® from Nanostring®. (A) Probes (capture and reporter) participating in the detection of target molecules in input sample. (B-D) Steps for detection of miRNA targets by digital barcoding hybridization: Solution phase hybridization (B), Purification and immobilization of linked probes (C), and Barcode quantification (D). Image adapted from the nCounter® brochure for Translational Research (Nanostring 2018).

Then, Nanostring® offers an option to run this analysis, the nCounter® system [65]. With this system, researchers can save time and process up to 800 targets per sample using a multiplex analysis based on three main steps. As shown in Figure 5, miRNA samples are first hybridized with a reporter and a capture probe (one of each type per target). Second, the mix is loaded into the

nCounter equipment to be washed (all excess probes discarded) and immobilized in the cartridge (using biotin ligation). Third, the cartridge is analyzed by a fluorescence microscope able to recognize barcodes (reporter probes) and export results as a comma-separated value (CSV) file.

Importantly, this technique can quantify miRNA targets directly to the RNA strand without conversion to complementary DNA (cDNA) or predictive alignment with previously described miRNA sequences. Once reliable features are crucial in exploratory phases, we used this technique to explore these miRNAs in their circulating form, but also protected by extracellular vesicles, as these forms are attracting the attention of researchers [38,66,67] for their potential applications in the field of theranostics.

1.4 Extracellular vesicles in Breast Cancer

Herein, we decided to focus on extracellular vesicles (EVs) because their biogenesis allows showing a preserved cargo (DNA, RNA, miRNA, and proteins) [67] that could be analyzed further. However, EVs are also characterized by their smaller size (30 nm-5 µm) and the ability of any cell to produce them [38,66–68]. EVs can be obtained from saliva, urine, blood, and tears for human research [69].

According to the up-to-date knowledge about EVs, they are divided into at least four main groups related to their notable differences in biogenesis [68]: exosomes, ectosomes, apoptotic bodies, and others (not classified). Exosomes (30-150 nm in size) are packaged in multivesicular bodies (cell membrane buds, MVB), whereas ectosomes (200 nm-5 µm) are generated from cell membrane protrusions. Then, apoptotic bodies are produced by cell fragmentation during programmed cell death [68,70]. Finally, not-classified particles refer to a broad spectrum of EVs that do not share biogenesis characteristics with any of the first groups, and they are material of further (and recent) research, like migrasomes [71], for example.

The study of EVs and their applications for diagnosis, prognosis, or treatment proposals for several diseases is a research field in development. As a quality parameter in the EVs research (according to the Minimal information for studies of extracellular vesicles, MISEV) [72], these particles must be characterized using membrane markers (CD9, CD81, ALIX, and TSG101),

electronic microscopy, and nanoparticle tracking analysis (NTA). Although these requirements are extremely necessary to define nanostructures as vesicles [72], there are still no specific markers for subpopulations of these EVs.

In cancer, these characteristics establish a recent research field intending to classify patients and estimate prognosis factors using minimally invasive methods. Recently, our group published a scientific review approaching the state-of-art about the diversity of extracellular vesicles studied from BC samples [70]. In this review, we associated elements of the EV cargo from BC cell lines or liquid biopsies of BC patients with tumor-related processes. Figure 6 presents a summary of these findings. In a nutshell, we analyzed different cargo types previously found in EVs, which include miRNA, long non-coding RNA (lncRNA), mRNA, and proteins. Then, these data were compared with functional studies to understand their participation in tumor processes. Thus, we associated EV cargo with four main events: modulation of tumor aggressiveness and growth, preparation of pre-metastatic niche, epithelial-to-mesenchymal transition (EMT), and drug-resistant phenotype.

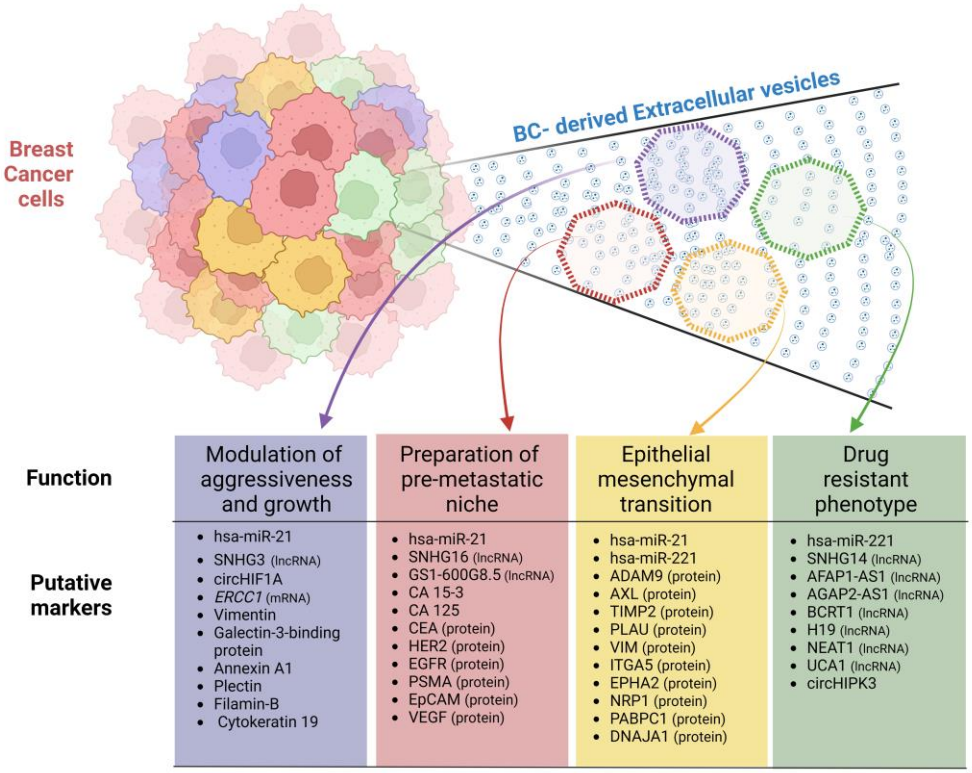

Figure 6. Putative BC biomarkers in Extracellular vesicles from BC-related samples. As BC cells are heterogeneous, this diversity can be translated into vesicles, which could contribute to different BC-related functions depending on their cargo. Image created on BioRender.com and adapted from the review of Murillo Carrasco et al. (2023).

In addition to the security offered by EVs to transport cargo to a receipt cell [67], these particles may participate in biodistribution once some specific biomarkers are projected in their membrane. Then, these proteins can determine which cell must receive their cargo.

Due to this reason, the presence of a lncRNA such as SNHG16 was not limited to one function. This lncRNA was associated with the formation of a pre-metastatic niche as it was demonstrated that this lncRNA suppresses the expression of hsa-miR-16-5p in γδT1 lymphocytes, which indirectly upregulates CD73 to favor the immune evasion [73]. However, this lncRNA can suppress another miRNA (hsa-miR-892) in BC cells. Vesicular SNHG16 can “educate” neighbor cancer cells to become more aggressive and affect EMT, migration, and BC invasion processes [74].

In this sense, EVs proved to be skillful in the dependence of their capacity of carrying different analytes in different subpopulations. Though there is no consensus about informative vesicular miRNA for BC patients, the implementation of exploratory and high-throughput technologies such as the RNA sequencing and RNA microarrays allow the discovery of new RNA subtypes in EVs from BC cell lines [75] and patient samples [76]. Among all RNA subtypes, miRNAs represent the group with more available information for cancer. Then, the small size of miRNAs makes them more likely to be transported by EVs when compared with other RNA types.

As an example of this versatility, the hsa-miR-21 has been studied in breast cancer [64,77,78], and this miRNA was found in EVs. In Figure 6, we described the participation of this miRNA in three out of four BC-related processes. The hsa-miR-21 was successfully detected in EVs from plasma, serum, and tears from BC patients [70,79]. In addition, this sequence was described to regulate different targets depending on their context. It was demonstrated that hsa-miR-21 can facilitate the BC expansion and EMT process by suppressing Wnt-11 [80], support the bone metastasis by repressing PDCD4 [81,82], and produce cancer-related thrombosis by inhibiting IL6R in progenitor cells [83].

Some studies have proposed the use of let-7a-5p, miR-222-3p, miR-142-5p, miR-4448, miR-2392, miR-2467-3p, miR-4800-3p, miR-150-5p, miR-1246 and miR-155 expression levels in vesicles from plasma as prognosis, classification or prediction markers in BC (AUC>0.7) [84–88]. For our study, we

decided to use a digital barcode hybridization platform as a high-resolution and high-throughput tool for obtaining exploratory data of circulating and vesicular miRNA expression in BC samples

After observing this diversity and regarding recent knowledge from the International Society of Extracellular Vesicles (ISEV), partial selections of extracellular vesicle subtypes (eventually called exosomes, microvesicles, small or large EVs, etc.) can be obtained by applying different isolation protocols [89,90]. Once there are different strategies for the selective capture and isolation of smaller particles, we propose to evaluate three of the principal methods for EV isolation from plasma (sedimentation by density, precipitation, and size exclusion). Although vesicular microRNAs have been reported as promising molecules for cancer diagnosis due to their protection from RNAse degradation. Their amount inside vesicles is predicted to be low and appropriate pipelines for analysis are still elusive.

After that, our proposal is to evaluate the miRNA cargo, observe differences between cf-miRNA and vesicular miRNA cargos, and learn about EV subpopulations.

1.5 The Tn antigen in cancer and their potential segregation on EV surface

According to our literature review, proteins can be isolated from EVs, and these vesicular proteins participate in the modulation of tumor processes in the BC environment (Figure 6). Regarding the EV heterogeneity in liquid biopsies [70], it would be interesting to focus on tumor-derived EVs. In this sense, proteins, different from nucleic acids, can be found anchored in the membrane of these EVs [91,92], which allow us to use them for selecting EV subpopulations. In addition, it was described that EVs can carry protein in their corona [93,94], and these proteins are usually modified with glycosylation patterns [70,93].

Then, cancer cells are been demonstrated to induce aberrant glycosylation profiles [95] (Figure 7). For example, derivatives of the Tn (GalNAcα1-Ser/Thr) antigen (p.e. Sialyl-Tn, T, and Tn antigens) are representations of aberrant glycosylation on the surface of cancer cells, including breast cancer [95,96]. In normal cells, a base residue of Serine or Threonine of surface proteins is

modified by the COSMC protein to produce complex glycans on the cell surface. However, in cancer cells occur a dysregulation of the function of COSMC leading to Tn (GalNAcα1-Ser/Thr) and sialyl-Tn (STn, Neu5Acα2,6GalNAcα1-Ser/Thr) formation. Thus, derivatives of Tn antigen were described for different stages of cancer as well as other human disorders, such as IgA nephropathy and Tn syndrome [96–99].

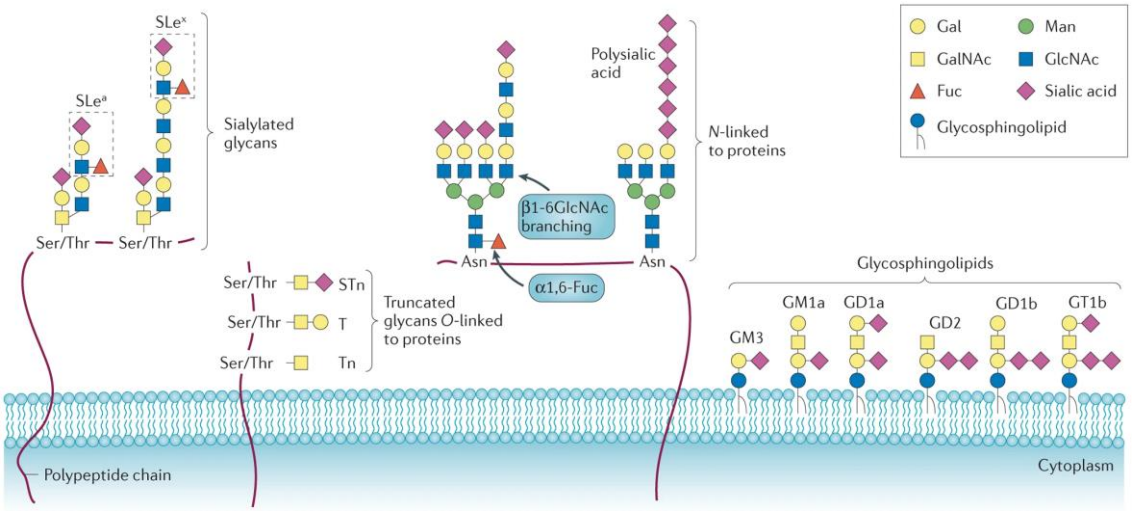

Figure 7. Common aberrant glycans found in tumors. These pathologic glycans are considered a hallmark of cancer cells. Aberrant glycosylation in cancer used to involve higher expression of sialyl Lewis x (SLex) and SLea antigens, as well as α2,6-sialylated structures, both in truncated O-linked glycans (for example, sialyl Tn -STn) and in N-linked glycans. Image adapted from the review of Pinho and Reis (2015). Gal, galactose; GalNAc, N-acetylgalactosamine; Man, mannose.

In this way, derivatives of Tn antigen (STn/Tn) might act as potential targets to select cancer cells by lectin affinity. To select cells or EVs that express these aberrant proteins, we can use glycan-binding proteins (GBPs) such as antibodies or lectins. Commonly, GBPs were used to detect and quantify their targets in breast (CA15-3/CA27-9), prostate (PSA), ovarian (CA125, HE4), colorectal (CEA), hepatocellular (AFP), Thyroid (Tg) and pancreatic (CA19-9) cancers [100,101].

GBPs were proposed as linkage to capture and quantify vesicles carrying their targets in breast cancer; this approach was previously used in prostate cancer to isolate EVs using affinity properties of Concanavalin A lectin and CD9/CD81/CD63 antibodies [102,103]. Then, this approach could be improved

by establishing an antibody-lectin sandwich to treat the same target, as suggested by Tang et al. (2015) [104].

The antibodies are produced such as defense tools against pathogen infection, whereas lectins are non-immune proteins capable of interacting with different sugars for molecular or cellular recognition. Thus, specific lectins and antibodies could select derivatives of Tn antigen but with some differences; the main is related to multivalent links [105].

Then, lectins look more feasible to select targets with high efficiency and strength but less specificity than antibodies. For breast cancer and Tn derivatives, some vegetable lectins have been described such as *Artocarpus integrifólia* (jackfruit) “Jacalin” and *Arachis hypogaea* (peanut) “PNA” [106]. Among these two species, it is important to add that Jacalin can be separated from jackfruit seeds following a well-standardized protocol [107]. Briefly, this protocol takes advantage of Jacalin's ability to link IgA1 using sepharose columns. On the other hand, PNA lectin is directly purified from peanuts using epoxy-activated Sepharose 6B columns [108].

In addition, jackfruit is one of the products of the colonization process in Brazil that has been adapted to climatic conditions and accepted by the population [109]. Brazilians used to eat the pulp of this fruit and discard the seeds, raw sources for the production of Jacalin. Then, researchers described different healthy properties in Jackfruit extracts from sections of the plant [110–112]. About jackfruit seeds, we know that they have the potential to stimulate selected phenotypes of B or T cells [113], and are rich in protease inhibitors [114] and antioxidants [115].

Unfortunately, jackfruit is one of the world's biggest fruits (4-50 Kgs), with a limited time of consumption due to its high water content [116], which reduces the industrial potential to culture this fruit. Due to these reasons, it is usual to find jackfruits in popular markets but not in commercial supermarkets, as it occurs with the top 5 fruits produced in Brazil (orange, banana, grape, apple, and pineapple) [117]. Making jackfruit less perishable is possible by drying protocols [116], but it requires high investment to render a large-scale production. In this opportunity, we evaluated Jacalin lectin as a strategy to increase their added value and offer new opportunities for these GBPs.

For this study, we hypothesized that the presence of aberrant surface proteins (including Tn derivatives) in the membrane of tumor-derived EVs can be used to specifically select EVs secreted by tumor cells. Then, we propose to use Jacalin lectin to select tumor-derived EVs. Figure 8 shows our hypothesis for using Jacalin for selecting tumor-derived EVs and then recovering them by incubating them with Jacalin's primary sugar (D-galactose).

Regarding the cellular heterogeneity in tumors and circulating fluids, we aim to identify and select tumor-derived EVs by targeting aberrant glycosylation on their surface proteins. Once a specific subpopulation of EVs is selected, researchers could use these particles to analyze further characteristics as their miRNA cargo. It is important to note that classification features of vesicular miRNAs would be enhanced if we conduct these expression analyses exclusively on tumor-derived EVs. However, there is still no consensus concerning a specific marker of breast cancer-derived EVs.

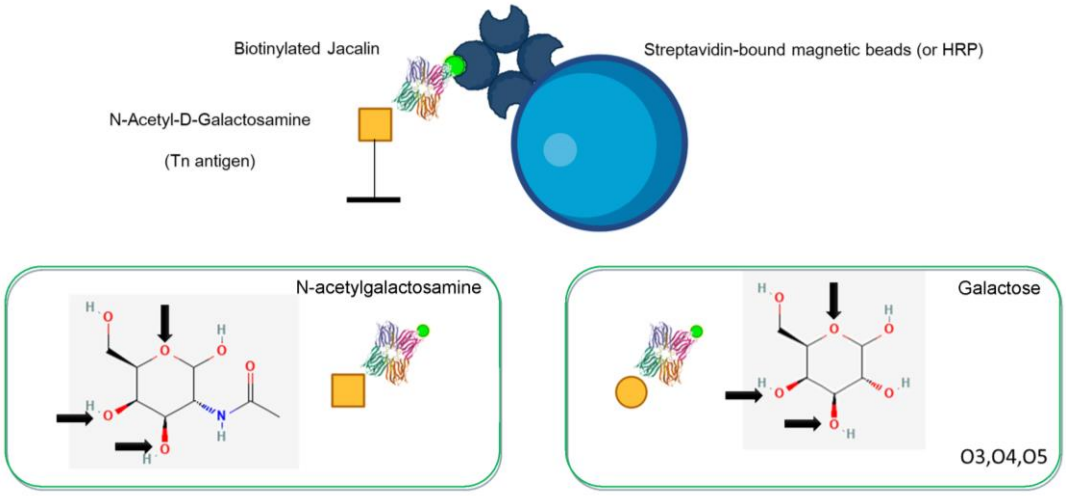

Figure 8. Schematic representation of Jacalin-Tn ligation. Reactions involving glycan-binding proteins (GBP) are performed based on this hypothesis. Tn antigens on the surface of EVs or BC cells will link to biotinylated Jacalin. Then, biotin will combine with streptavidin-bound molecules (magnetic beads for separation or horseradish peroxidase for labeling). Therefore, this reaction can be removed by incubation with the primary sugar of Jacalin, D-galactose. This reaction is possible since Jacalin molecules react with N-acetylgalactosamine or D-galactose by linking oxygens in positions 3,4, and 5 as shown in black arrows. The Jacalin 3D structure was provided by Protein Data Bank (https://www.rcsb.org/), accession 1KU8. HRP: horseradish peroxidase.

2. OBJECTIVES

- To standardize the protocol for isolating miRNA from plasma.

- To standardize the protocol for isolating EVs and their miRNA from plasma.

- To standardize the protocol for labeling tissue and liquid biopsy samples from BC patients with Jacalin.

- To evaluate whether cell-free (cf-miRNA) and vesicular (EV-miRNA) miRNA cargo differs between BC subtypes and age-related groups focusing on TNBC and young diagnosed (early onset) patients.

- To compare cf-miRNA and EV-miRNA profiles between BC patients.

- To test the ability of Jacalin to separate EVs potentially produced by the tumor of BC patients.

3. MATERIAL AND METHODS

3.1 Analyses with external data

Informative data presented in the Introduction of this thesis were provided by secondary analysis of data deposited in public repositories. For Kaplan-Meier curves with external data, we used the R2 tool [118]. We selected the appropriate dataset, excluded samples with no available information and plotted the overall survival curves based on the combination of two parameters (Estrogen receptor and HER2 receptor).

3.2 Experimental Design for cf-miRNA experiments

Initially, we evaluated the cf-miRNA content in the plasma of breast cancer patients (green section in Figure 9). According to sample availability for each immunohistochemical subtype, we selected 30 samples from Cohort A (Appendix 1) classified into 12 sample tubes: Elderly HER2 (one individual sample), Elderly Luminal A (one pool of three samples), Elderly Luminal B (one pool of three samples), Elderly Luminal HER2 (one pool of three samples), Elderly TNBC (two pools of three samples each), Young HER2 (two individual samples), Young Luminal B (one pool of three samples), Young Luminal HER2 (one pool of three samples), Young TNBC (two pools of three samples each). We isolated cf-miRNA from individual samples by following the steps described in the section “miRNA isolation” starting with 200 µL for each sample. For pooled samples, we combined 200 µL of each participant sample to obtain pools of 600 µL. Then, we ran the standard protocol thrice collecting all miRNA fractions in the same tube. After collecting the 12 cf-miRNA tubes, we quantify them by spectrophotometry and follow the “cf-miRNA profiling by digital barcode hybridization” and “nCounter raw data preprocessing for total cf-miRNA” sections to obtain cf-miRNA normalized counts.

3.3 Experimental Design for vesicular miRNA experiments

After observing the cf-miRNA results, we evaluated the vesicular miRNA profile (purple section in Figure 9). To do this, we evaluated the three best-known strategies to obtain vesicles apart from human plasma: ultracentrifugation, precipitation by chemical reagent, and size exclusion chromatography.

After evaluating the EV profile from samples of cohort B (Appendix 2), we extracted vesicular miRNA to assess its quality by spectrophotometry (section “miRNA quantification by spectrophotometry”) and capillary electrophoresis (section “Vesicular miRNA quantification by capillary electrophoresis”). Next, we quantified specific vesicular miRNAs using the nCounter (Nanostring) platform by inputting the total vesicular miRNA mass extracted from 600 µL of plasma.

For cohort A (Appendix 1), we performed miRNA isolation according to the strategy (individual or pool) of all samples. We isolated vesicular miRNA from individual samples by following the steps described in the section “miRNA isolation” starting with ~630 µL for each sample.

For pooled samples, we combined 600 µL of each participant sample to obtain pools of 1800 µL. Then, we ran the standard protocol thrice to collect all miRNA fractions in the same tube. After collecting all vesicular miRNA tubes, we quantified them by spectrophotometry/capillary electrophoresis. Then, we followed the “Vesicular miRNA profiling by digital barcode hybridization” step with ~65 ng of vesicular miRNA mass. Finally, we followed the “nCounter raw data preprocessing for vesicular miRNA” section to obtain normalized counts of vesicular miRNA.

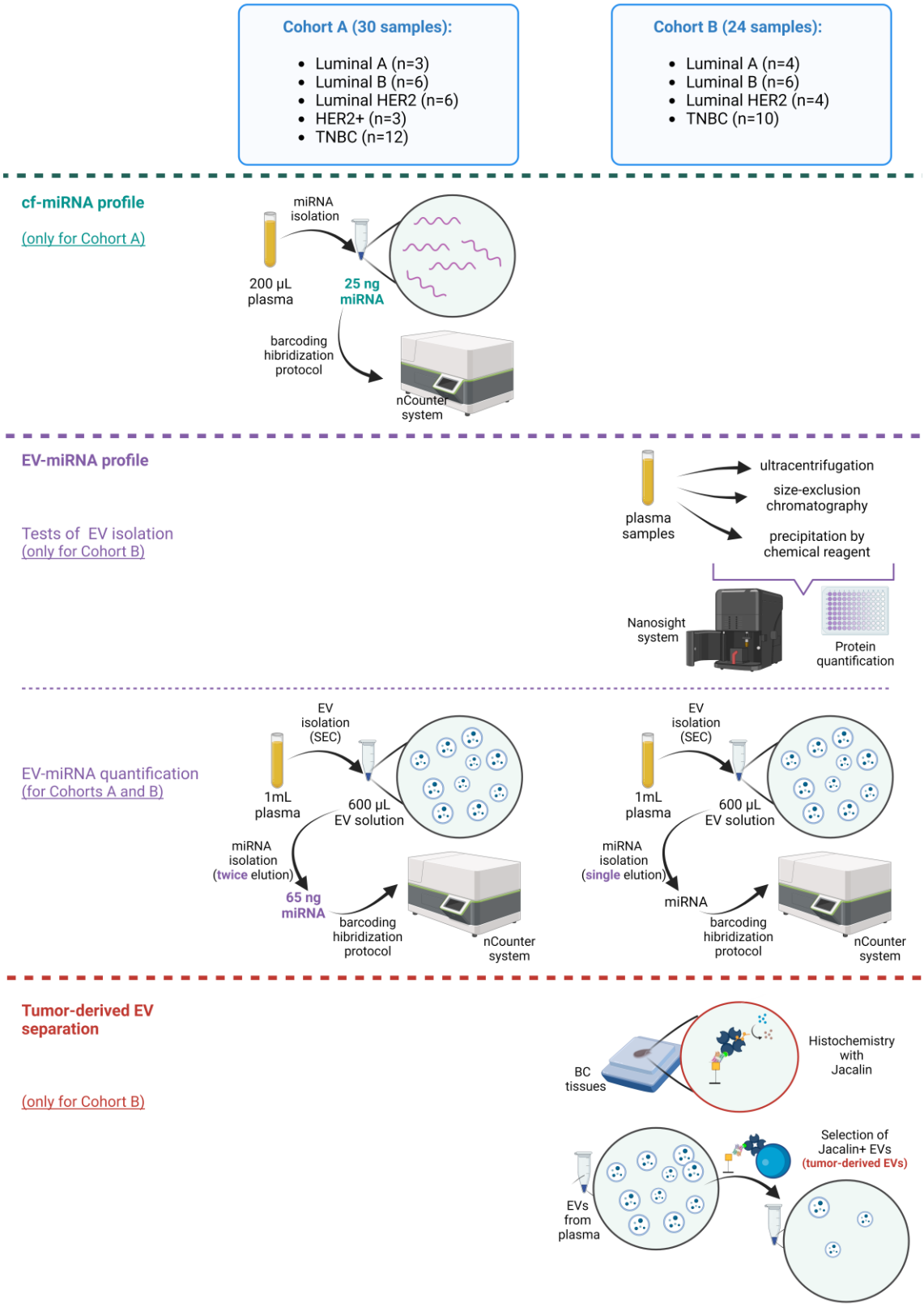

Figure 9. Visual outline for the experimental design of this thesis. This study is divided into three main groups of experiments: cf-miRNA profile (green), EV-miRNA profile (purple), and Tumor-derived EV separation (red). For each section, the main details of the experimental design are shown. Relevant information was stressed with the corresponding color of each section. For miRNA profiles, referential volume corresponds to one individual sample. Image created on BioRender.com. BC: breast cancer; SEC: Size-exclusion chromatography; EV: extracellular vesicles.

3.4 Experimental Design for evaluating tumor-derived EVs

After evaluating cf-miRNA and EV-miRNAs, we tested the hypothesis of selecting tumor-derived EVs using Jacalin as a glycan-binding protein (red section in Figure 9). We started evaluating levels of Jacalin targets in tissues of BC patients from Cohort B (Appendix 2). These observations are obtained by the interaction between Tn derivatives, biotinylated Jacalin, streptavidin-bound HRP, and chemiluminescent reagents described in the “Lectin histochemistry of FFPE tissues” section.

Then, we evaluated the ability of Jacalin to select BC cells using an indirect interaction mediated by Tn derivatives, biotinylated Jacalin, and streptavidin-bound magnetic beads following the “Selection of Jacalin lectin-positive cells” and “Removal of Jacalin lectin labeling in cells” sections.

To confirm that EVs can carry Tn signals on their surface, we run dot blot experiments with a similar rationale to lectin histochemistry, following steps of the “Dot blot of plasma and EV samples with Jacalin”.

Finally, we tested Jacalin and their primary sugar (D-galactose) to separate EVs based on the expression of the Tn antigen and their derivatives using the same interaction previously performed in cells. Herein we followed the methods described in the “Selection of Jacalin lectin-positive EVs”.

3.5 Breast Cancer patients

This study used plasma samples from BC patients and healthy individuals and Formalin Fixed Paraffin Embedded (FFPE) tissue samples of BC patients. All samples were used as a part of the sample collection from the Academic Biobank of Research on Cancer from the University of São Paulo, complemented by the cohort participant of the “Retratos da Mama” project.

The “Retratos da Mama” project is an observational study that aims to characterize genetic profiles by whole exome sequencing of BC patients classified as TNBC and diagnosed before 40 years old (young diagnosed, early onset BC). Then, genetic variations will be evaluated to determine their association with clinical outcomes and quality of life of these patients.

For this thesis, we included patients diagnosed with invasive breast cancer after 18 years old, classified as C50 according to the International Classification

of Diseases (ICD). Samples were classified into five groups according to their immunohistochemical subtype in agreement with the classification of Cirqueira et al. (2011) [21]: Luminal A, Luminal B, Luminal HER2, HER2+, and Triple-negative breast cancer (TNBC). Written informed consent and epidemiological questionnaire of Biobank and the project “Retratos da Mama” (*Certificado de Apresentação de Apreciação Ética*, CAAE nº 99542818.0.0000.0065, *Comitê de Ética em Pesquisa*, CEP nº 3.007.737/18) were obtained from all patients enrolled in the study. Ethical approval and written informed consent can be reviewed in Attachment 1, Attachment 2, and Attachment 3. For each sample, available information about age, sex, self-declared race, education level, Body-Mass Index (BMI), nutritional status, physical activity, drugs use, smoking, alcohol use, comorbidities, cancer familial history (known hereditary cancer syndrome criteria), previous surgeries, diabetes, high blood pressure, chronic obstructive pulmonary disease, chronic gastritis, presence of malign or benign tumors, tissue pathologic status, expression of receptors (estrogen, progesterone, and HER2) in the tissue, tumor stage, tumor relapse, treatment, survival/follow-up data, and the number of available plasma tubes were retrieved from the clinical records deposited on the Research Electronic Data Capture (REDCap) application.

3.6 Plasma samples

The patients' blood was collected in Ethylenediaminetetraacetic acid (EDTA) tubes at diagnosis (before surgery or adjuvant treatments). In agreement with previous studies, we obtained six EDTA tubes per patient. To reduce potential epithelial, platelet, or immune cell contamination [119,120], we used one of the 2^{nd}-6^{th} tubes for processing plasma for EV-related downstream analysis. Blood samples were processed using the protocol for plasma separation of the “Retratos da Mama” project (PRONON 25000.069252/2015-79). Briefly, blood tubes were centrifuged at 800xg for 10 min; the supernatant was separated and centrifuged at 11 000xg for 10 min. All centrifugation steps were performed at 4 °C. Finally, the second supernatant was preserved as debris and platelets-free plasma and frozen in 2mL tubes at -80 °C.

3.7 FFPE samples

Formalin-Fixed Paraffin-Embedded (FFPE) tissue blocks from breast cancer patients were used as a part of the sample collection from Academic Biobank of Research on Cancer from the University of São Paulo, located in Centro de Investigação Translacional em Oncologia, Instituto do Câncer do Estado de São Paulo (ICESP), São Paulo, Brazil. This Biobank protocol was approved by the Local Ethics Committee (CEP n° 031/12), and National Ethics Committee (CONEP n° 023/2014). For this study, we included tumor samples having more than 80% of tumor viable cells.

3.8 EV isolation by size-exclusion chromatography

Extracellular vesicles were isolated using qEV original columns (cat. 100666, IZON). For this step, we followed the manufacturer's recommendations starting with 1 mL of plasma. After rinsing the columns with filtered phosphate-buffered saline (PBS), pH 7.4, we loaded the plasma sample and immediately collected 1 mL fractions into 1.5 mL Eppendorf® tubes. The first three fractions (void volume) were discarded. The fourth and fifth fractions containing EVs were collected and stored at -80°C until the next procedure.

3.9 EV isolation by ultracentrifugation

Here, we diluted 1mL of human plasma up to 10mL with a filtered PBS pH 7.4 solution and set the ultracentrifuge with 28 500 rpm (~100 000xg in SW41Ti rotor, Optima XE-90 ultracentrifuge, Beckman Coulter) for two hours at 4 °C. Then, we resuspended the pellet in 300 µL of filtered PBS pH 7.4.

3.10 EV isolation by chemical precipitation

For this step, we used the miRCURY Exosome Serum/Plasma Kit (cat. 76603, Qiagen) with a starting volume input of 1mL of human plasma and following the manufacturer's recommendations.

3.11 EV quantification by NTA

We used a Nanoparticle Tracking Analysis (NTA) in the Nanosight® NS300 equipment (Malvern) to quantify EVs. For each sample, five measurements of 60 s each were taken using 50 µL per time. We also run the PBS pH 7.4 solutions as the negative control for checking quantification values.

3.12 Quantification of proteins

We performed a modification of the Lowry assay [121] to quantify proteins. We treated 40 µL of eluted EVs with 40 µL of RIPA detergent (cat. S8830. Sigma) and incubated the mix at 4 °C for 15 minutes. Then, we centrifuged the samples at 16000xg for 15 minutes and collected the supernatant in a new tube. After we put five microliters of each sample in a 96-well plate and stained with a copper solution diluted in bicinchoninic acid (1:50). The GloMax® reader (Promega) was used for the estimation of protein concentration by absorbance spectra at wavelengths ranging from 560 to 600 nm. Later, protein concentrations were estimated using a standard curve previously elaborated with 1:2 serial dilutions of BSA 5 µg/µL.

3.13 Protein gel electrophoresis

Proteins from each sample were separated using a polyacrylamide gel (SDS/PAGE). The gel was composed of two phases: stacking gel (4% polyacrylamide) and separating phase (12% polyacrylamide). Six micrograms of each sample were diluted in the Laemmli buffer [122] and loaded onto the stacking gel. An additional well was used to load 5 µL of the PageRuler Plus Stained Protein Ladder (ThermoFisher). The stacking gel was run for 15 minutes at 80v and the separating gel for 80 minutes at 120v. Subsequently, the gel was stained for 6 hours with a Coomassie blue solution: 0.05% Coomassie Brilliant Blue R-250 (w/v), 50% methanol (v/v), and 10% acetic acid (v/v) in distilled water. Finally, the gel was destained overnight by incubation with a solution composed of 5% methanol (v/v) and 7.5% acetic acid solution.

3.14 EV characterization by western blot

We sonicated EV samples (~5x10^7 particles) using the Fisherbrand™ Sonic Dismembrator device (cat. FB50, Fisher Scientific) by three pulses of one second each at low amplitude. Proteins were obtained using the RIPA buffer (Sigma) containing protease and phosphatase inhibitors and incubated for 15 min at 4 °C. Then, vesicular proteins were loaded onto 12% SDS-PAGE: 0.375 M Tris, pH 8.8, 0.1% SDS, 10% acrylamide, 0.03% ammonium persulfate (APS), and 0.06% N, N, N′, N′-tetramethyl ethylenediamine (TEMED). After the electrophoretic run, samples were transferred using the Mini Trans-Blot® Cell system (cat. 1703930, Bio-Rad) to polyvinylidene difluoride (PVDF) membranes. These membranes were then blocked with 5% BSA in 0.1% TBS-Tween for one hour at room temperature, followed by incubation with primary antibodies overnight at 4 °C and secondary antibodies for one hour at room temperature For this thesis, we used anti-CD9 (1:500, cat. PA5-85955, Invitrogen), anti-apoAI (1:500, cat. sc-376818, Santa Cruz Biotechnology), anti-rabbit IgG peroxidase (1:7000, cat. A9169, Sigma), and anti-mouse IgG peroxidase (1:4000, cat. NXA931, GE Healthcare). Protein bands were visualized with Amersham ECL Western Blotting Detection Reagent (cat. RPN2109. GE Healthcare) and Amersham ECL Prime Western Blotting Detection Reagent (cat. RPN2232, GE Healthcare). Chemiluminescent figures were acquired using the ImageQuant™ LAS 4000 equipment (GE Healthcare).

3.15 EV characterization by transmission electron microscopy

We used previously a previously published protocol [123] for performing the transmission electron microscopy (TEM). Briefly, EVs were fixed in a 2% paraformaldehyde and 2% glutaraldehyde solution (1:1) in sodium cacodylate buffer (pH 7.4) for 30 min at 4 °C. Next, we washed EVs with PBS and ultracentrifuged at 100 000× g. 10 µL of EV-containing solution were mounted in TEM grids, contrasted with uranyl acetate 2% for 15 min, and washed in distilled water. Fluid excess was blotted in filter paper, air-dried, and examined using a ZEISS Leo 906 electron microscope (Carl Zeiss, Jena, Germany).

3.16 miRNA isolation

For plasma total cell-free miRNA (cf-miRNA) performed in samples from Cohort A (Appendix 1), we followed the miRNeasy Serum/plasma kit manufacturer's recommendations starting with 200 µL of human plasma. For vesicular miRNA, this procedure was performed in agreement with the recommendations from the International Society of Extracellular Vesicles (ISEV-MISEV2018) [72]. 30 µL of proteinase K (20mg/mL, cat. P2308, Sigma-Aldrich) were added to 600 µL of EVs (fourth fraction of the isolation step) and incubated for 10 minutes at 37 °C. Then the mixture was added with 3 µL of RNAse A (20mg/mL, cat. 12091021, ThermoFisher) and then incubated for 30 minutes at 37 °C. Afterward, the total volume (~ 630 µL) was processed with the miRNeasy Serum/plasma kit (cat. 217184, Qiagen) according to the manufacturer's recommendations.

3.17 miRNA quantification by spectrophotometry

Vesicular miRNA and cf-miRNA were quantified using spectrophotometry in Nanodrop 4.0 equipment (ThermoFisher). 1.5 µL of each sample was used to estimate their optical density (OD) at 230, 260, and 280 nm wavelengths.

3.18 Vesicular miRNA quantification by capillary electrophoresis

Vesicular miRNA was quantified using small RNA chips (cat. 5067-1548, Agilent). Each chip can analyze up to 11 samples using one µL of each sample. Chips were loaded according to the manufacturer’s recommendations and then read in the 2100 Bioanalyzer equipment (Agilent) using the recommended settings for miRNA samples.

3.19 cf-miRNA profiling by digital barcode hybridization

40 (individual samples) or 120 (pooled samples) µL of each tube were concentrated up to 4 µL using the Eppendorf® 5301 concentrator for 20 or 35 minutes at 45 °C following the manufacturer’s recommendations. After concentration, 0.5 µL of each sample was loaded into the NanoDrop™ 8000 Spectrophotometer (ThermoFisher) to verify the miRNA mass. Then, ~25 ng of

cf-miRNA were hybridized for 16.5 hours with molecular barcoding for 827 experimentally validated human miRNAs (from miRBase v21) using the nCounter Master Mix (NanoString® Technologies, cat. NAA-AKIT-012). Subsequently, miRNAv3 NanoString® cartridges (NanoString® Technologies, cat. CSO-MIR3-12) were loaded with the mix per sample, sealed, and transferred to an nCounter® Digital Analyzer device (NanoString® Technologies) for data collection.

3.20 Vesicular miRNA profiling by digital barcode hybridization

We used two approaches for this step. In the first one (Cohort B, Appendix 2), 20 µL of each sample were concentrated up to 4 µL using the Eppendorf® 5301 concentrator for 10 minutes at 45 °C following the manufacturer's recommendations. Then, all samples were hybridized for 16.5 hours with molecular barcoding for 827 experimentally validated human miRNAs (from miRBase v21) using the nCounter Master Mix (NanoString® Technologies, cat. NAA-AKIT-012). While the second approach (Cohort A, Appendix 1) starts concentrating 40 µL of each sample using the Eppendorf® 5301 concentrator for 20 minutes at 45 °C. After concentration, 0.5 µL of each sample was loaded into the NanoDrop™ 8000 Spectrophotometer (ThermoFisher) to verify the miRNA mass. Then, ~65ng of EV-miRNA were hybridized for 16.5 hours with molecular barcoding for 827 experimentally validated human miRNAs (from miRBase v21) using the nCounter Master Mix (NanoString® Technologies, cat. NAA-AKIT-012). After hybridization, all samples from the two approaches were loaded into miRNAv3 NanoString® cartridges (NanoString® Technologies, cat. CSO-MIR3-12), sealed, and transferred to an nCounter® Digital Analyzer device (NanoString® Technologies) for data collection.

3.21 nCounter raw data preprocessing for total cf-miRNA

miRNA expression data were analyzed in the nSolver™ Data Analysis v.4.0 software (NanoString® Technologies) with the default protocol by the manufacturer. For cf-miRNA, we normalize the expression of human miRNAs by the geometric mean of all negative (negative normalization) and positive (positive normalization) probes. Then, we used the top 15 more stable regions

(up to 15% of the coefficient of variation) to normalize the content set data. Data were exported in comma-separated value (*.csv) format for further analysis.

3.22 nCounter raw data preprocessing for vesicular miRNA

miRNA expression data were analyzed in the nSolver™ Data Analysis v.4.0 software (NanoString® Tech.). Herein, we tested the following normalization parameters: (i) Negative normalization by the maximum value of any probe, Positive normalization by the geometric mean of all probes, and Content set normalization adjusted by EVs concentration; (ii) Negative normalization by the geometric mean of all probes, Positive normalization by the geometric mean of all probes, and Content set normalization adjusted by EVs concentration (obtained by NTA); and (iii) Negative normalization by the geometric mean of all probes, Positive normalization by the geometric mean of all probes, and Content set normalization adjusted for miRNAs with the lowest coefficient of variation (top15 stable regions). Data were exported in comma-separated value (*.csv) format for further analysis. The classification characteristics of these preprocessing protocols were evaluated using principal component analysis (PCA).

3.23 Breast cancer cell lines

We cultured cell lines for four main subtypes of breast cancer (Luminal A, Luminal B, HER2+, and Triple-negative) using standard conditions (37 °C in an atmosphere of 5% CO_2) up to obtain at least 7.9 x 10^5 cells. T-47D, HCC70, MDA-MB-468, MDA-MB-231, ZR-75, and SK-BR-3 cell lines were grown and maintained in RPMI-1640 medium (ThermoFischer Scientific) containing 10% fetal bovine serum (FBS, ThermoFischer Scientific). Hs578T cell line was grown and maintained in Dulbecco's modified Eagle medium (DMEM, Thermo Fischer Scientific) containing 10% fetal bovine serum (FBS). MCF-7 cell line was grown and maintained in Dulbecco's modified Eagle medium/Nutrient mixture F12 (DMEM/F12, ThermoFischer Scientific) containing 10% fetal bovine serum (FBS). We monitored cell grown by microscopy observation and use a sterile cell scraper (cat. 3010, StemCell) to harvest cells when required. For subculture and further experiments, cells were collected by centrifugation at 180xg for five

minutes and resuspend in proper medium (for subculture) or Phosphate-Buffered Saline (PBS) free of Ca2+ and Mg2+ pH 7.4 for further experiments. The quantification of breast cancer cells was performed using a Neubauer chamber with cells previously stained with Trypan blue 1:1. All cell lines were frequently tested for mycoplasma infection. Only aliquots with negative results for the mycoplasma infection were used in experiments.

3.24 Selection of Jacalin lectin-positive cells

Breast cancer cells (~$8x10^5$ cells/mL) were combined with 10 µg of biotinylated Jacalin lectin (cat. B-1155-5. Vector Labs) and incubated in a cold room at 4 °C for 10 minutes, under gentle agitation (Tube Shaker, LabQuake®). Cells were centrifuged at 400xg and added to $1x10^7$streptavidin-coupled magnetic beads (cat. 11047. ThermoFisher Scientific) previously resuspended in the standard isolation buffer composed by Bovine Serum Albumin (BSA) 0.1% and 2mM EDTA in PBS pH 7.4. The mix was incubated in a cold room at 4 °C for 20 minutes with gentle agitation. Then, we used a magnetic stand to attract Jacalin-bound magnetic beads with cells and wash twice them with the isolation buffer. Jacalin-positive cells were recuperated in PBS pH 7.4 to be quantified using a Neubauer chamber.

3.25 Removal of Jacalin lectin labeling in cells

Once Jacalin-positive cells were selected using magnetic beads, we use D-galactose (a primary sugar for Jacalin) to elute these cells. We added galactose to Jacalin-bound cells to obtain final concentrations of 50, 100, or 200 mM. Then, each mix was incubated in a cold room at 4 °C for 1 hour with gentle agitation. After, we used the magnetic stand to attract the beads and recuperate the selected cells from the supernatant. Selected cells were quantified again by Neubauer's cytometry.

3.26 Lectin histochemistry of FFPE tissues

FFPE tissue was sliced (3 µm thick), heated in dry at 60 °C for one hour, and deparaffinized. Then, we treated tumor slices with hydrogen peroxide 3% in

methanol to blockade endogenous peroxidase for 25 minutes at room temperature, and then we washed three times with PBS pH 7.4. No antigen retrieval was performed. We treated the slices with Tris-buffered saline (TBS) solution added with 5% or 10% of BSA for one hour to blockade nonspecific proteins with posterior washing with PBS pH 7.4. We have tested two concentrations of biotinylated Jacalin lectin: 4 ng/ µL (1:1250), 20 ng/ µL (1:250), and 100 ng/µL (1:50) by incubation for one and a half hours at room temperature and washed with PBS pH7.4. After, we incubated samples with 1:250 streptavidin-HRP (horseradish peroxidase) reagent (cat. SA1007, ThermoFisher Scientific) for one hour at 37 °C, and washed them with a PBS pH 7.4 solution. The slices were treated with a DAB (3, 3 –diaminobenzidine) substrate kit (cat. 550880, BD Biosciences) according to the manufacturer conditions (incubation at room temperature for 30 seconds). Finally, we performed a hematoxylin staining for one and a half minutes and mounted the slice on a glass slide properly identified.

3.27 Dot blot of plasma and EV samples with Jacalin

A section of a nitrocellulose membrane 0.45 µm (cat. 88018. ThermoFisher Scientific) was hydrated with PBS pH 7.4 and mounted in a Hybri-dot manifold (cat. 1050MM. Bethesda Research). Then we washed all wells with 200 µL of Tris-buffered saline (TBS) pH 7.4 solution. After that, we loaded up to 5 µL of serial dilutions of human plasma (Pl), EV-depleted plasma, EVs (ePl), TBS (Tris-buffered saline solution as negative control), and asialofetuin (AS, positive control for Jacalin) (cat. 11210238001. Roche) in the membrane. Then proteins were transferred to the membrane by the gravity principle for one hour. Later, we incubated the membrane with TBS with 0.1% Tween® 20 detergent (TBST) supplemented with 2.5% Bovine Serum Albumin (BSA) for 40 minutes with gentle agitation in a rocking shaker (cat. OSC12, ARSEC). We washed the membrane with TBST three times and then incubated it with 20 ng/µL of biotinylated Jacalin in TBST for 40 minutes under gentle agitation. Again, we washed the membrane and incubated it with streptavidin-HRPO 1:5000 (cat. SA1007, ThermoFisher Scientific) for 40 minutes with gentle agitation. Finally, we washed the membrane and used Amersham ECL Western Blotting

Detection Reagent (cat. RPN2109. GE Healthcare) and/or Amersham ECL Prime Western Blotting Detection Reagent (cat. RPN2232. GE Healthcare) for jacalin detection according to the manufacturer's recommendations. Chemiluminescent figures were acquired using the ImageQuant™ LAS 4000 equipment (GE Healthcare).

3.28 Selection of Jacalin lectin-positive EVs

Plasma EVs were combined with 10 µg of biotinylated Jacalin lectin (cat. B-1155-5. Vector Labs) and incubated at 4 °C for 1 hour, under gentle agitation (Tube Shaker, LabQuake®). Then, $1x10^7$ streptavidin-coupled magnetic beads (cat. 11047. ThermoFisher Scientific) were added. The mix was incubated at 4 °C for 40 minutes with gentle agitation. Next, we used a MagnaRack magnetic stand (cat. CS15000, ThermoFisher) for the recovery of jacalin positive EVs or cells. Samples were washed twice with PBS and, afterward, we tested D-galactose as a primary sugar for Jacalin to dissolve the interaction between Jacalin and derivatives of the Tn antigen. We added galactose to Jacalin-bound EVs up to 30 or 300 mM of D-galactose. Each mix was incubated at 4 °C for 1 hour with gentle agitation (Tube Shaker, LabQuake®). Finally, we used the magnetic stand to attach the magnetic beads releasing the previously selected EVs on the supernatant.

3.29 Statistical Analyses

Regarding the sample size and statistical power, we defined two cohorts based on convenience sampling that intend to include all immunohistochemical BC subtypes reported in our Institute using the biobank cohort. Due to the nature of the study, regarding their exploratory aim to analyze miRNAs and the proof-of-concept of selecting tumor-derived EVs, we defined at least one of these two cohorts to run specific experiments, as shown in Figure 9.

We used the Kruskal-Wallis test to evaluate the distribution of our data. After finding that our data did not follow a normal distribution, the Wilcoxon test was used to analyze mean differences between two paired groups, the Mann-Whitney test was used to evaluate mean differences between two unpaired groups, the Kruskal-Wallis test was used to analyze differences between more

than two groups, and Spearman's test was used to assess the correlation between values. For multiple comparisons, we used the False Discovery Rate (FDR) method to adjust p-values. Regarding the exploratory nature of this study, no region was excluded from the analysis, not even due to its low expression. All significant comparisons were $p<0.05$. For the p-based determination of putative markers, a fold change (FC) greater than two was set for choosing relevant regions.

Heatmaps with grouped data from nCounter experiments were plotted using the nSolver™ Data Analysis v.4.0 software (NanoString® Technologies). To calculate the distance between two samples (or two groups of samples) in dendrograms, we estimated the Euclidean distance by calculating the square root of the sum of squared differences of their count values. Other statistical analyses, heatmaps, survival plots, scatter plots, and violin plots were built on the R software v.4.3.1 and GraphPad Prism v8 for Windows.

3.30 Data Availability and Transparent Reporting

Regarding high-throughput experiments, raw and pre-processed data of cf-miRNA samples were deposited to the Gene Expression Omnibus (GEO) database under accession GSE240872 (Appendix 3), whereas vesicular miRNA data was submitted under accessions GSE241784 (Appendix 4) and GSE241785 (Appendix 5). All videos for NTA analysis of Jacalin-positive EVs and 3D representations of density plots for selection of relevant miRNAs between BC subtypes and age-related groups are stored in the figshare repository: https://figshare.com/projects/cf-miRNA_EV-miRNA_and_EVs_from_BC_patients/176259. Individual DOI links are given in each corresponding 2D snapshot.

We have submitted all relevant data of our experiments to the EV-TRACK knowledgebase (EV-TRACK ID: EV230978) [124]. This thesis is in agreement with the European Society for Medical Oncology (ESMO) Guidance for Reporting Oncology real-World evidence (GROW) [125] by the checklist in Appendix 6 and the Minimal Information for Blood EV research (MIBlood-EV) [126] by the Appendix 7.

4. RESULTS AND DISCUSSION

4.1 Study cohorts

We selected groups of patients to be independently analyzed according to specific questions during this thesis. We avoided including any sample in the two cohorts to reduce potential bias in experimental observations. For cohorts A and B, patients were classified according to their age at diagnosis as young (diagnosed before 40 years old) or elderly (diagnosed after 40 years old) patients.

Table 1 shows a summary of the clinical and self-reported characteristics of patients in cohorts A and B. A detailed description of these cohorts is provided in Appendix 1and Appendix 2.

Table 1. Summary of patient characteristics for Cohorts A and B.

Characteristic	**Cohort A**, N = 30[1]	**Cohort B**, N = 24[1]	**p-value**[2]
Group (IHC and age at diagnosis)			0.042
Elderly (late onset) HER2	1 / 30 (3.3%)	0 / 24 (0%)	
Elderly (late onset) Luminal A	3 / 30 (10%)	0 / 24 (0%)	
Elderly (late onset) Luminal B	3 / 30 (10%)	0 / 24 (0%)	
Elderly (late onset) Luminal HER2	3 / 30 (10%)	0 / 24 (0%)	
Elderly (late onset) TNBC	6 / 30 (20%)	6 / 24 (25%)	
Young (early onset) HER2	2 / 30 (6.7%)	0 / 24 (0%)	
Young (early onset) Luminal A	0 / 30 (0%)	4 / 24 (17%)	
Young (early onset) Luminal B	3 / 30 (10%)	6 / 24 (25%)	
Young (early onset) Luminal HER2	3 / 30 (10%)	4 / 24 (17%)	
Young (early onset) TNBC	6 / 30 (20%)	4 / 24 (17%)	
Age at admission to the biobank	47 (25-79)	40 (26-67)	0.3
Self-reported race			0.14
White	13 / 30 (43%)	10 / 24 (42%)	
Black	2 / 30 (6.7%)	6 / 24 (25%)	
Other	1 / 30 (3.3%)	2 / 24 (8.3%)	
Brown	14 / 30 (47%)	6 / 24 (25%)	

BMI	28 (18-40)	38 (19-80)	0.2
T			0.7
T1	4 / 26 (15%)	5 / 22 (23%)	
T2	8 / 26 (31%)	8 / 22 (36%)	
T3	8 / 26 (31%)	7 / 22 (32%)	
T4	5 / 26 (19%)	1 / 22 (4.5%)	
Tis	1 / 26 (3.8%)	1 / 22 (4.5%)	
Unknown	4	2	
N			0.2
N0	8 / 26 (31%)	11 / 22 (50%)	
N1	14 / 26 (54%)	6 / 22 (27%)	
N2	2 / 26 (7.7%)	4 / 22 (18%)	
N3	2 / 26 (7.7%)	1 / 22 (4.5%)	
Unknown	4	2	
M			0.2
M0	25 / 25 (100%)	20 / 22 (91%)	
M1	0 / 25 (0%)	2 / 22 (9.1%)	
Unknown	5	2	
Tumor Relapse			0.5
No	14 / 19 (74%)	20 / 24 (83%)	
Yes	5 / 19 (26%)	4 / 24 (17%)	
Unknown	11	0	

[1] n / N (%); Mean (Minimum-Maximum)

[2] Fisher's exact test; Wilcoxon rank sum test; Wilcoxon rank sum exact test; Pearson's Chi-squared test

BMI: Body-Mass Index, IHC: Immunohistochemistry, TNM Classification 8th edition.

4.1.1 Cohort A

This cohort was used for comparing miRNA expression levels in both forms (cf-miRNA and EV-miRNA) between BC immunohistochemical subtypes and age-related groups. It is composed by 30 samples distributed between the following immunohistochemical subtypes: Luminal A (n=3), Luminal B (n=6), Luminal HER2 (n=6), HER2 (n=3), and Triple-negative Breast Cancer (TNBC, n=12). A summary of their clinical and pathological features is described in Appendix 1.

We aimed to use this group of samples as a discovery cohort involving a pooling strategy. Due to this, we selected patients with similar characteristics for sex, self-reported race, education levels, body mass index (BMI), nutritional status, physical activity, drug use, smoking, alcohol use, Diabetes Mellitus, High Blood Pressure (HBP), Chronic Obstructive Pulmonary Disease (COPD), and Chronic Gastritis ($p>0.05$), since many of these conditions have been indicated as potential modulators of the cell-free or vesicular miRNAs [119,127–133]. Then, we aimed to avoid potential biological or clinical interferences in our results. In addition, none of these patients received any treatment before blood collection.

Regarding the family history of cancer, though potential genetic contributions (i.e., contribution of hereditary genes) are associated with patients diagnosed before 40 years [134–136], we focused on patients with less genetic impact (known hereditary cancer syndrome criteria). Furthermore, we selected a cohort of patients with no family history of breast and ovarian cancer in the first degree of kinship.

Regarding pathologic features, we intended to collect a group of patients with similar stages of the disease. As shown in Appendix 1, this selection was primarily diagnosed with early stages of the disease. Also, most of these cases have not presented tumor relapse during the follow-up of this study (1.4-87.4 months).

4.1.2 Cohort B

This cohort was used to (i) evaluate vesicular miRNA quantification profiles, (ii) test strategies for isolating extracellular vesicles, and (iii) test labeling of Tn antigen derivatives in plasma and tissue sections. It is composed by 24 samples distributed between the following immunohistochemical subtypes: Luminal A (n=4), Luminal B (n=6), Luminal HER2 (n=4), and Triple-negative Breast Cancer (TNBC, n=10). A summary of their clinical and pathological features is described in Appendix 2.

Our goal was to use this group of samples as a cohort to compare one individual per sample (not in a pooling strategy). Though we do not have control of many clinical and pathological factors, we selected patients with similar characteristics for self-reported race, education level, body mass index (BMI), nutritional status, physical activity, drug use, smoking, alcohol use, Diabetes Mellitus, High Blood Pressure (HBP), Chronic Obstructive Pulmonary Disease (COPD), and Chronic Gastritis ($p>0.05$), and reduced the number of missing (unknown) data in comparison with Cohort A.

For Cohort B, we did not include the HER2+ subtype. Though the high relevance of HER2+ BC patients as poor-prognosis individuals, cohort B aims to analyze the TNBC group in the context of young diagnosed BC patients. Due to this, cohort B includes young BC patients of all luminal subtypes (n=14) and TNBC patients (four young TNBC individuals and six elderly TNBC individuals).

In addition, this cohort has different profiles for family history of cancer and reports of treatments before blood collection (Appendix 2). As this cohort involves independent samples, we can include patients with more diverse features since these factors have no statistical differences between groups ($p>0.05$).

4.2 cf-miRNA levels in breast cancer patients

After concentrating cf-miRNA samples for the twelve tubes described for Cohort A, we obtained 4 µL of each sample with a mean cf-miRNA total concentration of 31.11 ng/µL (7.1-61.6 ng/µL, Figure 10A) and quality ratios of 1.37 (1.23-1.76) and 0.16 (0.02-0.93) for 260/280 and 260/230, respectively.

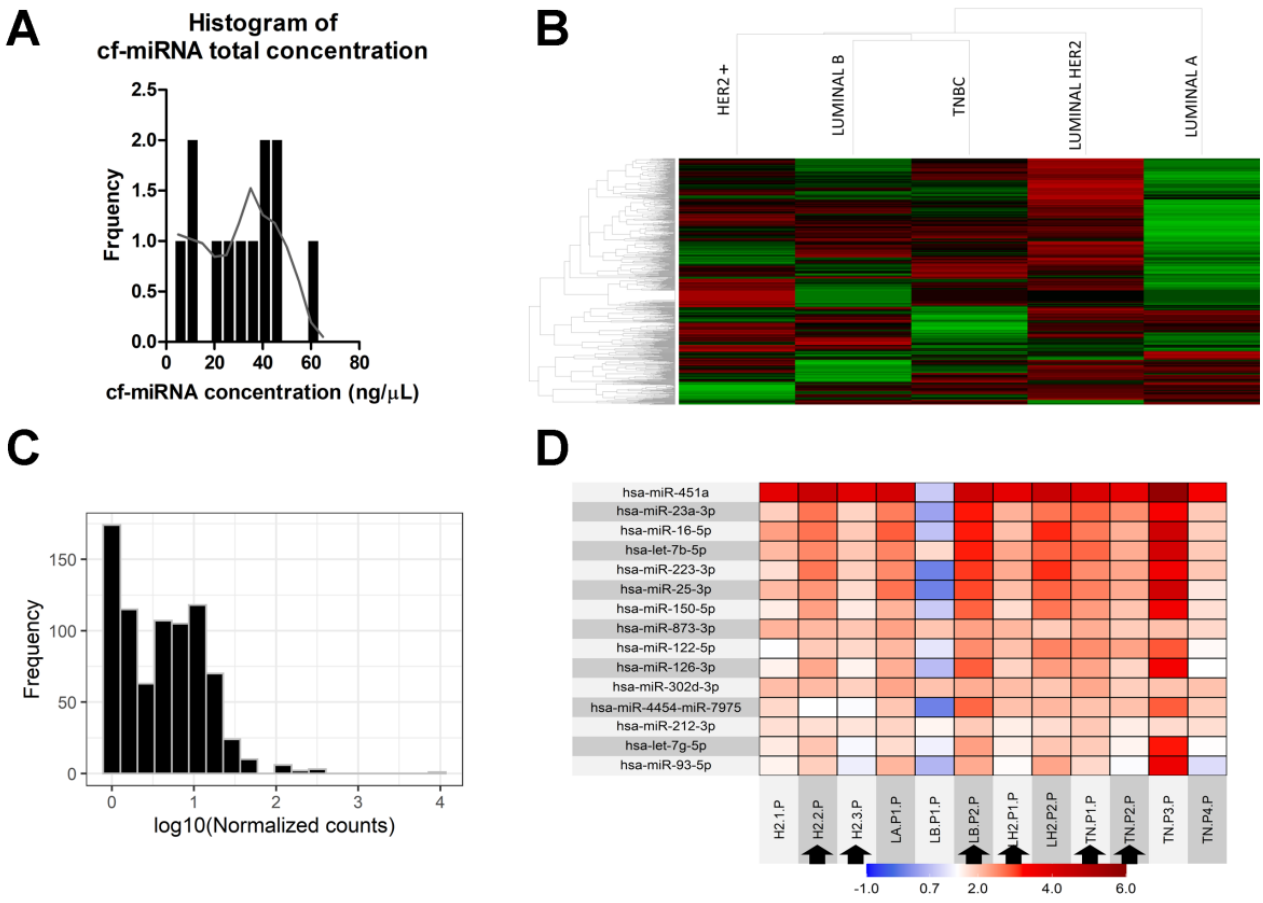

Figure 10. Profile of cf-miRNA in breast cancer patients according to molecular subtypes. (A) Histogram of cf-miRNA total concentration measured by spectrophotometry. Figure built on GraphPad Prism v8 for Windows. (B) Heatmap comparing miRNA levels from five main molecular subtypes included in this study. This panel shows the preliminary profile obtained in the nSolver software. (C) Histogram showing median level expression of evaluated miRNAs. (D) Heatmap showing the top 15 miRNAs expressed in all samples. Black arrows indicate samples from patients diagnosed with breast cancer before 40 years old (Young groups). Figures C and D were built on the R software v.4.3.1. H2: HER2+ subtype, LA: Luminal A subtype, LB: Luminal B subtype, LH2: Luminal HER2 subtype, TN: Triple-Negative

Though the concentration and quality features of the cf-miRNA isolated from our samples are comparable with previous studies in human plasma [64,137,138], we have a limited concentration in one of the samples (7.1 ng/µL). Then, we used it to determine the input mass (~25ng) of miRNA for this nCounter assay.

4.2.1 Top abundant cf-miRNA regions in plasma of BC patients

After verifying that all samples passed the quality parameters of the nSolver system, we ran a heatmap to observe the landscape of cf-miRNA expression between immunohistochemical subtypes (Figure 10B). It is possible to observe different patterns representing all probes in the nCounter system. Nevertheless, it is unlikely that all miRNAs are circulating in a cell-free form in blood of BC patients [139]. Raw and pre-processed data of these samples were deposited to the Gene Expression Omnibus (GEO) database under accession GSE240872 (Appendix 3).

Based on that, by observing the histogram of the mean expression of each miRNA (Figure 10C), we realized that almost 500 (out of 798 probes) have a low expression level (10 or fewer relative units). Then, we plotted the top 15 most highly expressed cf-miRNAs (Figure 10D), which includes hsa-miR-451a, hsa-miR-23a-3p, hsa-miR-16-5p, hsa-let-7b-5p, hsa-miR-223-3p, hsa-miR-25-3p, hsa-miR-150-5p, hsa-miR-873-3p, hsa-miR-122-5p, hsa-miR-126-3p, hsa-miR-302d-3p, hsa-miR-4454/miR-7975, hsa-miR-212-3p, hsa-let-7g-5p, and hsa-miR-93-5p.

Interestingly, almost all samples presented higher levels of hsa-miR-451a in their plasma. This miRNA presented controversial information in the literature regarding their pro- or anti-tumor effect. In cell culture, it was demonstrated that hsa-miR-451a sensitizes breast cancer cells to tamoxifen or carboplatin therapy [140,141] or suppress cancer growth by blocking tumor-promoting genes [142,143]. Nevertheless, some studies have described the presence of higher hsa-miR-451a levels in the plasma of breast or ovarian cancer patients [144–146]. In particular, the study of Emmenegger et al. (2014) used the same platform as this study (nCounter® miRNA expression assay) with further validation by qRT-PCR [142]. Then, Chang et al. (2015) evaluated miRNA

levels in peripheral blood mononuclear cells (PBMC) of breast cancer patients and controls and found the hsa-mir-451a was overexpressed in the patient groups [147].

In addition, the hsa-miR-451a (alone or combined with hsa-miR-23a) has also been indicated as an indicator of hemolysis in plasma samples [148,149]. Plasma samples are sensitive to carrying RNA from other circulating sources, for example, red blood cells and PBMCs. According to Shkurnikov et al. (2016), the hemolysis of ~0.05% of erythrocytes could be enough to alter the levels of hsa-miR-451a [148]. In this study, we took all appropriate care for processing samples, as indicated in the "Plasma samples" and “miRNA isolation” sections. Nevertheless, other factors can potentially participate to get this outcome [150]. We collected six EDTA tubes per patient and used one of the 2^{nd}-6^{th} tubes for this step. Some authors have demonstrated that delayed processing, excessive suction, and prolonged tourniquet could affect hemolysis ratios [150–153]. Then, our protocol is susceptible to this condition, despite this protocol reduces potential contamination with platelets and immune cells [119,120].

Though this potential contamination suggests focusing future research on enveloped circulating structures (p.e. EVs), other cf-miRNAs were most related to cancer-related processes. The hsa-miR-23a-3p was associated with tumor cell motility [154] and G1/S cell cycle transition [155]. The hsa-miR-16-5p was also found in the plasma of lung cancer patients [156] and the milk of mothers of preterm children [157]. Our results found the hsa-let-7b-5p consistently expressed in the plasma of BC patients, independent of their immunohistochemical subtype. This finding is consistent with a previous report on Saudi [158] and Chinese [76] breast cancer females. Interestingly, the hsa-let-7b-5p was included in a logistic regression model to evaluate the presence of elderly breast cancer in pre-diagnostic women by combining miRNA ratios with common characteristics being assessed as body mass index (BMI), menopausal status (MS), the interaction term BMI * MS, lifestyle score and breast density [159].

Moreover, the hsa-miR-223-3p presents some cancer-related features [160–162], indicating that this miRNA could be a candidate to be evaluated in liquid biopsies. It has been demonstrated that this miRNA can be exported in high-density lipoproteins (HDLs), one of the components of plasma cf-miRNA, of

Brazilian breast cancer patients [163]. Also consistent with our results, circulating levels of hsa-miR-25-3p were overexpressed in samples of cancer patients [158,164–166]. In addition, Zhao et al. (2021) determined that this miRNA contributes to breast cancer progression by targeting *TOB1*, a tumor suppressor, transducer of ERBB2 [167].

Other miRNAs abundantly expressed in the plasma of the BC cohort of this thesis have been related to tumor-related features. For example, hsa-miR-150-5p was upregulated in plasma samples of cancer patients [144,168,169]. The hsa- miR-122-5p was included in minimally invasive panels for early detection of breast and gastric cancers [76,170–172]. Then, this miRNA was indicated as key to determining the expression of *ADAM10*, which indirectly affects the HER2 shedding and modulates the effectiveness of Trastuzumab-including treatment schemes [173]. The hsa-miR-4454 was detected in systemic (plasma) or local (urine) liquid biopsy sources of cancer patients [146,174,175]. Though their function is not fully understood, the hsa-miR-212-3p was indicated as a potential biomarker of breast cancer diagnosis or prognosis as this miRNA can be detected in tumors, plasma, and serum samples [176]. Finally, the hsa-let-7g-5p was detected in the serum of cancer patients [177] as well milk of women with Low milk supply (LMS), which represents the potential participation of this miRNA in breast cell reorganization [178].

4.2.2 Differentially expressed cf-miRNAs between BC patients

In addition to commonly expressed cf-miRNAs, we focused on comparing age-related groups and immunohistochemical BC subtypes between these samples analyzing the cf-miRNA profile.

Figure 11 shows differentially expressed cf-miRNAs (p-value<0.01 and fold change >2) between BC groups. This figure aims to show specific signatures according to immunohistochemical subtypes or age-related groups. According to our observations, none of the luminal subtypes (Luminal A, Luminal B, or Luminal HER2) showed relevant differences in the cf-miRNA profile at this statistical level (p<0.01). Interestingly, BC subtypes with poor survival (HER2 and TNBC) showed specific cf-miRNA signatures. Thus, hsa-miR-548ar-3p and hsa-miR-585-3p were down-expressed in the plasma of TNBC patients when

compared with other subtypes (Figure 11A), while hsa-miR-3147, hsa-miR-320e, hsa-miR-497-5p, and hsa-miR-548ai-miR-570-5p characterized patients overexpressing HER2 receptors in their tissues (Figure 11B). In addition, we found that patients diagnosed with BC after 40 years old express higher levels of hsa-miR-95-3p in their plasma (Figure 11C).

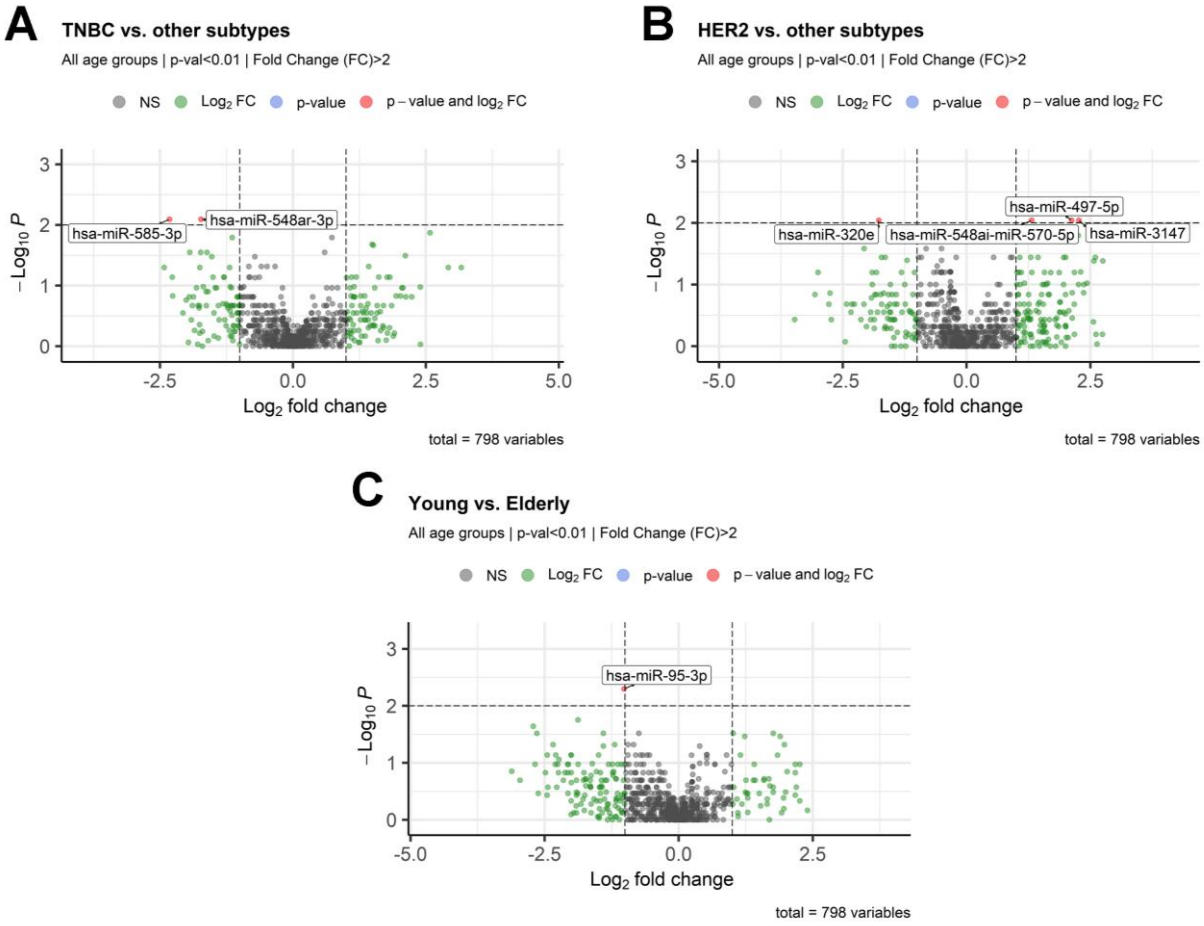

Figure 11. Volcano plots showing differentially expressed cf-miRNAs according to BC subtypes. Comparison between patients belonging to a specific breast cancer group (immunohistochemical subtype or age-related group). (A) Triple-Negative Breast Cancer (TNBC, n=4) vs. other subtypes (n=8). (B) HER2+ subtype (n=3) vs. other subtypes (n=9). (C) Young (n=6) vs. Elderly (n=6) diagnosed cases of breast cancer. Differentially expressed regions were determined by a nominal p-value <0.01 and Fold Change >2. Volcano plots were built on the R software v.4.3.1.

In a comprehensive view of this result, Tables 1-6 show remarkable cf-miRNA regions in our study (not limited to p<0.01 or FC>2). As we have a

limited number of samples in each subtype, we started comparing all patients without age-related classifications inside each subtype. Nevertheless, for each comparison, we ran a descriptive analysis regarding the fold change between BC subtypes in young or elderly patient cohorts. Though we adjusted p-values for multiple comparisons, our observations are based on the nominal p-value since the number of samples can affect the estimation of these p-values and their adjusted values [179,180].

4.2.3 Relevant cf-miRNA regions in TNBC patients

Table 2 shows differentially expressed cf-miRNAs ($p<0.05$) between TNBC patients and BC patients with other subtypes (Luminal A, Luminal B, Luminal HER2, and HER2+). The hsa-miR-548ar-3p was studied in the breast tumor context, and it was found that high levels of this miRNA are related to apoptosis induction by targeting *NEAT1* [181]. The hsa-miR-585-3p levels were previously analyzed in tissues of TNBC patients (not classified by age at diagnosis) to describe a correlation between low levels of hsa-miR-585-3p and poor prognosis [182].

In addition to hsa-miR-548ar-3p and hsa-miR-585-3p, we observed almost 20 cf-miRNAs characterizing the TNBC subtype when we included all patients in this study. From this group of cf-miRNA candidates, some have been directly studied in breast cancer plasma samples in a cell-free (not vesicular) approach. The hsa-miR-571 was observed in BC patients diagnosed at early stages [183] and as a response to chemotherapy schemes [184]. The hsa-miR-197-3p was found in the serum of BC patients [185,186] and showed treatment response prediction features in plasma [187].

About hsa-miR-381-3p, it was demonstrated that their downregulation can exacerbate breast tumors [188] and their lower levels in plasma can be a sign of gynecological disorders such as endometriosis [189]. A previous study reported that hsa-miR-887-5p is usually downregulated in serum samples of Luminal A/HER2 BC patients compared with healthy individuals [166]. Then, Haakensen et al. (2016) reported lower levels of this miRNA in TNBC patients [190]. Though the present thesis did not include healthy individuals for this analysis, the TNBC cohort presented lower hsa-miR-887-5p levels than Luminal

subtypes, which can support the inclusion of hsa-miR-887-5p in prognosis panels. In addition, hsa-miR-887-5p has been indicated as a promising biomarker for drug resistance in breast and ovarian cancers [191,192]. Finally, the hsa-miR-505-3p has been identified as a circulating biomarker for early diagnosis of BC [193,194], it is downregulated in Luminal BC samples [190], and this miRNA exerts its function through inhibition of the *RUNX2* expression [195].

Table 2. Differentially expressed cf-miRNAs ($p<0.05$) between TNBC (n=4) and other BC subtypes (n=8)

miRNA	Relative expression in the TNBC subtype (n=4)	Relative expression in other BC subtypes (n=8)	Log_2 Fold Change (TNBC/others)	p-value	Adjusted p-value
hsa-miR-548ar-3p	1.73	5.72	-1.73	0.008	1.00
hsa-miR-585-3p	1.35	6.72	-2.32	0.008	1.00
hsa-miR-219a-2-3p	6.87	1.15	2.58	0.013	1.00
hsa-miR-3690	10.95	6.59	0.73	0.016	1.00
hsa-miR-4536-5p	10.14	22.36	-1.14	0.016	1.00
hsa-miR-561-3p	3.03	1.08	1.49	0.021	1.00
hsa-miR-571	3.28	1.15	1.51	0.022	1.00
hsa-miR-10a-5p	9.67	6.39	0.60	0.028	1.00
hsa-miR-197-3p	1.35	4.12	-1.62	0.028	1.00
hsa-miR-381-3p	1.29	4.93	-1.94	0.028	1.00
hsa-miR-887-5p	2.31	7.67	-1.73	0.028	1.00
hsa-miR-505-3p	4.81	1.11	2.11	0.032	1.00
hsa-miR-5196-3p-miR-6732-3p	1.08	1.77	-0.72	0.033	1.00
hsa-miR-548m	1.08	3.10	-1.53	0.033	1.00
hsa-miR-203a-5p	19.57	24.69	-0.33	0.048	1.00
hsa-miR-2113	5.48	2.04	1.42	0.048	1.00
hsa-miR-365a-3p-miR-365b-3p	9.49	13.29	-0.49	0.048	1.00
hsa-miR-3928-3p	9.48	14.32	-0.59	0.048	1.00
hsa-miR-4707-3p	9.49	16.87	-0.83	0.048	1.00

BC: breast cancer; TNBC: Triple-negative breast cancer
P-values were obtained using the Mann-Whitney test and adjusted with the False Discovery Rate (FDR) method. Bold miRNAs indicate absolute fold change values higher than 2.

After observing the main profile of differentially expressed cf-miRNAs in TNBC patients, we evaluated these potential differences in the young

diagnosed BC cohort. However, the analysis between young diagnosed individuals cannot be analyzed based on their p-value due to the number of individuals (two TNBC patients vs. four patients with other BC subtypes).

Herein, Figure 12 shows a density plot comparing the abundance of each probe (x-axis) related to the fold change obtained between their expression in young diagnosed TNBC patients and young diagnosed BC patients with other BC subtypes (y-axis). In this graph, we labeled the top 1% of miRNA probes with higher fold change (FC) between TNBC and other subtypes in young diagnosed patients as well as miRNA probes showing a balance between median abundance in all analyzed samples (top 20%) and higher FC (top 20%). Remarkably, several miRNA probes presented lower FC or lower general expression (Figure 12).

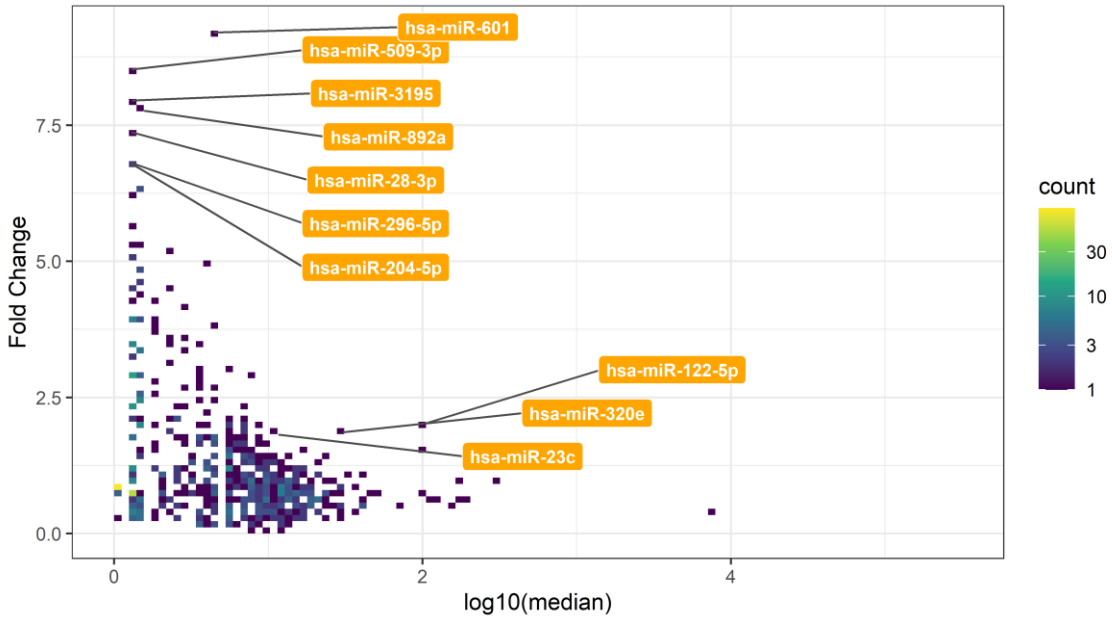

Figure 12. Relevant cf-miRNAs in young diagnosed TNBC patients. This density plot shows all miRNA probes scanned in the Nanostring platform comparing Fold Change between TNBC (n=2) vs. other BC subtypes (n=4) in young diagnosed individuals (y-axis) in comparison with their median expression (log10) in all young diagnosed individuals (x-axis). Labeled miRNA fulfill some of these conditions: i) top 1% of Fold Change or ii) top 20% of Fold Change and top 20% of median abundance. Figure built on the R software v.4.3.1. The 3D representation of this plot can be accessed here: https://doi.org/10.6084/m9.figshare.24002067

In addition to miRNAs presented in Table 2, Figure 12 shows a list of relevant cf-miRNA that includes hsa-miR-122-5p, hsa-miR-204-5p, hsa-miR-23c, hsa-miR-28-3p, hsa-miR-296-5p, hsa-miR-3195, hsa-miR-320e, hsa-miR-509-3p, hsa-miR-601, and hsa-miR-892a.

Despite hsa-miR-122-5p, hsa-miR-23c, or hsa-miR-320e have not the highest fold change values, they are more likely to be detected in less sensitive techniques such as quantitative real-time polymerase chain reaction (qRT-PCR). In particular, the hsa-miR-122-5p has been identified in liquid biopsies of BC patients, especially in more aggressive subtypes and models [76,144,196,197]. Interestingly, Gallo et al. (2022) demonstrated that mesenchymal stem cells (MSCs) export hsa-miR-23c which seems to control the growth of TNBC cells [198]. Although the hypothesis that MSCs express hsa-miR-23c and this miRNA can reach the bloodstream is valid, it is somewhat difficult to define whether the miRNA present in plasma comes from MSCs or tumor cells, complicating diagnostic approaches of this putative biomarker.

4.2.4 Relevant cf-miRNA regions in HER2+ BC patients

Table 3 shows differentially expressed cf-miRNAs ($p<0.05$) between HER2+ patients and BC patients with other subtypes (Luminal A, Luminal B, Luminal HER2, and TNBC). In addition to cf-miRNAs identified in Figure 5B (hsa-miR-3147, hsa-miR-320e, hsa-miR-497-5p, and hsa-miR-548ai-miR-570-5p, $p<0.01$), we observed 28 cf-miRNA regions dysregulated in the HER2+ BC cohort. Interestingly, hsa-miR-585-3p and hsa-miR-571 appear in this comparison besides in Table 2 (TNBC vs. other BC subtypes). However, they follow different expression patterns according to each BC subtype. While hsa-miR-571 was downregulated in HER2+ and upregulated in TNBC subtypes, hsa-miR-585-3p was upregulated in HER2+ and downregulated in TNBC samples.

Among other remarkable miRNAs, circulating hsa-miR-3147 was proven to predict lymph node metastasis in patients with early-stage cervical squamous cell carcinoma [199]. The hsa-miR-497-5p was indicated as a contributor to the immune evasion of breast cancer cells by targeting *CD274* [200], and independent studies suggested targeting this miRNA as a novel strategy to treat

breast and ovarian cancers [201,202]. Then, another study involving nCounter technology for evaluating circulating miRNA of advanced BC patients determined that hsa-miR-548ai contributes to the treatment response prediction [144]. About hsa-miR-1271-5p, different levels of this miRNA were found in BC subtypes in Brazilian patients, and the HER2+ subtype showed the most homogeneous values [203]. Then, the circulating version of hsa-miR-1271-5p was proposed as a biomarker for predicting the BC patient's response to letrozole [204] and diagnosing patients with endometriosis [205].

Consistent with our results, Chan et al. (2013) described the overexpression of hsa-miR-4284 in HER2+ BC patients [206]. This miRNA has been reported as a plasma biomarker of gynecological conditions such as endometriosis or endometriosis-associated ovarian cancer [207]. Then, hsa-miR-4647 was identified as a miRNA associated with more aggressive subtypes of BC [208] and recognized as a circulating biomarker [209]. Same as hsa-miR-136-5p, previously described as a circulating marker differentiating BC cases of patients with in situ carcinomas or healthy individuals [210] despite other authors having presented controversial results [211].

The hsa-miR-376a has been identified as a potential circulating biomarker of BC diagnosis and treatment response [187,212], especially in young-diagnosed patients [213] or cases detected at early-stages [183]. Another member of the miR-376 family, hsa-miR-376c-5p, was found elevated in the plasma of BC patients [183,212,214,215], especially in those with poor prognosis [214,215].

Finally, hsa-miR-382-3p [216–219], hsa-miR-605-5p [220], hsa-miR-675-5p [221–223], and hsa-miR-589 [224] were found overexpressed in serum/plasma of BC samples. In addition, Muller et al. (2019) described an interplay between miRNA and long non-coding (lncRNA) in breast cancer by proposing different proportions of plasma levels of H19/miR-675 in different BC subtypes [222]. Moreover, the hsa-miR-140-5p, found at low levels in the plasma of HER2+ BC patients in this study, was identified as responsible for suppressing the BC glycolysis by targeting *GLUT1* [225], and found in higher concentration in plasma of young BC patients [213].

Interestingly, the study of Zhao et al. (2010) found higher levels of hsa-miR-589-5p in the plasma of Caucasian Americans diagnosed with BC [224], differently from the African American BC cohort included in that study. Studies

such as this by Zhao et al. (2010) show the possibility that different ancestry groups affect miRNA levels in body fluids, even in the context of cancer, suggesting that more biological factors might be considered in sample selection for high throughput analysis based on circulating material. Though we did not include molecular ancestry identification for patients in the present thesis, we intended to compare samples with similar self-reported race information (p-value =0.3, Appendix 1) to mitigate the interference of non-cancer factors in our results.

However, we observed that the cf-miRNA content is highly variable due to the various sources that can export material into the bloodstream and subsequently into human plasma [226,227]. As we evaluated this for patients with TNBC, we refined the comparative analysis by focusing on young patients diagnosed with HER2+ BC (Figure 13). Nevertheless, we found a different set of relevant cf-miRNAs than Table 3. This result shows different patterns of segregated cellular components in the bloodstream, even according to the age of patients, which can complicate the standardized determination of potential biomarkers based on cf-miRNAs.

In a descriptive approach of the HER2+ versus other BC subtypes comparison, we observed that young patients overexpressing HER2 receptors in tumor tissue presented higher ratios (fold change> 5) of hsa-miR-3605-3p, hsa-miR-32-5p, hsa-miR-513b-5p, hsa-miR-193a-5p/hsa-miR-193b-5p, hsa-miR-3161, hsa-miR-1272, hsa-miR-523-3p, and hsa-miR-6511a-3p cf-miRNAs.

In addition, some cf-miRNAs were marked by their relatively high fold change and median abundance. This list includes hsa-miR-144-3p, hsa-miR-5001-5p, hsa-miR-451a, hsa-miR-4286, hsa-miR-424-5p, hsa-miR-548j-3p, hsa-miR-3928-3p, and hsa-miR-196a-5p. It is worth mentioning that hsa-miR-451a and hsa-miR-144-3p, present remarkable rations between HER2+ and other young diagnosed BC patients (above 2.5) with a median expression higher than 20 relative units. As described before, the hsa-miR-451a miRNA is used as a sensor of hemolysis [148,149]. However, this cf-miRNA may also show a role in cancer communication [142,144–147]. In this context, circulating miRNAs could be targets for testing this hypothesis since cell-free miRNAs are provided from different sources, which include the tumor itself and anti- and pro-tumor surrounding cells [226,227].

Table 3. Differentially expressed cf-miRNAs ($p<0.05$) between HER2+ (n=3) and other BC subtypes (n=9)

miRNA	Relative expression in the HER2+ BC subtype (n=3)	Relative expression in other BC subtypes (n=9)	Log_2 Fold Change (HER2+/others)	p-value	Adjusted p-value
hsa-miR-3147	12.48	2.59	2.27	0.009	0.85
hsa-miR-320e	15.7	53.7	-1.77	0.009	0.85
hsa-miR-497-5p	5.53	1.27	2.12	0.009	0.85
hsa-miR-548ai-miR-570-5p	12.48	5.01	1.32	0.009	0.85
hsa-miR-1271-5p	4.58	1.19	1.94	0.016	0.85
hsa-miR-135b-5p	5.69	1.19	2.26	0.016	0.85
hsa-miR-4284	3.62	1.19	1.61	0.016	0.85
hsa-miR-6720-3p	1	5.11	-2.35	0.016	0.85
hsa-miR-1249-3p	2.37	1.25	0.92	0.018	0.85
hsa-miR-379-5p	9.26	13.12	-0.50	0.018	0.85
hsa-miR-4647	5.23	1.42	1.88	0.018	0.85
hsa-miR-3195	1	4.2	-2.07	0.026	0.85
hsa-miR-571	1	1.76	-0.82	0.026	0.85
hsa-miR-642a-3p	1	1.42	-0.51	0.026	0.85
hsa-miR-136-5p	1.26	4.15	-1.72	0.036	0.85
hsa-miR-1972	14.55	16.81	-0.21	0.036	0.85
hsa-miR-376a-2-5p	10.08	4.1	1.30	0.036	0.85
hsa-miR-376c-5p	5.69	1.42	2.00	0.036	0.85
hsa-miR-382-3p	9.17	1.51	2.60	0.036	0.85
hsa-miR-487a-3p	2.37	1.25	0.92	0.036	0.85
hsa-miR-512-5p	17.35	9.38	0.89	0.036	0.85
hsa-miR-548q	4.58	14.31	-1.64	0.036	0.85
hsa-miR-585-3p	7.35	2.7	1.44	0.036	0.85
hsa-miR-605-5p	7.35	3.49	1.07	0.036	0.85
hsa-miR-675-5p	5.53	1.42	1.96	0.036	0.85
hsa-miR-758-5p	2.37	4.64	-0.97	0.036	0.85
hsa-miR-769-5p	5.69	10.72	-0.91	0.036	0.85
hsa-miR-770-5p	10.87	7.44	0.55	0.036	0.85
hsa-miR-140-5p	1	2.3	-1.20	0.041	0.85
hsa-miR-548i	1	1.42	-0.51	0.041	0.85
hsa-miR-153-3p	9.17	1.36	2.75	0.042	0.85
hsa-miR-589-5p	8.45	1.42	2.57	0.042	0.85

BC: breast cancer

P-values were obtained using the Mann-Whitney test and adjusted with the False Discovery Rate (FDR) method. Bold miRNAs indicate absolute fold change values higher than 2.

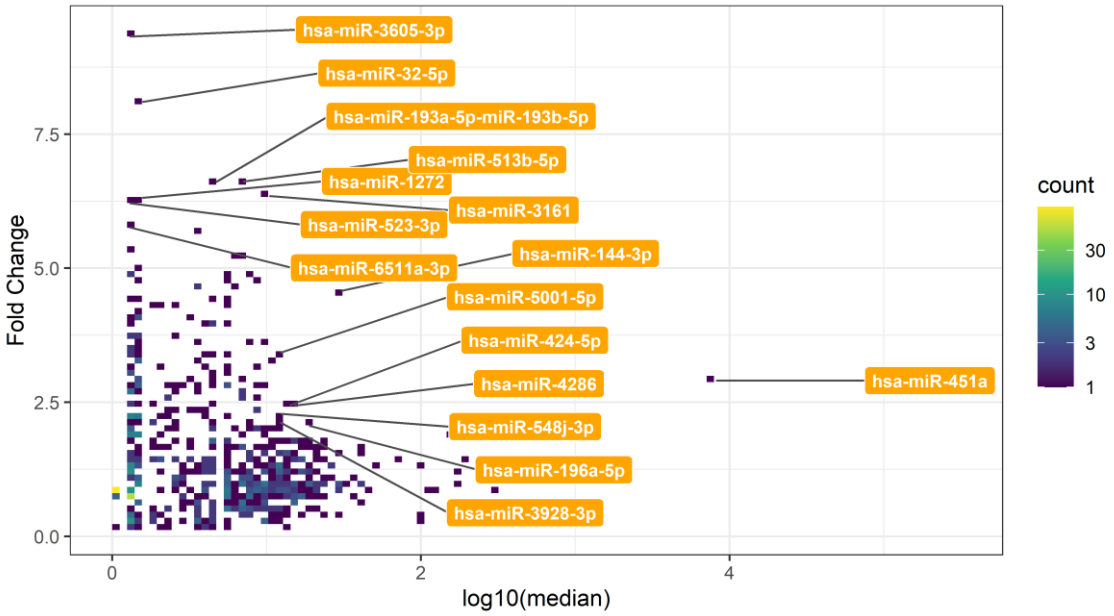

Figure 13. Relevant cf-miRNAs in young diagnosed HER2+ BC patients. This density plot shows all miRNA probes scanned in the Nanostring platform comparing Fold Change between HER2+ (n=2) vs. other BC subtypes (n=4) in young diagnosed individuals (y-axis) in comparison with their median expression (log10) in all young diagnosed individuals (x-axis). Labeled miRNA fulfill some of these conditions: i) top 1% of Fold Change or ii) top 20% of Fold Change and top 20% of median abundance. Figure built on the R software v.4.3.1. The 3D representation of this plot can be accessed here:
https://doi.org/10.6084/m9.figshare.24021006

Then, controversial results were published about the expression level of hsa-miR-144-3p in plasma samples of BC patients [228–232], but it has been recognized as a prognosis circulating biomarker for metastatic BC [147,230,231]. In addition, it was demonstrated that hsa-miR-144 regulates breast cancer progression via targeting *CEP55* [233].

4.2.5 Relevant cf-miRNA regions in Luminal BC patients

Regarding that Luminal (A, B, and HER2) subtypes are most responsive to treatment schemes or show a better survival [234–237], we found a highly diverse set of markers (for Luminal B or HER2) or no significant regions (for Luminal A), and then we only described our main findings in this section.

We only included one pool of Luminal A patients diagnosed before 40 years old in this cohort (Appendix 1). Then, we did not observe any cf-miRNA differentially expressed, but Table 4 presents the top 15 cf-miRNAs with higher ratios between Luminal A and other BC subtypes. This list includes hsa-miR-323a-5p, hsa-miR-510-3p, hsa-miR-190a-3p, hsa-miR-1178-3p, hsa-miR-125a-5p, hsa-miR-502-3p, hsa-miR-412-3p, hsa-miR-362-5p, hsa-let-7f-5p, hsa-miR-19a-3p, hsa-miR-6511a-3p, hsa-miR-124-3p, hsa-miR-3180-3p, hsa-miR-208a-3p, and hsa-miR-1233-3p cf-miRNAs that show fold change values between 7.93-16.94. It is important to note that none of these miRNAs were described in the previous comparisons against a specific subtype in all patients (Table 2 and Table 3).

Table 4. Top 15 cf-miRNAs between Luminal A (n=1) and other BC subtypes (n=11)

miRNA	Relative expression in the Luminal A subtype (n=1)	Relative expression in other BC subtypes (n=11)	Log_2 Fold Change (LumA/others)	p-value	Adjusted p-value
hsa-miR-323a-5p	20.16	1.19	4.08	0.145	0.96
hsa-miR-510-3p	16.58	1.25	3.73	0.147	0.96
hsa-miR-190a-3p	16.58	1.25	3.73	0.167	0.96
hsa-miR-1178-3p	16.58	1.25	3.73	0.246	0.96
hsa-miR-125a-5p	15.39	1.25	3.62	0.140	0.96
hsa-miR-502-3p	17.77	1.51	3.56	0.167	0.96
hsa-miR-412-3p	11.82	1.11	3.41	0.140	0.96
hsa-miR-362-5p	11.82	1.25	3.24	0.147	0.96
hsa-let-7f-5p	11.82	1.27	3.22	0.147	0.96
hsa-miR-19a-3p	13.01	1.42	3.20	0.560	0.96
hsa-miR-6511a-3p	10.63	1.25	3.09	0.238	0.96
hsa-miR-124-3p	11.82	1.42	3.06	0.147	0.96
hsa-miR-3180-3p	9.44	1.15	3.04	0.140	0.96
hsa-miR-208a-3p	18.97	2.34	3.02	0.147	0.96
hsa-miR-1233-3p	9.44	1.19	2.99	0.145	0.96

BC: breast cancer; LumA: Luminal A
P-values were obtained using the Mann-Whitney test and adjusted with the False Discovery Rate (FDR) method. Bold miRNAs indicate absolute fold change values higher than 2.

Luminal B samples showed 12 cf-miRNAs differentially expressed ($p<0.05$). This list includes hsa-miR-1254, hsa-miR-1827, hsa-miR-23c, hsa-miR-298, hsa-miR-301a-5p, hsa-miR-323a-3p, hsa-miR-335-5p, hsa-miR-492, hsa-miR-518f-3p, hsa-miR-1185-1-3p, hsa-miR-1252-5p, and hsa-miR-517b-3p (Table 5). Furthermore, the comparison of young diagnosed Luminal B (n=1) versus other young diagnosed BC subtypes (n=5) retrieved 15 relevant miRNAs (Figure 14) including hsa-let-7b-5p, hsa-miR-126-3p, hsa-miR-1283, hsa-miR-130a-3p, hsa-miR-150-5p, hsa-miR-15a-5p, hsa-miR-16-5p, hsa-miR-185-5p, hsa-miR-191-5p, hsa-miR-19a-3p, hsa-miR-205-5p, hsa-miR-27b-3p, hsa-miR-371a-5p, hsa-miR-4454-miR-7975, hsa-miR-498, and hsa-miR-92a-3p.

Table 5. Differentially expressed cf-miRNAs ($p<0.05$) between Luminal B (n=2) and other BC subtypes (n=10)

miRNA	Relative expression in the Luminal B subtype (n=2)	Relative expression in other BC subtypes (n=10)	Log_2 Fold Change (LumB/others)	p-value	Adjusted p-value
hsa-miR-1254	10.02	4.09	1.29	0.030	1.00
hsa-miR-1827	34.24	18.17	0.91	0.030	1.00
hsa-miR-23c	20.88	10.57	0.99	0.030	1.00
hsa-miR-298	13.10	5.45	1.26	0.030	1.00
hsa-miR-301a-5p	2.55	11.42	-2.18	0.030	1.00
hsa-miR-323a-3p	13.05	3.09	2.08	0.030	1.00
hsa-miR-335-5p	1.80	7.05	-2.00	0.030	1.00
hsa-miR-492	19.50	3.96	2.30	0.030	1.00
hsa-miR-518f-3p	12.18	2.36	2.37	0.030	1.00
hsa-miR-1185-1-3p	2.86	1.08	1.40	0.038	1.00
hsa-miR-1252-5p	2.04	1.08	0.92	0.038	1.00
hsa-miR-517b-3p	4.07	1.08	1.91	0.038	1.00

BC: breast cancer; LumB: Luminal B
P-values were obtained using the Mann-Whitney test and adjusted with the False Discovery Rate (FDR) method. Bold miRNAs indicate absolute fold change values higher than 2.

Finally, the Luminal HER2 subtype was characterized by the differential expression of 22 miRNAs (Table 6): hsa-miR-125a-3p, hsa-miR-1262, hsa-miR-1264, hsa-miR-141-3p, hsa-miR-25-5p, hsa-miR-324-3p, hsa-miR-3613-5p, hsa-miR-378d, hsa-miR-4421, hsa-miR-4425, hsa-miR-4443, hsa-miR-4485-3p, hsa-miR-4787-5p, hsa-miR-489-3p, hsa-miR-491-3p, hsa-miR-5001-5p, hsa-miR-518c-3p, hsa-miR-519d-3p, hsa-miR-548ad-3p, hsa-miR-627-5p, hsa-miR-874-3p, and hsa-miR-874-5p.

Though all cf-miRNAs reported in the whole comparison were downregulated in Luminal HER2 patients, using the descriptive approach between young diagnosed patients, it is possible to propose additional miRNA-based biomarkers for young diagnosed Luminal HER2 patients (Figure 15), for example: hsa-miR-127-5p, hsa-miR-181b-5p/hsa-miR-181d-5p, hsa-miR-208b-5p, hsa-miR-2113, hsa-miR-331-3p, hsa-miR-486-3p, hsa-miR-519e-3p, and hsa-miR-6720-3p.

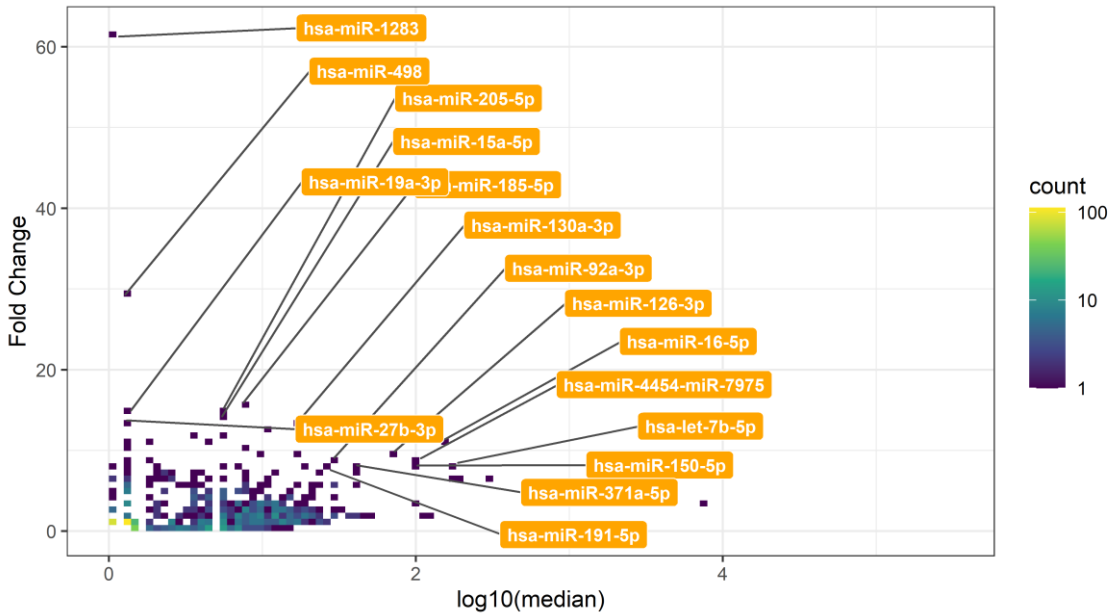

Figure 14. Relevant cf-miRNAs in young diagnosed Luminal B BC patients. This density plot shows all miRNA probes scanned in the Nanostring platform comparing Fold Change between Luminal B (n=1) vs. other BC subtypes (n=5) in young diagnosed individuals (y-axis) in comparison with their median expression (log10) in all young diagnosed individuals (x-axis). Labeled miRNA fulfill some of these conditions: i) top 1% of Fold Change or ii) top 5% of Fold Change and top 5% of median abundance. Figure built on the R software v.4.3.1. The 3D representation of this plot can be accessed here: https://doi.org/10.6084/m9.figshare.24021387

Table 6. Differentially expressed cf-miRNAs ($p<0.05$) between Luminal HER2 (n=2) and other BC subtypes (n=10)

miRNA	Relative expression in the Luminal HER2 subtype (n=2)	Relative expression in other BC subtypes (n=10)	Log_2 Fold Change (LumH2/others)	p-value	Adjusted p-value
hsa-miR-125a-3p	1.15	8.76	-2.94	0.030	0.99
hsa-miR-1262	1.18	4.50	-1.94	0.030	0.99
hsa-miR-1264	2.23	15.32	-2.74	0.030	0.99
hsa-miR-141-3p	1.15	11.25	-3.32	0.030	0.99
hsa-miR-25-5p	1.70	5.82	-1.79	0.030	0.99
hsa-miR-324-3p	1.15	3.14	-1.43	0.030	0.99
hsa-miR-3613-5p	2.59	10.34	-2.00	0.030	0.99
hsa-miR-378d	2.66	11.72	-2.12	0.030	0.99
hsa-miR-4421	4.16	12.34	-1.56	0.030	0.99
hsa-miR-4425	7.09	22.58	-1.69	0.030	0.99
hsa-miR-4443	2.04	16.82	-3.06	0.030	0.99
hsa-miR-4485-3p	1.70	7.50	-2.12	0.030	0.99
hsa-miR-4787-5p	1.15	4.31	-1.89	0.030	0.99
hsa-miR-489-3p	10.96	24.84	-1.18	0.030	0.99
hsa-miR-491-3p	3.92	14.69	-1.89	0.030	0.99
hsa-miR-5001-5p	1.44	10.71	-2.94	0.030	0.99
hsa-miR-518c-3p	1.15	9.62	-3.06	0.030	0.99
hsa-miR-519d-3p	7.61	19.57	-1.36	0.030	0.99
hsa-miR-548ad-3p	1.15	4.95	-2.12	0.030	0.99
hsa-miR-627-5p	4.85	16.23	-1.74	0.030	0.99
hsa-miR-874-3p	1.15	10.36	-3.18	0.030	0.99
hsa-miR-874-5p	1.15	13.88	-3.64	0.030	0.99

BC: breast cancer; LumH2: Luminal HER2

P-values were obtained using the Mann-Whitney test and adjusted with the False Discovery Rate (FDR) method. Bold miRNAs indicate absolute fold change values higher than 2.

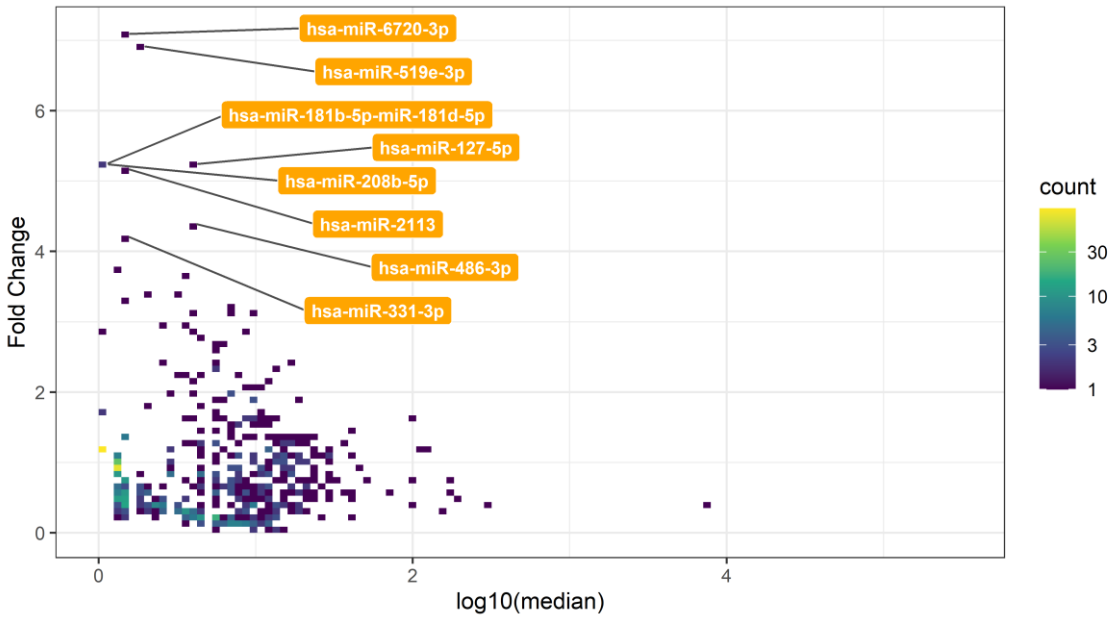

Figure 15. Relevant cf-miRNAs in young diagnosed Luminal HER2 BC patients. This density plot shows all miRNA probes scanned in the Nanostring platform comparing Fold Change between Luminal HER2 (n=1) vs. other BC subtypes (n=5) in young diagnosed individuals (y-axis) in comparison with their median expression (log10) in all young diagnosed individuals (x-axis). Labeled miRNA fulfill some of these conditions: i) top 1% of Fold Change or ii) top 5% of Fold Change and top 5% of median abundance. Figure built on the R software v.4.3.1. The 3D representation of this plot can be accessed here: https://doi.org/10.6084/m9.figshare.24021441

4.2.6 Relevant cf-miRNA regions related to age at diagnosis in BC patients

Some authors have reported that BC patients diagnosed after or before 40 years old have differences in their overall survival in dependence on tumor and environmental factors [4,6]. Thus, it was characterized that elderly diagnosed BC patients are sensitive to aging effects and environmental changes despite their tumors being less aggressive, whereas young diagnosed BC patients deal with highly clonal tumors showing a fast disease progression [238–241].

As a consequence of tumor- or aging-related factors, several miRNAs can be secreted into the bloodstream. Then, we decided to evaluate this factor by comparing the cf-miRNA levels between young and elderly BC patients (n=6 in each group) of Cohort A. Table 6 shows the differentially expressed cf-miRNAs in these two groups.

Table 7. Differentially expressed cf-miRNAs (p<0.05) between young (n=6) and elderly BC subtypes (n=6)

miRNA	Relative expression in the Young BC group (n=6)	Relative expression in the Elderly BC group (n=6)	Log_2 Fold Change (Young/Elderly)	p-value	Adjusted p-value
hsa-miR-95-3p	5.37	10.87	-1.02	0.005	1
hsa-miR-30c-5p	3.72	13.67	-1.88	0.018	1
hsa-miR-3202	1.25	8.18	-2.71	0.023	1
hsa-miR-1275	4.04	1.19	1.76	0.030	1
hsa-miR-1291	3.02	7.99	-1.40	0.030	1
hsa-miR-3074-3p	4.04	6.76	-0.74	0.030	1
hsa-miR-764	12.81	6.34	1.01	0.030	1
hsa-miR-937-3p	1.51	9.44	-2.64	0.030	1
hsa-miR-135b-5p	4.27	1.15	1.89	0.034	1
hsa-miR-615-3p	2.7	1.15	1.23	0.034	1
hsa-miR-101-3p	5.53	9.91	-0.84	0.048	1
hsa-miR-1287-5p	9.01	17.32	-0.94	0.048	1
hsa-miR-136-5p	2.03	4.64	-1.19	0.048	1
hsa-miR-28-3p	1.92	7.40	-1.95	0.048	1
hsa-miR-501-3p	9.01	2.3	1.97	0.048	1

BC: breast cancer
P-values were obtained using the Mann-Whitney test and adjusted with the False Discovery Rate (FDR) method. Bold miRNAs indicate absolute fold change values higher than 2

In addition to hsa-miR-95-3p (shown in Figure 11C), we found 14 additional miRNAs deregulated in the plasma of young BC patients. The entire list includes hsa-miR-95-3p, hsa-miR-30c-5p, hsa-miR-3202, hsa-miR-1275, hsa-miR-1291, hsa-miR-3074-3p, hsa-miR-764, hsa-miR-937-3p, hsa-miR-135b-5p, hsa-miR-615-3p, hsa-miR-101-3p, hsa-miR-1287-5p, hsa-miR-136-5p, hsa-miR-28-3p, and hsa-miR-501-3p.

Although hsa-miR-95-3p [203,242], hsa-miR-30c-5p [194,243–245], hsa-miR-1275 [242,246–250], hsa-miR-1291 [245,251–253], hsa-miR-937-3p [254–256], hsa-miR-135b-5p [257–261], hsa-miR-615-3p [166,262–264], hsa-miR-136-5p [210,211,265,266], hsa-miR-28-3p [206,220], and hsa-miR-501-3p [267,268] have been studied in the breast cancer context. This is the first evidence of their possible impact on the circulating miRNA composition of age-based BC groups.

Curiously, hsa-miR-28-3p was downregulated in the whole group of young diagnosed patients (log_2Fold Change= -1.95, p-value=0.048). However, among

young diagnosed patients, this miRNA is upregulated (log_2Fold change= 2.88) in the TNBC group (Figure 12). To validate these findings, we plotted a point-to-point graph in Figure 16.

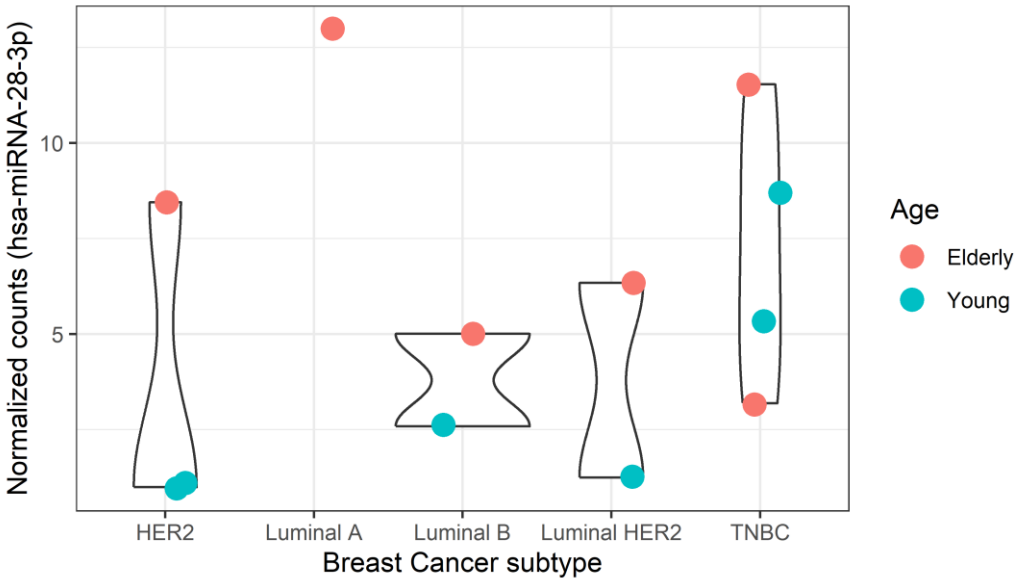

Figure 16. Dot plot of normalized values of hsa-miR-28-3p in plasma of Breast Cancer patients. Circulating levels of the hsa-miR-28-3p in samples of cohort A were plotted as a violin-dot plot stratifying samples according to their immunohistochemical subtype and age-related group. Figure built on the R software v.4.3.1. TNBC: Triple-negative breast cancer.

4.2.7 Challenges, lessons, and insights from the analysis of cf-miRNAs

We selected to work with liquid biopsies because our objective is to offer a minimally invasive test, which can improve the screening of patient candidates and then also serve to monitor the development of the tumor within them. To do this, we started from the hypothesis that tumor cells secrete material into the bloodstream that can be collected through venous puncture. In this context, plasma seems to be the most viable, fastest, and easiest option to evaluate putative cancer biomarkers [269–273]. Then, among the possible targets to be studied, miRNAs represent short regions, relatively easy to detect, and with limited diversity (compared to mRNA), as far as we know [274–276].

As the diversity of miRNA is still in development, many studies run RNA-seq experiments to evaluate miRNA-like regions. Nevertheless, they usually obtain a significant percentage of unaligned or unknown sequences [277–280]. Then,

more research is required to identify and annotate a new miRNA correctly. For these reasons, we decided to use the barcoding technology for analyzing specific regions previously determined by vast literature, according to information from miRBase v.21. However, the Nanostring technology requires at least 100 ng of input per sample.

In this analysis, we reached an average concentration of ~31.11 ng/µL, but the minimum sample content was ~25 ng, our input for cf-miRNA analysis. Then, it is suggested to include the total miRNA concentration after concentration as a sample exclusion criterion in the nCounter (Nanostring) analysis.

We then decided to implement a sample pool strategy to achieve a higher concentration. According to our results, this strategy is functional, contributing to improving the input mass. However, each plasma sample may present different degradation rates since the miRNAs evaluated at this stage are disseminated in various forms (as extracellular particle cargo, in a soluble form, or protein-coupled, etc.) [274–276]. Although we could increase our miRNA input by increasing the initial plasma input used in miRNA extraction, the goal of our molecular screening is to avoid causing any additional discomfort to the patient and collect a reasonable amount of blood. So, the objective involves starting with small volumes of plasma (in this case, 200 µL), despite the lower amount of miRNA.

Another alternative to increase miRNA input includes performing a pre-amplification. However, this process inlays the biases of the polymerase responsible for this process [281]. This factor could imply a different result since miRNAs are short sequences. Then, minimal differences in the miRNA sequence could be interpreted as another member of a miRNA family. On the other hand, we have the biological and technical implications of working with total miRNA extracted from plasma. According to our results, we found potential signs of hemolysis in our samples. This suggests that, in future analyses, a hemolysis assessment step could be added before processing these samples. The hemolysis status could be verified by evaluating plasma absorbance at 414 nm, as suggested by previous research [229,282]. In the present study, all plasma samples are separated up to 2 hours after collection following well-standardized guidelines [283–285], which exclude the time of processing as a

factor of hemolysis. Then, we hypothesize that hemolysis in samples of this study could be produced by the extended collection time.

On the one hand, since we followed the same protocols for all the samples, we can compare cf-miRNAs between BC groups. After running these analyses, we found a wide diversity of miRNA candidates as hsa-miR-28-3p. It is important to remark that exploratory studies are planned to propose putative biomarkers to be technically and biologically validated, especially to use affordable techniques such as qRT-PCR that allow us to approximate molecular protocols to the clinical routine.

On the other hand, cf-miRNA can include information from various cell sources [286], including tumor cells as well as anti-tumor responses. Then, we could refine and focus our analysis on one of these sources: extracellular vesicles (EVs). In this way, we hypothesize that we could reduce the contamination or noise found in cf-mirNA by analyzing EVs in plasma.

4.3 Vesicular miRNA levels in breast cancer patients

4.3.1 Selection of the best method for obtaining EVs from human plasma

We have tested three different methods to isolate EVs from plasma. Ultracentrifugation is a method that sediments particles of different density according to the speed at which this procedure is executed. For extracellular vesicles, we used high speeds (100 000 xg), and it takes approximately 4 hours to isolate EVs from 6 samples simultaneously. The miRCURY kit for EV isolation (Qiagen) uses a chemical reagent to diminish the water molecules in the sample, allowing precipitation of smaller particles (<100nm) taking one and a half days to isolate EVs from up to 24 samples. Finally, the qEV ready-to-use column (IZON) isolates extracellular vesicles by size exclusion principle, which takes around two hours to purify EVs from plasma samples (up to five samples).

In our experiment, we obtained one tube containing EVs for ultracentrifugation and miRCURY methods, whereas the qEV method generates six tubes (elution fractions). Then, we analyzed the quantity and size distribution of isolated vesicles produced by these methods. The qEV IZON column (Figure 17A) and the ultracentrifugation samples (Figure 17C) showed a similar EV profile compared to miRCURY kit (Figure 17B), that could be produced by the

presence of contaminants (Figure 18). In fact, the miRCURY tube showed a yellowish hue as a signal of plasma proteins (and/or other components), as it was reported in a previous study [287]. However, the miRCURY method seems to capture more EVs than other methods, although it is not possible to discriminate any contaminant having nanoscale dimension from EVs using NTA.

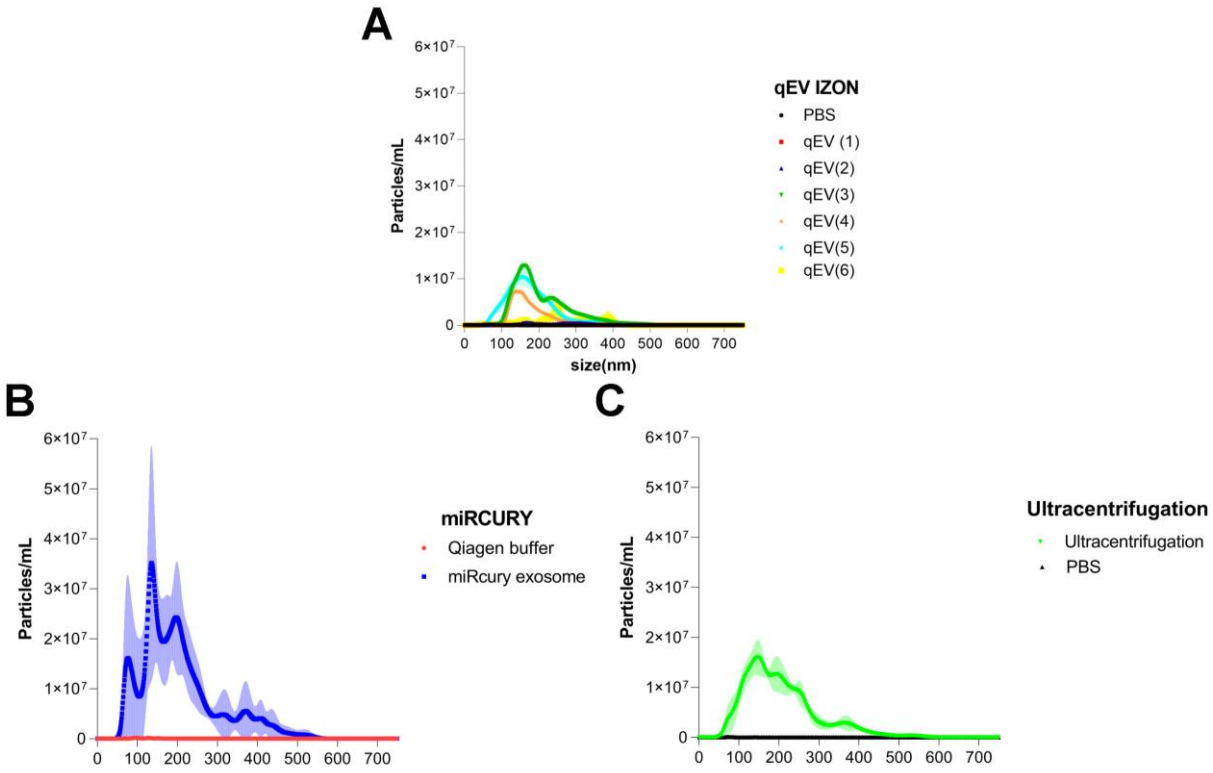

Figure 17. Nanotracking particle profiles for different methods to isolate EVs. Eluted samples from three strategies to isolate EVs: (A) qEV IZON-Size Exclusion Chromatography, (B) miRCURY-Chemical Precipitation, and (C) Ultracentrifugation. All samples were quantified using Nanoparticles Tracking Analysis (NTA). For each method, we also quantify the elution solution as a negative control (PBS or Qiagen buffer). All results are expressed in particles per mL and five technical replicates were considered for each curve. Figures built on GraphPad Prism v8 for Windows.

Another important criterion is related to particle size. Here, the miRCURY sample showed a higher number of smaller particles (<100nm). It is consistent with the principle of this method to reduce water exposition and drives the

precipitation of tiny particles with low-speed centrifugation. In general, we observed a common peak among 100 and 200 nm for all isolation methods (Figure 17), characterizing the extracellular vesicle profile in plasma as described in the literature [67,288].

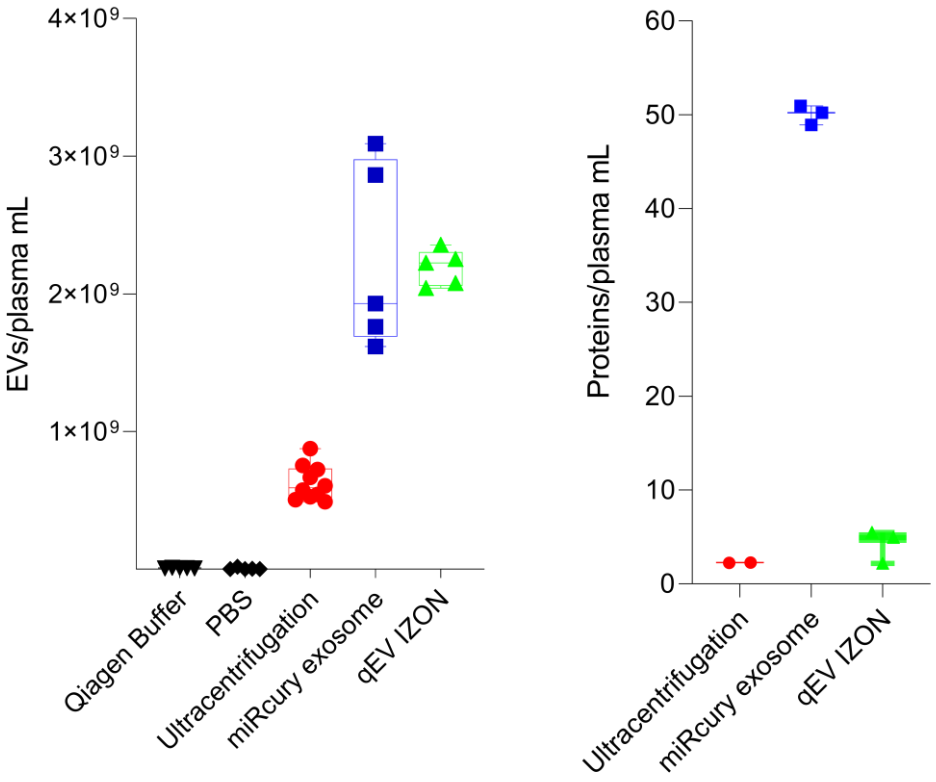

Figure 18. Quantification of particles and proteins according to EVs isolation method. The left panel shows the quantification of extracellular vesicles in NTA equipment (five replicates each). The right panel shows the quantification of proteins using a modification of the Lowry assay (three replicates each). For the quantification of EVs, we include data for Qiagen Buffer and PBS as negative controls. These results represent observations in at least three technical replicates. Figures built on GraphPad Prism v8 for Windows.

Regarding the importance of having highly pure samples for downstream applications, we have assessed the quantification of EVs and proteins for these three methods. We normalized all values considering the volume of plasma for EV isolation. According to our results, we obtained approximately $2x10^9$ particles per plasma mL using the miRCURY or the qEV IZON kits, followed by

the ultracentrifugation method that recovers almost $1x10^9$ particles per plasma mL. Therefore, qEV IZON and miRCURY methods seem to offer more yield than ultracentrifugation to isolate EVs; however, the miRCURY method also isolates a high concentration of proteins (~50mg/plasma mL), differently from ultracentrifugation or qEV IZON methods (Figure 18).

Table 8 shows that protein levels were undetectable in EVs from the qEV method (size-exclusion chromatography) and supernatant from the miRCURY method (precipitation by chemical reagent). This result is consistent with other experiences in the literature that reported high amounts of plasma proteins present in precipitation methods with chemical reagents, such as ExoQuick, Total Exosome Isolation, and Exoeasy [289–291]. On the other hand, qEV original (IZON) is becoming one of the most used size-exclusion columns for EV isolation with optimal results [289,290].

Table 8. Protein concentration for EV and supernatants fractions according to different isolation methods

Sample	Dilution	Protein concentration (µg/mL)
Whole human plasma	1:500	211.0
EV isolated by ultracentrifugation	1:1	996.0
EV isolated by size-exclusion chromatography	1:7	< detection threshold
EV isolated by precipitation with chemical reagent	1:12	2 657.0
Supernatant from ultracentrifugation	1:500	191.0
Supernatant from size-exclusion chromatography	1:500	< detection threshold
Supernatant from the method using chemical reagent	1:500	< detection threshold

EV: Extracellular Vesicles
Dilution factors are dependent on input and output volumes recommended by each protocol.
Detection threshold: 156.25 µg/mL

In our study, EVs fraction from the miRCURY method showed a higher concentration of proteins, probably depleting them on their supernatant fraction. Therefore, we decided to observe the protein profile of these EVs. We loaded ~6 µg of proteins from all three methods and the whole plasma in an electrophoresis gel. For EVs from size-exclusion chromatography, we considered the maximum volume (40 µL). As we expected, this sample did not

show any bands (Figure 19). Then we can explain this result by two factors: (i) the low sensitivity offered in gel electrophoresis and (ii) the high purity rate in EV isolated with size-exclusion columns. For other samples, the gel revealed a pattern band where estimated weights are related to common proteins in human plasma, for example, transferrin, albumin, and the heavy/light chains of IgG (According to the study of Qui et al., 2015 [292]).

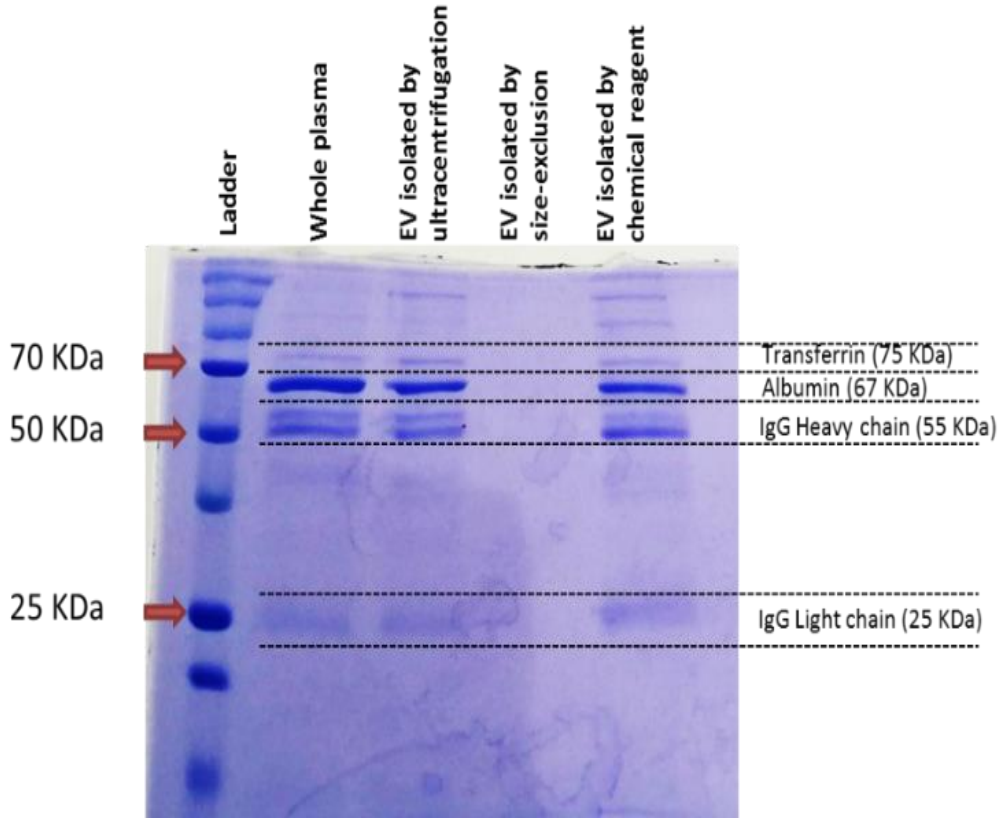

Figure 19. Polyacrylamide gel with protein profiles for plasma and EV isolated by different methods. Information on the molecular weight for transferrin, albumin, and IgG proteins was obtained from Qiu et al. (2015).

4.3.2 Characterization of EVs from plasma samples

After selecting the size exclusion chromatography method for the following steps in this thesis, we followed the guidelines for the publication of studies in extracellular vesicles [72]. We have submitted all relevant data of our experiments to the EV-TRACK knowledgebase (EV-TRACK ID: EV230978) [124]. Next, we used transmission electron microscopy (TEM) and western blotting to characterize the EVs that will be analyzed by barcoding hybridization.

Figure 20A and Figure 20B show the TEM profile of our EVs isolated by the SEC method. Using 20 000x magnification (Figure 20A), we observed many aggregates in the grid, whereas 30 000x allowed us to see corpuscles clustered with a round shape and matching with the expected size (50-200 nm) but partially lysed (Figure 20B). The appearance of EVs observed in Figures 14A-B could be affected by the concentration step (ultracentrifugation after the fixation).

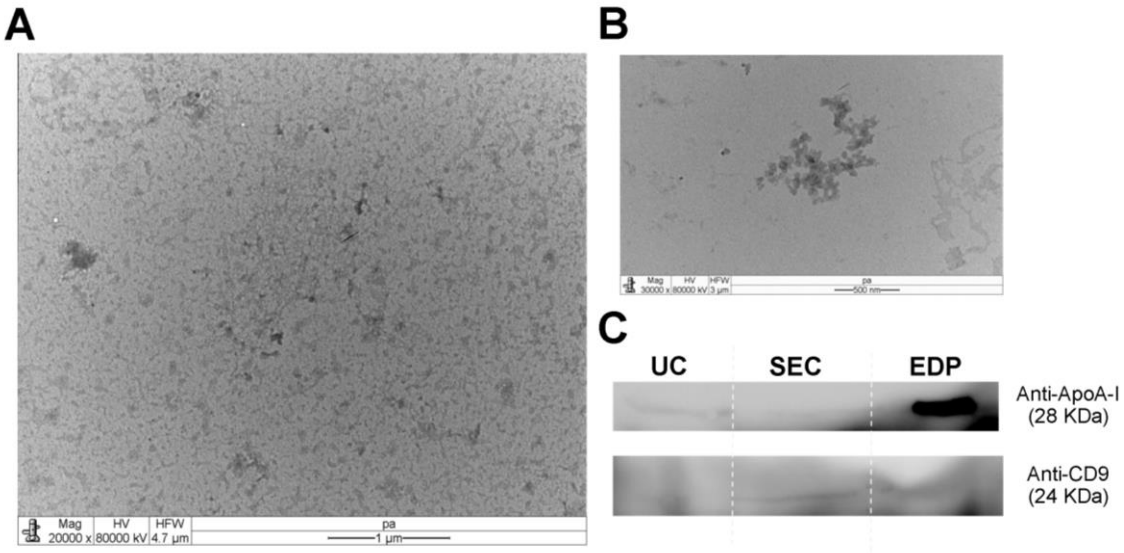

Figure 20. Characterization of EVs by TEM and WB. We used transmission electron microscopy (TEM) and western blot (WB) techniques to characterize the EV population included in downstream analysis. The TEM analysis demonstrated the presence of EVs and their morphology at 20 000x (A) and 30 000x (B) magnifications. Next, WB analysis showed a higher presence of CD9 (EV marker) in the sample isolated from the SEC method, whereas ApoA-I (lipoprotein marker) was more expressed in EVs obtained by ultracentrifugation (C). UC: EVs isolated from ultracentrifugation. SEC: EVs isolated from size-exclusion chromatography, EDP: EV-depleted plasma (supernatant from ultracentrifugation) diluted 1:50 in PBS buffer.

Though we followed a previously published protocol of our group [123], we started the protocol with 100-1000x less EV concentration, which could affect our final results. Furthermore, previous EV-related research has demonstrated that TEM results depend on the operator and protocol [293,294].

According to our results, the low concentration of vesicles collected per 1 mL of plasma from BC patients challenges the sensitivity of the TEM and WB techniques. However, this study must keep the input volume relatively low enough to be collected in one 3mL-EDTA tube because, by this input volume, we could foresee a practical and fast implementation of the clinical routine.

To characterize the presence of corona proteins or other contaminants present in blood, we evaluate the presence of lipoproteins that are described as the main contaminants in EVs isolation protocols. As shown in Figure 20C, EVs isolated by SEC are more likely to content EVs free of high-density lipoproteins (HDL). This finding is consistent with our current knowledge about plasma circulating components that have characterized HDL with a similar density to EVs (1.06–1.21 g/mL) [289], which could induce non-specific collection by density-based protocols such as ultracentrifugation.

Regarding our downstream application, it is essential to prevent EV contamination with HDL since it was discovered that these particles can also carry RNA fragments and have the potential to regulate receiving cells [163,295–297]. Then, other components present in plasma, such as very low- (VLDL), low- (LDL), or intermediate-density lipoproteins (IDL) and chylomicrons, have different densities or sizes [289], and could not represent the potential risk to be collected together with EVs.

4.3.3 EVs and vesicular miRNA total quantification in patient samples

EVs were isolated from all plasma samples of the cohort B (n = 24) using ultracentrifugation and size exclusion columns. As it was shown in Figure 18, both techniques collected a similar concentration of EVs (p = 0.4988) in samples of the cohort B (Figure 21A). For the following experiments, we used EV isolated by size exclusion chromatography as this method shows ultra-low rates of soluble protein (Figure 19). Then, the qEV IZON method was the best strategy to obtain extracellular vesicles from plasma with a good purity ratio, as reported in a previous analysis [290]. However, a crucial point for choosing the best method to isolate EVs is directly related to the final application [287,290].

We did not find statistical differences in EV levels for different BC subtypes in younger patients (Figure 21B), or in young vs. elderly comparison for TNBC samples (Figure 21C). This result can be influenced by the low number of samples used. Nevertheless, it is important to remark that BC patients with different ages or subtypes could show differences in the RNA cargo of these EVs [298,299].

Regarding the RNA content of the vesicles, we initially tested their quantification with a spectrophotometry-based method. With this method, we found an estimate of the amount of RNA for each of the 24 samples, which ranged between 3 and 15 ng/µL (Figure 22A). In this thesis, the RNA values were not related to the EV concentration (p=0.5335). As it is considered a high concentration for EV cargo [300], we decided to evaluate the quality parameters. We found that both ratios (260/230 and 260/280) were mostly outside the accepted limits (1.8-2.0, Figure 22B). In this way, the values shown in Figure 22A would not be real quantification [301]. Then, we required a more specific quantification for miRNAs, such as quantification by bioanalyzer.

After we carried out the experiments in the 2100 Bioanalyzer equipment, we saw that the miRNA concentration also showed no correlation with the number of vesicles previously quantified for each sample (Figure 23A). However, at this time all samples passed the quality indicators. Samples with acceptable quality showed their miRNA concentration in a text box with a green background. We found this for both low (Figure 23B) and high (Figure 23C) concentrated samples.

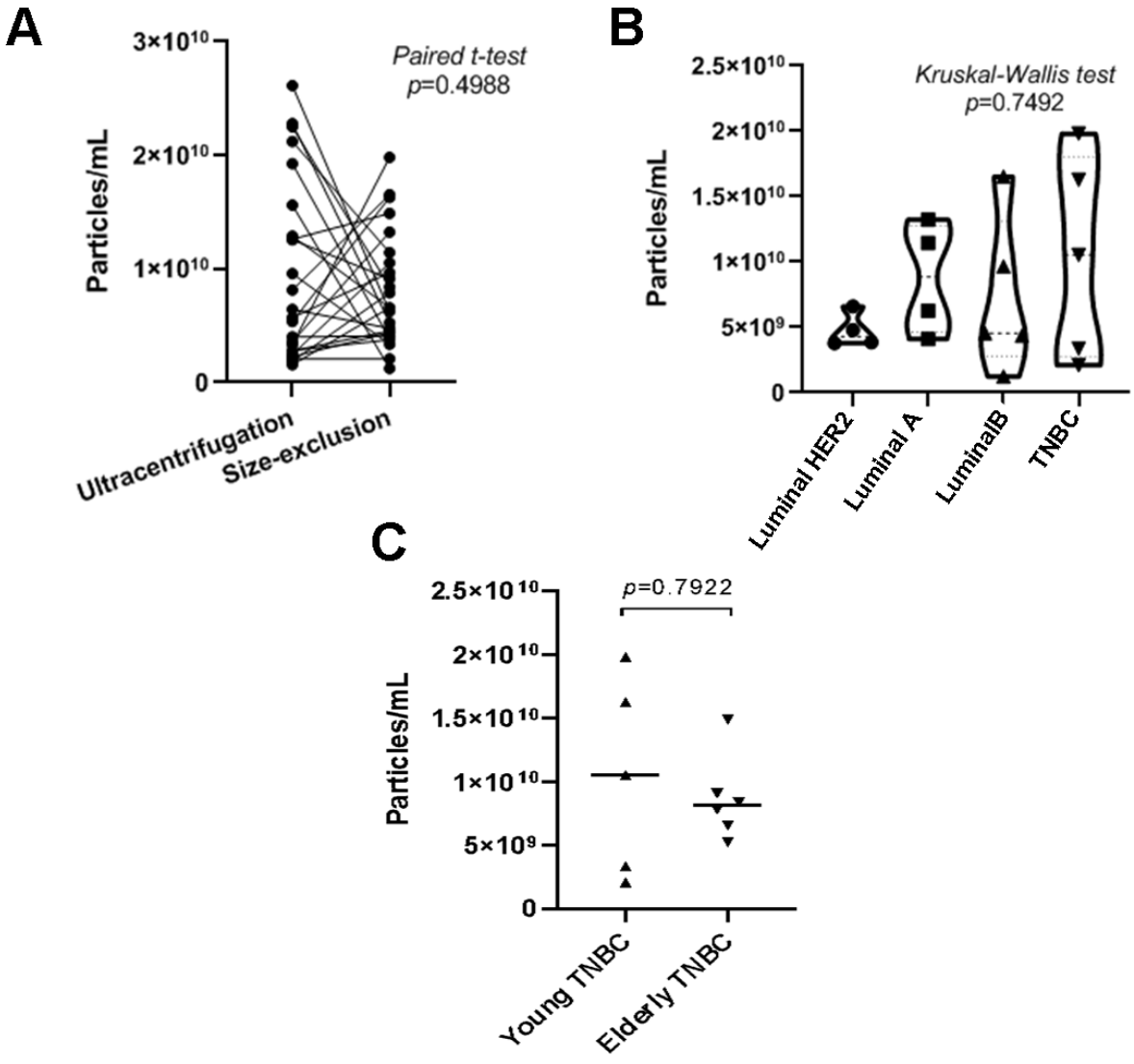

Figure 21. EV concentration in patient plasma samples. (A) Comparison between EVs isolated by ultracentrifugation and size-exclusion methods. (B) Comparison of EV concentration by BC subtype in young patients. (C) Comparison of EV concentration by age in TNBC patients. Each observation represents five technical replications. For unpaired comparisons, p-values were estimated using the Kruskal-Wallis test. For paired comparisons, we applied the Wilcoxon test. Figures built on GraphPad Prism v8 for Windows.

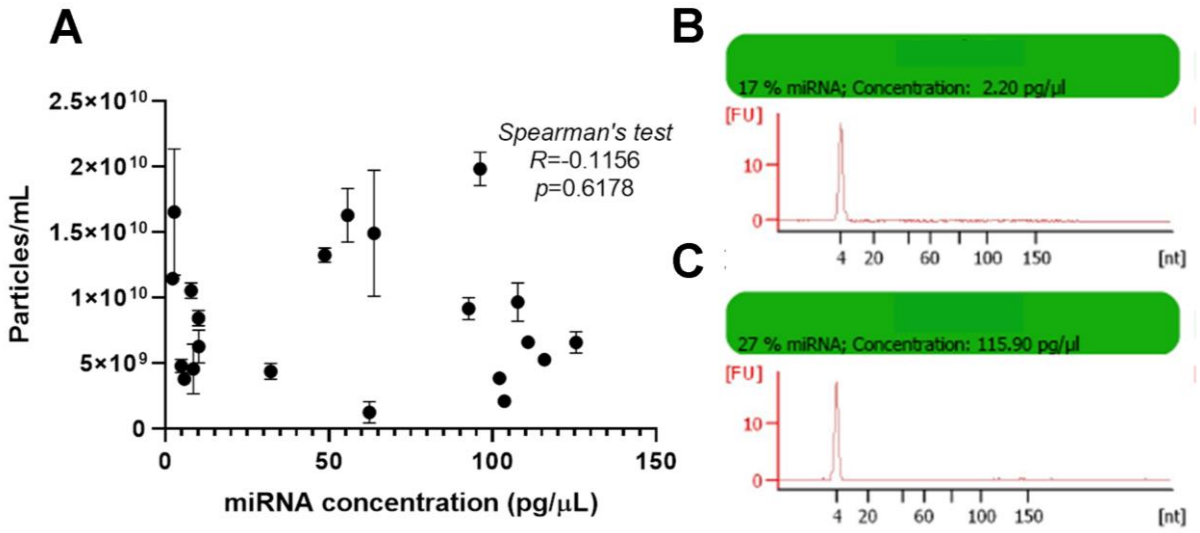

Figure 23. miRNA concentration in EVs measured by capillary electrophoresis. (A) Scatterplot showing miRNA and EV concentration values for each sample. Each point includes five technical replicates for EV concentration. We applied the Spearman's test for evaluating correlation between numerical variables. Figure built on GraphPad Prism v8 for Windows. (B and C) Representations of the capillary electrophoresis profile for low (B) and high (C) concentrated samples.

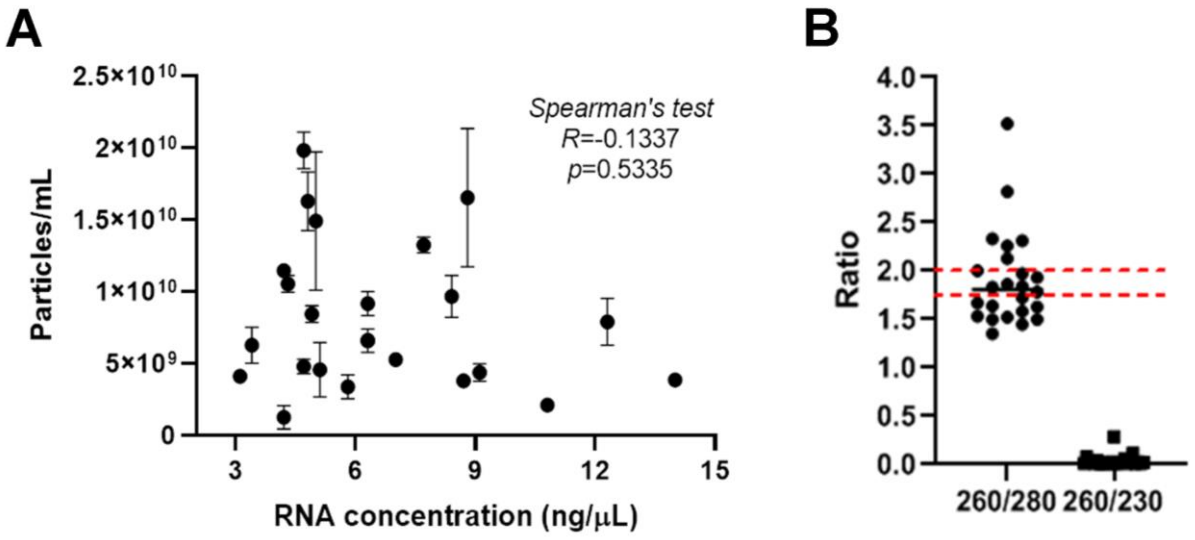

Figure 22. RNA concentration in EVs measured by spectrophotometry. (A) Scatterplot showing RNA and EV concentration values for each sample. Each point includes five technical replicates for EV concentration. We applied the Spearman's test for evaluating correlation between numerical variables. (B) Dot graph showing the proportions 260/230 and 260/280 obtained by each sample. The red lines delimit the optimal range for both values (1.8-2.0). Figures built on GraphPad Prism v8 for Windows.

The bioanalyzer assay showed a picogram-order mass of miRNA (Figure 23B and Figure 23C) present in EVs. Combining these results with the previously described vesicular RNA diversity (miRNA, lncRNA, and circRNA) [302], we have a new factor for our EV analysis. Our results showed that the concentrations of EV (Figure 21) or vesicular RNA (Figure 23 and Figure 22) are not uniform or follow a normal distribution. These levels could vary according to EV subpopulations that the scientific community has not fully characterized. After this analysis, we performed the nCounter (Nanostring®) analysis to evaluate potential differences in the vesicular miRNA expression between BC subtypes and age-related groups.

4.3.4 First observations of vesicular miRNA expression data

NanoString® technology allows obtaining expression data in a high-throughput format. After following the default settings for analyzing this data, we were able to find miRNAs with an absolute number of copies between 1 and more than 10 000 (minimum and maximum values in Figure 24).

The nCounter Nanostring® array for miRNA analysis includes 798 probes for evaluating the expression of all human validated miRNAs (miRBase v21, published in 2014), and 30 regulatory regions (system probes, spike-in regions, and housekeeping genes). Here are two of the most challenging factors to analyze vesicular miRNAs. First, there is no consistent-expression miRNA (housekeeping) for data normalization. Due to this, the insertion of traditional housekeeping probes (for example, *ACTB*, *B2M*, *GAPDH*, *RPL19*, and *RPLP0* for the NanoString® array) in the default pipeline are not relevant for the analysis of vesicular RNA. Second, vesicular miRNA levels are low. As previous studies have been described, the expected concentration of vesicular RNA is around one molecule from 1-100 EVs [303]. Regarding EV mass used for RNA extraction, we loaded between $3x10^9$ -$1.8x10^{10}$ EVs per sample, which could mean around $3x10^7$ -$1.8x10^8$ RNA molecules. However, the EV cargo is not only composed of miRNA. It also includes messenger RNA (mRNA) [303], long non-coding RNA (lncRNA), circular RNA (circRNA) [304], double-stranded DNA (dsDNA), mitochondrial DNA (mtDNA) [305], and proteins [306] as lumen components. Therefore, the actual vesicular miRNA concentration is lower than

expected. Due to this, the geometric mean of the eight negative probes that compose this array is higher than 75% of all tested probes (Figure 24).

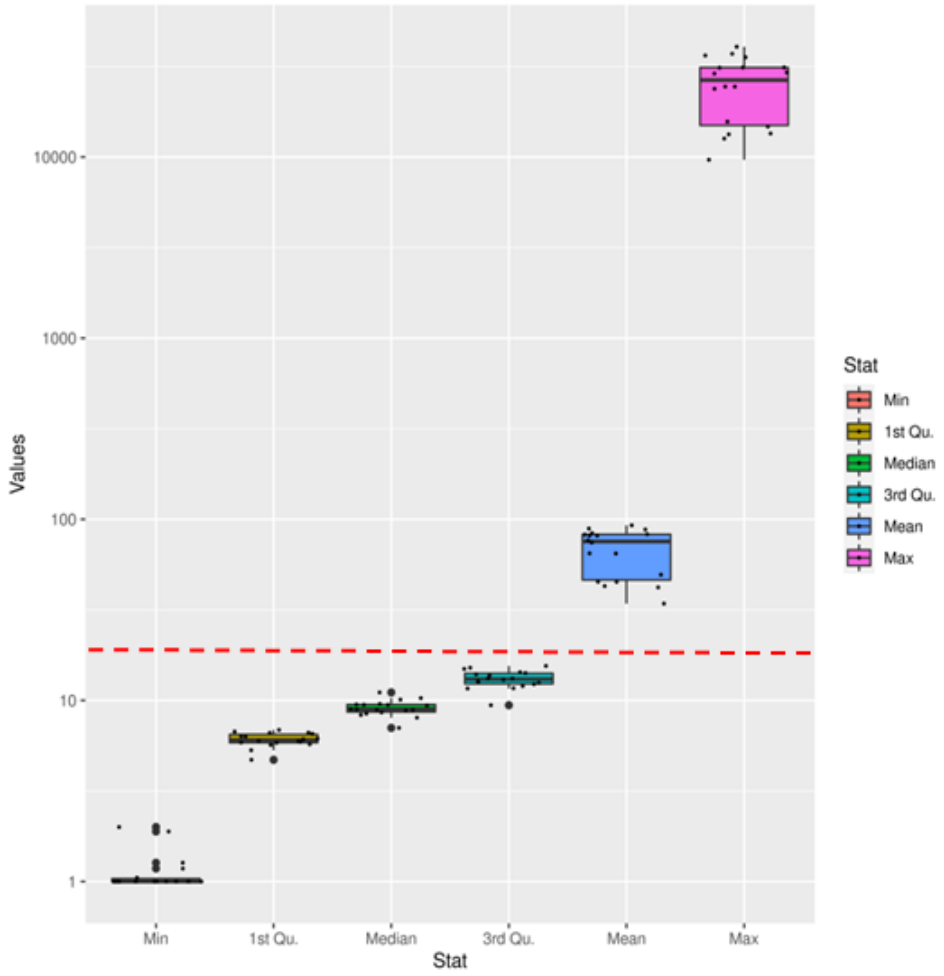

Figure 24. Summary of descriptive statistics of miRNA expression data after default processing. The red dotted line represents the geometric mean of negative controls. Min: Minimal value. 1st Qu: First Quartile value. 3rd Qu: Third Quartile value. Max: Maximum value. A log10 scale was used for the y-axis. Figure built on the R software v.4.3.1.

To validate that vesicular miRNA required a non-default normalization pre-processing (as the one proposed by the Nanostring® nSolver™), we performed an unsupervised analysis for both informative (798 probes) and normalizing (30 probes) regions with samples of the cohort B. Figure 25 shows the distribution of expression values for the informative regions after the default pre-processing procedure. Based on this result, our data set has many highly expressed miRNAs (colored in green and yellow). It could help to propose candidate miRNA markers to characterize breast cancer samples, as well as to

classify prognosis between patients. However, the profile of normalizing regions in Figure 26 shows highly heterogeneous levels across the samples. In the unsupervised analysis, the dendrogram shows three main clusters, which are partially coincident with the batch where these samples were analyzed (For example, all young TNBC and the Young_Luminal_5 samples were run on the same day, different from the other samples).

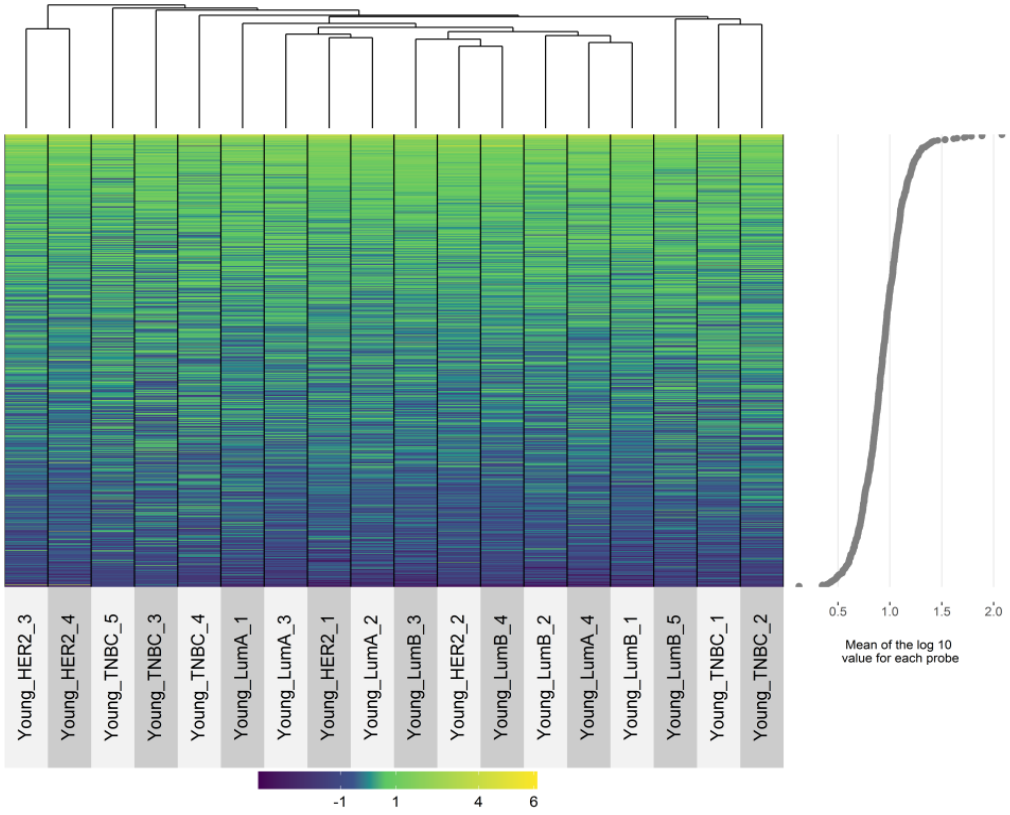

Figure 25. Heatmap of the expression of informative probes of the NanoString® miRNA array processed with the default protocol. Expression values are shown as log10, each row represents one miRNA, and each column indicates all values for one sample. The rows are ordered by their mean expression level in the samples (right panel). The columns are classified according to the unsupervised dendrogram (top panel). HER2: Luminal HER2, TNBC: Triple-negative breast cancer, LumA: Luminal A, LumB: Luminal B. Figure built on the R software v.4.3.1.

In addition, this data does not meet important technical parameters according to the NanoString® expected results [307]. In particular, Positive,

Negative, and Endogenous probes should not have similar expression levels. Then, Negative probes should have the lowest levels after normalization when run correctly. On the other hand, the lower expression of Endogenous probes could be comprehensible since these probes are very useful in cellular RNA but not in vesicular RNA. After our observations and the lack of consensus for this type of analysis, we conclude that a custom pipeline is required to preprocess vesicular miRNA data.

4.3.5 Evaluation of protocols for vesicular miRNA data normalization

The preprocessing of Nanostring® data is a process that involves three main steps: Negative Normalization, Positive Normalization and Content Set Normalization [308]. The Negative Normalization or Subtraction aims to eliminate the noise produced by the fluorescent background of each chip. Here, we can choose which algorithm (maximum, median, geometric mean, etc.) will be applied to the negative probes (n=8) to obtain the value that will be discounted from all samples. Positive normalization will adjust expression values relative to measurements of overexpressed (positive) probes also detected on the same chip. Again, we can choose the algorithm to define the value among all positive probes (n=6). Lastly, the Content Set Normalization aims to adjust the abundance of each miRNA regarding endogenous probes with an expected constant expression. In the quantification of cellular RNA, housekeeping probes (n=5) are used for this step. However, this could not be applicable for the vesicular content. Another method registered in the default protocol of Nanostring® nSolver^{TM} 4.0 considers the mean of the 100 most expressed probes. Concerning vesicular miRNA cargo, this is an unstable method since small differences in vesicular RNA can be overrated by their low abundance.

After these considerations, we tested many parameters for each normalization step while evaluating their biological relevance. As a selection of these tests, we present three of the compared models. We found that the geometric mean was our best option to estimate the normalization value for positive probes. Indeed, some authors agree that the geometric mean is the

most accurate way to process positive and housekeeping probes for RNA quantification [309,310]. For the negative normalization, we proposed two approaches. The most restrictive uses the maximum value of all negative probes, while the second approach uses the geometric mean following the same logic of positive normalization. Finally, the content set normalization was performed using the EV concentration of each sample (measured by NTA) or the geometric mean of the less variable informative probes (top15 stable regions).

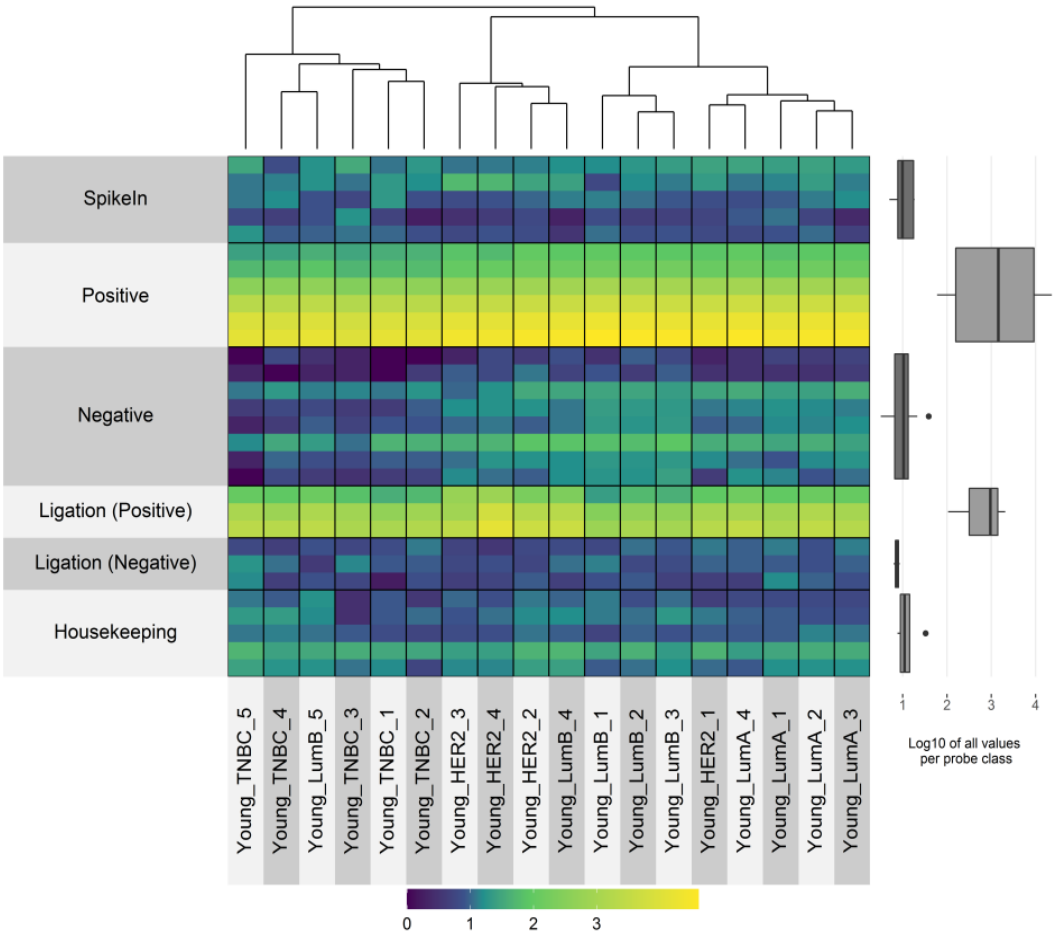

Figure 26. Heatmap of the expression of normalizing probes of the NanoString® miRNA array processed with the default protocol. Expression values are shown as log10, each row represents one probe, classified according to their class, and each column indicates all values for one sample. The columns are classified according to the unsupervised dendrogram (top panel). The right panel shows box plots made with the mean values of all the probes grouped by their classes. HER2: Luminal HER2, TNBC: Triple-negative breast cancer, LumA: Luminal A, LumB: Luminal B. Figure built on the R software v.4.3.1.

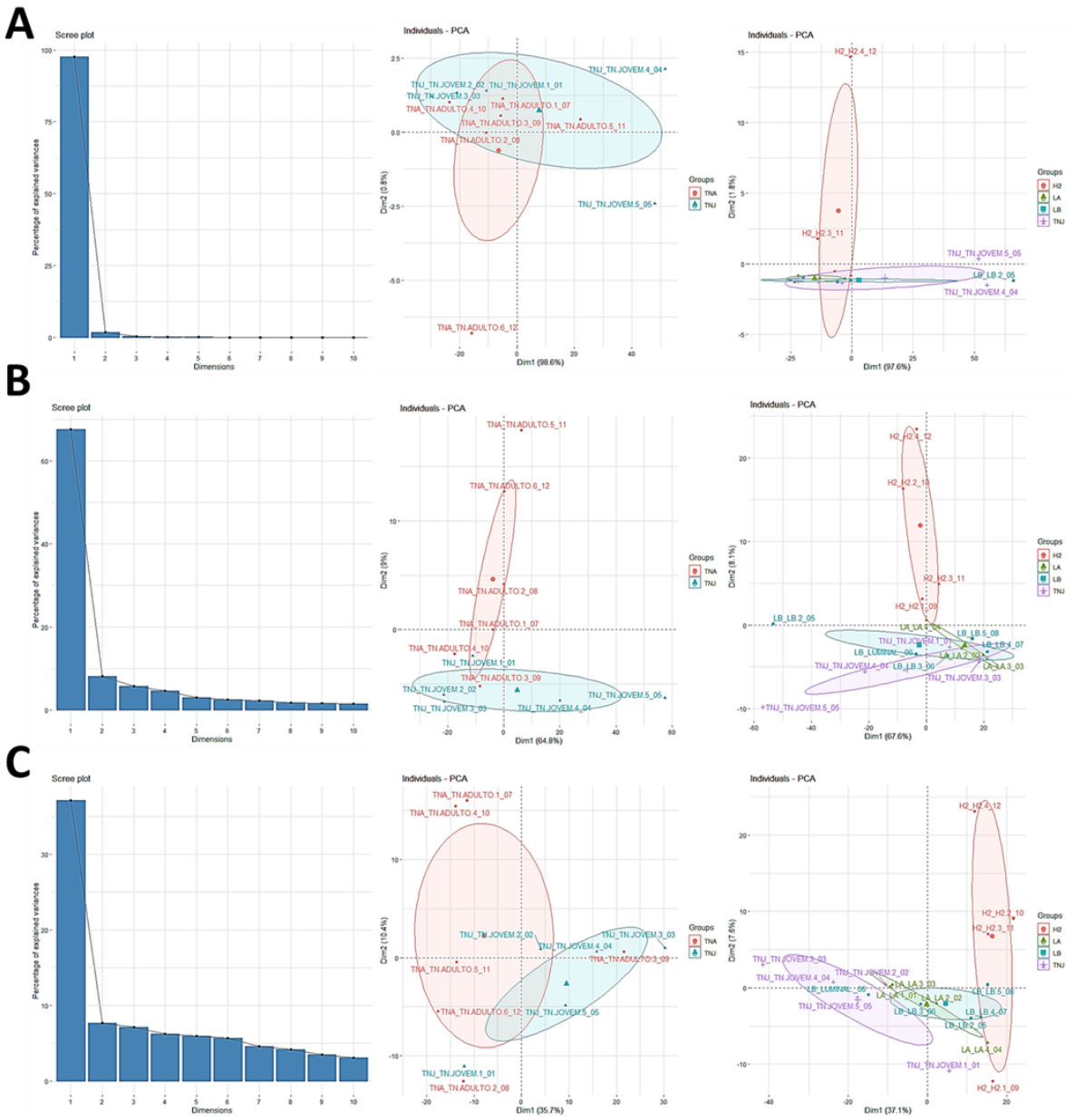

Figure 27. Principal Component Analysis (PCA) of the classification features of normalizing protocols in vesicular miRNA data. Three methods were selected for evaluating the contribution of preprocessed miRNA levels in the classification of BC samples. For all figures, the left panel shows the explained variance produced by the components generated in each case. The middle and right panels show the ability of each method to classify TNBC (young vs. elderly age-related groups) and young samples (Triple-negative, Luminal HER2, Luminal A or Luminal B subtypes), respectively. (A) Method using the maximum value of negative probes, the geometric mean of positive mean and EV concentration for content set normalization. (B) Method using the geometric mean of negative probes, the geometric mean of positive mean and EV concentration for content set normalization. (C) Method using the geometric mean of negative probes, the geometric mean of positive mean and less variable miRNAs (<50%) for content set normalization. TNA: Elderly TNBC (patients diagnosed with more than 40 years old), TNJ: Young TNBC (patients diagnosed with less than 40 years old), H2: Young Luminal HER2, LA: Young Luminal A, LB: Young Luminal B. Figures built on the R software v.4.3.1.

In the absence of a housekeeping region and despite its possible contamination with plasma lipoproteins [311,312], EV quantification appears to be one of the few biological ways to standardize vesicular RNA concentration. On the other hand, following the traditional rationale for selecting housekeeping regions, we can evaluate the less variable regions for our sample cohort, despite it could vary across experiment sets.

Figure 27 shows Principal Component Analysis (PCA) results of three selected protocols to preprocess vesicular miRNA data. Figure 27A and Figure 27B represent data normalized using the geometric mean of positive probes and the EV concentration of each sample as content normalizer. The difference of these methods is related to the negative normalization. In Figure 27A, the maximum value of the negative probes was used for the background subtraction. Many probes were then affected by suppressing their expression values. Due to this, a high percentage of the variance is explained uniquely by the first component (Figure 27A, left panel). Additionally, this method failed to separate TNBC or young BC patients (Figure 27A, middle and right panels). The second method (Figure 27B), which uses the geometric mean of negative probes for background subtraction, has a better performance for separating TNBC samples (Figure 27B, middle panel) but failed to separate young BC patients (Figure 27B, right panel). For the latter model, we decided to retain geometric means for positive and negative probe normalization and evaluate the most stable miRNAs for content normalization. According to Figure 27C, this model had a better distribution of explained variance across the predicted components (Figure 27C, left panel). Moreover, this model can separate TNBC and young BC subgroups more efficiently than the other models (Figure 27C, middle and right panel).

After selecting the third method, we evaluated its ability to separate young BC samples without supervision. For this step, we performed two separate analyses. The first analysis was for TNBC samples (including young and elderly samples, Figure 29A and Figure 28A), and the second for young BC samples (including TNBC, Luminal HER2, Luminal A, and Luminal B subtypes in young patients, Figure 29B and Figure 28B).

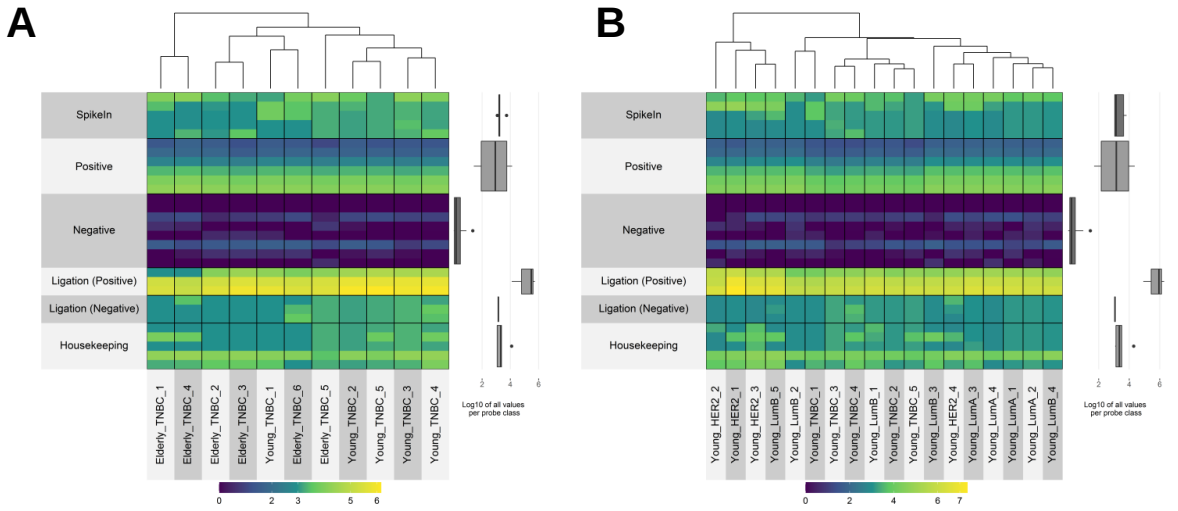

Figure 29. Heatmap of the expression of normalizing probes of the NanoString® miRNA array processed with our improved protocol. Expression values are shown as log10, each row represents one probe, classified according to their class, and each column indicates all values for one sample. The columns are classified according to the unsupervised dendrogram (top panel). The right panel shows box plots made with the mean values of all the probes grouped by their classes. (A) Heatmap of TNBC (young vs. elderly) samples. (B) Heatmap of young BC samples (classified by subtype). HER2: Luminal HER2, TNBC: Triple-negative breast cancer, LumA: Luminal A, LumB: Luminal B. Figure built on the R software v.4.3.1.

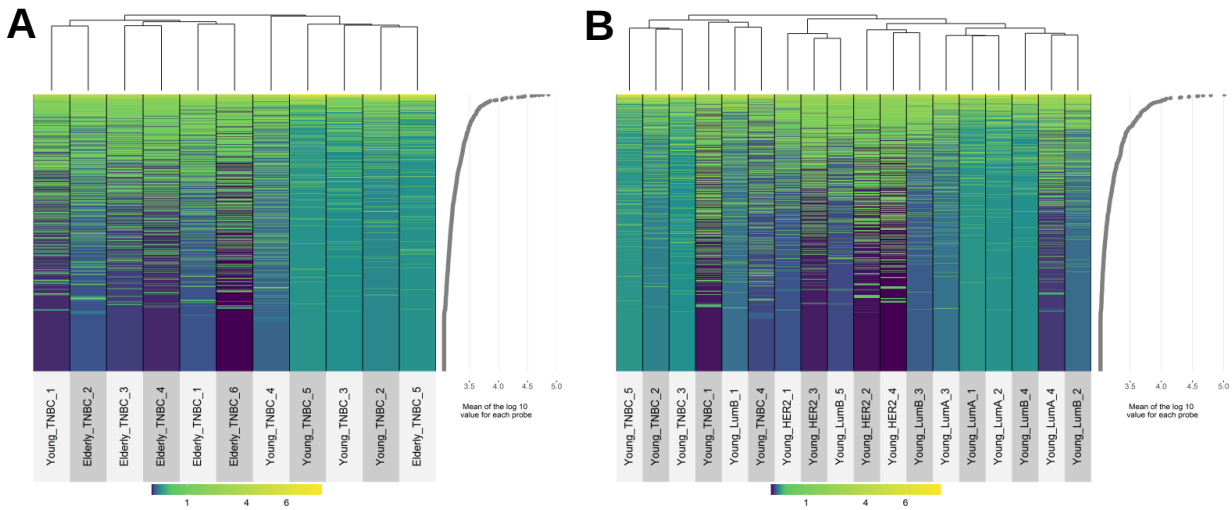

Figure 28. Heatmap of the expression of informative probes of the NanoString® miRNA array processed with our improved protocol. Expression values are shown as log10, each row represents one miRNA, and each column indicates all values for one sample. The rows are ordered by their mean expression level in the samples (right panel). The columns are classified according to the unsupervised dendrogram (top panel). (A) Heatmap of TNBC (young vs. elderly) samples. (B) Heatmap of young BC samples (classified by subtype). HER2: Luminal HER2, TNBC: Triple-negative breast cancer, LumA: Luminal A, LumB: Luminal B. Figure built on the R software v.4.3.1.

From these observations, we realized that the median values for the informative probes (Figure 28, scatterplot in the right panel) have a different profile compared to the default data processing (Figure 25, scatter plot in the right panel). After this normalization, the least informative miRNAs were standardized for showing similar patterns between samples. We can then remove them to avoid overvalued results. In addition, profiles of calibrating probes (Figure 29) were homogeneous across samples and in agreement with expected profiles for system probes according to the manufacturer manual [308]. These results warrant the use of this normalization method to obtain miRNA data for future comparison with clinical data.

4.3.6 Top abundant vesicular miRNAs in BC patients

Differentially from the analysis of cf-miRNA regions, we evaluated two different cohorts of vesicular miRNA. Samples of cohort B were independently analyzed, vesicular miRNA was eluted in 20 µL (one elution step at isolation), and the total miRNA mass obtained from 600 µL of plasma was inputted to the nCounter system. Whereas samples of cohort A were analyzed in a pooling strategy, vesicular miRNA was eluted in 40 µL (two elution steps at isolation), and the total miRNA mass was concentrated to input ~65ng of miRNA mass to the nCounter system. It is essential to mention that the strategy applied to Cohort A yields 65-200 ng of total miRNA measured by spectrophotometry after concentration by vacuum centrifuge. Raw and pre-processed data of these samples were deposited to the Gene Expression Omnibus (GEO) database under accessions GSE241784 (Appendix 4) and GSE241785 (Appendix 5).

Figure 30 shows the histogram profile of the vesicular miRNAs reported by the two strategies. Notably, by eluting the vesicular miRNA twice, we obtained a more homogeneous result between samples (Figure 30 B). Next, we observed that there are four vesicular miRNAs present in both lists: hsa-miR-212-3p, hsa-miR-302d-3p, hsa-miR-28-5p, and hsa-miR-873-3p. Despite the technical and biological differences between cohorts A and B, the report of common miRNAs present in these EVs represents a relevant finding to our understanding of the EV cargo in the plasma of BC patients. It is interesting because the scientific community is concentrating efforts on determining the main content of EVs from BC patients [70].

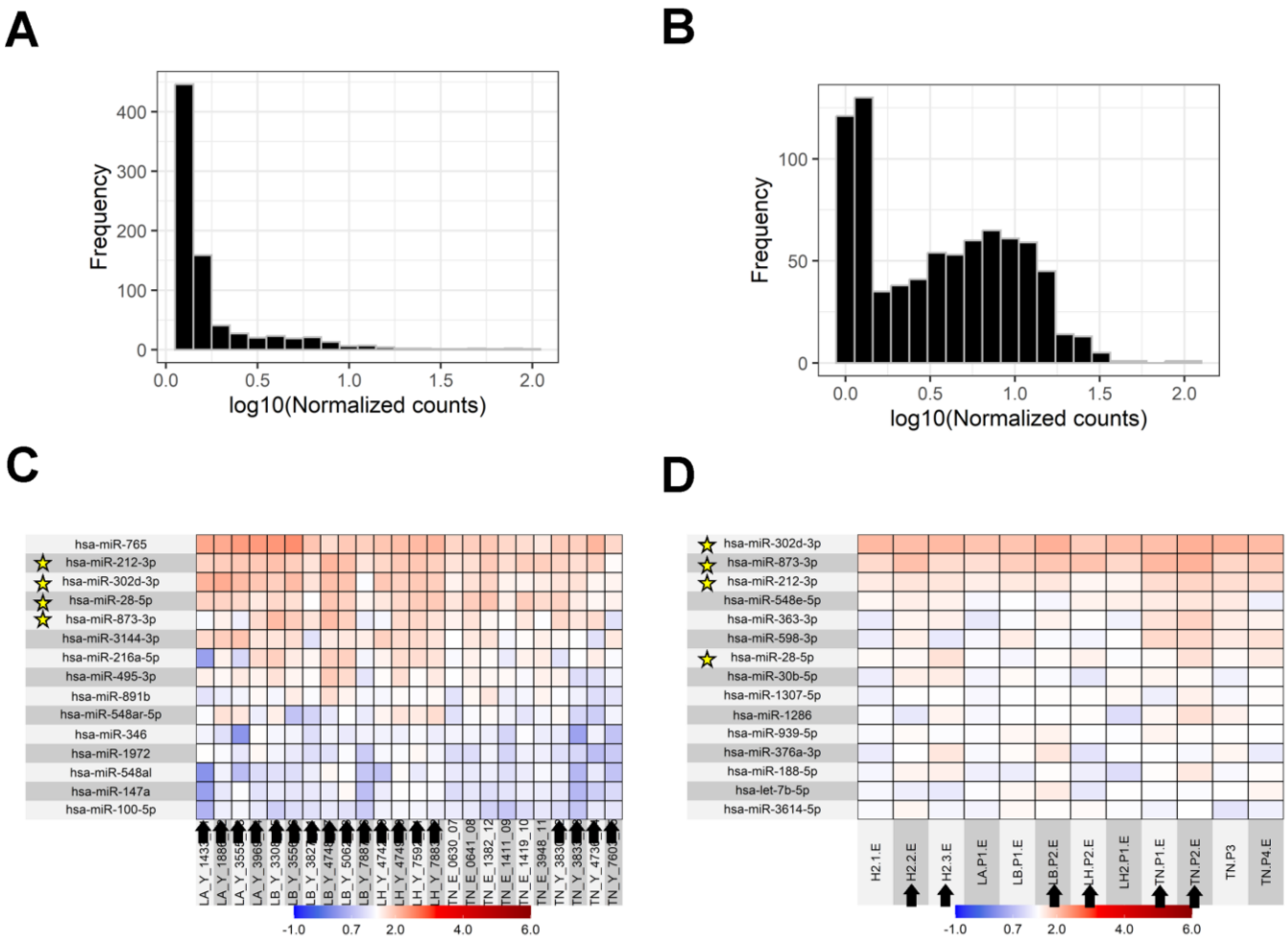

Figure 30. Profile of vesicular miRNA in the two evaluated cohorts. (A-B) Histogram showing median level expression of evaluated miRNAs isolated by one (A) or two (B) elution steps. (C-D) Heatmap showing the top 15 miRNAs expressed in both cohorts: (C) Cohort B eluted one time and (D) Cohort A eluted twice. Black arrows indicate samples from patients diagnosed with breast cancer before 40 years old (Young groups). Yellow stars indicate repeated miRNAs between both lists. Figures were built on the R software v.4.3.1. H2: HER2+ subtype, LA: Luminal A subtype, LB: Luminal B subtype, LH2: Luminal HER2 subtype, TN: Triple-Negative subtype.

More importantly, two of these four miRNAs were also represented in the plasma cf-miRNA profile (Figure 10). The presence of the top two common vesicular miRNAs (hsa-miR-212-3p and hsa-miR-302d-3p) in the cf-miRNA profile could be indicative of the contribution of vesicular cargo to the circulating material that can be obtained from plasma.

As research on vesicular cargo for cancer specimens is still under development, there is restricted information for these miRNAs in the BC context. However, according to previous functional studies, many of these miRNAs have dual functions pro- or anti-tumor.

The hsa-miR-212-3p was found to be upregulated in BC tumors [313]. However, it was proven to regulate *VEGFA* via *SP1* to inhibit angiogenesis [314]. Then, the inhibition of hsa-miR-212-3p could promote BC progression [315,316]. However, the combined overexpression of hsa-miR-132 and hsa-miR-212 can induce drug resistance in BC tumors and cells [317].

Though some studies have associated overexpression of hsa-miR-302d-3p with inhibition of tumor features (for example, migration, metastasis, and epithelium-to-mesenchymal transition) and sensitization to anti-cancer treatment [318–320], this miRNA has been indicated as a biomarker of occurrence of BC cancer [321].

Regarding hsa-miR-28-5p, previous research has featured this miRNA as a BC biomarker [210,322] despite other studies that suggest that inhibiting this miRNA could increase the aggressiveness of BC tumors [323]. Finally, hsa-miR-873-3p was also described as overexpressed in BC tumors against non-tumor samples [324].

Though there is no consensus about the miRNA marker of BC samples in EVs, it is a short list of miRNAs found between different liquid biopsy samples from BC patients [70]. Interestingly, hsa-miR-188 has been found in EVs isolated from plasma and serum of BC patients [268], and we found it as hsa-miR-188-5p in samples of cohort A (eluted twice, Figure 30D).

As a technical observation and according to our hypothesis, we reduced the presence of hemolysis-related miRNAs (hsa-miR-451a and hsa-miR-23a-3p) by performing an analysis only in EVs. Differentially from Figure 10, Figure 30 does not show these miRNAs. However, our collection of EVs may include a compilation of EV subpopulations produced by different cell types, including tumor cells. In addition, it is suggested to evaluate vesicular profiles performing a twice elution to ensure the detection of relevant regions for these samples (Figure 30B), avoiding misrepresented miRNA regions (Figure 30A) or the inclusion of contaminant factors (Figure 10C).

4.3.7 Differentially expressed vesicular miRNAs between BC patients

For this section, we ran similar comparisons between samples of cohort A as we did before for cf-miRNA. Interestingly, after applying the most restrictive cutoff (p<0.01 and Fold Change >2), we only found differences between Young vs. Elderly BC patients, TNBC vs. other subtypes, and HER2+ vs. other subtypes (Figure 31). As vesicular cargo contributes to the circulating material, but EVs are less abundant when compared with other plasma components [57–59,325,326], it is expected to see a different profile in the vesicular miRNA profile than in cf-miRNA analysis (Figure 11).

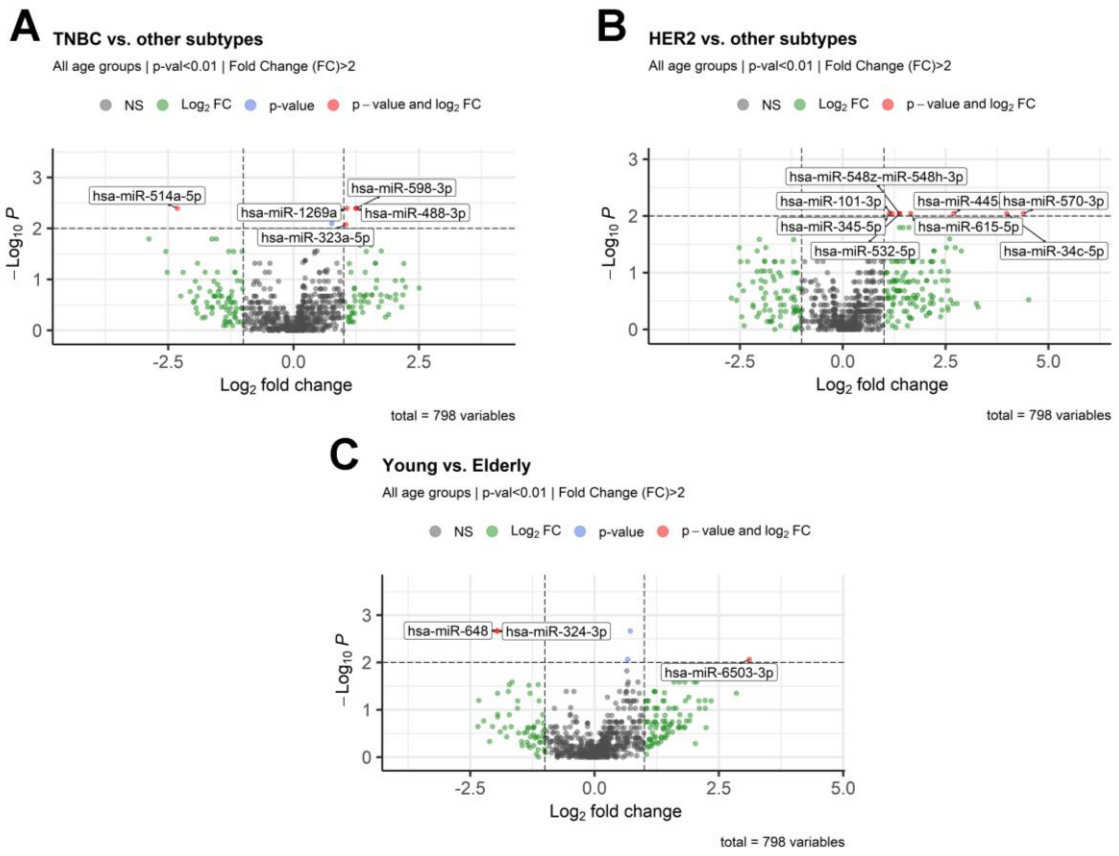

Figure 31. Volcano plots showing differentially expressed vesicular miRNAs according to BC subtypes (Cohort A). Comparison between patients belonging to a specific breast cancer group (immunohistochemical subtype or age-related group). (A) Triple-Negative Breast Cancer (TNBC, n=4) vs. other subtypes (n=8). (B) HER2+ subtype (n=3) vs. other subtypes (n=9). (C) Young (n=6) vs. Elderly (n=6) diagnosed cases of breast cancer. Differentially expressed regions were determined by a nominal p-value <0.01 and Fold Change >2. Volcano plots were built on the R software v.4.3.1.

Remarkably, patients of the TNBC subtype (n=4) presented overexpression of hsa-miR-598-3p, hsa-miR-1269a, hsa-miR-488-3p, and hsa-miR-323a-5p, whereas hsa-miR-514a-5p was downregulated when compared with vesicular miRNA cargo of patients with different subtypes (Figure 31A). Patients diagnosed with HER2+ BC subtype (n=3) were characterized by the overexpression of hsa-miR-548z/hsa-miR-548h-3p, hsa-miR-101-3p, hsa-miR-4458, hsa-miR-570-3p, hsa-miR-345-5p, hsa-miR-532-5p, hsa-miR-615-5p, and hsa-miR-34c-5p in their vesicles (Figure 31B).

Young diagnosed patients (n=6) showed higher levels of hsa-miR-6503-3p, whereas elderly diagnosed BC patients (n=6) were characterized by higher vesicular levels of hsa-miR-648 and hsa-miR-324-3p (Figure 31C). As reported in cf-miRNA levels, patients diagnosed with luminal subtypes did not show any representative vesicular miRNA using p-value<0.01 and fold change>2 as cutoffs.

4.3.8 Relevant vesicular miRNA regions in TNBC patients

In addition to miRNAs shown in Figure 31A, Table 9 presents 36 differentially expressed miRNAs (p<0.05). Among them, hsa-miR-30d-5p, hsa-miR-613, hsa-miR-514a-5p, hsa-miR-4421, hsa-miR-3605-3p, hsa-miR-128-3p, hsa-miR-3164, hsa-miR-1257, and hsa-miR-589-5p, were notably (FC>2) expressed in vesicles of non-TNBC patients and hsa-miR-323a-5p, hsa-miR-1269a, hsa-miR-1307-3p, hsa-miR-1273c, hsa-miR-450b-3p, hsa-miR-598-3p, hsa-miR-488-3p, hsa-miR-1278, hsa-miR-511-5p, hsa-miR-626, hsa-miR-323b-5p, hsa-miR-6511a-5p, hsa-miR-548i, and hsa-miR-331-5p were upregulated (FC>2) in vesicles from TNBC patients.

Interestingly, the hsa-miR-197-3p was downregulated in vesicular (Table 9) and circulating miRNA (Table 2) samples of TNBC patients. To validate these findings, we explored dot plots of these samples comparing TNBC and non-TNBC patients. Thus, Figure 32 shows these differences in circulating (Figure 32A) and vesicular (Figure 32B) profiles. In addition, young TNBC patients appear to have higher levels of this miRNA than elderly diagnosed patients of the same subtype, but we were unable to validate it in data from cohort B (p=0.48).

Table 9. Differentially expressed EV-miRNAs (p<0.05) between TNBC (n=4) and other BC subtypes (n=8) from cohort A.

miRNA	Relative expression in the TNBC subtype	Relative expression in other BC subtypes	Log_2 Fold Change (TNBC/others)	p-value	Adjusted p-value
hsa-miR-1269a	36.86	17.60	1.07	0.004	0.537
hsa-miR-1972	20.18	12.26	0.72	0.004	0.537
hsa-miR-212-3p	58.23	44.03	0.40	0.004	0.537
hsa-miR-488-3p	9.25	3.88	1.26	0.004	0.537
hsa-miR-514a-5p	1.15	5.72	-2.31	0.004	0.537
hsa-miR-598-3p	57.08	24.14	1.24	0.004	0.537
hsa-miR-363-3p	46.30	27.25	0.76	0.008	0.806
hsa-miR-323a-5p	3.38	1.64	1.05	0.008	0.806
hsa-miR-1273c	18.17	8.48	1.10	0.016	0.806
hsa-miR-128-3p	1.15	3.35	-1.54	0.016	0.806
hsa-miR-1307-3p	17.46	8.16	1.10	0.016	0.806
hsa-miR-302e	34.65	20.53	0.76	0.016	0.806
hsa-miR-30d-5p	1.16	8.52	-2.88	0.016	0.806
hsa-miR-3144-3p	30.80	20.43	0.59	0.016	0.806
hsa-miR-3605-3p	2.09	6.45	-1.63	0.016	0.806
hsa-miR-885-3p	24.77	13.90	0.83	0.016	0.806
hsa-miR-1278	4.11	1.64	1.33	0.022	0.868
hsa-miR-626	9.91	3.38	1.55	0.022	0.868
hsa-miR-548i	3.37	1.00	1.75	0.028	0.868
hsa-miR-556-5p	1.39	1.00	0.47	0.028	0.868
hsa-miR-1257	4.75	10.87	-1.19	0.028	0.868
hsa-miR-1286	35.11	26.08	0.43	0.028	0.868
hsa-miR-3164	2.38	5.83	-1.29	0.028	0.868
hsa-miR-511-5p	8.86	3.24	1.45	0.028	0.868
hsa-miR-589-5p	1.18	2.39	-1.02	0.028	0.868
hsa-miR-613	1.16	6.75	-2.55	0.028	0.868
hsa-miR-517b-3p	1.38	1.03	0.42	0.031	0.878
hsa-miR-1249-3p	1.18	1.00	0.23	0.043	0.878
hsa-miR-582-3p	1.18	1.00	0.23	0.043	0.878
hsa-miR-7-5p	1.18	1.00	0.23	0.043	0.878
hsa-miR-767-5p	1.18	1.00	0.23	0.043	0.878
hsa-let-7a-5p	1.18	1.03	0.19	0.047	0.878
hsa-miR-1226-3p	6.23	9.93	-0.67	0.048	0.878
hsa-miR-147a	23.15	12.71	0.86	0.048	0.878
hsa-miR-197-3p	2.30	3.91	-0.77	0.048	0.878
hsa-miR-323b-5p	9.85	3.18	1.63	0.048	0.878
hsa-miR-3614-5p	20.02	27.73	-0.47	0.048	0.878
hsa-miR-4421	3.51	13.19	-1.91	0.048	0.878
hsa-miR-6511a-5p	8.36	2.70	1.63	0.048	0.878
hsa-miR-331-5p	5.06	1.10	2.20	0.049	0.878
hsa-miR-450b-3p	2.38	1.10	1.11	0.049	0.878

BC: breast cancer; TNBC: Triple-negative breast cancer
P-values were obtained using the Mann-Whitney test and adjusted with the False Discovery Rate (FDR) method. Bold miRNAs indicate absolute fold change values higher than 2

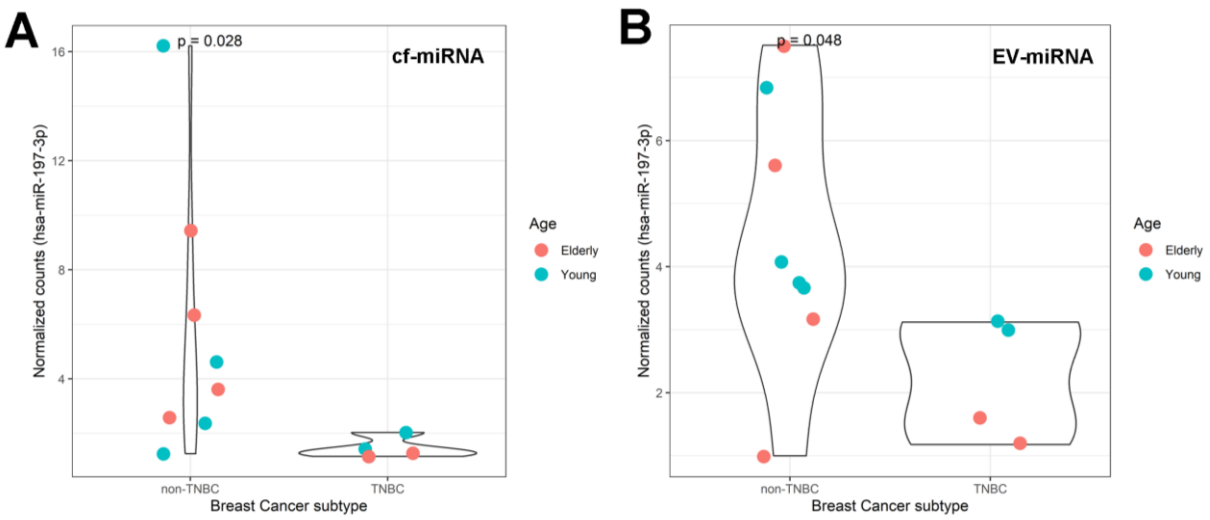

Figure 32. Dot plot of normalized values of hsa-miR-197-3p in plasma and EVs of Breast Cancer patients. Circulating (A) and Vesicular (B) levels of the hsa-miR-197-3p miRNA in samples of cohort A were plotted as a violin-dot plot stratifying samples according to their immunohistochemical subtype (into TNBC or non-TNBC groups) and age-related group. P-values were obtained using the Mann-Whitney test. Figure built on the R software v.4.3.1. TNBC: Triple-negative breast cancer.

The hsa-miR-197-3p was previously described as a circulating biomarker of prognosis in luminal BC patients [185,186,327]. In the context of BC, it was demonstrated that hsa-miR-197-3p can induce angiogenesis by regulating the expression of the *CYP4Z1* gene [328]. Therefore, it is possible that hsa-miR-197-3p could contribute to the prognosis assessment of non-TNBC patients, a group that includes luminal subtypes and the HER2+ subtype.

After evaluating the general profile of TNBC patients, we focused on the young diagnosed group. Using data from cohort A, Figure 33 shows relevant miRNAs between young TNBC (n=2) vs. other BC subtypes (n=4) diagnosed before 40 years old. This list of miRNAs includes hsa-miR-106a-5p/hsa-miR-17-5p, hsa-miR-1206, hsa-miR-198, hsa-miR-33a-5p, hsa-miR-484, hsa-miR-511-5p, hsa-miR-627-3p, and hsa-miR-630. Among them, the hsa-miR-511-5p was described in the analysis of all TNBC patients vs. other subtypes (Table 9), but this behavior was not observed in the cohort B (p=0.26).

According to the literature, the hsa-miR-511-5p miRNA is downregulated in BC tissues [329,330]. However, vesicular levels of this miRNA are attracting the attention of researchers [302,331–333] because hsa-miR-511-5p can be

upregulated in tumor-associated immune cells and act as a biomarker of immune response to BC [333,334].

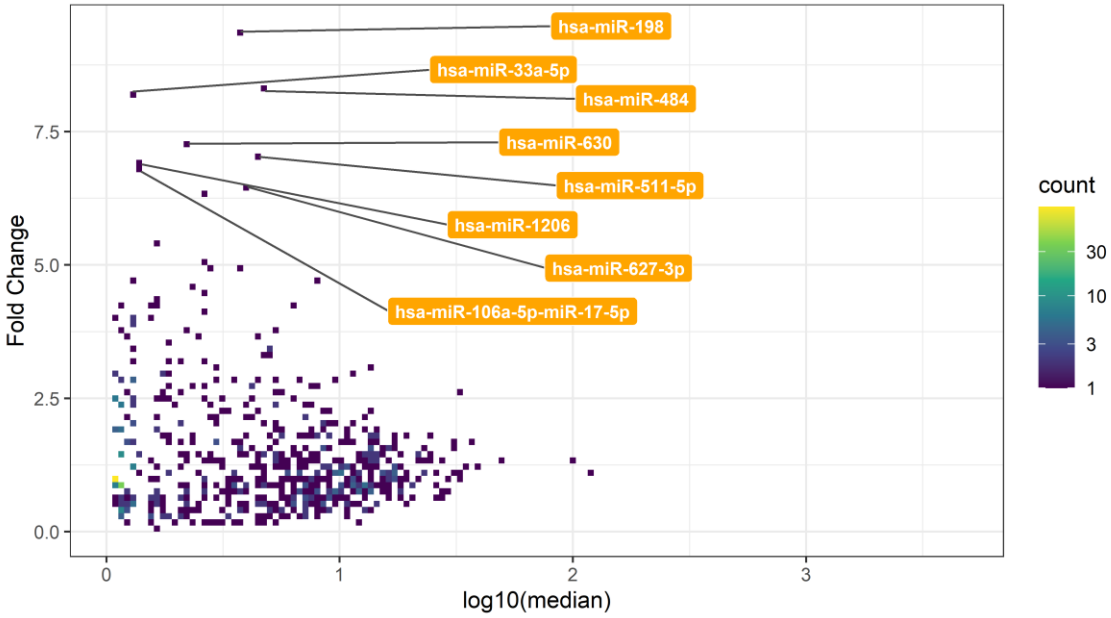

Figure 33. Relevant vesicular miRNAs in young diagnosed TNBC patients (Cohort A). This density plot shows all miRNA probes scanned in the Nanostring platform comparing Fold Change between TNBC (n=2) vs. other BC subtypes (n=4) in young diagnosed individuals (y-axis) in comparison with their median expression (log10) in all young diagnosed individuals (x-axis). Labeled miRNA fulfill some of these conditions: i) top 1% of Fold Change or ii) top 5% of Fold Change and top 5% of median abundance. Figure built on the R software v.4.3.1. The 3D representation of this plot can be accessed here: https://doi.org/10.6084/m9.figshare.24061572

Complementing the above-described results, data from cohort B can offer a statistical parameter about differentially expressed miRNAs between TNBC and non-TNBC young diagnosed patients. Though miRNAs indicated by Figure 33 did not retrieve a statistically significant result ($p<0.05$) in the analysis of young TNBC vs. non-TNBC samples from cohort B, it could be attributable to the differences in the processing of these cohorts. Nevertheless, this approach could be useful to propose additional miRNAs for this comparison. Thus, Figure 34 shows differentially expressed vesicular miRNAs from cohort B (young TNBC vs. young non-TNBC groups).

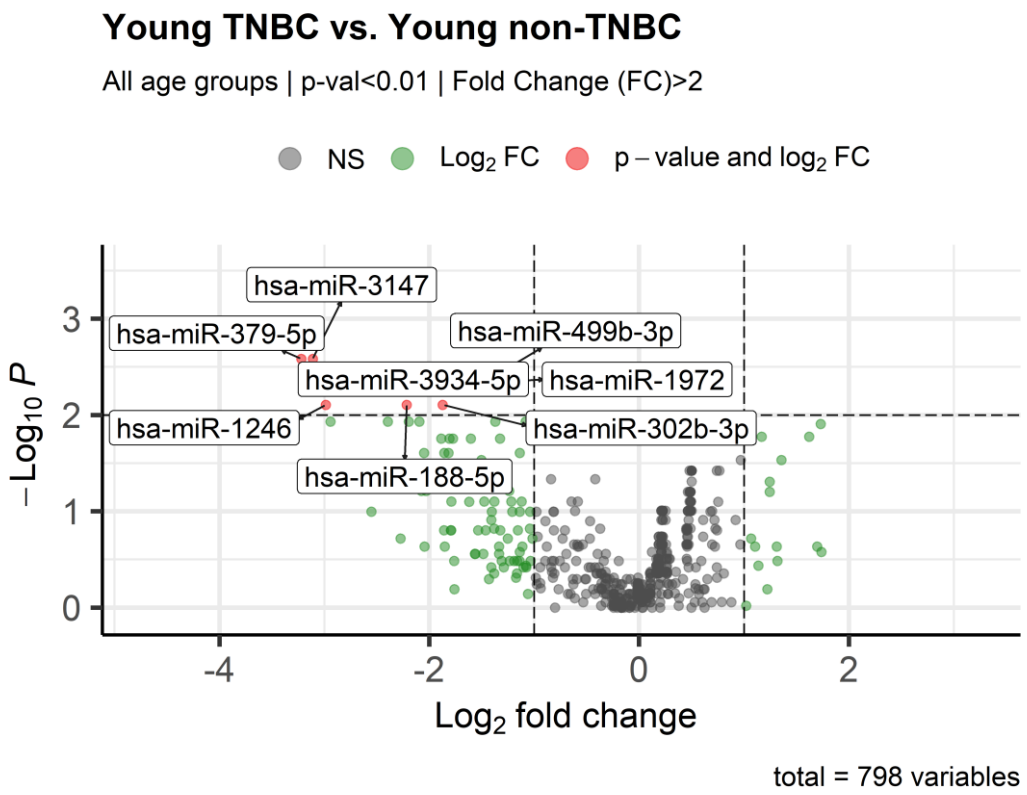

Figure 34. Volcano plot showing differentially expressed vesicular miRNAs in young diagnosed patients (Cohort B). Comparison between Triple-Negative Breast Cancer (TNBC, n=4) vs. other young-diagnosed subtypes (non-TNBC, n=14). Differentially expressed regions were determined by a nominal p-value <0.01 and Fold Change >2. Volcano plot built on the R software v.4.3.1.

According to this analysis, hsa-miR-3147, hsa-miR-379-5p, hsa-miR-1972, hsa-miR-3934-5p, hsa-miR-499b-3p, hsa-miR-1246, hsa-miR-188-5p, and hsa-miR-302b-3p are downregulated (p<0.01) in EVs from young TNBC patients from cohort B. In addition to the previously described research on hsa-miR-3147 [199] and hsa-miR-188-5p [268], other miRNAs haven been analyzed in the BC context.

For example, it was described that hsa-miR-379 belongs to a regulatory region called C14 (located at the 14q32.31 chromosomal band) that acts as a tumor suppressor [335–337]. Then, its subexpression in young TNBC patients could be related to a worse prognosis. The hsa-miR-3934-5p was

downregulated in plasma samples of colorectal cancer patients [338], suggesting their function against tumors. In addition, it was verified that cancer cells package and release hsa-miR-3934-5p into vesicles by the action of EWI-2 [339].

The hsa-miR-1972 was upregulated in blood samples of BC patients [340] and it has been proved the presence of this miRNA in plasma and EVs from cancer patients [341,342]. As the hsa-miR-1246 is overexpressed in EVs and other circulating forms in non-TNBC patients, this miRNA was extensively characterized and used to standardize protocols evolving non-TNBC subtypes [88,216,343–353], which include modern strategies to select EVs using Au nanoflare probes [347], molecular beacons [352], and a universal catalytic hairpin assembly system [353].

Regarding hsa-miR-302b-3p, it is known that some controversial reports have been published related to their over- or sub-expression in BC samples [354–356]. However, this observation could be biased as there is unknown information about the immunohistochemical subtype of these patients. Moreover, it was reported that hsa-miR-302b has a modulatory function of p21 [224], and this miRNA can sensitize BC cells to the chemotherapeutic drug cisplatin by inhibiting the E2F family [357].

After these observations, data from cohort B can offer a statistical parameter about differentially expressed miRNAs in EVs of young and elderly TNBC patients. Figure 35 shows differentially expressed miRNAs ($p<0.01$ and Fold Change>2) in patients whose sample input was established by the volume of EVs collected from plasma. According to these results, elderly TNBC patients express more hsa-miR-1266-5p, hsa-miR-1287-5p, hsa-miR-199a-5p, hsa-miR-520h, and hsa-miR-584-5p levels in their EVs. In addition, Table 10 shows the relevant miRNAs of this comparison in a less restrictive cutoff ($p<0.05$, Fold Change>2).

Interestingly, we found that some miRNAs altered between young and elderly TNBC patients from cohort B (Table 10) also demonstrated a trend to be dysregulated in patients from cohort A (Figure 36). In vesicular miRNA observations from cohort A, we did not consider the statistical values since there were not enough samples to do it.

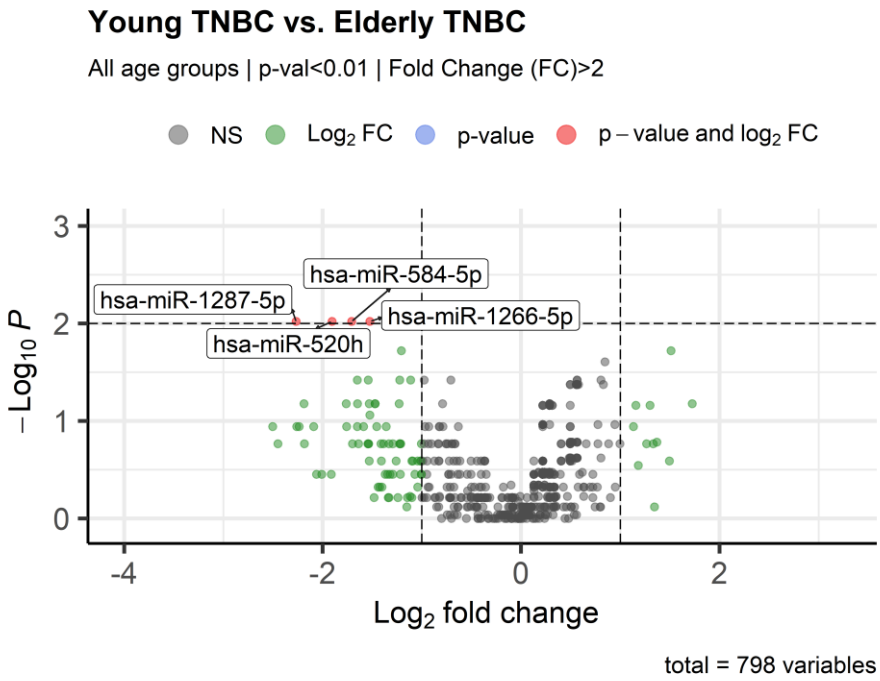

Figure 35. Volcano plot showing differentially expressed vesicular miRNAs according to age-related groups in TNBC patients (cohort B). Analysis performed with vesicular levels of miRNAs from Young TNBC (n=4) and Elderly TNBC (n=6) patients. Differentially expressed regions were determined by a nominal p-value <0.01 and Fold Change >2. Volcano plot built on the R software v.4.3.1.

Table 10. Differentially expressed EV-miRNAs (p<0.05, FC>2) between young TNBC (n=4) and elderly TNBC (n=6) patients from cohort B.

miRNA	Relative expression in young TNBC patients	Relative expression in elderly TNBC patients	Log_2 Fold Change (young TNBC/ elderly TNBC)	p-value	Adjusted p-value
hsa-miR-1266-5p	4.87	14.00	-1.52	0.010	0.239
hsa-miR-1287-5p	1.93	9.30	-2.27	0.010	0.239
hsa-miR-520h	1.35	5.06	-1.90	0.010	0.239
hsa-miR-584-5p	2.21	7.20	-1.71	0.010	0.239
hsa-miR-2053	2.92	6.74	-1.21	0.019	0.239
hsa-miR-423-5p	3.15	1.11	1.51	0.019	0.239
hsa-miR-499b-3p	1.38	5.72	-2.06	0.019	0.239
hsa-miR-507	1.35	4.18	-1.63	0.019	0.239
hsa-miR-520c-3p	1.96	8.07	-2.04	0.019	0.239
hsa-miR-525-5p	1.35	5.32	-1.98	0.019	0.239
hsa-miR-616-3p	1.35	4.09	-1.60	0.019	0.239
hsa-miR-487a-3p	1.35	4.24	-1.65	0.038	0.239
hsa-miR-548e-5p	5.29	11.43	-1.11	0.038	0.239
hsa-miR-642a-5p	1.70	3.97	-1.22	0.038	0.239
hsa-miR-939-5p	2.96	8.61	-1.54	0.038	0.239

BC: breast cancer; TNBC: Triple-negative breast cancer
P-values were obtained using the Mann-Whitney test and adjusted with the False Discovery Rate (FDR) method. Bold miRNAs indicate absolute fold change values higher than 2

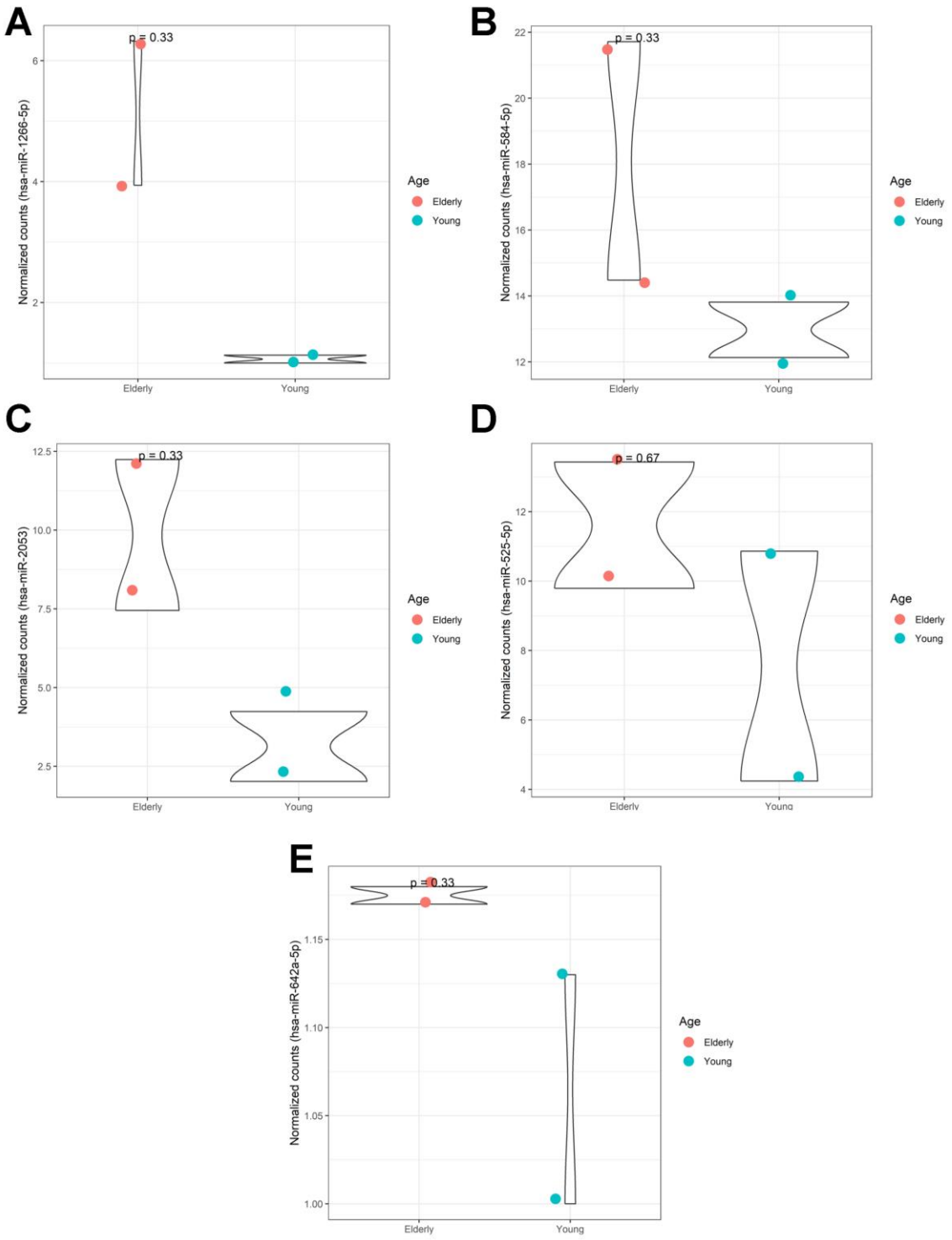

Figure 36. Cohort A profile of differentially expressed vesicular miRNAs between young vs. elderly TNBC patients from cohort B. After selecting differentially expressed miRNAs from cohort B samples ($p<0.05$, $FC>2$), we showed miRNAs with similar trend in TNBC samples from cohort A. Vesicular levels of hsa-miR-1266-5p (A), hsa-miR-584-5p (B), hsa-miR-2053 (C), hsa-miR-525-5p (D), and hsa-miR-642a-5p (E) miRNAs in samples of cohort A were plotted as a violin-dot plot stratifying samples according to their age-related group. P-values were obtained using the Mann-Whitney test. Figures built on the R software v.4.3.1.

Among potential biomarkers of young and elderly TNBC patients, we found vesicular versions of hsa-miR-1266-5p, hsa-miR-584-5p, hsa-miR-2053, hsa-miR-525-5p, and hsa-miR-642a-5p. Although this type of comparison is less studied worldwide, proposed miRNAs have been studied in the BC context.

The hsa-miR-1266 was overregulated in BC tumors expressing Estrogen receptors (Luminal-like subtypes) that presented metastasis/occurrence [358]. In a study involving BC cell lines expressing Estrogen receptors, hsa-miR-584 was activated by a progesterone receptor (PR-A) [359]. Interestingly, the hsa-miR-2053 has been compared between TNBC and non-TNBC samples of patients with Hispanic or Latin ancestries to evaluate if their levels are influenced by copy number alterations in their corresponding chromosomal region (8q23.3) [360]. The patients of this study were elderly diagnosed with TNBC and showed higher levels of hsa-miR-2053 [360], consistent with the present thesis. Then, it is possible that copy number variations subsequent to the tumoral process could be a genome-based cause of miRNA dysregulation in liquid biopsy sources.

The overexpression of hsa-miR-525-5p in BC tissues was associated with lower tumor relapse rates [361].Then, a study using cells and tissue samples of TNBC determined that the inhibition of hsa-miR-525-5p can increase the aggressiveness of tumors [362], while other researchers demonstrated that the genomic regions of this miRNA is differentially methylated in BC [363]. Finally, circulating levels of hsa-miR-642a were indicated as a biomarker for treatment prediction response in HER2+ BC patients from the NeoALTTO trial [364].

4.3.9 Relevant vesicular miRNA regions in HER2+ BC patients

Table 11 shows differentially expressed vesicular miRNAs ($p<0.05$) between HER2+ patients and BC patients with other subtypes (Luminal A, Luminal B, Luminal HER2, and TNBC). Notably, HER2+ BC subtypes showed several dysregulated vesicular miRNAs, similar to results reported in cf-miRNAs (Table 3). Nevertheless, no miRNAs were found repeated in both lists. The hsa-miR-376c-3p, hsa-miR-205-5p, hsa-miR-2110, hsa-miR-298, hsa-miR-4741, hsa-miR-147a, hsa-miR-1273c, hsa-miR-323a-5p were downregulated in EVs of HER2+ BC patients ($p<0.05$, $FC<0.5$).

Table 11. Differentially expressed EV-miRNAs ($p<0.05$) between HER2+ (n=3) and other BC subtypes (n=9) from cohort A

miRNA	Relative expression in the HER2+ BC subtype (n=3)	Relative expression in other BC subtypes (n=9)	Log_2 Fold Change (HER2+/others)	p-value	Adjusted p-value
hsa-miR-101-3p	20.42	8.90	1.20	0.009	0.700
hsa-miR-345-5p	16.31	7.45	1.13	0.009	0.700
hsa-miR-34c-5p	18.56	1.17	3.99	0.009	0.700
hsa-miR-4458	10.33	1.59	2.70	0.009	0.700
hsa-miR-532-5p	13.00	4.97	1.39	0.009	0.700
hsa-miR-548z-miR-548h-3p	12.89	4.97	1.37	0.009	0.700
hsa-miR-570-3p	24.52	1.17	4.39	0.009	0.700
hsa-miR-615-5p	20.42	6.50	1.65	0.009	0.700
hsa-miR-1233-3p	5.59	1.13	2.31	0.015	0.700
hsa-miR-1224-5p	10.22	1.17	3.13	0.016	0.700
hsa-miR-1910-5p	15.45	5.95	1.38	0.016	0.700
hsa-miR-491-5p	10.33	3.74	1.47	0.016	0.700
hsa-miR-506-3p	12.08	3.96	1.61	0.016	0.700
hsa-miR-1273c	5.06	12.68	-1.33	0.018	0.700
hsa-miR-147a	8.37	22.75	-1.44	0.018	0.700
hsa-miR-3164	8.37	4.23	0.98	0.018	0.700
hsa-miR-383-5p	11.19	3.00	1.90	0.018	0.700
hsa-miR-4741	1.39	4.08	-1.55	0.018	0.700
hsa-miR-450b-5p	6.92	1.14	2.60	0.025	0.700
hsa-miR-2110	1.00	4.08	-2.03	0.026	0.700
hsa-miR-323a-5p	1.00	2.28	-1.19	0.026	0.700
hsa-miR-181a-3p	14.60	10.86	0.43	0.036	0.700
hsa-miR-18b-5p	2.81	1.14	1.30	0.036	0.700
hsa-miR-195-5p	7.78	1.17	2.73	0.036	0.700
hsa-miR-298	2.28	8.35	-1.87	0.036	0.700
hsa-miR-3605-5p	12.08	7.51	0.69	0.036	0.700
hsa-miR-374a-3p	13.75	5.28	1.38	0.036	0.700
hsa-miR-374c-5p	10.33	3.96	1.38	0.036	0.700
hsa-miR-376c-3p	1.39	7.96	-2.52	0.036	0.700
hsa-miR-409-3p	13.00	2.26	2.52	0.036	0.700
hsa-miR-450a-1-3p	13.93	5.90	1.24	0.036	0.700
hsa-miR-514a-3p	6.92	2.68	1.37	0.036	0.700
hsa-miR-519b-3p	8.37	2.76	1.60	0.036	0.700
hsa-miR-548d-5p	16.71	6.78	1.30	0.036	0.700
hsa-miR-548j-3p	14.86	9.12	0.70	0.036	0.700
hsa-miR-664a-3p	16.18	7.62	1.09	0.036	0.700
hsa-miR-660-5p	2.66	1.13	1.24	0.041	0.700
hsa-miR-125a-5p	2.66	1.14	1.22	0.042	0.700
hsa-miR-205-5p	1.00	4.23	-2.08	0.042	0.700
hsa-miR-378h	5.22	1.13	2.21	0.042	0.700
hsa-miR-887-3p	8.63	1.17	2.88	0.042	0.700
hsa-miR-890	7.44	1.59	2.23	0.042	0.700

BC: breast cancer

P-values were obtained using the Mann-Whitney test and adjusted with the False Discovery Rate (FDR) method. Bold miRNAs indicate absolute fold change values higher than 2.

On the other hand, vesicular versions of hsa-miR-664a-3p, hsa-miR-345-5p, hsa-miR-101-3p, hsa-miR-125a-5p, hsa-miR-660-5p, hsa-miR-450a-1-3p, hsa-miR-548d-5p, hsa-miR-18b-5p, hsa-miR-514a-3p, hsa-miR-548z-miR-548h-3p, hsa-miR-1910-5p, hsa-miR-374a-3p, hsa-miR-374c-5p, hsa-miR-532-5p, hsa-miR-491-5p, hsa-miR-519b-3p, hsa-miR-506-3p, hsa-miR-615-5p, hsa-miR-383-5p, hsa-miR-378h, hsa-miR-890, hsa-miR-1233-3p, hsa-miR-409-3p, hsa-miR-450b-5p, hsa-miR-4458, hsa-miR-195-5p, hsa-miR-887-3p, hsa-miR-1224-5p, hsa-miR-34c-5p, and hsa-miR-570-3p were consistently overexpressed in HER2+ BC patients from cohort A ($p<0.05$, $FC>2$).

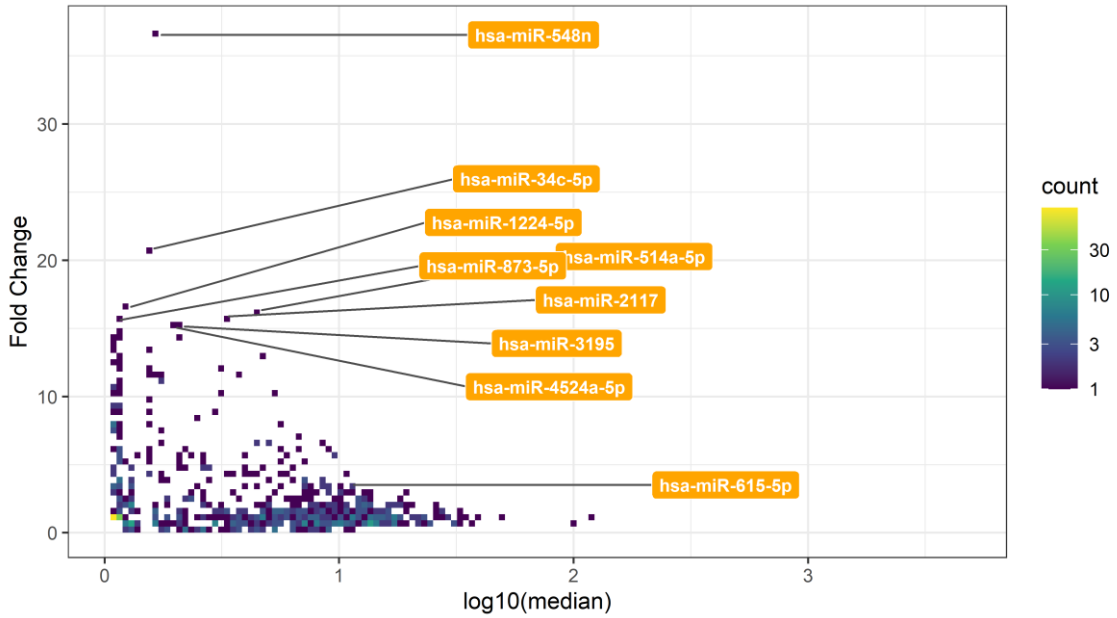

Figure 37. Relevant vesicular miRNAs in young diagnosed HER2+ BC patients (Cohort A). This density plot shows all miRNA probes scanned in the Nanostring platform comparing Fold Change between HER2+ (n=2) vs. other BC subtypes (n=4) in young diagnosed individuals (y-axis) in comparison with their median expression (log10) in all young diagnosed individuals (x-axis). Labeled miRNA fulfill some of these conditions: i) top 1% of Fold Change or ii) top 20% of Fold Change and top 20% of median abundance. Figure built on the R software v.4.3.1. The 3D representation of this plot can be accessed here: https://doi.org/10.6084/m9.figshare.24081507

Then, we explored the landscape of relevant vesicular miRNAs in young diagnosed patients from cohort A. Figure 37 shows relevant miRNAs found in

EVs from HER2+ BC patients. Remarkably, hsa-miR-1224-5p, hsa-miR-2117, hsa-miR-3195, hsa-miR-34c-5p, hsa-miR-4524a-5p, hsa-miR-514a-5p, hsa-miR-548n, hsa-miR-615-5p, and hsa-miR-873-5p showed higher fold change values between young diagnosed HER2+ BC patients and individuals diagnosed with other BC subtypes.

We found three miRNAs in common from both lists (Table 11 and Figure 37): hsa-miR-1224-5p, hsa-miR-34c-5p, and hsa-miR-615-5p. To validate these findings in cohort A, we plotted comparative dot plots for all samples (colored by age-related groups) and young diagnosed BC patients. Figure 38 confirms that these three miRNAs are more expressed in vesicles from BC patients overexpressing HER2 receptors in their tumors. From the literature, we get information about these miRNAs. The subexpression of hsa-miR-1224-5p in BC tissues was related to better overall survival [365]. In contrast, low hsa-miR-34c plasma levels were associated with worse prognosis in TNBC patients [366], this miRNA was considered as tumor suppressor [367–369], and it could be indirectly regulated by hsa-miR-21 [367]. Though we previously described some studies in hsa-miR-615-3p, there is limited information for their -5p counterpart. Then, it was published that hsa-miR-615-5p can act as an anti-angiogenic miRNA by targeting endothelial cell (EC) VEGFAKT/eNOS signaling [370]. As cohort B does not include a group of HER2+ BC patients, we cannot evaluate this profile in additional samples.

4.3.10 Relevant vesicular miRNA regions in Luminal BC patients

Due to the limited number of samples belonging to the Luminal A subtype in cohort A (n=1), we performed a comparative analysis focusing on vesicular miRNAs with higher fold change values between the Luminal A BC patient vs. all others. Table 12 shows the top15 expressed miRNAs that include: hsa-miR-144-3p, hsa-miR-128-3p, hsa-miR-578, hsa-miR-206, hsa-miR-1204, hsa-miR-30a-5p, hsa-miR-148a-3p, hsa-miR-675-5p, hsa-miR-499a-3p, hsa-miR-1287-3p, hsa-miR-1305, hsa-miR-30e-5p, hsa-miR-1272, hsa-miR-130a-3p, and hsa-miR-211-3p. None of these miRNAs were found in the top15 cf-miRNA list from the same cohort (Table 4).

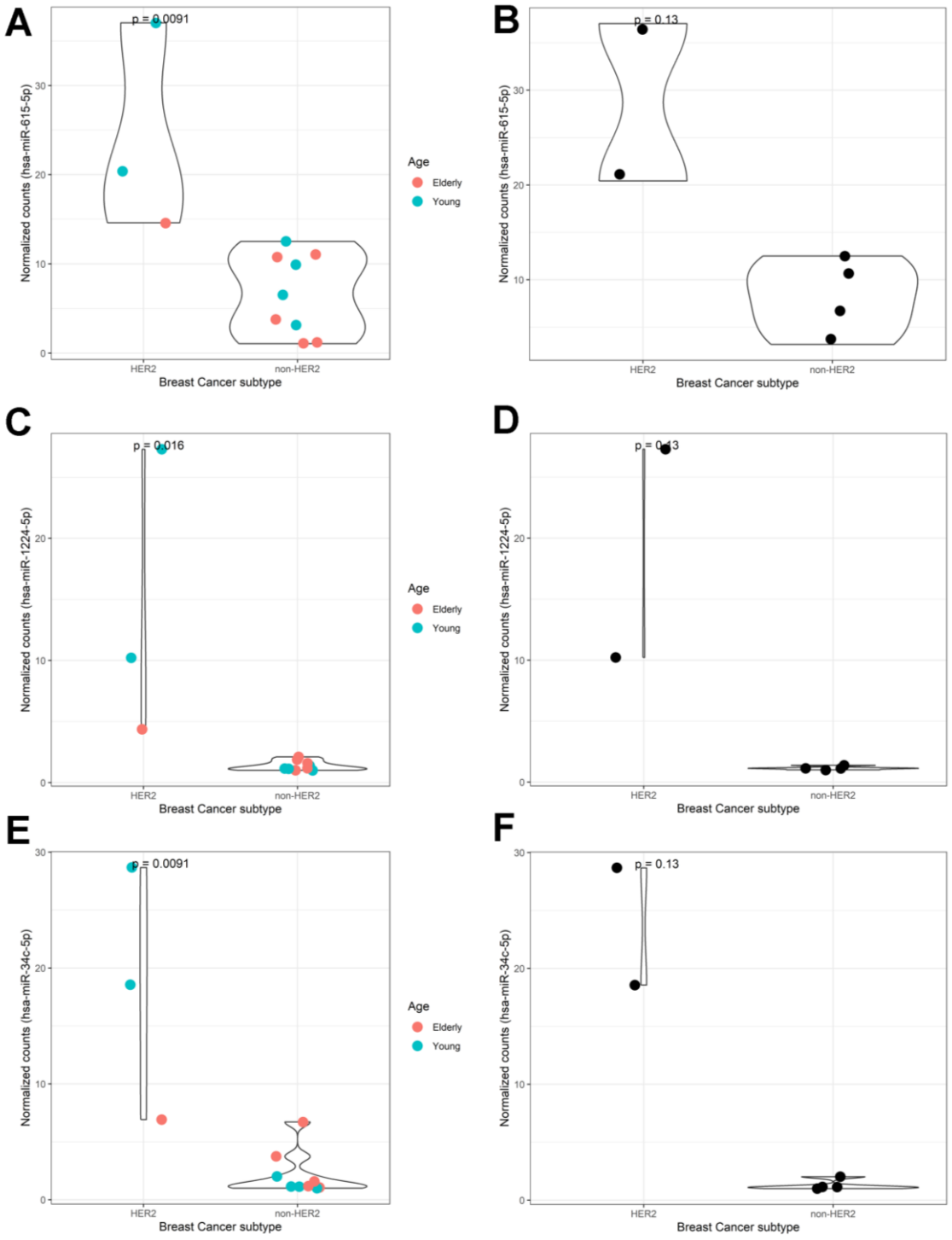

Figure 38. Cohort A profile of differentially expressed vesicular miRNAs between HER2+ BC patients and other subtypes. After selecting differentially expressed miRNAs in HER2+ BC patients ($p<0.05$, $FC>2$), we showed that some miRNAs have a similar trend in young diagnosed patients of this cohort. Vesicular levels of hsa-miR-615-5p (A and B), hsa-miR-1224-5p (C and D), and hsa-miR-34c-5p (E and F) miRNAs in all samples (A, C, and E) or young diagnosed (B, D, and F) of cohort A were plotted as a violin-dot plot. Figures A, C, and E show samples color-stratified according to their age-related group. P-values were obtained using the Mann-Whitney test. Figures built on the R software v.4.3.1.

Table 12. Top 15 EV-miRNAs between Luminal A (n=1) and other BC subtypes (n=11) from Cohort A

miRNA	Relative expression in the Luminal A subtype (n=1)	Relative expression in other BC subtypes (n=11)	Log_2 Fold Change (LumA/others)	p-value	Adjusted p-value
hsa-miR-144-3p	11.63	1.18	3.30	0.243	1.000
hsa-miR-128-3p	12.68	1.39	3.19	0.167	1.000
hsa-miR-578	10.57	1.17	3.18	0.246	1.000
hsa-miR-206	10.57	1.18	3.16	0.147	1.000
hsa-miR-1204	7.40	1.13	2.71	0.230	1.000
hsa-miR-30a-5p	6.34	1.13	2.49	0.133	1.000
hsa-miR-148a-3p	6.34	1.14	2.48	0.238	1.000
hsa-miR-675-5p	7.40	1.39	2.41	0.381	1.000
hsa-miR-499a-3p	11.63	2.28	2.35	0.167	1.000
hsa-miR-1287-3p	9.51	1.90	2.32	0.145	1.000
hsa-miR-1305	13.74	2.82	2.28	0.167	1.000
hsa-miR-30e-5p	5.28	1.14	2.21	0.238	1.000
hsa-miR-1272	5.28	1.14	2.21	0.555	1.000
hsa-miR-130a-3p	5.28	1.17	2.17	0.140	1.000
hsa-miR-211-3p	5.28	1.17	2.17	0.243	1.000

BC: breast cancer; LumA: Luminal A
P-values were obtained using the Mann-Whitney test and adjusted with the False Discovery Rate (FDR) method. Bold miRNAs indicate absolute fold change values higher than 2.

In addition, data from cohort B allow us to get differentially expressed vesicular miRNAs by inputting the same volume of plasma. According to Table 13, there are 21 deregulated vesicular miRNAs in the young diagnosed Luminal A group ($p<0.05$, $FC>2$).

This list includes hsa-miR-23c, hsa-miR-513a-5p, hsa-miR-325, hsa-miR-526a/hsa-miR-518c-5p/hsa-miR-518d-5p, hsa-miR-1295a, hsa-miR-6724-5p, hsa-miR-548i, hsa-miR-548z/hsa-miR-548h-3p, hsa-miR-513c-5p, hsa-miR-381-3p, hsa-miR-340-5p, hsa-miR-765, hsa-miR-548e-5p, hsa-miR-612, hsa-miR-2053, hsa-miR-764, hsa-miR-1270, hsa-miR-616-3p, hsa-miR-1266-5p, hsa-miR-507, and hsa-miR-519d-3p. Among them, the hsa-miR-765 showed a higher abundance in the sample, which could offer more chances to detect this miRNA using affordable and less sensitive techniques [371,372].

In a more restrictive filter (p<0.01, FC>2), hsa-miR-23c, hsa-miR-513a-5p, and hsa-miR-325 demonstrated to have their vesicular expression altered in the Luminal A group from cohort B (Figure 39).

Table 13. Differentially expressed EV-miRNAs (p<0.05, FC>2) between Luminal A (n=4) and other BC subtypes (n=14) from Cohort B

miRNA	Relative expression in the young Luminal A subtype (n=4)	Relative expression in other young BC subtypes (n=14)	Log_2 Fold Change (LumA/others)	p-value	Adjusted p-value
hsa-miR-23c	1.59	10.34	-2.70	0.001	0.379
hsa-miR-513a-5p	1.66	9.12	-2.46	0.001	0.379
hsa-miR-325	8.83	3.94	1.16	0.008	0.379
hsa-miR-526a-miR-518c-5p-miR-518d-5p	12.79	3.55	1.85	0.012	0.379
hsa-miR-1295a	4.47	11.05	-1.31	0.018	0.379
hsa-miR-6724-5p	6.49	1.38	2.24	0.018	0.379
hsa-miR-548i	8.93	1.44	2.63	0.025	0.379
hsa-miR-381-3p	9.77	1.35	2.86	0.029	0.379
hsa-miR-513c-5p	3.34	1.28	1.39	0.029	0.379
hsa-miR-548z-miR-548h-3p	2.78	1.23	1.18	0.029	0.379
hsa-miR-2053	18.43	4.72	1.97	0.035	0.379
hsa-miR-340-5p	1.59	4.24	-1.41	0.035	0.379
hsa-miR-548e-5p	20.84	9.61	1.12	0.035	0.379
hsa-miR-612	19.05	5.90	1.69	0.035	0.379
hsa-miR-764	9.24	1.44	2.68	0.035	0.379
hsa-miR-765	197.10	94.65	1.06	0.035	0.379
hsa-miR-1270	3.54	1.22	1.54	0.038	0.379
hsa-miR-616-3p	5.05	1.28	1.98	0.038	0.379
hsa-miR-1266-5p	1.60	5.91	-1.89	0.044	0.379
hsa-miR-507	4.33	1.31	1.72	0.046	0.379
hsa-miR-519d-3p	4.62	1.31	1.82	0.049	0.379

BC: breast cancer; LumA: Luminal A
P-values were obtained using the Mann-Whitney test and adjusted with the False Discovery Rate (FDR) method. Bold miRNAs indicate absolute fold change values higher than 2.

Consistently with our findings, the low expression of hsa-miR-23c was associated with good prognosis in BC tissues [373], and recently, Gallo et al. (2022) described a mechanism to induce a cross-talk between Mesenchymal Stem Cells (MSCs) and TNBC cells [198]. Then, it was proven that hsa-miR-

513a-5p can inhibit the expression of progesterone receptors in BC tissues [374]. Consequently, the expression of PRs in Luminal A patients (100% positive in cohort B, Appendix 2) could be related to the low expression of hsa-miR-513a-5p in vesicles. Finally, the hsa-miR-325 was related to modulation of the aggressiveness of BC tumors by targeting *S100A2* [375].

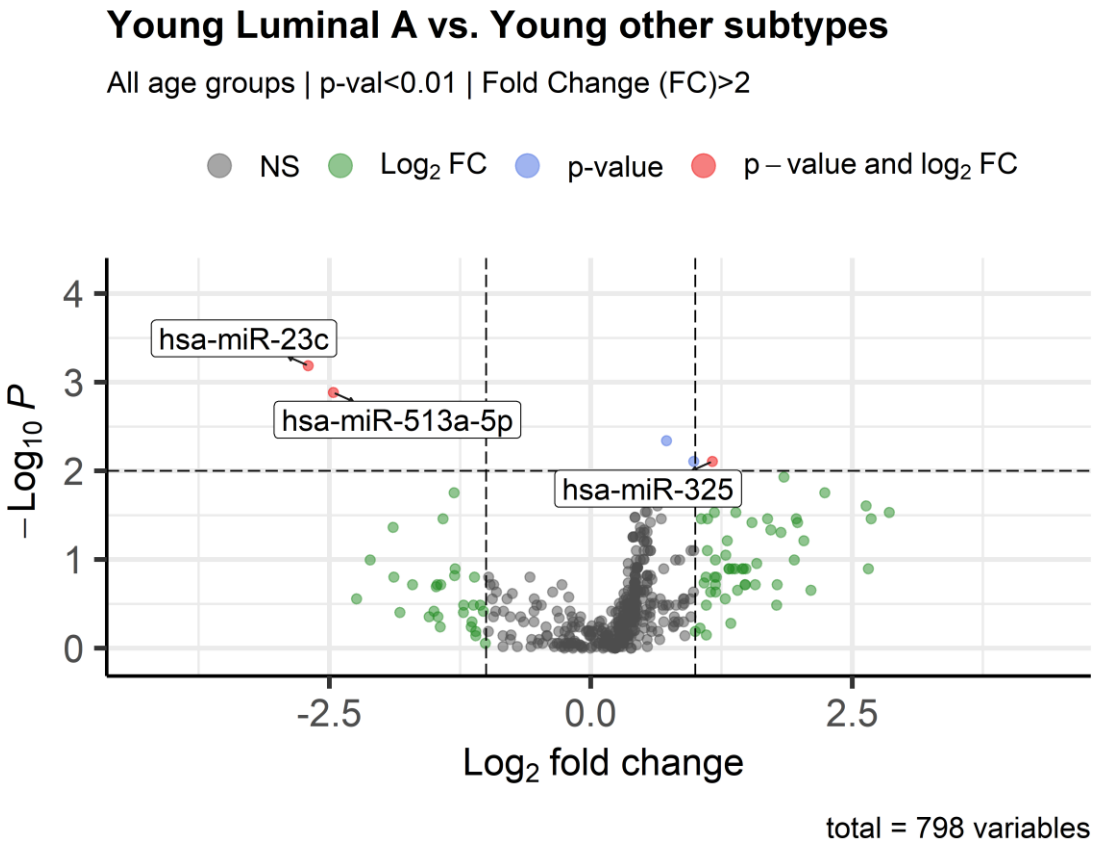

Figure 39. Volcano plot showing differentially expressed vesicular miRNAs between young Luminal A (n=4) and young other BC subtypes (n=14) from Cohort B. Differentially expressed regions were determined by a nominal p-value <0.01 and Fold Change >2. Volcano plot built on the R software v.4.3.1.

Regarding Luminal B patients, we initially explored differentially expressed vesicular miRNAs in cohort A. Table 14 shows miRNAs deregulated in EVs from Luminal B patients (p<0.05). Among remarkably regions (FC>2), we found the following miRNAs: hsa-miR-1302, hsa-miR-197-3p, hsa-miR-3168, hsa-miR-410-3p, hsa-miR-5001-3p, hsa-miR-5196-3p/hsa-miR-6732-3p, hsa-miR-876-5p, hsa-miR-330-5p, hsa-miR-642a-3p, hsa-miR-28-3p, and hsa-miR-617.

Interestingly, almost all of these regions were overexpressed in Luminal B patients, except hsa-miR-3168, which was notably sub-expressed.

Table 14. Differentially expressed EV-miRNAs (p<0.05) between Luminal B (n=2) and other BC subtypes (n=10) from Cohort A

miRNA	Relative expression in the Luminal B subtype (n=2)	Relative expression in other BC subtypes (n=10)	Log_2 Fold Change (LumB/others)	p-value	Adjusted p-value
hsa-miR-1302	12.59	5.02	1.33	0.030	1.000
hsa-miR-197-3p	7.17	3.15	1.19	0.030	1.000
hsa-miR-199b-5p	6.20	11.59	-0.90	0.030	1.000
hsa-miR-208b-3p	17.62	10.18	0.79	0.030	1.000
hsa-miR-3168	7.97	19.05	-1.26	0.030	1.000
hsa-miR-361-3p	19.15	10.00	0.94	0.030	1.000
hsa-miR-410-3p	14.37	6.96	1.05	0.030	1.000
hsa-miR-5001-3p	20.76	9.69	1.10	0.030	1.000
hsa-miR-5196-3p-miR-6732-3p	9.35	1.94	2.27	0.030	1.000
hsa-miR-876-5p	5.46	1.03	2.40	0.034	1.000
hsa-miR-330-5p	2.47	1.10	1.17	0.038	1.000
hsa-miR-642a-3p	6.43	1.16	2.48	0.039	1.000
hsa-miR-28-3p	11.45	4.08	1.49	0.041	1.000
hsa-miR-617	9.44	2.79	1.76	0.041	1.000

BC: breast cancer; LumB: Luminal B
P-values were obtained using the Mann-Whitney test and adjusted with the False Discovery Rate (FDR) method.
Bold miRNAs indicate absolute fold change values higher than 2.

Then, we focus on young diagnosed patients. Figure 41 shows relevant EV-miRNAs in Luminal B patients from cohort A. Among these miRNAs, we found hsa-miR-182-3p, hsa-miR-215-5p, hsa-miR-302f, hsa-miR-4488, hsa-miR-589-5p, hsa-miR-630, hsa-miR-887-3p, and hsa-miR-92b-3p. Subsequently, we explored differentially expressed miRNAs in vesicles from Luminal B patients of cohort B. Here we found ten miRNAs (p<0.05, FC>2) that includes hsa-miR-574-5p, hsa-miR-1234-3p, hsa-miR-877-5p, hsa-miR-382-3p, hsa-miR-1290, hsa-miR-665, hsa-miR-1307-3p, hsa-miR-764, hsa-miR-1268b, and hsa-miR-519d-3p. Figure 40 shows a restrictive selection of these results (p<0.01, FC>2). For Luminal B patients, we did not find miRNAs in more than one list.

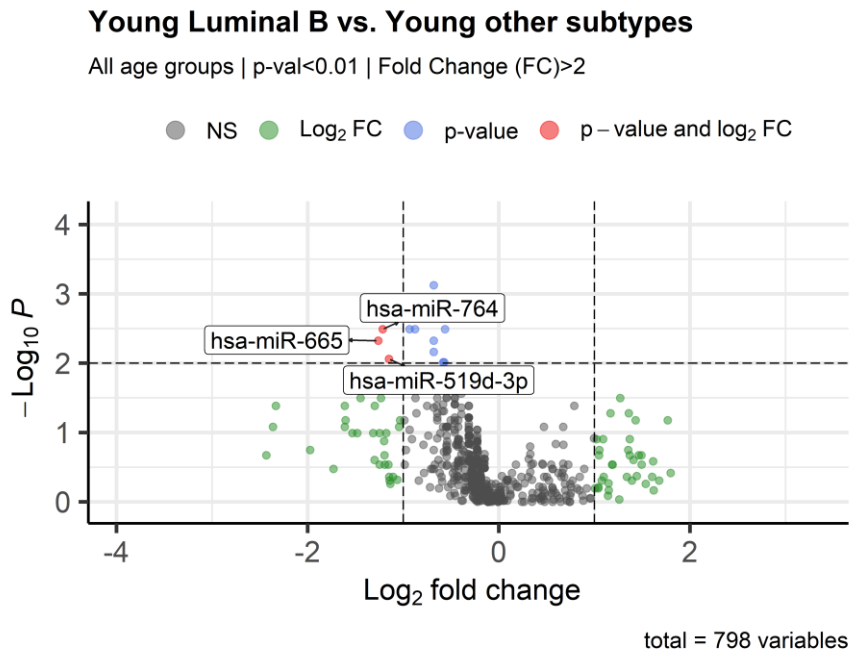

Figure 40. Volcano plot showing differentially expressed vesicular miRNAs between young Luminal B (n=6) and young other BC subtypes (n=12) from Cohort B. Differentially expressed regions were determined by a nominal p-value <0.01 and Fold Change >2. Volcano plot built on the R software v.4.3.1.

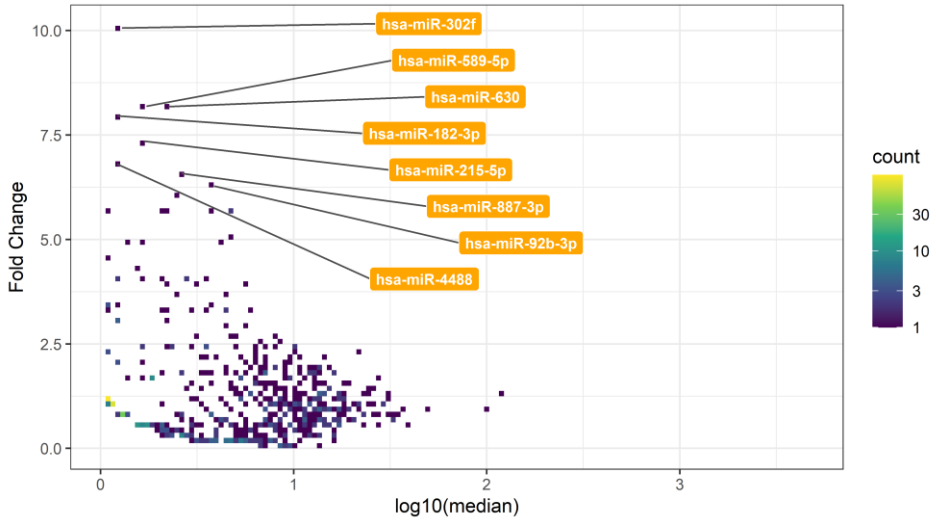

Figure 41. Relevant vesicular miRNAs in young diagnosed Luminal B patients (Cohort A). This density plot shows all miRNA probes scanned in the Nanostring platform comparing Fold Change between Luminal B (n=1) vs. other BC subtypes (n=5) in young diagnosed individuals (y-axis) in comparison with their median expression (log10) in all young diagnosed individuals (x-axis). Labeled miRNA fulfill some of these conditions: i) top 1% of Fold Change or ii) top 5% of Fold Change and top 5% of median abundance. Figure built on the R software v.4.3.1. The 3D representation of this plot can be accessed here: https://doi.org/10.6084/m9.figshare.24082293

Using data from Cohort A, we explored deregulated miRNAs in EVs of patients classified as Luminal HER2. In comparison with patients from other BC subtypes, patients of Luminal HER2 subtype showed altered expression of 25 miRNA regions (p<0.05, FC>2) as shown in Table 15. In this analysis, no miRNA showed a p-value less than 0.01.

Table 15. Differentially expressed EV-miRNAs (p<0.05, FC>2) between Luminal HER2 (n=2) and other BC subtypes (n=10) from Cohort A

miRNA	Relative expression in the Luminal HER2 subtype (n=2)	Relative expression in other BC subtypes (n=10)	Log_2 Fold Change (LumH2/others)	p-value	Adjusted p-value
hsa-miR-539-3p	1.19	5.64	-2.24	0.030	0.686
hsa-miR-664a-3p	2.37	10.12	-2.09	0.030	0.686
hsa-miR-515-3p	11.24	2.69	2.06	0.030	0.686
hsa-miR-142-3p	2.37	9.50	-2.00	0.030	0.686
hsa-miR-593-3p	9.85	2.79	1.82	0.030	0.686
hsa-miR-23b-3p	7.56	2.20	1.78	0.030	0.686
hsa-miR-769-5p	3.00	8.65	-1.53	0.030	0.686
hsa-miR-651-5p	5.76	16.05	-1.48	0.030	0.686
hsa-miR-92a-1-5p	8.02	3.09	1.38	0.030	0.686
hsa-miR-323b-3p	7.55	16.12	-1.10	0.030	0.686
hsa-miR-196a-5p	8.01	16.78	-1.07	0.030	0.686
hsa-miR-339-3p	10.73	5.30	1.02	0.030	0.686
hsa-miR-328-5p	3.47	1.10	1.66	0.038	0.686
hsa-miR-506-3p	1.00	6.95	-2.80	0.041	0.686
hsa-miR-548ak	1.00	5.02	-2.33	0.041	0.686
hsa-miR-576-5p	1.00	4.88	-2.29	0.041	0.686
hsa-miR-149-5p	1.00	4.68	-2.22	0.041	0.686
hsa-miR-5001-5p	1.64	7.51	-2.20	0.041	0.686
hsa-miR-1909-3p	1.00	3.82	-1.93	0.041	0.686
hsa-miR-625-5p	1.00	3.69	-1.88	0.041	0.686
hsa-miR-1255b-5p	1.00	3.20	-1.68	0.041	0.686
hsa-miR-3140-5p	1.00	2.97	-1.57	0.041	0.686
hsa-miR-345-3p	3.00	1.14	1.40	0.041	0.686
hsa-miR-411-5p	3.00	1.14	1.40	0.041	0.686
hsa-miR-3136-5p	1.00	2.27	-1.18	0.041	0.686

BC: breast cancer; LumH2: Luminal HER2
P-values were obtained using the Mann-Whitney test and adjusted with the False Discovery Rate (FDR) method. Bold miRNAs indicate absolute fold change values higher than 2.

Among these miRNAs, the hsa-miR-5001-5p calls attention as it was downregulated in Luminal HER2 patients in both vesicular and circulating versions (Table 6). To validate this finding, we plotted individual levels of this

miRNA in Figure 42. Though Zhou et al. (2020) have described that hsa-miR-5001-5p could be sponged by linc-ROR, a lncRNA promoter of oncogenesis [376], there is still limited information about this miRNA in the BC context.

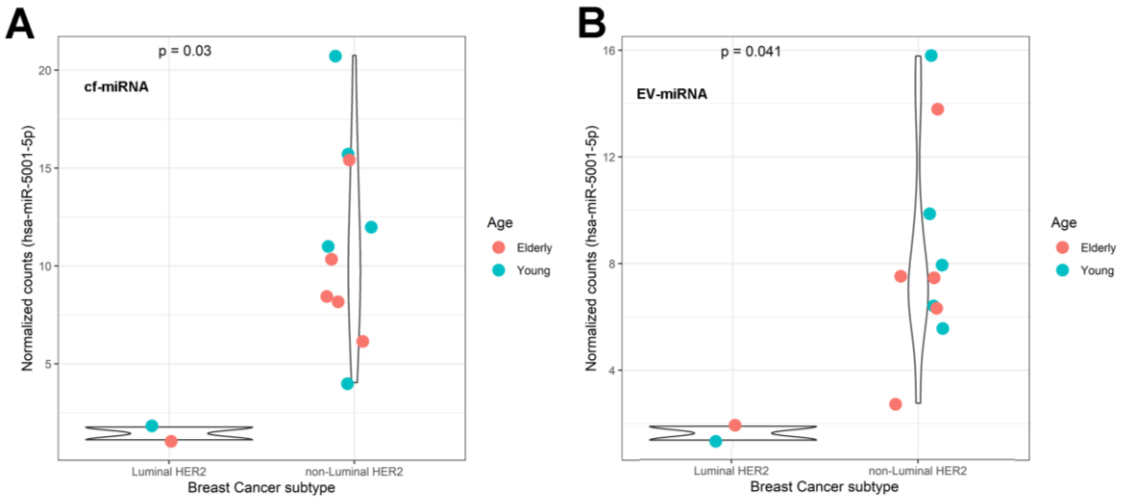

Figure 42. Dot plot of normalized values of hsa-miR-5001-5p in plasma and EVs of Breast Cancer patients. Circulating (A) and Vesicular (B) levels of the hsa-miR-5001-5p miRNA in samples of cohort A were plotted as a violin-dot plot stratifying samples according to their immunohistochemical subtype (into Luminal HER2 or non-Luminal HER2 groups) and age-related group. P-values were obtained using the Mann-Whitney test. Figure built on the R software v.4.3.1.

In addition, Figure 43 shows relevant miRNAs associated with the Luminal HER2 subtype found in the abundance-related analysis performed on young diagnosed patients (Cohort A). This list includes hsa-miR-1295a, hsa-miR-198, hsa-miR-205-5p, hsa-miR-301a-5p, hsa-miR-30d-5p, hsa-miR-325, hsa-miR-3916, hsa-miR-494-5p, hsa-miR-614, and hsa-miR-671-5p.

As we performed before, we also look for relevant miRNA regions in young Luminal HER2 samples from Cohort B. In this analysis, we found a high number of differentially expressed miRNAs: 46 ($p<0.05$, $FC>2$) and 20 ($p<0.01$, $FC>2$). Differentially expressed miRNAs in vesicles of Luminal HER2 (Cohort B) includes hsa-miR-374a-5p, hsa-miR-548a-5p, hsa-miR-2116-5p, hsa-miR-378e, hsa-miR-378h, hsa-miR-411-5p, hsa-miR-574-5p, hsa-miR-628-3p, hsa-miR-644a, hsa-miR-675-5p, hsa-miR-1266-5p, hsa-miR-1234-3p, hsa-miR-3614-5p, hsa-miR-4455, hsa-miR-503-5p, hsa-miR-570-3p, hsa-miR-141-3p, hsa-miR-

379-5p, hsa-miR-382-3p, and hsa-miR-620. Table 16 shows representative regions of this comparison.

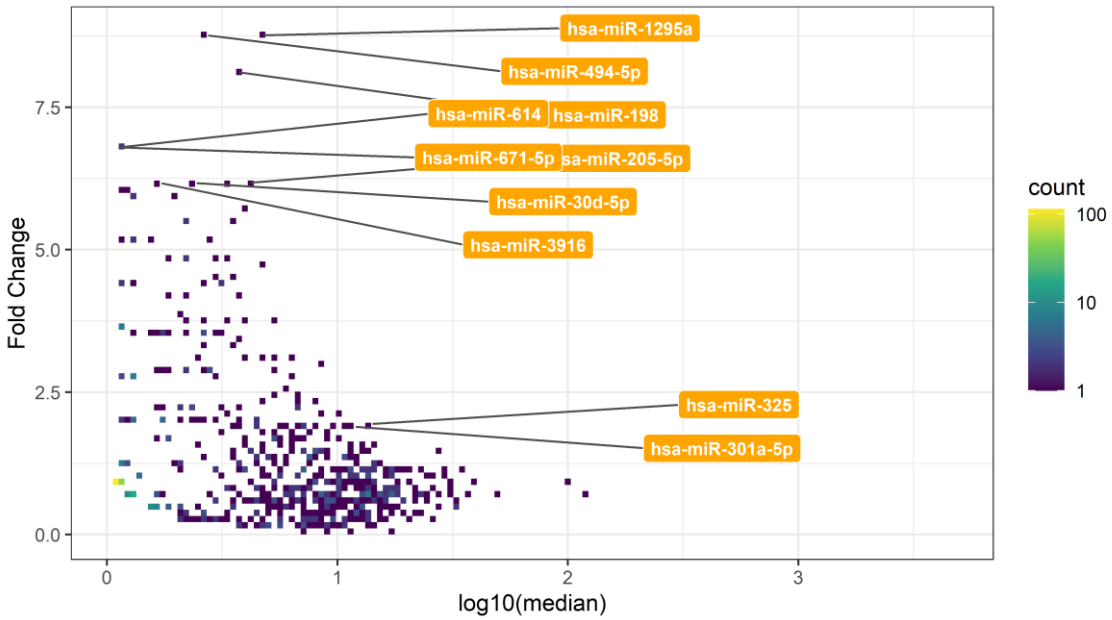

Figure 43. Relevant vesicular miRNAs in young diagnosed Luminal HER2 patients (Cohort A). This density plot shows all miRNA probes scanned in the Nanostring platform comparing Fold Change between Luminal HER2 (n=1) vs. other BC subtypes (n=5) in young diagnosed individuals (y-axis) in comparison with their median expression (log10) in all young diagnosed individuals (x-axis). Labeled miRNA fulfill some of these conditions: i) top 1% of Fold Change or ii) top 20% of Fold Change and top 20% of median abundance. Figure built on the R software v.4.3.1. The 3D representation of this plot can be accessed here: https://doi.org/10.6084/m9.figshare.24082380

After these analyses, we realized that hsa-miR-411-5p was previously found in another comparison involving Luminal HER2 patients (Table 15 and Table 16). Remarkably, the hsa-miR-411-5p miRNA was overexpressed in EVs from patients diagnosed with the Luminal HER2 subtype of BC. These results are representative as they appeared in two different datasets of patients (Cohort A and Cohort B). Then, these samples were inputted into the nCounter system with different criteria: Cohort A was inputted by the same RNA mass (65ng per well), whereas Cohort B samples were inputted using the same starting volume of EVs (before miRNA isolation). In addition, the comparison performed on samples from Cohort A includes both young and elderly patients, whereas Cohort B focuses on BC patients diagnosed before 40 years old.

Table 16. Differentially expressed EV-miRNAs (p<0.01, FC>2) between young Luminal HER2 (n=4) and other young BC subtypes (n=14) from Cohort B

miRNA	Relative expression in the young Luminal HER2 subtype (n=4)	Relative expression in other young BC subtypes (n=14)	Log_2 Fold Change (LumH2/others)	p-value	Adjusted p-value
hsa-miR-374a-5p	9.55	1.35	2.82	0.001	0.099
hsa-miR-548a-5p	7.53	1.35	2.48	0.001	0.099
hsa-miR-2116-5p	5.58	1.43	1.97	0.001	0.099
hsa-miR-378e	48.88	2.12	4.53	0.001	0.099
hsa-miR-378h	30.63	1.52	4.34	0.001	0.099
hsa-miR-411-5p	63.12	3.26	4.28	0.001	0.099
hsa-miR-574-5p	13.59	3.14	2.12	0.001	0.099
hsa-miR-628-3p	3.55	1.35	1.39	0.003	0.099
hsa-miR-644a	18.19	1.35	3.75	0.003	0.099
hsa-miR-675-5p	5.91	1.28	2.21	0.003	0.099
hsa-miR-1266-5p	16.62	3.16	2.40	0.003	0.099
hsa-miR-1234-3p	14.91	4.86	1.62	0.005	0.099
hsa-miR-3614-5p	9.39	1.60	2.56	0.005	0.099
hsa-miR-4455	4.49	1.35	1.73	0.005	0.099
hsa-miR-503-5p	15.63	4.99	1.65	0.005	0.099
hsa-miR-570-3p	12.37	1.59	2.96	0.007	0.099
hsa-miR-141-3p	7.50	1.73	2.12	0.008	0.099
hsa-miR-379-5p	60.28	15.06	2.00	0.008	0.099
hsa-miR-382-3p	7.67	1.73	2.15	0.008	0.099
hsa-miR-620	8.85	2.87	1.62	0.008	0.099

BC: breast cancer; LumH2: Luminal HER2
P-values were obtained using the Mann-Whitney test and adjusted with the False Discovery Rate (FDR) method. Bold miRNAs indicate absolute fold change values higher than 2.

According to Figure 44, hsa-miR-411-5p was significantly deregulated in the vesicular cargo of Luminal HER2 BC patients in two cohorts without regard for age at diagnosis. Some authors have demonstrated that hsa-miR-411 is sub-expressed in tumors and serum samples of BC patients compared with healthy controls [377], especially in groups with recurrence [378]. Then, functional experiments validated tumor suppressor features of hsa-miR-411-5p [355,379,380]. In this way, some regulatory RNAs have been proposed to inhibit the expression of this miRNA, for example, circ_001569 [379], as well as other circular and long non-coding RNAs compiled by Zou et al. (2022) [380].

Therefore, hsa-miR-411-5p is associated with less aggressive BC models as Luminal-like subtypes. Since many articles studying hsa-miR-411-5p have not described specific subtypes of their cohort, we cannot compare them directly.

However, we believe our results are consistent with the main findings proposed by these authors.

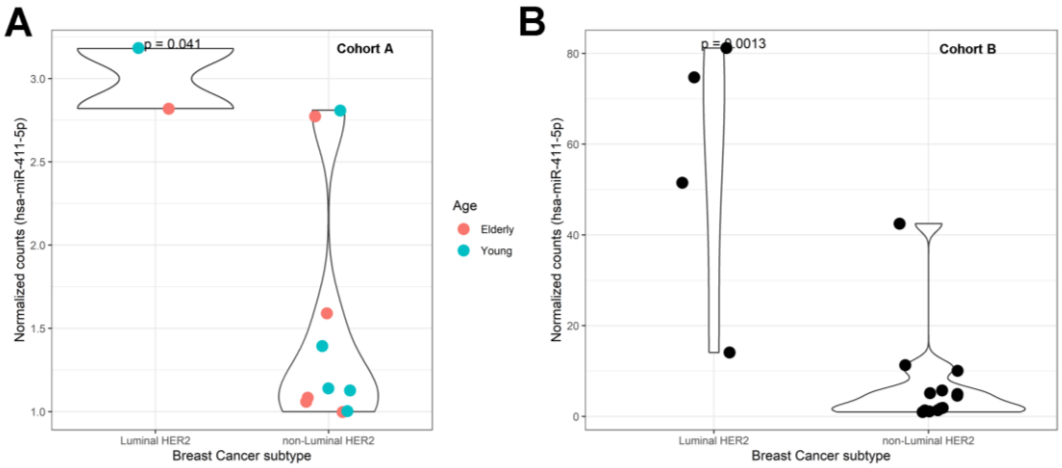

Figure 44. Dot plot of normalized values of hsa-miR-411-5p in EVs of Breast Cancer patients. Vesicular levels of hsa-miR-411-5p from cohorts A (A) and B (B) were plotted as a violin-dot plot stratifying samples according to their immunohistochemical subtype (into Luminal HER2 or non-Luminal HER2 groups). For Cohort A, a color-based legend was added to show age-related groups. P-values were obtained using the Mann-Whitney test. Figure built on the R software v.4.3.1.

4.3.11 Relevant vesicular miRNA regions related to age at diagnosis in BC patients

After comparing BC subtypes from both Cohorts, we observed some differentially expressed miRNAs between age-related groups (Figure 31). In addition to hsa-miR-324-3p, hsa-miR-648, and hsa-miR-6503-3p, Table 17 shows 18 other miRNAs deregulated between young and elderly diagnosed BC patients from Cohort A. Applying statistical ($p<0.05$) and fold change ($FC>2$) relevant filters, we found the following differentially expressed miRNAs between age-related groups: hsa-miR-324-3p, hsa-miR-648, hsa-miR-6503-3p, hsa-miR-603, hsa-miR-3918, hsa-miR-548h-5p, hsa-miR-548y, hsa-miR-519e-3p, hsa-miR-496, hsa-miR-129-5p, hsa-miR-1268a, hsa-miR-3144-5p, hsa-miR-499b-5p, hsa-miR-5010-3p, hsa-miR-381-5p, hsa-miR-1183, hsa-miR-487b-5p, hsa-miR-487b-3p, hsa-miR-361-5p, hsa-miR-486-3p, and hsa-miR-758-5p. None of these miRNAs were described in the same comparison using cf-miRNA (Table 7) or other comparisons on vesicular miRNAs.

Table 17. Differentially expressed EV-miRNAs (p<0.05, FC>2) between young (n=6) and elderly BC subtypes (n=6) from Cohort A

miRNA	Relative expression in the Young BC group (n=6)	Relative expression in the Elderly BC group (n=6)	Log_2 Fold Change (Young/Elderly)	p-value	Adjusted p-value
hsa-miR-324-3p	1.27	4.89	-1.95	0.002	0.576
hsa-miR-648	2.15	8.40	-1.97	0.002	0.576
hsa-miR-6503-3p	10.17	1.18	3.11	0.009	0.927
hsa-miR-603	5.92	1.87	1.66	0.020	0.927
hsa-miR-3918	4.88	1.18	2.05	0.026	0.927
hsa-miR-548h-5p	4.52	1.13	2.01	0.026	0.927
hsa-miR-548y	6.95	1.97	1.82	0.026	0.927
hsa-miR-519e-3p	8.83	2.71	1.71	0.026	0.927
hsa-miR-496	11.75	3.88	1.60	0.026	0.927
hsa-miR-129-5p	1.27	3.99	-1.66	0.026	0.927
hsa-miR-1268a	1.07	2.34	-1.13	0.029	0.927
hsa-miR-3144-5p	1.07	3.50	-1.72	0.029	0.927
hsa-miR-499b-5p	1.09	2.71	-1.32	0.030	0.927
hsa-miR-5010-3p	6.34	2.72	1.22	0.041	0.927
hsa-miR-381-5p	18.10	7.86	1.20	0.041	0.927
hsa-miR-1183	12.32	5.37	1.20	0.041	0.927
hsa-miR-487b-5p	1.27	4.20	-1.73	0.041	0.927
hsa-miR-487b-3p	2.74	1.03	1.41	0.044	0.927
hsa-miR-361-5p	8.10	1.12	2.85	0.045	0.927
hsa-miR-486-3p	1.14	2.79	-1.30	0.045	0.927
hsa-miR-758-5p	1.27	4.89	-1.95	0.045	0.927

BC: breast cancer
P-values were obtained using the Mann-Whitney test and adjusted with the False Discovery Rate (FDR) method. Bold miRNAs indicate absolute fold change values higher than 2

Then, we compared vesicular miRNA levels between young and elderly BC patients from Cohort B. Table 18 shows relevant miRNAs from this analysis. Among these miRNAs, we found outstanding regions (p<0.01), for example, hsa-miR-1266-5p and hsa-miR-642a-5p, overexpressed in EVs from patients diagnosed after 40 years old. In particular, hsa-miR-1266-5p and hsa-miR-642a-5p were previously overexpressed in vesicles of elderly diagnosed TNBC patients in both cohorts (Table 10 and Figure 36). Since the elderly subgroup of Cohort B (Appendix 2) is uniquely composed of TNBC patients, overexpression of hsa-miR-1266-5p and hsa-miR-642a-5p shown in Table 18 could be influenced by previous observations.

Table 18. Differentially expressed EV-miRNAs (p<0.05, FC>2) between young (n=18) and elderly BC subtypes (n=6) from Cohort B

miRNA	Relative expression in the Young BC group (n=18)	Relative expression in the Elderly BC group (n=6)	Log_2 Fold Change (Young/Elderly)	p-value	Adjusted p-value
hsa-miR-1266-5p	4.87	14.00	-1.52	0.008	0.520
hsa-miR-642a-5p	1.52	3.97	-1.39	0.009	0.520
hsa-miR-451a	2.83	1.15	1.31	0.010	0.520
hsa-miR-1234-3p	7.33	1.43	2.36	0.012	0.520
hsa-miR-1287-5p	2.54	9.30	-1.87	0.018	0.520
hsa-miR-507	1.44	4.18	-1.54	0.018	0.520
hsa-miR-892a	1.29	2.83	-1.13	0.019	0.520
hsa-miR-522-3p	1.43	2.98	-1.06	0.021	0.520
hsa-miR-379-5p	17.92	3.53	2.35	0.022	0.520
hsa-miR-487a-3p	1.35	4.24	-1.65	0.027	0.520
hsa-miR-148a-3p	1.60	4.35	-1.45	0.030	0.520
hsa-miR-519e-3p	1.19	3.92	-1.72	0.033	0.520
hsa-miR-4755-5p	12.87	3.92	1.71	0.040	0.520
hsa-miR-520c-3p	2.83	8.07	-1.51	0.040	0.520
hsa-miR-302d-3p	82.24	38.85	1.08	0.040	0.520
hsa-miR-188-5p	14.35	4.48	1.68	0.047	0.520
hsa-miR-499a-5p	1.68	5.17	-1.62	0.047	0.520
hsa-miR-302b-3p	16.24	5.32	1.61	0.047	0.520
hsa-miR-3131	5.39	1.84	1.55	0.047	0.520
hsa-miR-499b-5p	1.44	3.75	-1.38	0.047	0.520

BC: breast cancer
P-values were obtained using the Mann-Whitney test and adjusted with the False Discovery Rate (FDR) method. Bold miRNAs indicate absolute fold change values higher than 2

Interestingly, the hsa-miR-451a, a biomarker previously found as a hemolysis signal in this thesis (Figure 10), was described as a relevant biomarker between elderly and young diagnosed BC patients (Cohort B). It is important to note that EVs are excluded from hemolysis effects once we treat EV solutions with proteinase K and RNase A before miRNA isolation. As a result of this treatment, hsa-miR-451a presents a low median expression in EVs (9.27 for Cohort A and 1.85 for Cohort B) compared with values reported in cf-miRNA (9906.24, Figure 10).

As a counterpart, high-expressed miRNAs in EVs can also determine differences between groups. For example, the hsa-miR-302d-3p was highly expressed in EVs (1st and 3rd more abundant miRNA for Cohort A and Cohort B,

respectively, Figure 30), differently from cf-miRNAs (11th more abundant miRNA), but this miRNA can also differentiate elderly TNBC patients from young BC cases (Table 18).

4.3.12 Relevant vesicular miRNAs in an individual analysis (Cohort B)

After all the exploratory analysis using collective and individual strategies for the main pathological data, we moved forward to deeply explore the individual-to-individual features by analyzing the vesicular miRNA levels of cohort B.

All participants of this thesis belong to the main study “Retratos da Mama”, which is still recruiting individuals as diverse tests are still ongoing. Among them, it is planned to evaluate prognostic factors, as we get enough information to build Kaplan-Meier plots of these cohorts. Today, the median follow-up time of BC patients of Cohort B is limited to 1193.5 days (43-2623 days, Figure 45), with 92% of alive patients. As we do not have the minimal follow-up time required to propose prognosis miRNA-based biomarkers (five years in median) [381–383], we get miRNA data available publicly to be compared with overall survival in the future.

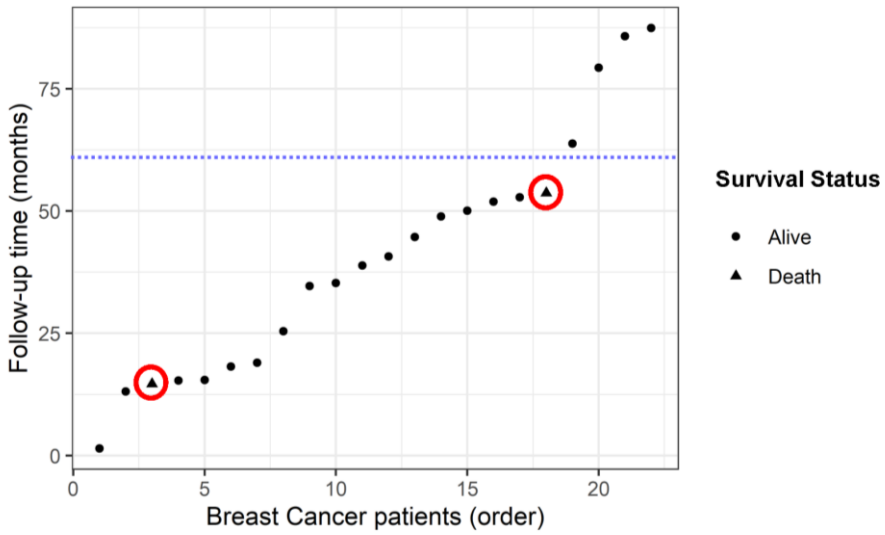

Figure 45. Follow-up time according to patients recruited in the Cohort B. Dot plot showing follow-up time in months for each patient. Shapes indicate the survival status (circles for alive, triangles for death). The dashed purple line indicates the reference time of five years. Then, many patients have a follow-up time lower than the reference

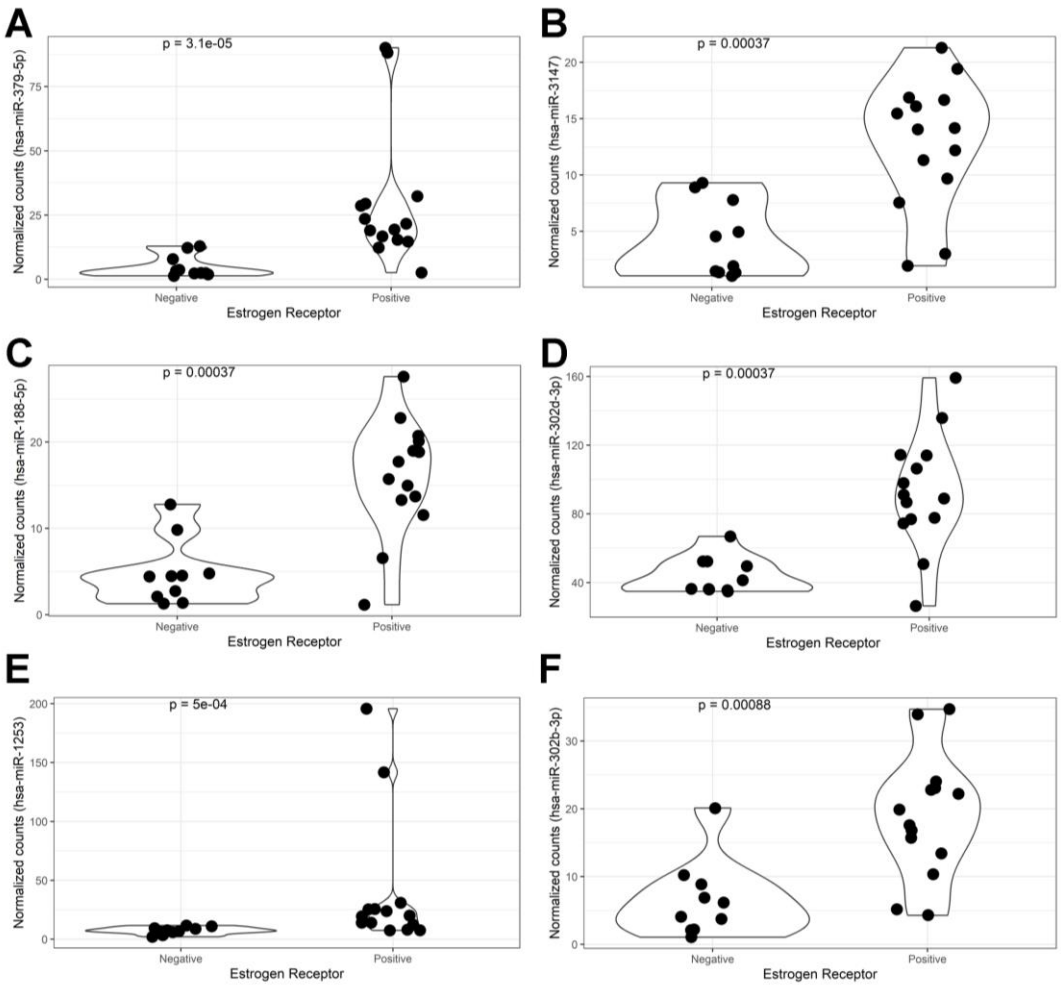

Figure 46. Dot plot of normalized values of selected miRNAs according to the estrogen receptor expression in BC tumors from Cohort B. Vesicular levels of hsa-miR-379-5p (A), hsa-miR-3147 (B), hsa-miR-188-5p (C), hsa-miR-302d-3p (D), hsa-miR-1253 (E), and hsa-miR-302b-3p (F) were plotted as a violin-dot plot stratifying samples according to their expression of estrogen receptor in tissues. P-values were obtained using the Mann-Whitney test. Figure built on the R software v.4.3.1.

In addition, other information beyond immunohistochemical subtypes can be compared. After running mean-comparing tests for qualitative variables and correlation analyses for quantitative variables, we determined additional miRNA-based markers in EVs from BC patients.

For qualitative variables, after applying a high restrictive filter (p-value< $1x10^{-3}$), we found some vesicular miRNAs associated with the expression of progesterone or estrogen receptors and high-blood pressure (HBP). For example, hsa-miR-379-5p, hsa-miR-3147, hsa-miR-188-5p, hsa-miR-302d-3p,

hsa-miR-1253, and hsa-miR-302b-3p were deregulated in EVs from patients whose tumors expressed estrogen receptors (Figure 46).

The hsa-miR-379-5p was also downexpressed in young TNBC patients of Cohort B (Figure 34). Then, some related references have been discussed for indicating this miRNA as a tumor suppressor [335–337]. About hsa-miR-3147, we found it overexpressed in the plasma of HER2+ BC patients (Figure 11B). Despite the given information on this miRNA [199] being limited, it could be a relevant region to be further validated.

Interestingly, hsa-miR-188 was abundant in EVs of BC patients (Figure 30D), consistent with a review that found this miRNA in EVs from both serum and plasma [70]. Then, hsa-miR-188 showed a relevant expression profile. This miRNA is low expressed in vesicles of young TNBC compared with non-TNBC young diagnosed patients (Figure 34); however, if all BC patients diagnosed before 40 years old are taken as a whole, the vesicular levels of hsa-miR-188 are higher than patients diagnosed after 40 years old (Table 18).

Another miRNA abundant in EVs with altered profiles among BC patients is hsa-miR-302d-3p (Figure 30). This miRNA was also present in the cf-miRNA profile (Figure 10) of BC samples and was overexpressed in young diagnosed BC patients (Cohort B, Table 18). In addition, their expression was downregulated in patients whose tumors do not express estrogen receptors (Figure 46). According to findings about this miRNA, previously discussed in this thesis, it seems to act against tumor features [318–320], but is still being detected as a BC biomarker [321]. This particular behavior could sign a corporal response against the tumor growth, as we described it for other miRNAs in this study. This hypothesis suggests that EVs collected from circulating sources represent a mixture of different subpopulations. Despite reliable results presented in this thesis, it is suggested to focus on specific subpopulations of EVs that can give a proper signature of tumor development.

About hsa-miR-302b-3p, researchers described controversial results about its expression in BC patients [354–356]. Nevertheless, the overexpression of this miRNA in vesicles of ER+ BC patients supports previous findings reported in Figure 34 since the expression of estrogen receptors is one of the parameters included in the determination of the BC immunohistochemical subtype. Moreover, the hsa-miR-1253 was overexpressed in ECM3, a

molecular BC subtype with poor survival in advanced stages [384]. In cohort B, we included a similar percentage of patients with early (I/II) and advanced (III/IV) stages (54.2% vs. 45.8%). Therefore, it is difficult to determine if our results are consistent with the previous report. In addition, this miRNA was found in a hypermethylated region in endometrial cancer patients [385], it was sub-expressed in exosomes from cancer-associated fibroblasts [386], and Ding et al. (2020) proposed that hsa-miR-1253 can control the tumor growth by regulating *DDAH1* [387].

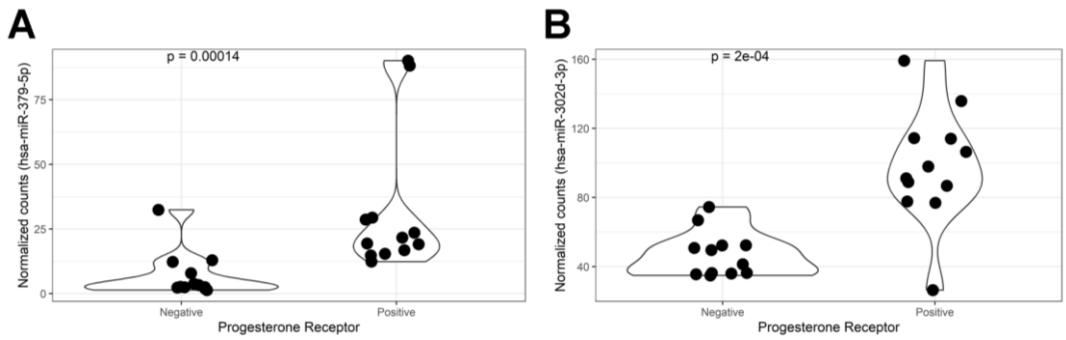

Figure 47. Dot plot of normalized values of selected miRNAs according to the progesterone receptor expression in BC tumors from Cohort B. Vesicular levels of hsa-miR-379-5p (A), and hsa-miR-302d-3p (B) were plotted as a violin-dot plot stratifying samples according to their expression of estrogen receptor in tissues. P-values were obtained using the Mann-Whitney test. Figure built on the R software v.4.3.1.

Figure 47 shows that hsa-miR-379-5p and hsa-miR-302d-3p have higher vesicular levels in patients who express progesterone receptors in their tumors. As shown in Figure 46, this finding can contribute to getting these miRNAs downregulated in young TNBC patients (Figure 34).

Finally, the vesicular expression of hsa-miR-642a-5p was altered in patients with High Blood Pressure (HBP) as shown in Figure 48. Once hsa-miR-642a-5p has proven to be upregulated in vesicles from elderly diagnosed TNBC patients from both Cohorts (Table 10 and Figure 36), it could be a signal of HBP as this characteristic surrounds older people [388]. However, it is relevant to mention that 50% of the elderly group from Cohort B presents HBP (Appendix 2). Of all HBP patients represented in Figure 48, three are from the Elderly TNBC group, while one is from the young Luminal HER2 group. For these reasons,

immunohistochemical subtypes or age-related groups could not be involved in these findings, and vesicular levels of hsa-miR-642a-5p are suggested to be a marker of patients with HBP.

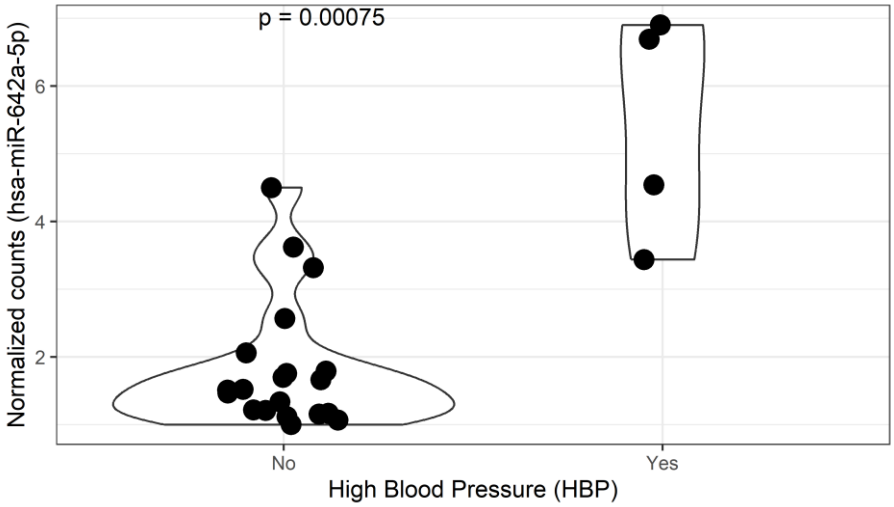

Figure 48. Dot plot of normalized values of selected miRNAs according to the high blood pressure (HBP) condition from Cohort B. Vesicular levels of hsa-miR-642a-5p were plotted as a violin-dot plot stratifying samples according to the diagnosis of HBP. P-values were obtained using the Mann-Whitney test. Figure built on the R software v.4.3.1.

For quantitative variables, we run the Spearman's test and select variables with significant strong correlation (R-values higher than 0.7 and p-value<0.01). Relevantly, we found two main correlations. The first one is between the number of individuals in the first degree of kinship with breast or ovarian cancer and vesicular levels of hsa-miR-664a-3p (R=0.75, $p=1.92x10^{-5}$, Figure 49A), and the second is between body mass index (BMI) and hsa-miR-423-3p (R=0.71, $p=2.11x10^{-4}$, Figure 49B).

Previously, in this thesis, we found deregulated vesicular levels of hsa-miR-664a-3p in patients from Cohort A. This miRNA was overexpressed in HER2+ BC patients (Table 11) but down-expressed in samples whose tumors were classified as Luminal HER2 subtype (Table 15). Despite there being no descriptions of the increase of expression levels in relationship with a growing number of relatives with cancer, and we did not include BC patients with HER2+ subtype in Cohort B, it could be a suggestion to evaluate the profile of different

inherited pro-tumor mutations. As part of the “Retratos da Mama” study, we expect to cross these expression levels with mutational profiles in the future.

Finally, the hsa-miR-423-3p was not previously described in this thesis. Then, data from the literature have evaluated levels of this miRNA in different contexts. It was overexpressed in the muscles of cachectic patients [389], and it was stably present in the serum of individuals [390], while a study focusing on in vivo models of obesity found higher levels of this miRNA in livers from mice fed with high-fat diet (HFD) and obese humans [391].

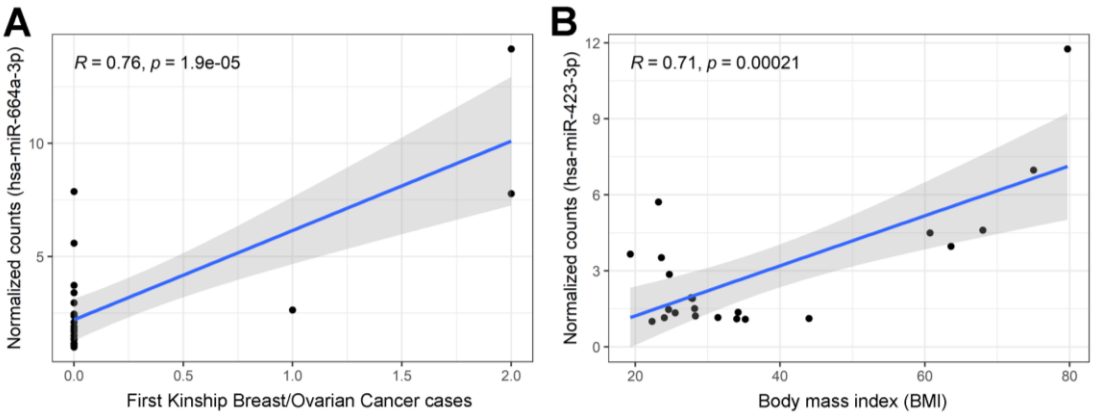

Figure 49. Dot plot of normalized values of selected miRNAs according to quantitative clinical conditions from Cohort B. Comparisons of vesicular levels of hsa-miR-642a-5p and the number of breast or ovarian cancer cases in first kinship (A) and vesicular levels of hsa-miR-423-3p and body mass index (B) were plotted as dot plots. P-values were obtained using the Spearman’s test. Figure built on the R software v.4.3.1.

4.3.13 Challenges, lessons, and insights from the analysis of vesicular miRNAs

In addition to the topics discussed in the cf-miRNA section, the information provided by vesicular miRNA unleashes some additional factors.

For this section, we included cohort B to carry out protocol standardization trials to isolate extracellular vesicles and make a point-to-point comparison between patients by not applying the pooling strategy (as was done with cohort A) despite the risk of losing sensitivity in this process.

Initially, we must comment that cohort B has a short follow-up time for its patients due to the recent training and collection of samples (Figure 45). This makes it impossible to carry out survival comparisons; however, it opens up

new possibilities for the future. By the end of the recruiting process, we will have more information on these patients, and the follow-up time will be prolonged. It is essential to mention that miRNA could be a perishable source, even stored at -80°C for many years. To the best of our knowledge, the stability of circulating miRNA has been evaluated only for up to one year stored at -80°C [57,227,392,393]. So, it is crucial to carry out molecular evaluations as soon as possible but save and make the data publicly available (Appendix 4 and Appendix 5) for when comparison factors can be added.

Regarding the information collected from patients, the construction of questionnaires for the evaluation and follow-up of these patients is constantly updated. These questionnaires must see the patients as part of a continuously changing society beyond individuals. Thus, in the patient selection process, we have some challenges, for example, self-reported information on ancestry. Despite the considerable impact of miscegenation in Brazilian samples, self-declared race information is still considered in many establishments [394]. Due to this, we included it as a factor in ensuring homogeneity in our cohorts (p-values equal to 0.3 and 0.2 for Cohorts A and B, respectively). Nevertheless, molecular tests to evaluate and determine ancestral components have been proposed for the Brazilian population [395–397]. It could be required once it is known that independent ethnic profiles can induce differences in the molecular and clinical features associated with cancer [398–401]. In the same way, these molecular tests could help certify the mutational status of patients who are not allowed to get information about their family history or help confirm the biological sex of individuals who have undergone gender transition processes.

About observations made on sample processing, we verified that the analysis of extracellular vesicles represents a sample free of clearly circulating components and other contaminants, such as the effect of hemolysis observed in cf-miRNA (Figure 10D, Figure 30C, and Figure 30D). However, by working with a circulating sample subselection, we reduced the yield per mL plasma that will go into the equipment. To improve this context, we increased the input volume by 3-fold (for cf-miRNA, we started with 200 µL of the sample, while EV-miRNA protocols started with 600 µL), and we tested the double elution process to collect the maximum possible miRNA total mass. As seen in the results of cohort A, by applying this double dilution step, it is possible to collect a

minimum of 65 ng of vesicular miRNA mass in a sample. Naturally, other samples obtained higher performance, regardless of whether they came from individual or pool samples.

Then, after observing the results of extracellular vesicles miRNome (Figure 24 and Figure 25), we evaluated different normalization protocols once we did not have endogenous or exogenous controls. There, we observed that normalizing by the most stable regions continues to be the most reliable (Figure 29 and Figure 28). Although the nCounter barcoding hybridization system has five slots for spike-in regions of non-homologous species (ath-miR159a, cel-miR-248, cel-miR-254, osa-miR414, and osa-miR442), it still there is a broad discussion about which regions should be used, even presenting the small nucleolar RNA U6 (RNU6B, U6) region as an alternative. Moreover, the moment in which these exogenous regions of known concentration should be placed: (i) before vesicle extraction, (ii) after the plasma separation, (iii) before treatment with proteinases, or (iv) before detection protocol, was not robustly defined either [402–405]. For this reason, we did not include exogenous regions in our assays, but it could be tested in the future.

Regarding the versatility of miRNAs, the vesicular component helped us understand that some regions may have more than one function, such as the hsa-miR-451a miRNA, which was reported as a hemolysis signal in cf-miRNA (Figure 10), but which could also differentiate between young and adult BC patients (Table 18). This suggests the hypothesis that a given miRNA can fulfill different functions in different cell types. Naturally, as these cell types secrete EVs into the bloodstream, we will find modulated levels of these miRNAs according to specific circumstances, as we saw with some miRNAs in this thesis; for example, hsa-miR-188-5p (Figure 30 and Figure 34) or hsa-miR-302d-3p (Figure 30 and Table 18).

Then, to understand the function of these miRNAs, we used information from previously published studies. Nevertheless, the nomenclature of miRNAs follows a growing process [406] that must be considered when drawing interpretations from scientific articles. In this thesis, according to the information available, we carefully confirmed which arm (-3p or -5p) is being referred to in each external study. For example, research done on hsa-mR-615. The -5p version (hsa-miR-615-5p) appeared overexpressed in vesicles from HER2+

patients (Figure 37 and Figure 38), while the -3p arm (hsa-miR-615-3p) was expressed in plasma from patients diagnosed before 40 years of age (Table 7). Next, we found several studies about hsa-miR-615-3p [166,262–264], but very few reports about hsa-miR-615-5p [370]. In addition, some miRNAs belong to some families, where their nomenclature can be more complex; for example, the miR-302 family: hsa-miR-302a/b/c/d. On the other hand, the tumor is capable of inducing mutations in the DNA of cells [407]. Then, miRNAs can also be targets of their effects [360]. Subsequently, the presence of mutations in regions that transcribe miRNAs can cause alterations in their determination and annotation, regardless of the applied technology (microarrays, barcode hybridization, RNAseq). In this way, we reinforce that the interpretations of external works on miRNAs of interest must be analyzed with caution.

After reviewing the information on each miRNA, we found some information consistent with our results, but also potentially controversial reports. For example, the case of hsa-miR-302d-3p has functional studies that show an antitumor effect [318–320] and others that indicate it as a biomarker [321]. In our results, this miRNA was consistently abundant in vesicle samples from two independent cohorts. However, its presence may not necessarily be provided by the tumor but rather by surrounding cells that seek to control it.

In this way, new questions are opened about the composition of extracellular vesicles at the subpopulation level. For the following section, we intend to evaluate the technical and technological capacity currently available to select extracellular vesicles that are potentially produced by the tumor using a strategy of labeling antigens already associated with the tumor process in breast cancer.

4.4 Selection of EVs potentially derived from BC tumors

After reviewing the literature about proposed miRNAs in previous sections of this thesis, there is the hypothesis that circulating material potentially overexpressed in specific BC subtypes or age-related groups are not only related to tumor-produced factors but also includes circulating miRNAs and EVs produced by other cells as a response of the tumor growth (i.e. immune cells). Herein, we present the establishment of initial protocols for using Jacalin lectin to label breast cancer cells from cell culture, sample tumors, and select EVs from BC patients. These data offer technical and biological information supporting the hypothesis of breast cancer cells producing Jacalin-positive EVs.

4.4.1 Ability of Jacalin lectin to bind BC cells

We used cell lines to verify the linkage of Jacalin lectin with aberrant glycoproteins on the surface of these tumor cells. Then, we also used cells to standardize laboratory protocols due to their major size when compared with their extracellular vesicles [67,288]. The expression of the Tn antigen and their derivatives are related to aberrant glycosylation occurring in cancer samples [96] and to the recognition of these targets by Jacalin lectin [106].

Our experiments confirmed the ability of Jacalin lectin to bind breast cancer cells. In Figure 50A, we show magnetic beads overlapping live or dead cells representing an interaction among derivatives of the Tn antigen on the surface of these cells and biotinylated Jacalin. Linked cells could be observed such as cell clusters connected by Jacalin lectin and magnetic beads. However, we realized that this does not occur in all cells and neither is it associated with the main subtypes of breast cancer (Figure 50B). Herein, we focus on differences among all Triple-Negative Breast Cancer (TNBC) cell lines and find highly variable percentages of Jacalin-positive cells (from 7.4% in MDA-MB-468 to 72.63% in MDA-MB-231 cell line). According to the Lehmann et al. (2011) study [27], the cell lines tested in our experiment represent different TNBC subtypes: MDA-MB-468 (Basal-like 1), HCC70 (Basal-like 2), MDA-MB-231 and HS578T (Mesenchymal stem-like), and this new classification could introduce different epigenetic and post-translational modifications.

Then, we tested representative cell lines for four of the main subtypes of breast cancer (Figure 50C) to confirm previous results. Here, we use biological

replicates to determine statistical differences among MDA-MB-231 (TNBC cell line) and others cultured at the same conditions (cell confluence, harvesting method, use of recommended cell media, etc.) verifying previously reported results. These differences are related to expression profiles of surface proteins among both breast cancer cells and tumors [408].

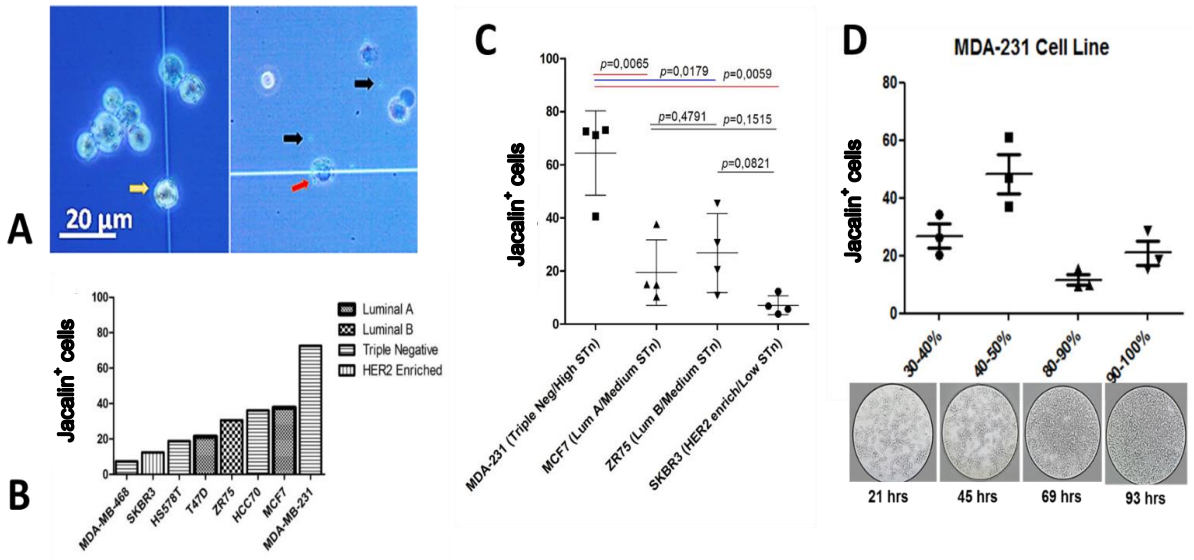

Figure 50. Jacalin lectin binds breast cancer cell lines. (A) Photomicrography of BC cells after treatment with Jacalin lectin and magnetic beads. Black arrows indicate magnetic beads alone (tiny and refractory circles), whereas red and yellow arrows show magnetic beads bound to dead and live cells, respectively. (B) Description of the percentage of cells expressing derivatives of the Tn antigen among BC cell lines. The cell line MDA-MB-231 shown Jacalin-bound cells, whereas the MDA-MB-468 cell line shown the lowest level, despite both MDA-468 and MDA-231 are TNBC cell lines. Cell lines were painted according to phenotypes defined by Holliday & Speirs (2011) study. (C) Comparison of cells expressing derivatives of the Tn antigen among BC subtypes. Experiments with four biological replicates indicate higher levels of Jacalin-bound cells from the TNBC subtype (MDA-MB-231 cell line) when compared with others. The Mann-Whitney test was applied to calculate all p-values. (D) Variable expression of derivatives of the Tn antigen with cell confluence. MDA-MB-231 cells have reported a peak at a middle level of confluence. For each cell confluence measure, we indicate the time that this phase occurred and attach photomicrography. Figures B-D were built on GraphPad Prism v8 for Windows.

Once we determine the differences between breast cancer cells, we need to analyze differences along with the growth of these cells. In order to determine if the expression of Jacalin targets also depends on cell confluence, we selected the MDA-MB-231 cell line due to its high percentage of Tn+ cells and compared their percentages of Jacalin-positive cells with their cell confluence. Here, we describe an increase in the number of cells expressing Jacalin targets up to 50% confluence. After that (above 70-80% confluence), this number decreases sharply and concomitantly with the production of EVs (Figure 50D). This variation occurs due to internal changes probably related to the production of EVs. In this step, proteins leave the cell membrane, suffer aberrant modifications, and are packaged in multivesicular bodies to be released [409]. It is important to remark that the endomembrane system participates in this cell reorganization and glycoprotein synthesis.

A

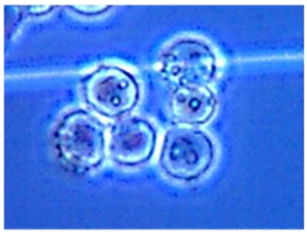

B

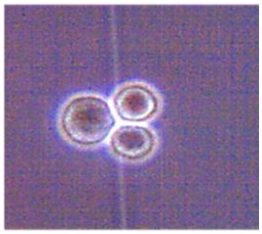

C

	Mean	SD
(50mM)	15%	4%
(100mM)	43%	1%
(200mM)	35%	9%

Figure 51. D-galactose treatment allows the release of Jacalin-bound cells. **(A)** Microscopy observation (40x) of BC cells treated with Jacalin. Magnetic beads are shown as refractory and tiny spheres. **(B)** Microscopy observation (40x) of BC cells that were selected by Jacalin lectin and after treated with galactose to remove lectin interactions. **(C)** Table with results of the percentage of cells recovered at each concentration. The standard deviation was estimated from three biological replicates performed for each treatment.

After cells (or EVs) are selected by Jacalin lectin, we need to remove this interaction to use these cells in further applications. For that, we tested three concentrations of D-galactose, a primary sugar for Jacalin lectin [106]. In this

experiment, we were able to recuperate selected cells without Jacalin labeling. However, we realize this method recovered very few Jacalin-positive cells (almost 50%). In order to improve it, we propose to increase the time of incubation with the best concentration of D-galactose that we have tested (100 mM) since this treatment showed consistent results in all treated samples (Figure 51).

4.4.2 Staining of breast cancer tissue with Jacalin lectin

We also found Jacalin labeling cellular regions in breast cancer tissues. Tissue staining allowed us to observe differences between tumor and normal adjacent tissues (Figure 52). Normal adjacent cells show tiny and organized nuclei with a weak Jacalin staining, whereas tumor cells show an aberrant organization and variable intensities of Jacalin staining. This reflects the intratumoral heterogeneity (50-90% cells) previously described in other experiments (Figure 50D) and other studies in the literature involving lectin histochemistry [410,411].

When we treated FFPE slices with fewer concentrations of BSA (5%), we were able to visualize remarkable spots in regions associated with the endomembrane system (Figure 52C). These results reinforce our hypothesis of breast cancer cells expressing and exporting aberrant glycoproteins. Then, the biogenesis of extracellular vesicles, and specifically exosomes, also involve the endomembrane system of the cell such as the Golgi apparatus, endoplasmic reticulum, and naturally, the own plasma membrane [412]. In consequence, the production of EVs and the exportation of aberrant glycoproteins could be related processes in cancer cells. Subsequently, this favors the main objective of our project to select tumor-derived EVs using Jacalin lectin.

About specifications of the protocol for lectin histochemistry, we performed a long protocol to blockade endogenous peroxidase, which is recommended by other studies working with lectins [410]. The blockade of endogenous biotin is not recommended for our type of sample due to their low expression in this tissue [413].

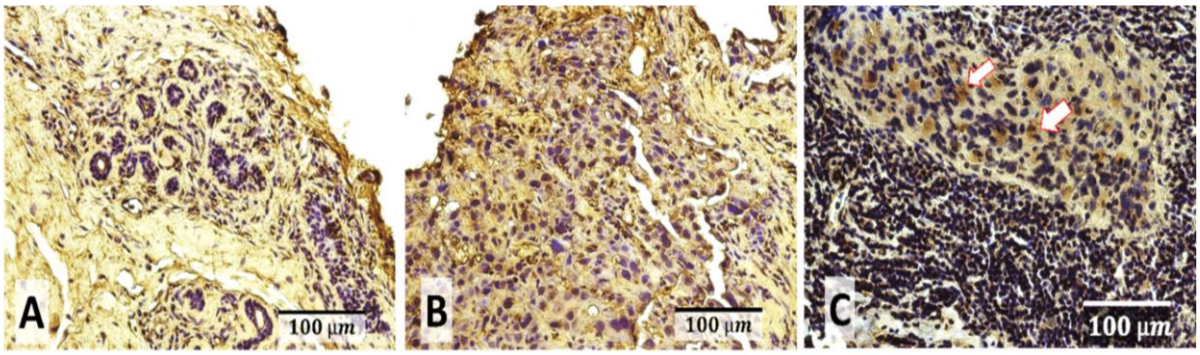

Figure 52. Comparison of normal and tumor tissues stained with Jacalin. Photomicrographs (40x) of FFPE sections from breast cancer patients showing differences among tumor and normal adjacent cells. (A) Normal adjacent section presenting a common distribution of organized cells and a very low expression of Jacalin targets. (B) Tumor section showing a highly heterogeneous group of unorganized cells with different-size nuclei. This tissue also shows strong staining with Jacalin, despite intratumoral heterogeneity. (C) Tumor section showing spots highly reagent with Jacalin (white arrows) in regions related to the endomembrane system.

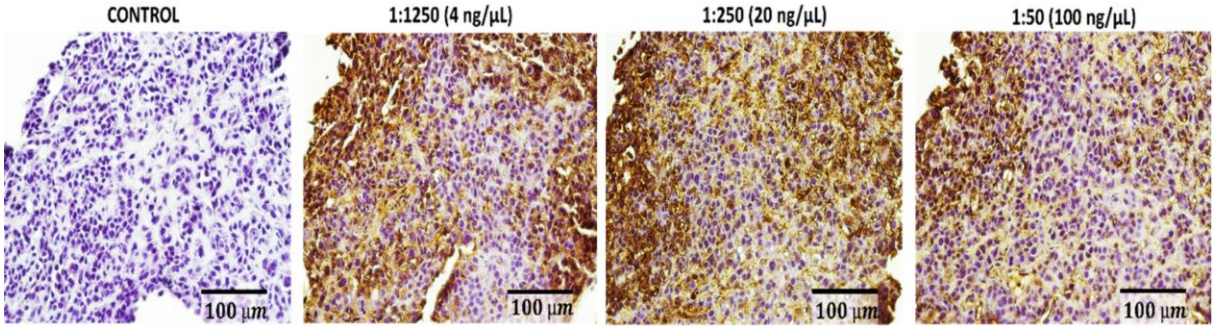

Figure 53. Breast cancer tissue stained with Jacalin lectin. Photomicrographs (40x) of FFPE tissues from breast cancer patients have shown differential labeling concomitant with Jacalin concentrations. Tumor regions are appreciable as a heterogeneous tissue where the Jacalin labeling is also differential between all cells.

The antigen retrieval is a step usually recommended in immunohistochemistry and lectin histochemistry [410]. However, this procedure could increase the damage of the tissue by exposition to high temperatures and then affect the visualization of cells. In our experiments, we were able to visualize a high interaction of Jacalin with their targets (Figure 53). In a broader observation, we evaluated tissues from Cohort B patients and found Jacalin staining in the stroma in 97% of cases. Then, cancer cells showed primarily high staining (72% of cases), followed by low (26%) and moderate (2%) staining

levels. In addition, there was no association with the subtype or age at diagnosis of these patients ($p>0.05$). It could be by the relatively low specificity of the Jacalin as a glycan-binding protein.

Nevertheless, it does not devalue their analysis since normal and tumor sections have shown different Jacalin profiles (Figure 52). In future experiments, it is suggested to reduce the current concentration of streptavidin-HRP (1:250) to highlight regions with a higher affinity for Jacalin.

4.4.3 Dot blot with Jacalin and modifications for low concentrated samples

After observing that BC tissues can express Jacalin targets, we move the protocol to a liquid biopsy approach using dot blots. We standardized the optimal conditions for the dot blot for EV protein detection (Figure 54). Here, we realized that common reagents for dot blot revealing did not work for EV samples. Then, we include an enhancer or prime (ECL Prime WB reagent) to improve these results (Figure 55).

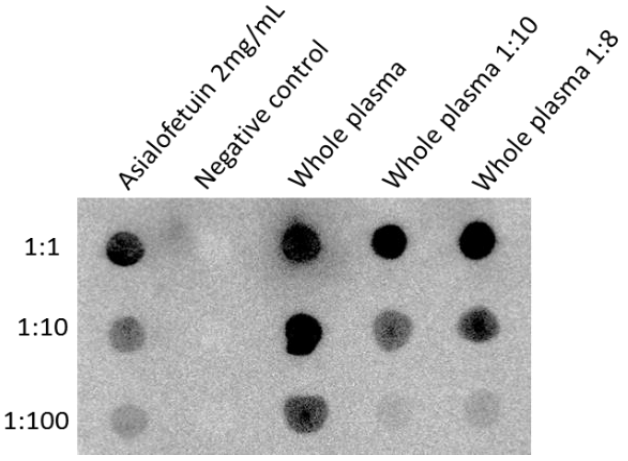

Figure 54. Dot blot of different dilutions of whole plasma used for standardization of the technique. Asialofetuin (positive control), Tris-buffered saline solution (negative control), and whole plasma were loaded to evaluate the formation of dots and their staining with Jacalin lectin.

In a brief comparison with the study by Koliha et al., 2016, they reported a protein concentration per particle ranging 10^{-2} and 10^{-4} picograms [414]. Considering the average value of our samples, a concentration of $1x10^{9}$ particles/mL would represent approximately 10^{2}-10^{4} pg of vesicular protein per

µL. So for each 5 µL of the sample, we could load around 500-5000 pg of total protein. However, lectin targets represent only a percentage of the total protein in human plasma [415] which was not detected by the ECL Western Blot reagent. For this reason, we choose to use the ECL Prime that increases the sensitivity up to ~ 1 pg.

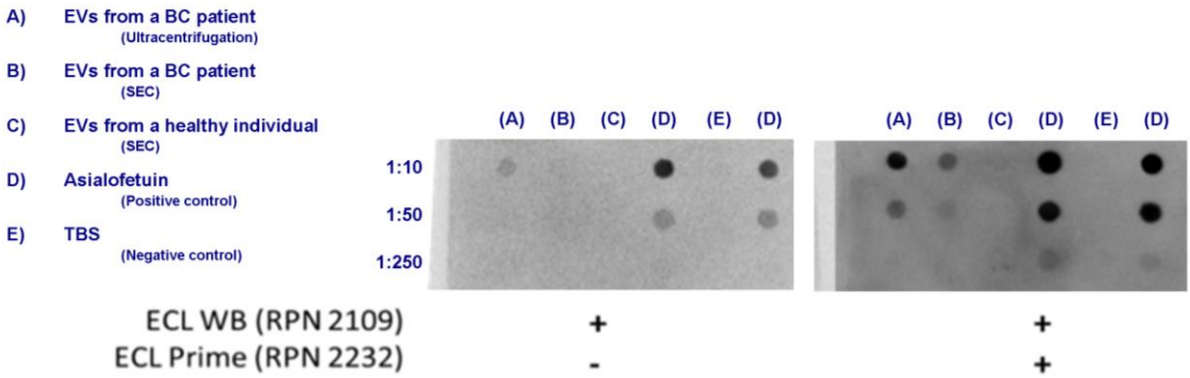

Figure 55. Increment in the sensitivity for detecting Jacalin interactions by using an enhancer reagent. A nitrocellulose membrane with Jacalin-reactive solutions was revealed with the traditional reagent alone (left panel) or combined with a chemical enhancer (right panel). The presence of the enhancer improves the sensitivity allowing the apparition of new dots, related to EV samples. SEC: Size-exclusion chromatography; TBS: Tris-buffered saline solution.

4.4.4 Differences in the expression of Jacalin targets in EVs from plasma of patients and controls

Once we defined all parameters to perform the dot blot and EVs were isolated from plasma of a training cohort of patients, we aimed to evaluate potential differences between patients and controls about the expression of Jacalin targets in EVs from plasma.

Interestingly, we observed higher levels of Jacalin targets in EVs isolated from patient plasma compared to a sample from a healthy individual (Figure 56A). Then patient samples would have enough Jacalin targets to perform a specific selection of this EV subpopulation. These results are remarkable even though the concentration of these vesicles (Figure 56B), nor the frequency profile about the size of these particles (Figure 56C), do not show statistically significant changes, which indicates that these profiles are not necessarily related.

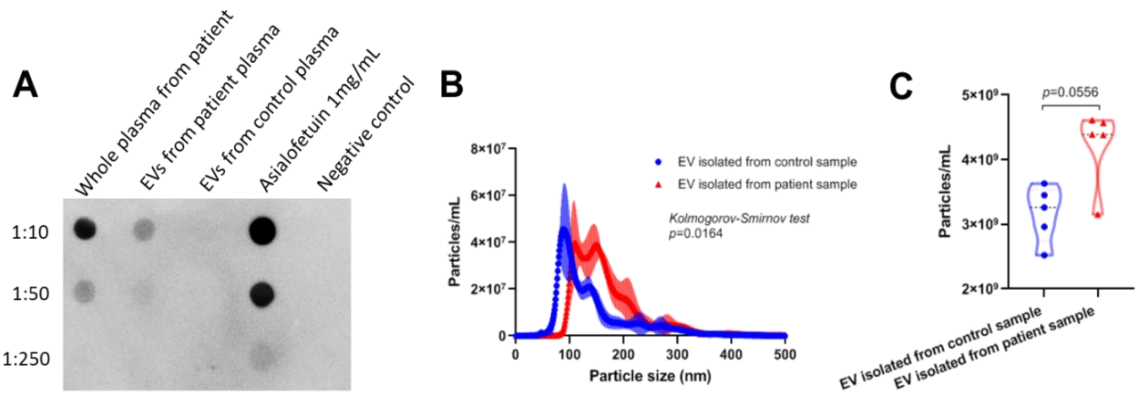

Figure 56. The patient sample shows a higher expression of Jacalin targets in EVs from plasma. (A) Dot blot membrane stained with Jacalin lectin. Asialofetuin is a positive control for Jacalin. The membrane was stained with the ECL Western Blotting reagent and enhanced with the ECL Prime reagent. (B) Distribution of the concentration of particles per size (nm) between patient and control samples. (C) Comparison of EV levels in patient and control samples. P-values were obtained using the Kolomogorov-Smirnov test for curves comparison and the Mann-whitney test for evaluating differences between the mean levels of two groups. Figures were built on the R software v.4.3.1.

Though the EV concentration profiles are not usually described in diverse studies, they are very similar between patients and healthy individuals [416–418]. By applying methods based on physical features to separate EVs (size-exclusion chromatography), it is possible to collect a mixed population of EVs [419–421], which opens opportunities for searching for new biomarkers in a combination of EVs from different sources. Differently, affinity-based strategies such as isolating EVs that express tetraspanins (CD9, CD63, or CD81), ALIX, or TSG101 on their surface could bias results once we know that not all EVs carry these markers in the same concentrations [91,92].

Due to these reasons, many studies involving extracellular vesicles in breast cancer have focused on analyzing their protein or nucleotide cargo instead of their crude EV concentration, as we have approached in a recent review [70]. In this manuscript, we showed that many vesicular biomarkers proposed for BC are related to miRNAs, messenger RNA (mRNA), other RNAs, or proteins despite several strategies for isolating these EVs have been tested (reviewed in [70]). Interestingly, cited studies involve all EVs, except the study of Kim et al. (2021), which focused on the EV subpopulation expressing CD49f

and EpCAM on their surface by passing samples through a microfluidic device [422].

By this evidence, after verifying that there are no reproducible differences in the total EV concentration between BC patients and healthy individuals, we observed that Jacalin can identify a subpopulation notably present in the sample from BC patients (Figure 56).

4.4.5 Separation of Jacalin+ EVs in a patient sample

As we have performed for BC cells (Figure 51), we also tested the ability of D-galactose to dissolve interactions between Jacalin and its targets on the EV surface. Considering that the experiments with cells yielded better results when incubated Jacalin-selected cells with 100 mM of D-galactose together with previous reports in lectins [423,424], we decided to evaluate a broad range (30-300 mM) to observe their ability to separate Jacalin-positive EVs.

Figure 57A shows the first NTA of EVs alone and after treatment with biotinylated Jacalin, biotin-binding magnetic beads, and D-galactose. We start the experiment with ~$6x10^9$ particles/mL (Figure 57B) isolated by size-exclusion chromatography. After incubation with biotinylated Jacalin and biotin-binder magnetic beads, the supernatant including molecular clusters by biotin-streptavidin interactions showed a higher concentration of low-size particles (Figure 57C) than the original sample. However, it could be explained by the presence of soluble biotinylated Jacalin in high concentrations from the treatment performed. As proof of this, the washing step fraction showed a low concentration of particles (~$1x10^8$ particles/mL, Figure 57B). At this moment, bound EVs were treated with 0.03 or 0.3 M of D-galactose, allowing us to recover $9x10^7$ and $6.4x10^8$ particles, respectively. Therefore, our method for selection and recovery of Jacalin-positive EVs was able to retrieve around 10% of the original sample. Then, our treatment could be efficient to select this biologically reduced fraction of total EVs from an individual.

Various previously published protocols chose to use magnetic beads surrounded by affinity proteins (antibodies or lectins) to select targets potentially associated with the tumor. Yoh et al. (2021) published a study that separated extracellular vesicles that express EpCAM in different types of cancer (including

BC) [425]. They lose 98-99% of total protein concentration between all EVs and EpCAM+ EVs. Despite this, the protein levels obtained were differentially expressed between cancer patients and healthy controls [425].

Then, some studies used lectin-based affinity assays for selecting EVs. Yamamoto et al. (2019) used a lectin from *Oscillatoria agardhii* (OAA) for purifying small EVs surrounded by high-mannose-type glycans from an EV collection produced by melanoma cell lines. Though this cohort of EVs could be considered pure, the efficiency of the lectin-based selection was equal to 60% [426]. Regarding liquid biopsies, Royo et al. (2016) evaluated different methods for isolating EVs from urine (local liquid biopsy). These methods included precipitation by chemical reagent, ultracentrifugation, and isolation by affinity using a *Solanum tuberosum* lectin. According to their results, the protocol with lectins showed a pure EV sample but lost 70-95% of RNA yield [427].

In this thesis, we proposed a method to select BC cells and EVs from a systemic liquid biopsy source (plasma). We recovered 10% of total EVs, which express Jacalin targets in their membrane. After revising related studies, we believe that our results are consistent, reliable, and comparable with those from the literature. Since plasma EVs are provided by different sources [66], it would be beneficial to focus on an EV subpopulation more related to breast tumors. However, this decision challenges the sensitivity features of detection systems.

There is no determined proportion of expected tumor-derived EVs in the bloodstream. Eventually, when this value is determined, it will depend on the methods followed for collecting these vesicles once these protocols can select specific groups of particles as we know today [90,428]. On the other hand, lectins and antibodies are useful tools for helping in this process; however, their use involves additional bias regarding their specificity and the establishment of the target. Antibodies have been proved to be more specific, but lectins can offer best cost-benefit estimation [429,430]. In addition, it is possible to profile glycans (one of the most interesting cancer-related protein modifications) in exploratory techniques, for example lectin microarrays or ELISA assays [101,431,432], to discover who is more abundant in EVs from cancer patients, and research other separating platforms beyond magnetic beads for improving affinity-based separations.

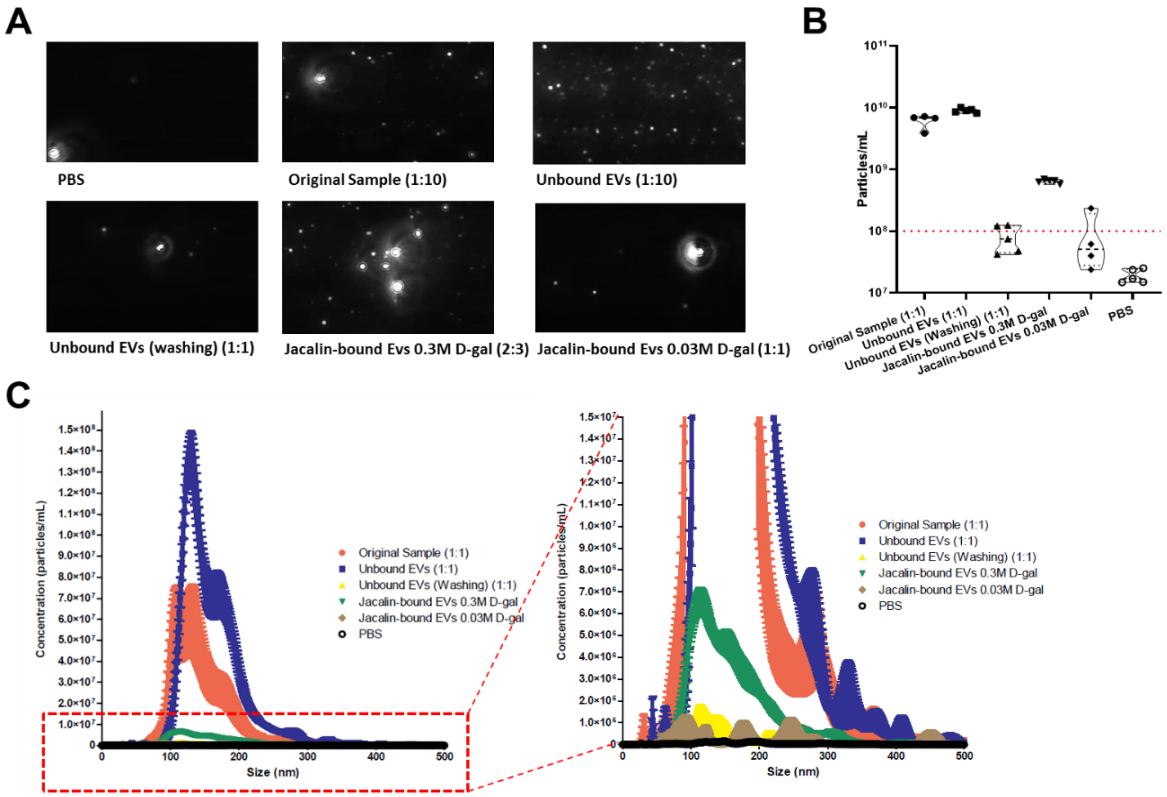

Figure 57. NTA of Jacalin-positive EVs. For different stages of the protocol, samples were collected for NTA analysis: Original samples (EV isolated from patient plasma), Unbound EVs (supernatant after Original samples were incubated with biotinylated Jacalin and biotin-binder magnetic beads), Unbound EVs-Washing (supernatant after washing step with PBS), Jacalin-bound EVs (supernatant after treatment of EV-bound magnetic beads with 0.03 or 0.3 M D-galactose). PBS buffer was included as a negative control. (A) Snapshot of EVs under NTA. Particles are shown as bright dots swinging when the analysis is running. (B) Nanoparticle concentration for all fractions analyzed. The red dotted line delimits the upper limit of PBS quantifications. (C) Distribution of the concentration of particles per size (nm) between all fractions analyzed. All results are expressed in particles per mL and five technical replicates were considered for each curve. The full videos of NTA analysis can be accesed here: https://doi.org/10.6084/m9.figshare.24073803. Figures B-C were built on GraphPad Prism v8 for Windows.

4.4.6 Challenges, lessons, and insights from the separation of EVs potentially derived from BC tumors

In this thesis, we observed differences in the cargo of EVs that could be associated with a body response in the presence of a tumor such as breast cancer, for example, the presence of anti-tumor miRNAs in plasma EVs. Thus, we decided to test a method of selecting EVs to favor those potentially produced by the tumor.

In this case, we decided to select EVs that express derivatives of the Tn antigen, targets of the Jacalin lectin [106,433,434]. However, it is possible to use exploratory technologies [101,431,432] to reveal the targets most expressed in tumor materials and less present in materials from healthy individuals.

The only detail of this exploratory approach is that it entails a high investment of resources since many known targets in the membrane of cells and EVs are made up of proteins. In that sense, in addition to canonical proteins, it would be possible to search for modified proteins [70,435–437], such as those analyzed in this thesis (modified by glycosylation-related processes). Thus, executing a broad spectrum search would require a cost-benefit analysis to preserve the balance between the number of samples necessary to generate consistent results and the number of analytes provided by this analysis.

Regarding our strategy for analyzing the Tn antigen and its derivatives, there is vast literature associating this antigen with tumor samples [96,98,99]. We then performed assays on cell lines (Figure 50 and Figure 51) and samples from cohort B with breast cancer (Figure 53 and Figure 52). Based on those results, we decided to try an experimental pilot to select extracellular vesicles expressing Jacalin targets.

After running the experiments, we consistently purified 10% of all EVs from patient samples (Figure 57). Although additional assays, such as dot blot or quantitative tests (ELISA) with this lectin are required to ensure the correct separation of these EVs, our results are consistent with other EV separation processes using affinity proteins.

Regarding this type of experiment, some points are still subjects of research, for example, the expected number of tumor-derived vesicles in human plasma from BC patients. To the best of our knowledge, tumors segregate vesicles to circulating media [438]. Nevertheless, we still do not know whether tumor-derived EV concentration is modulated by clinical or pathological factors.

Additionally, we have certain biases with the type of affinity protein and the system used. Antibodies and lectins can act as affinity proteins [429,430]. In this thesis, we primarily used Jacalin lectin to select EVs that express derivatives of the Tn antigen.

It is possible to use an antibody, such as the anti-STn antibody produced by B72.3 cells, which has already demonstrated selection against STn and Tn [439,440]. However, this is a still unexplored field. In the same way, we also do not know if there are derivatives of Tn (in addition to T and STn antigens) that may not be selected by the antibody but by the antigen.

As a summary of this section, we support the possibility of continuing trials that objectify the selection of EVs based on the expression of aberrant molecules (such as derivatives of the Tn antigen). Nevertheless, we emphasize the need to perform confirmatory tests to evaluate whether the enriched material (Jacalin+ EVs) shows sufficient EVs and miRNA yield to perform subsequent tests while intending to maintain the input volume handled throughout this project (1mL of plasma). Once this step has been carried out, it will be possible to validate in BC-derived EVs previous knowledge about the Tn antigen in BC tissues, such as its ability to show correlations with tumor stages, levels of aggressiveness, and prognosis [429].

CONCLUSIONS

- Protocols for i) isolating EVs from plasma, ii) isolating miRNA from plasma, iii) isolating miRNA from plasmatic EVs, iv) labeling Jacalin targets by dot blot in vesicular samples, and v) labeling Jacalin targets by lectin-histochemistry in BC tissues were established.

- BC subgroups (based on IHC profiles or age at diagnosis) show different miRNA profiles in cell-free (cf-miRNA) and vesicular (EV-miRNA) content.

- EV-miRNA represents a purest cargo than cf-miRNA. In addition, it is possible to separate EV subpopulations regarding the cell of origin and their biogenesis.

- Jacalin has the potential to label the tissues and plasma of BC patients. Then, it is possible to use this glycan-binding protein to separate EV subpopulations expressing Jacalin targets (Tn derivatives).

- The circulating (cf-miRNA) hsa-miR-28-3p was overexpressed in elderly (late onset) BC patients compared with young BC patients. In addition, young TNBC patients (early onset) showed higher levels of this miRNA when compared with young BC patients diagnosed with other subtypes.

- The miRNA hsa-miR-197-3p was downregulated in TNBC samples in their cf-miRNA and EV-miRNA forms.

- The hsa-miR-212-3p, hsa-miR-302d-3p, hsa-miR-28-5p, and hsa-miR-873-3p miRNAs proven to be highly expressed in EVs from plasma of BC patients.

SUGGESTIONS FOR FURTHER STUDIES

- To characterize the immunohistochemical, clinical, pathological, and sociodemographic profile of patients or cell lines used in experiments. It would avoid any overestimation of results.

- To run pre-analytical tests (including hemolysis checking) on plasma to ensure the quality of these samples, especially before evaluating non-vesicular cargoes.

- Once miRNAs are highly versatile, it is essential to have an adequate annotation (nomenclature and studied arm, -3p or -5p).

- In experiments with multiple comparisons, p-values must be adjusted, but in pilot studies (or those with a low number of samples per group), the interpretation of adjusted p-values should be revised.

- To explore protocols for concentrating EVs from bodily fluids to reach required volumes for conventional EV characterization protocols (TEM, WB, others).

- To get publicly available omics data from patient cohorts and keep it updated to open the possibility of running survival analysis and secondary comparisons later.

- To compare mechanisms for separating EV subpopulations using different platforms (carbon-based, magnetic beads, microfluidics, etc.) and ligation proteins (antibodies or lectins).

REFERENCES

[1] Sung H, Ferlay J, Siegel RL, Laversanne M, Soerjomataram I, Jemal A, et al. Global Cancer Statistics 2020: GLOBOCAN Estimates of Incidence and Mortality Worldwide for 36 Cancers in 185 Countries. CA Cancer J Clin 2021;71:209–49. https://doi.org/10.3322/CAAC.21660.

[2] Ferlay J, Ervik M, Lam F, Colombet M, Mery L, Piñeros M, et al. Global Cancer Observatory: Cancer Today. Lyon, Fr Int Agency Res Cancer 2020. https://gco.iarc.fr/today (accessed August 11, 2023).

[3] World Health Organization. Breast Cancer Fact Sheet. Breast Cancer 2023. https://www.who.int/news-room/fact-sheets/detail/breast-cancer (accessed August 11, 2023).

[4] De Lima Vazquez F, Silva TB, Da Costa Vieira RA, Da Costa AM, Scapulatempo C, Fregnani JHTG, et al. Retrospective analysis of breast cancer prognosis among young and older women in a Brazilian cohort of 738 patients, 1985–2002. Oncol Lett 2016;12:4911–24. https://doi.org/10.3892/ol.2016.5360.

[5] Han W, Kim SW, Ae Park I, Kang D, Kim S-W, Youn Y-K, et al. Young age: an independent risk factor for disease-free survival in women with operable breast cancer. BMC Cancer 2004;4:82. https://doi.org/10.1186/1471-2407-4-82.

[6] Sundquist M, Thorstenson S, Brudin L, Wingren S, Nordenskjöld B. Incidence and prognosis in early onset breast cancer. The Breast 2002;11:30–5. https://doi.org/10.1054/brst.2001.0358.

[7] Silva JDDE, de Oliveira RR, da Silva MT, Carvalho MD de B, Pedroso RB, Pelloso SM. Breast Cancer Mortality in Young Women in Brazil. Front Oncol 2021;10:569933. https://doi.org/10.3389/fonc.2020.569933.

[8] Guo L, Kong D, Liu J, Zhan L, Luo L, Zheng W, et al. Breast cancer heterogeneity and its implication in personalized precision therapy. Exp Hematol Oncol 2023;12:3. https://doi.org/10.1186/s40164-022-00363-1.

[9] Tan PH, Ellis I, Allison K, Brogi E, Fox SB, Lakhani S, et al. The 2019 World Health Organization classification of tumours of the breast. Histopathology 2020;77:181–5. https://doi.org/10.1111/his.14091.

[10] Vuong D, Simpson PT, Green B, Cummings MC, Lakhani SR. Molecular classification of breast cancer. Virchows Arch 2014;465:1–14. https://doi.org/10.1007/s00428-014-1593-7.

[11] American Cancer Society. Types of Breast Cancer. ACS 2021. https://www.cancer.org/cancer/types/breast-cancer/about/types-of-breast-

cancer.html (accessed August 15, 2023).

[12] Cianfrocca M, Gradishar W. New Molecular Classifications of Breast Cancer. CA Cancer J Clin 2009;59:303–13. https://doi.org/10.3322/caac.20029.

[13] Garrido-Castro AC, Lin NU, Polyak K. Insights into Molecular Classifications of Triple-Negative Breast Cancer: Improving Patient Selection for Treatment. Cancer Discov 2019;9:176–98. https://doi.org/10.1158/2159-8290.CD-18-1177.

[14] Zhang X. Molecular Classification of Breast Cancer: Relevance and Challenges. Arch Pathol Lab Med 2023;147:46–51. https://doi.org/10.5858/arpa.2022-0070-RA.

[15] Rakha EA, Green AR. Molecular classification of breast cancer: what the pathologist needs to know. Pathology 2017;49:111–9. https://doi.org/10.1016/j.pathol.2016.10.012.

[16] Dobruch-Sobczak K, Gumowska M, Mączewska J, Kolasińska-Ćwikła A, Guzik P. Immunohistochemical subtypes of the breast cancer in the ultrasound and clinical aspect – literature review. J Ultrason 2022;22:93–9. https://doi.org/10.15557/JoU.2022.0016.

[17] Yersal O. Biological subtypes of breast cancer: Prognostic and therapeutic implications. World J Clin Oncol 2014;5:412. https://doi.org/10.5306/wjco.v5.i3.412.

[18] Rydén L, Heibert Arnlind M, Vitols S, Höistad M, Ahlgren J. Aromatase inhibitors alone or sequentially combined with tamoxifen in postmenopausal early breast cancer compared with tamoxifen or placebo – Meta-analyses on efficacy and adverse events based on randomized clinical trials. The Breast 2016;26:106–14. https://doi.org/10.1016/j.breast.2016.01.006.

[19] Garreau JR, DeLaMelena T, Walts D, Karamlou K, Johnson N. Side effects of aromatase inhibitors versus tamoxifen: the patients' perspective. Am J Surg 2006;192:496–8. https://doi.org/10.1016/j.amjsurg.2006.06.018.

[20] Buzdar A, Howell A. Advances in Aromatase Inhibition: Clinical Efficacy and Tolerability in the Treatment of Breast Cancer. Clin Cancer Res 2001;7:2620–35.

[21] Cirqueira MB, Moreira MAR, Soares LR, Freitas-Júnior R. Molecular subtypes of breast cancer. Femina 2011;39:499–503.

[22] Furrer D, Sanschagrin F, Jacob S, Diorio C. Advantages and Disadvantages of Technologies for HER2 Testing in Breast Cancer Specimens: Table 1. Am J Clin Pathol 2015;144:686–703. https://doi.org/10.1309/AJCPT41TCBUEVDQC.

[23] Bartlett JMS, Going JJ, Mallon EA, Watters AD, Reeves JR, Stanton P, et al. EvaluatingHER2 amplification and overexpression in breast cancer. J Pathol

2001;195:422–8. https://doi.org/10.1002/path.971.

[24] Dalal H, Dahlgren M, Gladchuk S, Brueffer C, Gruvberger-Saal SK, Saal LH. Clinical associations of ESR2 (estrogen receptor beta) expression across thousands of primary breast tumors. Sci Rep 2022;12:4696. https://doi.org/10.1038/s41598-022-08210-3.

[25] Gonçalves H, Guerra MR, Duarte Cintra JR, Fayer VA, Brum IV, Bustamante Teixeira MT. Survival Study of Triple-Negative and Non–Triple-Negative Breast Cancer in a Brazilian Cohort. Clin Med Insights Oncol 2018;12:1–10. https://doi.org/10.1177/1179554918790563.

[26] Li X, Yang J, Peng L, Sahin AA, Huo L, Ward KC, et al. Triple-negative breast cancer has worse overall survival and cause-specific survival than non-triple-negative breast cancer. Breast Cancer Res Treat 2017;161:279–87. https://doi.org/10.1007/s10549-016-4059-6.

[27] Lehmann BD, Bauer JA, Chen X, Sanders ME, Chakravarthy AB, Shyr Y, et al. Identification of human triple-negative breast cancer subtypes and preclinical models for selection of targeted therapies. J Clin Invest 2011;121:2750–67. https://doi.org/10.1172/JCI45014.

[28] Yin L, Duan J-J, Bian X-W, Yu S. Triple-negative breast cancer molecular subtyping and treatment progress. Breast Cancer Res 2020;22:61. https://doi.org/10.1186/s13058-020-01296-5.

[29] Le Du F, Eckhardt BL, Lim B, Litton JK, Moulder S, Meric-Bernstam F, et al. Is the future of personalized therapy in triple-negative breast cancer based on molecular subtype? Oncotarget 2015;6:12890–908. https://doi.org/10.18632/oncotarget.3849.

[30] Lee Y-M, Oh MH, Go J-H, Han K, Choi S-Y. Molecular subtypes of triple-negative breast cancer: understanding of subtype categories and clinical implication. Genes Genomics 2020;42:1381–7. https://doi.org/10.1007/s13258-020-01014-7.

[31] Paik S, Shak S, Tang G, Kim C, Baker J, Cronin M, et al. A Multigene Assay to Predict Recurrence of Tamoxifen-Treated, Node-Negative Breast Cancer. N Engl J Med 2004;351:2817–26. https://doi.org/10.1056/NEJMoa041588.

[32] Parker JS, Mullins M, Cheang MCU, Leung S, Voduc D, Vickery T, et al. Supervised Risk Predictor of Breast Cancer Based on Intrinsic Subtypes. J Clin Oncol 2009;27:1160–7. https://doi.org/10.1200/JCO.2008.18.1370.

[33] Buyse M, Loi S, van't Veer L, Viale G, Delorenzi M, Glas AM, et al. Validation and Clinical Utility of a 70-Gene Prognostic Signature for Women With Node-Negative Breast Cancer. JNCI J Natl Cancer Inst 2006;98:1183–92.

https://doi.org/10.1093/jnci/djj329.

[34] Mittempergher L, Delahaye LJ, Witteveen AT, Snel MH, Mee S, Chan BY, et al. Performance Characteristics of the BluePrint® Breast Cancer Diagnostic Test. Transl Oncol 2020;13:100756. https://doi.org/10.1016/j.tranon.2020.100756.

[35] Thennavan A, Beca F, Xia Y, Garcia-Recio S, Allison K, Collins LC, et al. Molecular analysis of TCGA breast cancer histologic types. Cell Genomics 2021;1:100067. https://doi.org/10.1016/j.xgen.2021.100067.

[36] Curtis C, Shah SP, Chin S-F, Turashvili G, Rueda OM, Dunning MJ, et al. The genomic and transcriptomic architecture of 2,000 breast tumours reveals novel subgroups. Nature 2012;486:346–52. https://doi.org/10.1038/nature10983.

[37] Halvaei S, Daryani S, Eslami-S Z, Samadi T, Jafarbeik-Iravani N, Bakhshayesh TO, et al. Exosomes in Cancer Liquid Biopsy: A Focus on Breast Cancer. Mol Ther - Nucleic Acids 2018;10:131–41. https://doi.org/10.1016/j.omtn.2017.11.014.

[38] Crowley E, Di Nicolantonio F, Loupakis F, Bardelli A. Liquid biopsy: Monitoring cancer-genetics in the blood. Nat Rev Clin Oncol 2013;10:472–84. https://doi.org/10.1038/nrclinonc.2013.110.

[39] Alix-Panabières C, Pantel K. Clinical applications of circulating tumor cells and circulating tumor DNA as liquid biopsy. Cancer Discov 2016;6:479–91. https://doi.org/10.1158/2159-8290.CD-15-1483.

[40] Best MG, Sol N, In ‘t Veld SGJG, Vancura A, Muller M, Niemeijer ALN, et al. Swarm Intelligence-Enhanced Detection of Non-Small-Cell Lung Cancer Using Tumor-Educated Platelets. Cancer Cell 2017;32:238-252.e9. https://doi.org/10.1016/j.ccell.2017.07.004.

[41] Mazzitelli C, Santini D, Corradini AG, Zamagni C, Trerè D, Montanaro L, et al. Liquid Biopsy in the Management of Breast Cancer Patients: Where Are We Now and Where Are We Going. Diagnostics 2023;13:1241. https://doi.org/10.3390/diagnostics13071241.

[42] Giacona MB, Ruben GC, Iczkowski KA, Roos TB, Porter DM, Sorenson GD. Cell-free DNA in human blood plasma: Length measurements in patients with pancreatic cancer and healthy controls. Pancreas 1998;17:89–97. https://doi.org/10.1097/00006676-199807000-00012.

[43] Murillo Carrasco A, Acosta O, Ponce J, Cotrina J, Aguilar A, Araujo J, et al. PUM1 and RNase P genes as potential cell-free DNA markers in breast cancer. J Clin Lab Anal 2021;35:1–10. https://doi.org/10.1002/jcla.23720.

[44] Fernandez-Garcia D, Hills A, Page K, Hastings RK, Toghill B, Goddard KS, et al. Plasma cell-free DNA (cfDNA) as a predictive and prognostic marker in patients

with metastatic breast cancer. Breast Cancer Res 2019;21:149. https://doi.org/10.1186/s13058-019-1235-8.

[45] Danos P, Giannoni-Luza S, Murillo Carrasco AG, Acosta O, Guevara-Fujita ML, Cotrina Concha JM, et al. Promoter hypermethylation of <scp> *RARB* </scp> and <scp> *GSTP1* </scp> genes in plasma cell-free <scp>DNA</scp> as breast cancer biomarkers in Peruvian women. Mol Genet Genomic Med 2023;00:1–12. https://doi.org/10.1002/mgg3.2260.

[46] Stastny I, Zubor P, Kajo K, Kubatka P, Golubnitschaja O, Dankova Z. Aberrantly Methylated cfDNA in Body Fluids as a Promising Diagnostic Tool for Early Detection of Breast Cancer. Clin Breast Cancer 2020;20:e711–22. https://doi.org/10.1016/j.clbc.2020.05.009.

[47] Chimonidou M, Tzitzira A, Strati A, Sotiropoulou G, Sfikas C, Malamos N, et al. CST6 promoter methylation in circulating cell-free DNA of breast cancer patients. Clin Biochem 2013;46:235–40. https://doi.org/10.1016/j.clinbiochem.2012.09.015.

[48] Giannoni-Luza S, Acosta O, Murillo Carrasco AG, Danos P, Cotrina Concha JM, Guerra Miller H, et al. Chip-based digital Polymerase Chain Reaction as quantitative technique for the detection of PIK3CA mutations in breast cancer patients. Heliyon 2022;8:e11396. https://doi.org/10.1016/j.heliyon.2022.e11396.

[49] Dawson S-J, Tsui DWY, Murtaza M, Biggs H, Rueda OM, Chin S-F, et al. Analysis of Circulating Tumor DNA to Monitor Metastatic Breast Cancer. N Engl J Med 2013;368:1199–209. https://doi.org/10.1056/NEJMoa1213261.

[50] Sobhani N, Generali D, Zanconati F, Bortul M, Scaggiante B. Cell-free DNA integrity for the monitoring of breast cancer: Future perspectives? World J Clin Oncol 2018;9:26–32. https://doi.org/10.5306/wjco.v9.i2.26.

[51] Kustanovich A, Schwartz R, Peretz T, Grinshpun A. Life and death of circulating cell-free DNA. Cancer Biol Ther 2019;20:1057–67. https://doi.org/10.1080/15384047.2019.1598759.

[52] Tong Y-K, Lo YMD. Diagnostic developments involving cell-free (circulating) nucleic acids. Clin Chim Acta 2006;363:187–96. https://doi.org/10.1016/j.cccn.2005.05.048.

[53] de Jong JS, Diest PJ van, Baak JPA. Number of apoptotic cells as a prognostic marker in invasive breast cancer. Br J Cancer 2000;82:368–73. https://doi.org/10.1054/bjoc.1999.0928.

[54] Paci P, Colombo T, Farina L. Computational analysis identifies a sponge interaction network between long non-coding RNAs and messenger RNAs in human breast cancer. BMC Syst Biol 2014;8:83. https://doi.org/10.1186/1752-

0509-8-83.

[55] Hardeland R. Melatonin, Noncoding RNAs, Messenger RNA Stability and Epigenetics—Evidence, Hints, Gaps and Perspectives. Int J Mol Sci 2014;15:18221–52. https://doi.org/10.3390/ijms151018221.

[56] LICHTENSTEIN A V., MELKONYAN HS, TOMEI LD, UMANSKY SR. Circulating Nucleic Acids and Apoptosis. Ann N Y Acad Sci 2006;945:239–49. https://doi.org/10.1111/j.1749-6632.2001.tb03892.x.

[57] Creemers EE, Tijsen AJ, Pinto YM. Circulating MicroRNAs. Circ Res 2012;110:483–95. https://doi.org/10.1161/CIRCRESAHA.111.247452.

[58] Wang H, Peng R, Wang J, Qin Z, Xue L. Circulating microRNAs as potential cancer biomarkers: the advantage and disadvantage. Clin Epigenetics 2018;10:59. https://doi.org/10.1186/s13148-018-0492-1.

[59] Pozniak T, Shcharbin D, Bryszewska M. Circulating microRNAs in Medicine. Int J Mol Sci 2022;23:3996. https://doi.org/10.3390/ijms23073996.

[60] Cacheux J, Bancaud A, Leichlé T, Cordelier P. Technological Challenges and Future Issues for the Detection of Circulating MicroRNAs in Patients With Cancer. Front Chem 2019;7:1–11. https://doi.org/10.3389/fchem.2019.00815.

[61] Letelier P, Riquelme I, Hernández A, Guzmán N, Farías J, Roa J. Circulating MicroRNAs as Biomarkers in Biliary Tract Cancers. Int J Mol Sci 2016;17:791. https://doi.org/10.3390/ijms17050791.

[62] Kozomara A, Birgaoanu M, Griffiths-Jones S. miRBase: from microRNA sequences to function. Nucleic Acids Res 2019;47:D155–62. https://doi.org/10.1093/nar/gky1141.

[63] Furuya TK, Bovolenta Murta C, Carrasco AGM, Uno M, Sichero L, Villa LL, et al. Disruption of miRNA-mRNA networks defines novel molecular signatures for penile carcinogenesis. Cancers (Basel) 2021;13:4745. https://doi.org/10.3390/CANCERS13194745/S1.

[64] Murillo Carrasco A, Giannoni S, Acosta Conchucos O, Cotrina J, Aguilar A, Rebaza P, et al. EVALUATION OF PLASMA MIRNAS FOR EARLY DIAGNOSIS OF BREAST CANCER. Conceitos Básicos da Genética, Atena Editora; 2019, p. 128–38. https://doi.org/10.22533/at.ed.214192106.

[65] nanoString. nCounter® Analysis System. 2018.

[66] Phan TH, Kim SY, Rudge C, Chrzanowski W. Made by cells for cells – extracellular vesicles as next-generation mainstream medicines. J Cell Sci 2022;135:jcs259166. https://doi.org/10.1242/jcs.259166.

[67] Lopez-Verrilli MA, Court FA. Exosomes: Mediators of communication in eukaryotes. Biol Res 2013;46:5–11. https://doi.org/10.4067/S0716-

97602013000100001.

[68] Dixson AC, Dawson TR, Di Vizio D, Weaver AM. Context-specific regulation of extracellular vesicle biogenesis and cargo selection. Nat Rev Mol Cell Biol 2023;24:454–76. https://doi.org/10.1038/s41580-023-00576-0.

[69] Doyle LM, Wang MZ. Overview of extracellular vesicles, their origin, composition, purpose, and methods for exosome isolation and analysis. Cells 2019;8:727. https://doi.org/10.3390/cells8070727.

[70] Murillo Carrasco AG, Otake AH, Macedo-da-Silva J, Feijoli Santiago V, Palmisano G, Andrade LN de S, et al. Deciphering the Functional Status of Breast Cancers through the Analysis of Their Extracellular Vesicles. Int J Mol Sci 2023;24:13022. https://doi.org/10.3390/ijms241613022.

[71] Ma L, Li Y, Peng J, Wu D, Zhao X, Cui Y, et al. Discovery of the migrasome, an organelle mediating release of cytoplasmic contents during cell migration. Cell Res 2015;25:24–38. https://doi.org/10.1038/cr.2014.135.

[72] Théry C, Witwer KW, Aikawa E, Alcaraz MJ, Anderson JD, Andriantsitohaina R, et al. Minimal information for studies of extracellular vesicles 2018 (MISEV2018): a position statement of the International Society for Extracellular Vesicles and update of the MISEV2014 guidelines. Https://DoiOrg/101080/2001307820181535750 2018;7. https://doi.org/10.1080/20013078.2018.1535750.

[73] Ni C, Fang QQ, Chen WZ, Jiang JX, Jiang Z, Ye J, et al. Breast cancer-derived exosomes transmit lncRNA SNHG16 to induce CD73+γδ1 Treg cells. Signal Transduct Target Ther 2020 51 2020;5:1–14. https://doi.org/10.1038/s41392-020-0129-7.

[74] Xia W, Liu Y, Cheng T, Xu T, Dong M, Hu X. Extracellular Vesicles Carry lncRNA SNHG16 to Promote Metastasis of Breast Cancer Cells via the miR-892b/PPAPDC1A Axis. Front Cell Dev Biol 2021;9:1319. https://doi.org/10.3389/FCELL.2021.628573.

[75] Feng T, Zhang P, Sun Y, Wang Y, Tong J, Dai H, et al. High throughput sequencing identifies breast cancer-secreted exosomal LncRNAs initiating pulmonary pre-metastatic niche formation. Gene 2019;710:258–64. https://doi.org/10.1016/J.GENE.2019.06.004.

[76] Li M, Zou X, Xia T, Wang T, Liu P, Zhou X, et al. A five-miRNA panel in plasma was identified for breast cancer diagnosis. Cancer Med 2019;8:7006–17. https://doi.org/10.1002/cam4.2572.

[77] Khalighfard S, Alizadeh AM, Irani S, Omranipour R. Plasma miR-21, miR-155, miR-10b, and Let-7a as the potential biomarkers for the monitoring of breast

cancer patients. Sci Rep 2018;8:17981. https://doi.org/10.1038/s41598-018-36321-3.

[78] Motamedi M, Hashemzadeh Chaleshtori M, Ghasemi S, Mokarian F. Plasma Level Of miR-21 And miR-451 In Primary And Recurrent Breast Cancer Patients. Breast Cancer Targets Ther 2019;11:293–301. https://doi.org/10.2147/BCTT.S224333.

[79] INUBUSHI S, KAWAGUCHI H, MIZUMOTO S, KUNIHISA T, BABA M, KITAYAMA Y, et al. Oncogenic miRNAs Identified in Tear Exosomes From Metastatic Breast Cancer Patients. Anticancer Res 2020;40:3091–6. https://doi.org/10.21873/ANTICANRES.14290.

[80] Arisan ED, Rencuzogullari O, Cieza-borrella C, Miralles Arenas F, Dwek M, Lange S, et al. MiR-21 Is Required for the Epithelial–Mesenchymal Transition in MDA-MB-231 Breast Cancer Cells. Int J Mol Sci 2021, Vol 22, Page 1557 2021;22:1557. https://doi.org/10.3390/IJMS22041557.

[81] Abdulhussain MM, Hasan NA, Hussain AG. Interrelation of the Circulating and Tissue MicroRNA-21 with Tissue PDCD4 Expression and the Invasiveness of Iraqi Female Breast Tumors. Indian J Clin Biochem 2017;34:26–38. https://doi.org/10.1007/s12291-017-0710-1.

[82] Yuan X, Qian N, Ling S, Li Y, Sun W, Li J, et al. Breast cancer exosomes contribute to pre-metastatic niche formation and promote bone metastasis of tumor cells. Theranostics 2021;11:1429–45. https://doi.org/10.7150/THNO.45351.

[83] Wang W, Yuan X, Xu A, Zhu X, Zhan Y, Wang S, et al. Human cancer cells suppress behaviors of endothelial progenitor cells through miR-21 targeting IL6R. Microvasc Res 2018;120:21–8. https://doi.org/10.1016/J.MVR.2018.05.007.

[84] Ahmed SH, Espinoza-Sánchez NA, El-Damen A, Fahim SA, Badawy MA, Greve B, et al. Small extracellular vesicle-encapsulated miR-181b-5p, miR-222-3p and let-7a-5p: Next generation plasma biopsy-based diagnostic biomarkers for inflammatory breast cancer. PLoS One 2021;16:e0250642. https://doi.org/10.1371/JOURNAL.PONE.0250642.

[85] Ozawa PMM, Vieira E, Lemos DS, Souza ILM, Zanata SM, Pankievicz VC, et al. Identification of miRNAs Enriched in Extracellular Vesicles Derived from Serum Samples of Breast Cancer Patients. Biomol 2020, Vol 10, Page 150 2020;10:150. https://doi.org/10.3390/BIOM10010150.

[86] Sueta A, Fujiki Y, Goto-Yamaguchi L, Tomiguchi M, Yamamoto-Ibusuki M, Iwase H, et al. Exosomal miRNA profiles of triple-negative breast cancer in

neoadjuvant treatment. Oncol Lett 2021;22:1–10. https://doi.org/10.3892/OL.2021.13080/HTML.

[87] Wu H, Wang Q, Zhong H, Li L, Zhang Q, Huang Q, et al. Differentially expressed microRNAs in exosomes of patients with breast cancer revealed by next-generation sequencing. Oncol Rep 2020;43:240–50. https://doi.org/10.3892/OR.2019.7401/HTML.

[88] Zhang Z, Zhang L, Yu G, Sun Z, Wang T, Tian X, et al. Exosomal miR-1246 and miR-155 as predictive and prognostic biomarkers for trastuzumab-based therapy resistance in HER2-positive breast cancer 2020;86:761–72.

[89] Royo F, Théry C, Falcón-Pérez JM, Nieuwland R, Witwer KW. Methods for Separation and Characterization of Extracellular Vesicles: Results of a Worldwide Survey Performed by the ISEV Rigor and Standardization Subcommittee. Cells 2020;9:1955. https://doi.org/10.3390/cells9091955.

[90] Mateescu B, Kowal EJK, van Balkom BWM, Bartel S, Bhattacharyya SN, Buzás EI, et al. Obstacles and opportunities in the functional analysis of extracellular vesicle RNA – an ISEV position paper. J Extracell Vesicles 2017;6:1286095. https://doi.org/10.1080/20013078.2017.1286095.

[91] Jankovičová J, Sečová P, Michalková K, Antalíková J. Tetraspanins, More than Markers of Extracellular Vesicles in Reproduction. Int J Mol Sci 2020;21:7568. https://doi.org/10.3390/ijms21207568.

[92] Mizenko RR, Brostoff T, Rojalin T, Koster HJ, Swindell HS, Leiserowitz GS, et al. Tetraspanins are unevenly distributed across single extracellular vesicles and bias sensitivity to multiplexed cancer biomarkers. J Nanobiotechnology 2021;19:250. https://doi.org/10.1186/s12951-021-00987-1.

[93] Buzas EI. Opportunities and challenges in studying the extracellular vesicle corona. Nat Cell Biol 2022;24:1322–5. https://doi.org/10.1038/s41556-022-00983-z.

[94] Tóth EÁ, Turiák L, Visnovitz T, Cserép C, Mázló A, Sódar BW, et al. Formation of a protein corona on the surface of extracellular vesicles in blood plasma. J Extracell Vesicles 2021;10:e12140. https://doi.org/10.1002/jev2.12140.

[95] Pinho SS, Reis CA. Glycosylation in cancer: Mechanisms and clinical implications. vol. 15. Nature Publishing Group; 2015. https://doi.org/10.1038/nrc3982.

[96] Munkley J. The role of sialyl-Tn in cancer. Int J Mol Sci 2016;17:275. https://doi.org/10.3390/ijms17030275.

[97] Ju T, Wang Y, Aryal RP, Lehoux SD, Ding X, Kudelka MR, et al. Tn and sialyl-Tn antigens, aberrant O -glycomics as human disease markers. PROTEOMICS -

Clin Appl 2013;7:618–31. https://doi.org/10.1002/prca.201300024.

[98] Fu C, Zhao H, Wang Y, Cai H, Xiao Y, Zeng Y, et al. Tumor-associated antigens: Tn antigen, sTn antigen, and T antigen. HLA 2016;88:275–86. https://doi.org/10.1111/tan.12900.

[99] Kölbl AC, Jeschke U, Friese K, Andergassen U. The role of TF- and Tn-antigens in breast cancer metastasis. Histol Histopathol 2016;31:613–21. https://doi.org/10.14670/HH-11-722.

[100] Tang MKS, Wong AST. Exosomes: Emerging biomarkers and targets for ovarian cancer. Cancer Lett 2015;367:26–33. https://doi.org/10.1016/j.canlet.2015.07.014.

[101] Syed P, Gidwani K, Kekki H, Leivo J, Pettersson K, Lamminmäki U. Role of lectin microarrays in cancer diagnosis. Proteomics 2016;16:1257–65. https://doi.org/10.1002/pmic.201500404.

[102] Samsonov R, Shtam T, Burdakov V, Glotov A, Tsyrlina E, Berstein L, et al. Lectin-induced agglutination method of urinary exosomes isolation followed by mi-RNA analysis: Application for prostate cancer diagnostic. Prostate 2016;76:68–79. https://doi.org/10.1002/pros.23101.

[103] Gerlach JQ, Maguire CM, Krüger A, Joshi L, Prina-Mello A, Griffin MD. Urinary nanovesicles captured by lectins or antibodies demonstrate variations in size and surface glycosylation profile. Nanomedicine 2017;12:1217–29. https://doi.org/10.2217/nnm-2017-0016.

[104] Tang H, Hsueh P, Kletter D, Bern M, Haab B. The Detection and Discovery of Glycan Motifs in Biological Samples Using Lectins and Antibodies: New Methods and Opportunities, 2015, p. 167–202. https://doi.org/10.1016/bs.acr.2014.11.003.

[105] Cummings RD, Etzler M. Chapter 45Antibodies and Lectins in Glycan Analysis. Essentials Glycobiol., Cold Spring Harbor Laboratory Press; 2009.

[106] Poiroux G, Barre A, van Damme EJM, Benoist H, Rougé P. Plant lectins targeting O-glycans at the cell surface as tools for cancer diagnosis, prognosis and therapy. Int J Mol Sci 2017;18:1232. https://doi.org/10.3390/ijms18061232.

[107] Hagiwara K, Collet-Cassart D, Kunihiko K, Vaerman J-P. Jacalin: isolation, characterization, and influence of various factors on its interaction with human IgA1, as assessed by precipitation and latex agglutination. Mol Immunol 1988;25:69–83. https://doi.org/10.1016/0161-5890(88)90092-2.

[108] Miller RL. Purification of peanut (Arachis hypogaea) agglutinin isolectins by chromatofocusing. Anal Biochem 1983;131:438–46. https://doi.org/10.1016/0003-2697(83)90196-3.

[109] Bergallo HG, Bergallo AC, Rocha HB, Rocha CFD. Invasion by Artocarpus heterophyllus (Moraceae) in an island in the Atlantic Forest Biome, Brazil: distribution at the landscape level, density and need for control. J Coast Conserv 2016;20:191–8. https://doi.org/10.1007/s11852-016-0429-9.

[110] Gonçalves JLS, Lopes RC, Oliveira DB, Costa SS, Miranda MMFS, Romanos MTV, et al. In vitro anti-rotavirus activity of some medicinal plants used in Brazil against diarrhea. J Ethnopharmacol 2005;99:403–7. https://doi.org/10.1016/j.jep.2005.01.032.

[111] SOUSA DF de, CAMPOS FILHO PC, CONCEIÇÃO AO da. Antibacterial activity of jackfruit leaves extracts and the interference on antimicrobial susceptibility of enteropathogen. Food Sci Technol 2022;42:1–5. https://doi.org/10.1590/fst.49220.

[112] Waghmare R, Memon N, Gat Y, Gandhi S, Kumar V, Panghal A. Jackfruit seed: an accompaniment to functional foods. Brazilian J Food Technol 2019;22:e2018207. https://doi.org/10.1590/1981-6723.20718.

[113] Bunn-Moreno MM, Campos-Neto A. Lectin(s) extracted from seeds of Artocarpus integrifolia (jackfruit): potent and selective stimulator(s) of distinct human T and B cell functions. J Immunol 1981;127:427–9. https://doi.org/10.4049/jimmunol.127.2.427.

[114] Bhat A V., Pattabiraman TN. Protease inhibitors from jackfruit seed (Artocarpus integrifolia). J Biosci 1989;14:351–65. https://doi.org/10.1007/BF02703421.

[115] Nagala S, Yekula M, Tamanam RR. Antioxidant and gas chromatographic analysis of five varieties of jackfruit (Artocarpus) seed oils. Drug Invent Today 2013;5:315–20. https://doi.org/10.1016/j.dit.2013.08.001.

[116] Evaristo RA. Elaboração de jaca passa por diferentes processos de secagem. Universidade Federal da Paraíba, 2016.

[117] IBGE. Instituto Brasileiro de Geografia e Estatística. Produção Frutas No Bras 2021. https://www.ibge.gov.br/.

[118] Koster J, Volckmann R, Zwijnenburg D, Molenaar P, Versteeg R. Abstract 2490: R2: Genomics analysis and visualization platform. Cancer Res 2019;79:2490–2490. https://doi.org/10.1158/1538-7445.AM2019-2490.

[119] Ramirez MI, Amorim MG, Gadelha C, Milic I, Welsh JA, Freitas VM, et al. Technical challenges of working with extracellular vesicles. Nanoscale 2018;10:881–906. https://doi.org/10.1039/C7NR08360B.

[120] Chung J, Kim KH, Yu N, An SH, Lee S, Kwon K. Fluid Shear Stress Regulates the Landscape of microRNAs in Endothelial Cell-Derived Small Extracellular Vesicles and Modulates the Function of Endothelial Cells. Int J Mol Sci

2022;23:1314. https://doi.org/10.3390/ijms23031314.

[121] Lowry O, Rosebrough N, Farr AL, Randall R. PROTEIN MEASUREMENT WITH THE FOLIN PHENOL REAGENT. J Biol Chem 1951;193:265–75. https://doi.org/10.1016/S0021-9258(19)52451-6.

[122] LAEMMLI UK. Cleavage of Structural Proteins during the Assembly of the Head of Bacteriophage T4. Nature 1970;227:680–5. https://doi.org/10.1038/227680a0.

[123] Santos NL, Bustos SO, Reis PP, Chammas R, Andrade LNS. Extracellular Vesicle-Packaged miR-195-5p Sensitizes Melanoma to Targeted Therapy with Kinase Inhibitors. Cells 2023;12:1317. https://doi.org/10.3390/cells12091317.

[124] Van Deun J, Mestdagh P, Agostinis P, Akay Ö, Anand S, Anckaert J, et al. EV-TRACK: transparent reporting and centralizing knowledge in extracellular vesicle research. Nat Methods 2017;14:228–32. https://doi.org/10.1038/nmeth.4185.

[125] Castelo-Branco L, Pellat A, Martins-Branco D, Valachis A, Derksen JWG, Suijkerbuijk KPM, et al. ESMO Guidance for Reporting Oncology real-World evidence (GROW). Ann Oncol Off J Eur Soc Med Oncol 2023;34:1097–112. https://doi.org/10.1016/j.annonc.2023.10.001.

[126] Lucien F, Gustafson D, Lenassi M, Li B, Teske JJ, Boilard E, et al. MIBlood-EV: Minimal information to enhance the quality and reproducibility of blood extracellular vesicle research. J Extracell Vesicles 2023;12:e12385. https://doi.org/10.1002/jev2.12385.

[127] Villard A, Marchand L. Diagnostic Value of Cell-free Circulating Micrornas for Obesity and Type 2 Diabetes: A Meta-analysis. J Mol Biomark Diagn 2015;06:251. https://doi.org/10.4172/2155-9929.1000251.

[128] Zhang Y, Jia Y, Zheng R, Guo Y, Wang Y, Guo H, et al. Plasma MicroRNA-122 as a Biomarker for Viral-, Alcohol-, and Chemical-Related Hepatic Diseases. Clin Chem 2010;56:1830–8. https://doi.org/10.1373/clinchem.2010.147850.

[129] Momen-Heravi F, Saha B, Kodys K, Catalano D, Satishchandran A, Szabo G. Increased number of circulating exosomes and their microRNA cargos are potential novel biomarkers in alcoholic hepatitis. J Transl Med 2015;13:261. https://doi.org/10.1186/s12967-015-0623-9.

[130] Sundar IK, Li D, Rahman I. Small RNA-sequence analysis of plasma-derived extracellular vesicle miRNAs in smokers and patients with chronic obstructive pulmonary disease as circulating biomarkers. J Extracell Vesicles 2019;8:1684816. https://doi.org/10.1080/20013078.2019.1684816.

[131] Zhu X-L, Ren L-F, Wang H-P, Bai Z-T, Zhang L, Meng W-B, et al. Plasma microRNAs as potential new biomarkers for early detection of early gastric cancer. World J Gastroenterol 2019;25:1580–91.

https://doi.org/10.3748/wjg.v25.i13.1580.

[132] Barone I, Gelsomino L, Accattatis FM, Giordano F, Gyorffy B, Panza S, et al. Analysis of circulating extracellular vesicle derived microRNAs in breast cancer patients with obesity: a potential role for Let-7a. J Transl Med 2023;21:232. https://doi.org/10.1186/s12967-023-04075-w.

[133] O'Farrell HE, Bowman R V, Fong KM, Yang IA. Plasma Extracellular Vesicle miRNA Profiles Distinguish Chronic Obstructive Pulmonary Disease Exacerbations and Disease Severity. Int J Chron Obstruct Pulmon Dis 2022;17:2821–33. https://doi.org/10.2147/COPD.S379774.

[134] Gómez-Flores-Ramos L, Álvarez-Gómez RM, Villarreal-Garza C, Wegman-Ostrosky T, Mohar A. Breast cancer genetics in young women: What do we know? Mutat Res Mutat Res 2017;774:33–45. https://doi.org/10.1016/j.mrrev.2017.08.001.

[135] Young S, Pilarski RT, Donenberg T, Shapiro C, Hammond LS, Miller J, et al. The prevalence of BRCA1 mutations among young women with triple-negative breast cancer. BMC Cancer 2009;9:86. https://doi.org/10.1186/1471-2407-9-86.

[136] Lynch HT, Watson P, Conway T, Fitzsimmons ML, Lynch J. Breast cancer family history as a risk factor for early onset breast cancer. Breast Cancer Res Treat 1988;11:263–7. https://doi.org/10.1007/BF01807285.

[137] Mompeón A, Ortega-Paz L, Vidal-Gómez X, Costa TJ, Pérez-Cremades D, Garcia-Blas S, et al. Disparate miRNA expression in serum and plasma of patients with acute myocardial infarction: a systematic and paired comparative analysis. Sci Rep 2020;10:5373. https://doi.org/10.1038/s41598-020-61507-z.

[138] Öberg H. Comparison of extraction method for miRNA as a biomarker for the diagnosis of sepsis: Future diagnostics of sepsis. University of Skövde, 2020.

[139] Foye C, Yan IK, David W, Shukla N, Habboush Y, Chase L, et al. Comparison of miRNA quantitation by Nanostring in serum and plasma samples. PLoS One 2017;12:e0189165. https://doi.org/10.1371/journal.pone.0189165.

[140] Khordadmehr M, Ezzati H, Shahbazfar A, Jigari-Asl F, Baradaran B, Baghbani E, et al. mir-451a-5p Modulates Breast Cancer Cell Apoptosis, Migration, and Chemosensitivity to Carboplatin through the PTEN Pathway. Pharm Sci 2023;29:328–37. https://doi.org/10.34172/PS.2022.28.

[141] Liu Z-R, Song Y, Wan L-H, Zhang Y-Y, Zhou L-M. Over-expression of miR-451a can enhance the sensitivity of breast cancer cells to tamoxifen by regulating 14-3-3ζ, estrogen receptor α, and autophagy. Life Sci 2016;149:104–13. https://doi.org/10.1016/j.lfs.2016.02.059.

[142] Zhang H, Chen P, Yang J. miR-451a suppresses the development of breast

cancer via targeted inhibition of CCND2. Mol Cell Probes 2020;54:101651. https://doi.org/10.1016/j.mcp.2020.101651.

[143] Zhang X, Cong L, Xu D, Leng Q, Shi M, Zhou Y. AC092127.1-miR-451a-AE binding protein 2 Signaling Facilitates Malignant Properties of Breast Cancer. J Breast Cancer 2021;24:389. https://doi.org/10.4048/jbc.2021.24.e37.

[144] Emmenegger U, Sousa BA, Hoang VC, Chow A, Clemons M, Dent S, et al. Generation of a Plasma Microrna (Mirna) Signature Predicting Response to Metronomic Chemotherapy (Mc) for Advanced Breast Cancer (Abc). Ann Oncol 2014;25:iv62. https://doi.org/10.1093/annonc/mdu326.12.

[145] Fang R, Zhu Y, Hu L, Khadka VS, Ai J, Zou H, et al. Plasma MicroRNA Pair Panels as Novel Biomarkers for Detection of Early Stage Breast Cancer. Front Physiol 2019;9:1879. https://doi.org/10.3389/fphys.2018.01879.

[146] Penyige A, Márton É, Soltész B, Szilágyi-Bónizs M, Póka R, Lukács J, et al. Circulating miRNA Profiling in Plasma Samples of Ovarian Cancer Patients. Int J Mol Sci 2019;20:4533. https://doi.org/10.3390/ijms20184533.

[147] Chang C-W, Wu H-C, Terry MB, Santella RM. microRNA Expression in Prospectively Collected Blood as a Potential Biomarker of Breast Cancer Risk in the BCFR. Anticancer Res 2015;35:3969–77.

[148] Shkurnikov MY, Knyazev EN, Fomicheva KA, Mikhailenko DS, Nyushko KM, Saribekyan EK, et al. Analysis of Plasma microRNA Associated with Hemolysis. Bull Exp Biol Med 2016;160:748–50. https://doi.org/10.1007/s10517-016-3300-y.

[149] Smith MD, Leemaqz SY, Jankovic-Karasoulos T, McAninch D, McCullough D, Breen J, et al. Haemolysis Detection in MicroRNA-Seq from Clinical Plasma Samples. Genes (Basel) 2022;13:1288. https://doi.org/10.3390/genes13071288.

[150] Wan Azman WN, Omar J, Koon TS, Tuan Ismail TS. Hemolyzed Specimens: Major Challenge for Identifying and Rejecting Specimens in Clinical Laboratories. Oman Med J 2019;34:94–8. https://doi.org/10.5001/omj.2019.19.

[151] Simundic A-M, Topic E, Nikolac N, Lippi G. Hemolysis detection and management of hemolysed specimens. Biochem Medica 2010;20:154–9. https://doi.org/10.11613/BM.2010.018.

[152] Lippi G, Avanzini P, da Pavesi F, Bardi M, Ippolito L, Aloe R, et al. Studies on in vitro hemolysis and utility of corrective formulas for reporting results on hemolyzed specimens. Biochem Medica 2011:297–305. https://doi.org/10.11613/BM.2011.040.

[153] Carraro P, Servidio G, Plebani M. Hemolyzed specimens: a reason for rejection or a clinical challenge? Clin Chem 2000;46:306–7.

[154] Wen Y-C, Lee W-J, Tan P, Yang S-F, Hsiao M, Lee L-M, et al. By inhibiting snail

signaling and miR-23a-3p, osthole suppresses the EMT-mediated metastatic ability in prostate cancer. Oncotarget 2015;6:21120–36. https://doi.org/10.18632/oncotarget.4229.

[155] Xiang Y, Yang Y, Lin C, Wu J, Zhang X. MiR-23a-3p promoted G1/S cell cycle transition by targeting protocadherin17 in hepatocellular carcinoma. J Physiol Biochem 2020;76:123–34. https://doi.org/10.1007/s13105-020-00726-4.

[156] Reis PP, Drigo SA, Carvalho RF, Lopez Lapa RM, Felix TF, Patel D, et al. Circulating miR-16-5p, miR-92a-3p, and miR-451a in Plasma from Lung Cancer Patients: Potential Application in Early Detection and a Regulatory Role in Tumorigenesis Pathways. Cancers (Basel) 2020;12:2071. https://doi.org/10.3390/cancers12082071.

[157] Floris I, Billard H, Boquien C-Y, Joram-Gauvard E, Simon L, Legrand A, et al. MiRNA Analysis by Quantitative PCR in Preterm Human Breast Milk Reveals Daily Fluctuations of hsa-miR-16-5p. PLoS One 2015;10:e0140488. https://doi.org/10.1371/journal.pone.0140488.

[158] Qattan A, Intabli H, Alkhayal W, Eltabache C, Tweigieri T, Amer S Bin. Robust expression of tumor suppressor miRNA's let-7 and miR-195 detected in plasma of Saudi female breast cancer patients. BMC Cancer 2017;17:799. https://doi.org/10.1186/s12885-017-3776-5.

[159] Chiorino G, Petracci E, Sehovic E, Gregnanin I, Camussi E, Mello-Grand M, et al. Plasma microRNA ratios associated with breast cancer detection in a nested case–control study from a mammography screening cohort. Sci Rep 2023;13:12040. https://doi.org/10.1038/s41598-023-38886-0.

[160] Wei Y, Yang J, Yi L, Wang Y, Dong Z, Liu Z, et al. MiR-223-3p targeting SEPT6 promotes the biological behavior of prostate cancer. Sci Rep 2014;4:7546. https://doi.org/10.1038/srep07546.

[161] Aziz F, Chakraborty A, Khan I, Monts J. Relevance of miR-223 as Potential Diagnostic and Prognostic Markers in Cancer. Biology (Basel) 2022;11:249. https://doi.org/10.3390/biology11020249.

[162] Zhou X, Wen W, Zhu J, Huang Z, Zhang L, Zhang H, et al. A six-microRNA signature in plasma was identified as a potential biomarker in diagnosis of esophageal squamous cell carcinoma. Oncotarget 2017;8:34468–80. https://doi.org/10.18632/oncotarget.16519.

[163] Santana M de FM, Sawada MIBAC, Santos AS, Reis M, Xavier J, Côrrea-Giannella ML, et al. Increased Expression of miR-223-3p and miR-375-3p and Anti-Inflammatory Activity in HDL of Newly Diagnosed Women in Advanced Stages of Breast Cancer. Int J Mol Sci 2023;24:12762.

https://doi.org/10.3390/ijms241612762.

[164] Li M, Song Q, Li H, Lou Y, Wang L. Circulating miR-25-3p and miR-451a May Be Potential Biomarkers for the Diagnosis of Papillary Thyroid Carcinoma. PLoS One 2015;10:e0132403. https://doi.org/10.1371/journal.pone.0132403.

[165] Qattan A, Al-Tweigeri T, Alkhayal W, Suleman K, Tulbah A, Amer S. Clinical Identification of Dysregulated Circulating microRNAs and Their Implication in Drug Response in Triple Negative Breast Cancer (TNBC) by Target Gene Network and Meta-Analysis. Genes (Basel) 2021;12:549. https://doi.org/10.3390/genes12040549.

[166] Souza KCB, Evangelista AF, Leal LF, Souza CP, Vieira RA, Causin RL, et al. Identification of Cell-Free Circulating MicroRNAs for the Detection of Early Breast Cancer and Molecular Subtyping. J Oncol 2019;2019:1–11. https://doi.org/10.1155/2019/8393769.

[167] Zhao T, Meng W, Chin Y, Gao L, Yang X, Sun S, et al. Identification of miR-25-3p as a tumor biomarker: Regulation of cellular functions via TOB1 in breast cancer. Mol Med Rep 2021;23:406. https://doi.org/10.3892/mmr.2021.12045.

[168] Paunescu IA, Bardan R, Marcu A, Nitusca D, Dema A, Negru S, et al. Biomarker Potential of Plasma MicroRNA-150-5p in Prostate Cancer. Medicina (B Aires) 2019;55:564. https://doi.org/10.3390/medicina55090564.

[169] Fogli S, Polini B, Carpi S, Pardini B, Naccarati A, Dubbini N, et al. Identification of plasma microRNAs as new potential biomarkers with high diagnostic power in human cutaneous melanoma. Tumor Biol 2017;39:101042831770164. https://doi.org/10.1177/1010428317701646.

[170] CHEN Q, GE X, ZHANG Y, XIA H, YUAN D, TANG Q, et al. Plasma miR-122 and miR-192 as potential novel biomarkers for the early detection of distant metastasis of gastric cancer. Oncol Rep 2014;31:1863–70. https://doi.org/10.3892/or.2014.3004.

[171] Zhang Y, Huang H, Zhang Y, Liao N. Combined Detection of Serum MiR-221-3p and MiR-122-5p Expression in Diagnosis and Prognosis of Gastric Cancer. J Gastric Cancer 2019;19:315. https://doi.org/10.5230/jgc.2019.19.e28.

[172] Maruyama S, Furuya S, Shiraishi K, Shimizu H, Akaike H, Hosomura N, et al. miR-122-5p as a novel biomarker for alpha-fetoprotein-producing gastric cancer. World J Gastrointest Oncol 2018;10:344–50. https://doi.org/10.4251/wjgo.v10.i10.344.

[173] Ergün S, Ulasli M, Igci YZ, Igci M, Kırkbes S, Borazan E, et al. The association of the expression of miR-122-5p and its target ADAM10 with human breast

cancer. Mol Biol Rep 2015;42:497–505. https://doi.org/10.1007/s11033-014-3793-2.

[174] Permuth-Wey J, Chen D-T, Fulp WJ, Yoder SJ, Zhang Y, Georgeades C, et al. Plasma MicroRNAs as Novel Biomarkers for Patients with Intraductal Papillary Mucinous Neoplasms of the Pancreas. Cancer Prev Res 2015;8:826–34. https://doi.org/10.1158/1940-6207.CAPR-15-0094.

[175] Armstrong DA, Green BB, Seigne JD, Schned AR, Marsit CJ. MicroRNA molecular profiling from matched tumor and bio-fluids in bladder cancer. Mol Cancer 2015;14:194. https://doi.org/10.1186/s12943-015-0466-2.

[176] Chen W, Song J, Bian H, Yang X, Xie X, Zhu Q, et al. The functions and targets of miR-212 as a potential biomarker of cancer diagnosis and therapy. J Cell Mol Med 2020;24:2392–401. https://doi.org/10.1111/jcmm.14966.

[177] Yang R, Fu Y, Zeng Y, Xiang M, Yin Y, Li L, et al. Serum miR-20a is a promising biomarker for gastric cancer. Biomed Reports 2017;6:429–34. https://doi.org/10.3892/br.2017.862.

[178] Hicks SD, Chandran D, Confair A, Ward A, Kelleher SL. Human Milk-Derived Levels of let-7g-5p May Serve as a Diagnostic and Prognostic Marker of Low Milk Supply in Breastfeeding Women. Nutrients 2023;15:567. https://doi.org/10.3390/nu15030567.

[179] Marino MJ. How often should we expect to be wrong? Statistical power, P values, and the expected prevalence of false discoveries. Biochem Pharmacol 2018;151:226–33. https://doi.org/10.1016/j.bcp.2017.12.011.

[180] Greenland S, Senn SJ, Rothman KJ, Carlin JB, Poole C, Goodman SN, et al. Statistical tests, P values, confidence intervals, and power: a guide to misinterpretations. Eur J Epidemiol 2016;31:337–50. https://doi.org/10.1007/s10654-016-0149-3.

[181] Ke H, Zhao L, Feng X, Xu H, Zou L, Yang Q, et al. NEAT1 is Required for Survival of Breast Cancer Cells through FUS and miR-548. Gene Regul Syst Bio 2016;10s1:GRSB.S29414. https://doi.org/10.4137/GRSB.S29414.

[182] Yao M, Wang S, Chen L, Wei B, Fu P. Research on correlations of miR-585 expression with progression and prognosis of triple-negative breast cancer. Clin Exp Med 2022;22:201–7. https://doi.org/10.1007/s10238-021-00704-0.

[183] Cuk K, Zucknick M, Heil J, Madhavan D, Schott S, Turchinovich A, et al. Circulating microRNAs in plasma as early detection markers for breast cancer. Int J Cancer 2013;132:1602–12. https://doi.org/10.1002/ijc.27799.

[184] Salih O, Mohamad D. Expression of miR-571 and miR-20a in Breast Cancer Patients as Diagnostic Biomarkers. Mosul J Nurs 2022;10:124–34.

https://doi.org/10.33899/mjn.2022.171438.

[185] Shaker O, Maher M, Nassar Y, Morcos G, Gad Z. Role of microRNAs -29b-2, −155, −197 and −205 as diagnostic biomarkers in serum of breast cancer females. Gene 2015;560:77–82. https://doi.org/10.1016/j.gene.2015.01.062.

[186] Lambrechts Y, Hatse, Sigrid ; Floris, Giuseppe ; Van Asten, Kathleen ; Punie, Kevin ; Neven, Patrick ; Nevelsteen, Ines ; Desmedt, Christine ; Richard, François ; Laenen, Annouschka ; Wildiers H. Relapsing and non-relapsing patients with luminal breast cancer exhibit differential serum expression of microRNA miR-197-3p at diagnosis. Leuven: 2022.

[187] Di Cosimo S, Appierto V, Pizzamiglio S, Tiberio P, Iorio M V., Hilbers F, et al. Plasma miRNA Levels for Predicting Therapeutic Response to Neoadjuvant Treatment in HER2-positive Breast Cancer: Results from the NeoALTTO Trial. Clin Cancer Res 2019;25:3887–95. https://doi.org/10.1158/1078-0432.CCR-18-2507.

[188] Bolandghamat Pour Z, Nourbakhsh M, Mousavizadeh K, Madjd Z, Ghorbanhosseini SS, Abdolvahabi Z, et al. Up-regulation of miR-381 inhibits NAD+ salvage pathway and promotes apoptosis in breast cancer cells. EXCLI J 2019;18:683–96. https://doi.org/10.17179/excli2019-1431.

[189] Bahramy A, Zafari N, Izadi P, Soleymani F, Kavousi S, Noruzinia M. The Role of miRNAs 340-5p, 92a-3p, and 381-3p in Patients with Endometriosis: A Plasma and Mesenchymal Stem-Like Cell Study. Biomed Res Int 2021;2021:1–15. https://doi.org/10.1155/2021/5298006.

[190] Haakensen VD, Nygaard V, Greger L, Aure MR, Fromm B, Bukholm IRK, et al. Subtype-specific micro-RNA expression signatures in breast cancer progression. Int J Cancer 2016;139:1117–28. https://doi.org/10.1002/ijc.30142.

[191] Aghaei M. The Breast Cancer, a Global Health Crisis. J New Find Heal Educ Sci 2023;2:107–17.

[192] Kazmierczak D, Jopek K, Sterzynska K, Nowicki M, Rucinski M, Januchowski R. The Profile of MicroRNA Expression and Potential Role in the Regulation of Drug-Resistant Genes in Cisplatin- and Paclitaxel-Resistant Ovarian Cancer Cell Lines. Int J Mol Sci 2022;23:526. https://doi.org/10.3390/ijms23010526.

[193] Matamala N, Vargas MT, González-Cámpora R, Miñambres R, Arias JI, Menéndez P, et al. Tumor MicroRNA Expression Profiling Identifies Circulating MicroRNAs for Early Breast Cancer Detection. Clin Chem 2015;61:1098–106. https://doi.org/10.1373/clinchem.2015.238691.

[194] Matamala N. Deregulated microRNAs in breast cancer and their potential role as diagnostic and prognostic biomarkers. Universidad Autónoma de Madrid, 2015.

[195] Liu S, Song A, Zhou X, Huo Z, Yao S, Yang B, et al. ceRNA network development and tumour-infiltrating immune cell analysis of metastatic breast cancer to bone. J Bone Oncol 2020;24:100304. https://doi.org/10.1016/j.jbo.2020.100304.

[196] Frères P, Josse C, Bovy N, Boukerroucha M, Struman I, Bours V, et al. Neoadjuvant Chemotherapy in Breast Cancer Patients Induces miR-34a and miR-122 Expression. J Cell Physiol 2015;230:473–81. https://doi.org/10.1002/jcp.24730.

[197] Fong MY, Zhou W, Liu L, Alontaga AY, Chandra M, Ashby J, et al. Breast-cancer-secreted miR-122 reprograms glucose metabolism in premetastatic niche to promote metastasis. Nat Cell Biol 2015;17:183–94. https://doi.org/10.1038/ncb3094.

[198] Gallo M, Carotenuto M, Frezzetti D, Camerlingo R, Roma C, Bergantino F, et al. The EGFR Signaling Modulates in Mesenchymal Stem Cells the Expression of miRNAs Involved in the Interaction with Breast Cancer Cells. Cancers (Basel) 2022;14:1851. https://doi.org/10.3390/cancers14071851.

[199] CHEN J, YAO D, LI Y, CHEN H, HE C, DING N, et al. Serum microRNA expression levels can predict lymph node metastasis in patients with early-stage cervical squamous cell carcinoma. Int J Mol Med 2013;32:557–67. https://doi.org/10.3892/ijmm.2013.1424.

[200] Yang L, Cai Y, Zhang D, Sun J, Xu C, Zhao W, et al. miR-195/miR-497 Regulate CD274 Expression of Immune Regulatory Ligands in Triple-Negative Breast Cancer. J Breast Cancer 2018;21:371. https://doi.org/10.4048/jbc.2018.21.e60.

[201] Wu Z, Li X, Cai X, Huang C, Zheng M. miR-497 inhibits epithelial mesenchymal transition in breast carcinoma by targeting Slug. Tumor Biol 2016;37:7939–50. https://doi.org/10.1007/s13277-015-4665-7.

[202] WANG W, REN F, WU Q, JIANG D, LI H, SHI H. MicroRNA-497 suppresses angiogenesis by targeting vascular endothelial growth factor A through the PI3K/AKT and MAPK/ERK pathways in ovarian cancer. Oncol Rep 2014;32:2127–33. https://doi.org/10.3892/or.2014.3439.

[203] Corrêa S, Lopes FP, Panis C, Basili T, Binato R, Abdelhay E. miRNome Profiling Reveals Shared Features in Breast Cancer Subtypes and Highlights miRNAs That Potentially Regulate MYB and EZH2 Expression. Front Oncol 2021;11:710919. https://doi.org/10.3389/fonc.2021.710919.

[204] Yu T, Yu H-R, Sun J-Y, Zhao Z, Li S, Zhang X-F, et al. miR-1271 inhibits ERα expression and confers letrozole resistance in breast cancer. Oncotarget 2017;8:107134–48. https://doi.org/10.18632/oncotarget.22359.

[205] Tahermanesh K, Hakimpour S, Govahi A, Rokhgireh S, Mehdizadeh M, Minaeian S, et al. Evaluation of expression of biomarkers of PLAGL1 (ZAC1), microRNA, and their non-coding RNAs in patients with endometriosis. J Gynecol Obstet Hum Reprod 2023;52:102568. https://doi.org/10.1016/j.jogoh.2023.102568.

[206] Chan M, Liaw CS, Ji SM, Tan HH, Wong CY, Thike AA, et al. Identification of Circulating MicroRNA Signatures for Breast Cancer Detection. Clin Cancer Res 2013;19:4477–87. https://doi.org/10.1158/1078-0432.CCR-12-3401.

[207] Suryawanshi S, Vlad AM, Lin H-M, Mantia-Smaldone G, Laskey R, Lee M, et al. Plasma MicroRNAs as Novel Biomarkers for Endometriosis and Endometriosis-Associated Ovarian Cancer. Clin Cancer Res 2013;19:1213–24. https://doi.org/10.1158/1078-0432.CCR-12-2726.

[208] Shen S, Song Y, Zhao B, Xu Y, Ren X, Zhou Y, et al. Cancer-derived exosomal miR-7641 promotes breast cancer progression and metastasis. Cell Commun Signal 2021;19:1–13. https://doi.org/10.1186/S12964-020-00700-Z/FIGURES/6.

[209] Hussain SA, Deepak KV, Nanjappa DP, Sherigar V, Nandan N, Suresh PS, et al. Comparative expression analysis of tRF-3001a and tRF-1003 with corresponding miRNAs (miR-1260a and miR-4521) and their network analysis with breast cancer biomarkers. Mol Biol Rep 2021;48:7313–24. https://doi.org/10.1007/s11033-021-06732-z.

[210] Shen J, Hu Q, Schrauder M, Yan L, Wang D, Medico L, et al. Circulating miR-148b and miR-133a as biomarkers for breast cancer detection. Oncotarget 2014;5:5284–94. https://doi.org/10.18632/oncotarget.2014.

[211] Borsos BN, Páhi ZG, Ujfaludi Z, Sükösd F, Nikolényi A, Bankó S, et al. BC-miR: Monitoring Breast Cancer-Related miRNA Profile in Blood Sera—A Prosperous Approach for Tumor Detection. Cells 2022;11:2721. https://doi.org/10.3390/cells11172721.

[212] Cuk K, Zucknick M, Madhavan D, Schott S, Golatta M, Heil J, et al. Plasma MicroRNA Panel for Minimally Invasive Detection of Breast Cancer. PLoS One 2013;8:e76729. https://doi.org/10.1371/journal.pone.0076729.

[213] Hatse S, Brouwers B, Dalmasso B, Laenen A, Kenis C, Schöffski P, et al. Circulating MicroRNAs as Easy-to-Measure Aging Biomarkers in Older Breast Cancer Patients: Correlation with Chronological Age but Not with Fitness/Frailty Status. PLoS One 2014;9:e110644. https://doi.org/10.1371/journal.pone.0110644.

[214] Shaheen J, Shahid S, Shahzadi S, Akhtar MW, Sadaf S. Identification of Circulating miRNAs as Non-Invasive Biomarkers of Triple Negative Breast

Cancer in the Population of Pakistan. Pak J Zool 2019;51:1113–21. https://doi.org/10.17582/journal.pjz/2019.51.3.1113.1121.

[215] Cizeron-Clairac G, Lallemand F, Vacher S, Lidereau R, Bieche I, Callens C. MiR-190b, the highest up-regulated miRNA in ERα-positive compared to ERα-negative breast tumors, a new biomarker in breast cancers? BMC Cancer 2015;15:499. https://doi.org/10.1186/s12885-015-1505-5.

[216] FU L, LI Z, ZHU J, WANG P, FAN G, DAI Y, et al. Serum expression levels of microRNA-382-3p, −598-3p, −1246 and −184 in breast cancer patients. Oncol Lett 2016;12:269–74. https://doi.org/10.3892/ol.2016.4582.

[217] Shih A, Korsunsky I, Guttadauria B, Bhuiya T, Liew A, Khalili H, et al. Abstract P2-07-09: Integrative analysis of miRNA and mRNA expression in metastatic versus non-metastatic triple negative breast cancer. Cancer Res 2018;78:P2-07-09-P2-07–9. https://doi.org/10.1158/1538-7445.SABCS17-P2-07-09.

[218] Guo L, Zhao Y, Yang S, Cai M, Wu Q, Chen F. Genome-wide screen for aberrantly expressed miRNAs reveals miRNA profile signature in breast cancer. Mol Biol Rep 2013;40:2175–86. https://doi.org/10.1007/s11033-012-2277-5.

[219] Mar-Aguilar F, Mendoza-Ramírez JA, Malagón-Santiago I, Espino-Silva PK, Santuario-Facio SK, Ruiz-Flores P, et al. Serum circulating microRNA profiling for identification of potential breast cancer biomarkers. Dis Markers 2013;34:163–9. https://doi.org/10.3233/DMA-120957.

[220] Jusoh AR, Mohan S, Lu Ping T, Tengku Din TADAA, Haron J, Romli R, et al. Plasma Circulating Mirnas Profiling for Identification of Potential Breast Cancer Early Detection Biomarkers. Asian Pacific J Cancer Prev 2021;22:1375–81. https://doi.org/10.31557/APJCP.2021.22.5.1375.

[221] Lagendijk M, Sadaatmand S, Koppert LB, Tilanus-Linthorst MMA, de Weerd V, Ramírez-Moreno R, et al. MicroRNA expression in pre-treatment plasma of patients with benign breast diseases and breast cancer. Oncotarget 2018;9:24335–46. https://doi.org/10.18632/oncotarget.25262.

[222] Müller V, Oliveira-Ferrer L, Steinbach B, Pantel K, Schwarzenbach H. Interplay of lncRNA H19/miR-675 and lncRNA NEAT1/miR-204 in breast cancer. Mol Oncol 2019;13:1137–49. https://doi.org/10.1002/1878-0261.12472.

[223] Wehida N, Abdel-Rehim W, El Mansy H, Karmouty A, Kamel MA. A Panel of Circulating Non-Coding RNAs in the Diagnosis and Monitoring of Therapy in Egyptian Patients with Breast Cancer. Biomedicines 2023;11:563. https://doi.org/10.3390/biomedicines11020563.

[224] Zhao H, Shen J, Medico L, Wang D, Ambrosone CB, Liu S. A Pilot Study of Circulating miRNAs as Potential Biomarkers of Early Stage Breast Cancer. PLoS

One 2010;5:e13735. https://doi.org/10.1371/journal.pone.0013735.

[225] He Y, Deng F, Zhao S, Zhong S, Zhao J, Wang D, et al. Analysis of miRNA–mRNA network reveals miR-140-5p as a suppressor of breast cancer glycolysis via targeting GLUT1. Epigenomics 2019;11:1021–36. https://doi.org/10.2217/epi-2019-0072.

[226] Amelio I, Bertolo R, Bove P, Buonomo OC, Candi E, Chiocchi M, et al. Liquid biopsies and cancer omics. Cell Death Discov 2020;6:131. https://doi.org/10.1038/s41420-020-00373-0.

[227] Keller A, Rounge T, Backes C, Ludwig N, Gislefoss R, Leidinger P, et al. Sources to variability in circulating human miRNA signatures. RNA Biol 2017;14:1791–8. https://doi.org/10.1080/15476286.2017.1367888.

[228] Li X, Zou W, Wang Y, Liao Z, Li L, Zhai Y, et al. Plasma-based microRNA signatures in early diagnosis of breast cancer. Mol Genet Genomic Med 2020;8:e1092. https://doi.org/10.1002/mgg3.1092.

[229] Pezuk JA, Miller TLA, Bevilacqua JLB, de Barros ACSD, de Andrade FEM, e Macedo LF de A, et al. Measuring plasma levels of three microRNAs can improve the accuracy for identification of malignant breast lesions in women with BI-RADS 4 mammography. Oncotarget 2017;8:83940–8. https://doi.org/10.18632/oncotarget.20806.

[230] Madhavan D, Peng C, Wallwiener M, Zucknick M, Nees J, Schott S, et al. Circulating miRNAs with prognostic value in metastatic breast cancer and for early detection of metastasis. Carcinogenesis 2016;37:461–70. https://doi.org/10.1093/carcin/bgw008.

[231] Escuin D, López-Vilaró L, Mora J, Bell O, Moral A, Pérez I, et al. Circulating microRNAs in Early Breast Cancer Patients and Its Association With Lymph Node Metastases. Front Oncol 2021;11:627811. https://doi.org/10.3389/fonc.2021.627811.

[232] Pezuk JA, Miller TLA, Bevilacqua JLB, Barros ACS, Andrade FEM de, Macedo LF de A e, et al. Abstract A54: Circulating miR-15a, miR-101, and miR-144 to distinguish between benign and malignant breast lesions in women with BI-RADS 4 mammography. Clin Cancer Res 2018;24:A54–A54. https://doi.org/10.1158/1557-3265.TCM17-A54.

[233] Yin Y, Cai J, Meng F, Sui C, Jiang Y. MiR-144 suppresses proliferation, invasion, and migration of breast cancer cells through inhibiting CEP55. Cancer Biol Ther 2018;19:306–15. https://doi.org/10.1080/15384047.2017.1416934.

[234] Lips EH, Mulder L, de Ronde JJ, Mandjes IAM, Koolen BB, Wessels LFA, et al. Breast cancer subtyping by immunohistochemistry and histological grade

outperforms breast cancer intrinsic subtypes in predicting neoadjuvant chemotherapy response. Breast Cancer Res Treat 2013;140:63–71. https://doi.org/10.1007/s10549-013-2620-0.

[235] Blows FM, Driver KE, Schmidt MK, Broeks A, van Leeuwen FE, Wesseling J, et al. Subtyping of Breast Cancer by Immunohistochemistry to Investigate a Relationship between Subtype and Short and Long Term Survival: A Collaborative Analysis of Data for 10,159 Cases from 12 Studies. PLoS Med 2010;7:e1000279. https://doi.org/10.1371/journal.pmed.1000279.

[236] Pinheiro JBF, Torres A de F, Paz AR da. Immunohistochemical profile of breast cancer subtypes in patients seen at Napoleão Laureano Hospital, Paraíba, Brazil. Mastology 2019;29:58–63. https://doi.org/10.29289/2594539420190000415.

[237] Prat A, Fan C, Fernández A, Hoadley KA, Martinello R, Vidal M, et al. Response and survival of breast cancer intrinsic subtypes following multi-agent neoadjuvant chemotherapy. BMC Med 2015;13:303. https://doi.org/10.1186/s12916-015-0540-z.

[238] Stava CJ, Lopez A, Vassilopoulou-Sellin R. Health profiles of younger and older breast cancer survivors. Cancer 2006;107:1752–9. https://doi.org/10.1002/cncr.22200.

[239] Wang M, Ren J, Tang L, Ren Z. Molecular features in young vs elderly breast cancer patients and the impacts on survival disparities by age at diagnosis. Cancer Med 2018;7:3269–77. https://doi.org/10.1002/cam4.1544.

[240] Johansson ALV, Trewin CB, Hjerkind KV, Ellingjord-Dale M, Johannesen TB, Ursin G. Breast cancer-specific survival by clinical subtype after 7 years follow-up of young and elderly women in a nationwide cohort. Int J Cancer 2019;144:1251–61. https://doi.org/10.1002/ijc.31950.

[241] de Kruijf EM, Bastiaannet E, Rubertá F, de Craen AJM, Kuppen PJK, Smit VTHBM, et al. Comparison of frequencies and prognostic effect of molecular subtypes between young and elderly breast cancer patients. Mol Oncol 2014;8:1014–25. https://doi.org/10.1016/j.molonc.2014.03.022.

[242] Liang G, Ling Y, Liu Z, Mehrpour M, Hamai A, Tian Z, et al. Abstract LB-307: Autophagy-associated circRNA AUACA1 mediates the proliferation of breast cancer cells via a miR-1275/ATG7/autophagic flux axis. Cancer Res 2019;79:LB-307-LB-307. https://doi.org/10.1158/1538-7445.AM2019-LB-307.

[243] Yang H, Ren L, Wang Y, Bi X, Li X, Wen M, et al. FBI-1 enhanced the resistance of triple-negative breast cancer cells to chemotherapeutic agents via the miR-30c/PXR axis. Cell Death Dis 2020;11:851. https://doi.org/10.1038/s41419-020-

03053-0.

[244] Egeland N, Lunde S, Jonsdottir K, Lende T, Cronin-Fenton D, Gilje B, et al. The Role of MicroRNAs as Predictors of Response to Tamoxifen Treatment in Breast Cancer Patients. Int J Mol Sci 2015;16:24243–75. https://doi.org/10.3390/ijms161024243.

[245] Escuin D, López-Vilaró L, Bell O, Mora J, Moral A, Pérez JI, et al. MicroRNA-1291 Is Associated With Locoregional Metastases in Patients With Early-Stage Breast Cancer. Front Genet 2020;11:562114. https://doi.org/10.3389/fgene.2020.562114.

[246] Han X, Li M, Xu J, Fu J, Wang X, Wang J, et al. miR-1275 targets MDK/AKT signaling to inhibit breast cancer chemoresistance by lessening the properties of cancer stem cells. Int J Biol Sci 2023;19:89–103. https://doi.org/10.7150/ijbs.74227.

[247] Vishnubalaji R, Alajez NM. Epigenetic regulation of triple negative breast cancer (TNBC) by TGF-β signaling. Sci Rep 2021;11:15410. https://doi.org/10.1038/s41598-021-94514-9.

[248] Shuaib M, Prajapati KS, Gupta S, Kumar S. Natural Steroidal Lactone Induces G1/S Phase Cell Cycle Arrest and Intrinsic Apoptotic Pathway by Up-Regulating Tumor Suppressive miRNA in Triple-Negative Breast Cancer Cells. Metabolites 2022;13:29. https://doi.org/10.3390/metabo13010029.

[249] Burgess KS, Ipe J, Swart M, Metzger IF, Lu J, Gufford BT, et al. Variants in the CYP2B6 3′UTR Alter In Vitro and In Vivo CYP2B6 Activity: Potential Role of MicroRNAs. Clin Pharmacol Ther 2018;104:130–8. https://doi.org/10.1002/cpt.892.

[250] Jafari SH, Saadatpour Z, Salmaninejad A, Momeni F, Mokhtari M, Nahand JS, et al. Breast cancer diagnosis: Imaging techniques and biochemical markers. J Cell Physiol 2018;233:5200–13. https://doi.org/10.1002/jcp.26379.

[251] Zhang X, Shen B, Cui Y. Signature microRNAs of nuclear Sm complex associated with breast cancer tumorigenesis. J Cell Biochem 2018;119:5426–36. https://doi.org/10.1002/jcb.26697.

[252] Chen Y, Zhou Y, Han F, Zhao Y, Tu M, Wang Y, et al. A novel miR-1291-ERRα-CPT1C axis modulates tumor cell proliferation, metabolism and tumorigenesis. Theranostics 2020;10:7193–210. https://doi.org/10.7150/thno.44877.

[253] Xin Y, Wang X, Meng K, Ni C, Lv Z, Guan D. Identification of exosomal miR-455-5p and miR-1255a as therapeutic targets for breast cancer. Biosci Rep 2020;40:20190303. https://doi.org/10.1042/BSR20190303/221318.

[254] Li D, Zhong J, Zhang G, Lin L, Liu Z. Oncogenic Role and Prognostic Value of

MicroRNA-937-3p in Patients with Breast Cancer. Onco Targets Ther 2019;12:11045–56. https://doi.org/10.2147/OTT.S229510.

[255] Shi W, Dong F, Jiang Y, Lu L, Wang C, Tan J, et al. Construction of prognostic microRNA signature for human invasive breast cancer by integrated analysis. Onco Targets Ther 2019;12:1979–2010. https://doi.org/10.2147/OTT.S189265.

[256] Fang H, Jiang W, Jing Z, Mu X, Xiong Z. miR-937 regulates the proliferation and apoptosis via targeting APAF1 in breast cancer. Onco Targets Ther 2019;12:5687–99. https://doi.org/10.2147/OTT.S207091.

[257] TRIANTAFYLLOU A, DOVROLIS N, ZOGRAFOS E, THEODOROPOULOS C, ZOGRAFOS GC, MICHALOPOULOS N V., et al. Circulating miRNA Expression Profiling in Breast Cancer Molecular Subtypes: Applying Machine Learning Analysis in Bioinformatics. Cancer Diagnosis Progn 2022;2:739–49. https://doi.org/10.21873/cdp.10169.

[258] Sun G, Sun L, Liu Y, Xing H, Wang K. Her-2 expression regulated by downregulation of miR-9 and which affects chemotherapeutic effect in breast cancer. Cancer Gene Ther 2017;24:194–202. https://doi.org/10.1038/cgt.2014.82.

[259] Darbeheshti F, Mansoori Y, Azizi-Tabesh G, Zolfaghari F, Kadkhoda S, Rasti A, et al. Evaluation of Circ_0000977-Mediated Regulatory Network in Breast Cancer: A Potential Discriminative Biomarker for Triple-Negative Tumors. Biochem Genet 2023;61:1487–508. https://doi.org/10.1007/s10528-023-10331-x.

[260] Yang F, Fu Z, Yang M, Sun C, Li Y, Chu J, et al. Expression pattern of microRNAs related with response to trastuzumab in breast cancer. J Cell Physiol 2019;234:16102–13. https://doi.org/10.1002/jcp.28268.

[261] Bertoli G, Cava C, Corsi F, Piccotti F, Martelli C, Ottobrini L, et al. Triple negative aggressive phenotype controlled by miR-135b and miR-365: new theranostics candidates. Sci Rep 2021;11:6553. https://doi.org/10.1038/s41598-021-85746-w.

[262] Lei B, Wang D, Zhang M, Deng Y, Jiang H, Li Y. miR-615-3p promotes the epithelial-mesenchymal transition and metastasis of breast cancer by targeting PICK1/TGFBRI axis. J Exp Clin Cancer Res 2020;39:71. https://doi.org/10.1186/s13046-020-01571-5.

[263] Malagobadan S, San Ho C, Hasima Nagoor N. MicroRNA-6744-5p promotes anoikis in breast cancer and directly targets NAT1 enzyme. Cancer Biol Med 2020;17:101–11. https://doi.org/10.20892/j.issn.2095-3941.2019.0010.

[264] Jayavelu ND, Bar N. Reconstruction of temporal activity of microRNAs from

gene expression data in breast cancer cell line. BMC Genomics 2015;16:1077. https://doi.org/10.1186/s12864-015-2260-3.

[265] Thiebaut C, Chesnel A, Merlin J-L, Chesnel M, Leroux A, Harlé A, et al. Dual Epigenetic Regulation of ERα36 Expression in Breast Cancer Cells. Int J Mol Sci 2019;20:2637. https://doi.org/10.3390/ijms20112637.

[266] Teoh SL, Das S. The Role of MicroRNAs in Diagnosis, Prognosis, Metastasis and Resistant Cases in Breast Cancer. Curr Pharm Des 2017;23:1845–59. https://doi.org/10.2174/1381612822666161027120043.

[267] Yin L, Ding Y, Wang Y, Wang C, Sun K, Wang L. Identification of Serum miR-501-3p and miR-338-3p as Novel Diagnostic Biomarkers for Breast Cancer and Their Target Genes Associated with Immune Infiltration. Int J Gen Med 2023;16:1279–94. https://doi.org/10.2147/IJGM.S406802.

[268] Zou X, Li M, Huang Z, Zhou X, Liu Q, Xia T, et al. Circulating miR-532-502 cluster derived from chromosome X as biomarkers for diagnosis of breast cancer. Gene 2020;722:144104. https://doi.org/10.1016/j.gene.2019.144104.

[269] Ozawa PMM, Jucoski TS, Vieira E, Carvalho TM, Malheiros D, Ribeiro EM de SF. Liquid biopsy for breast cancer using extracellular vesicles and cell-free microRNAs as biomarkers. Transl Res 2020;223:40–60. https://doi.org/10.1016/j.trsl.2020.04.002.

[270] Alimirzaie S, Bagherzadeh M, Akbari MR. Liquid biopsy in breast cancer: A comprehensive review. Clin Genet 2019;95:643–60. https://doi.org/10.1111/cge.13514.

[271] Karachaliou N, Mayo-de-Las-Casas C, Molina-Vila MA, Rosell R. Real-time liquid biopsies become a reality in cancer treatment. Ann Transl Med 2015;3:36. https://doi.org/10.3978/j.issn.2305-5839.2015.01.16.

[272] Pittella-Silva F, Chin YM, Chan HT, Nagayama S, Miyauchi E, Low S-K, et al. Plasma or Serum: Which Is Preferable for Mutation Detection in Liquid Biopsy? Clin Chem 2020;66:946–57. https://doi.org/10.1093/clinchem/hvaa103.

[273] Wu H-J, Chu P-Y. Current and Developing Liquid Biopsy Techniques for Breast Cancer. Cancers (Basel) 2022;14:2052. https://doi.org/10.3390/cancers14092052.

[274] Izzotti A, Carozzo S, Pulliero A, Zhabayeva D, Ravetti JL, Bersimbaev R. Extracellular MicroRNA in liquid biopsy: applicability in cancer diagnosis and prevention. Am J Cancer Res 2016;6:1461–93.

[275] Larrea E, Sole C, Manterola L, Goicoechea I, Armesto M, Arestin M, et al. New Concepts in Cancer Biomarkers: Circulating miRNAs in Liquid Biopsies. Int J Mol Sci 2016;17:627. https://doi.org/10.3390/ijms17050627.

[276] Liu X, Papukashvili D, Wang Z, Liu Y, Chen X, Li J, et al. Potential utility of miRNAs for liquid biopsy in breast cancer. Front Oncol 2022;12:940314. https://doi.org/10.3389/fonc.2022.940314.

[277] Bahmer T, Krauss-Etschmann S, Buschmann D, Behrends J, Watz H, Kirsten A, et al. RNA-seq–based profiling of extracellular vesicles in plasma reveals a potential role of miR-122-5p in asthma. Allergy 2021;76:366–71. https://doi.org/10.1111/all.14486.

[278] Huang X, Yuan T, Tschannen M, Sun Z, Jacob H, Du M, et al. Characterization of human plasma-derived exosomal RNAs by deep sequencing. BMC Genomics 2013;14:319. https://doi.org/10.1186/1471-2164-14-319.

[279] Freedman JE, Gerstein M, Mick E, Rozowsky J, Levy D, Kitchen R, et al. Diverse human extracellular RNAs are widely detected in human plasma. Nat Commun 2016;7:11106. https://doi.org/10.1038/ncomms11106.

[280] Galvanin A, Dostert G, Ayadi L, Marchand V, Velot É, Motorin Y. Diversity and heterogeneity of extracellular RNA in human plasma. Biochimie 2019;164:22–36. https://doi.org/10.1016/j.biochi.2019.05.011.

[281] DE BARBA M, WAITS LP. Multiplex pre-amplification for noninvasive genetic sampling: is the extra effort worth it? Mol Ecol Resour 2010;10:659–65. https://doi.org/10.1111/j.1755-0998.2009.02818.x.

[282] Givens RC, Moore D, Akashi H, Kato T, Naka Y, Takayama H, et al. Micro-RNA-451 and Measures of Hemolysis Associated with Left Ventricular Assist Device Implantation. J Hear Lung Transplant 2013;32:S279. https://doi.org/10.1016/j.healun.2013.01.733.

[283] Vu BT, Tan Le D, Van Pham P. Liquid biopsies: tumour diagnosis and treatment monitoring. Biomed Res Ther 2016;3:35. https://doi.org/10.7603/s40730-016-0035-3.

[284] Fernández-Lázaro D, García Hernández JL, García AC, Córdova Martínez A, Mielgo-Ayuso J, Cruz-Hernández JJ. Liquid Biopsy as Novel Tool in Precision Medicine: Origins, Properties, Identification and Clinical Perspective of Cancer's Biomarkers. Diagnostics 2020;10:215. https://doi.org/10.3390/diagnostics10040215.

[285] Zhou H, Zhu L, Song J, Wang G, Li P, Li W, et al. Liquid biopsy at the frontier of detection, prognosis and progression monitoring in colorectal cancer. Mol Cancer 2022;21:86. https://doi.org/10.1186/s12943-022-01556-2.

[286] Pritchard CC, Kroh E, Wood B, Arroyo JD, Dougherty KJ, Miyaji MM, et al. Blood Cell Origin of Circulating MicroRNAs: A Cautionary Note for Cancer Biomarker Studies. Cancer Prev Res 2012;5:492–7. https://doi.org/10.1158/1940-

6207.CAPR-11-0370.

[287] Peng C, Wang J, Bao Q, Wang J, Liu Z, Wen J, et al. Isolation of extracellular vesicle with different precipitation-based methods exert a tremendous impact on the biomarker analysis for clinical plasma samples. Cancer Biomarkers 2020:1–13. https://doi.org/10.3233/cbm-201651.

[288] Kalluri R, Lebleu VS. Discovery of double-stranded genomic DNA in circulating exosomes. Cold Spring Harb Symp Quant Biol 2016;81:275–80. https://doi.org/10.1101/sqb.2016.81.030932.

[289] Brennan K, Martin K, FitzGerald SP, O'Sullivan J, Wu Y, Blanco A, et al. A comparison of methods for the isolation and separation of extracellular vesicles from protein and lipid particles in human serum. Sci Rep 2020;10:1039. https://doi.org/10.1038/s41598-020-57497-7.

[290] Stranska R, Gysbrechts L, Wouters J, Vermeersch P, Bloch K, Dierickx D, et al. Comparison of membrane affinity-based method with size-exclusion chromatography for isolation of exosome-like vesicles from human plasma. J Transl Med 2018;16:1. https://doi.org/10.1186/s12967-017-1374-6.

[291] Tang YT, Huang YY, Zheng L, Qin SH, Xu XP, An TX, et al. Comparison of isolation methods of exosomes and exosomal RNA from cell culture medium and serum. Int J Mol Med 2017;40:834–44. https://doi.org/10.3892/IJMM.2017.3080/HTML.

[292] Qiu F, Hou T, Huang D, Xue Z, Liang D, Li Q, et al. Evaluation of two high-abundance protein depletion kits and optimization of downstream isoelectric focusing. Mol Med Rep 2015;12:7749–55. https://doi.org/10.3892/MMR.2015.4417/HTML.

[293] van der Pol E, Coumans FAW, Grootemaat AE, Gardiner C, Sargent IL, Harrison P, et al. Particle size distribution of exosomes and microvesicles determined by transmission electron microscopy, flow cytometry, nanoparticle tracking analysis, and resistive pulse sensing. J Thromb Haemost 2014;12:1182–92. https://doi.org/10.1111/jth.12602.

[294] Rikkert LG, Nieuwland R, Terstappen LWMM, Coumans FAW. Quality of extracellular vesicle images by transmission electron microscopy is operator and protocol dependent. J Extracell Vesicles 2019;8:1555419. https://doi.org/10.1080/20013078.2018.1555419.

[295] Michell DL, Vickers KC. Lipoprotein carriers of microRNAs. Biochim Biophys Acta - Mol Cell Biol Lipids 2016;1861:2069–74. https://doi.org/10.1016/j.bbalip.2016.01.011.

[296] Vickers KC, Palmisano BT, Shoucri BM, Shamburek RD, Remaley AT.

MicroRNAs are transported in plasma and delivered to recipient cells by high-density lipoproteins. Nat Cell Biol 2011;13:423–33. https://doi.org/10.1038/ncb2210.

[297] Rossi-Herring G, Belmonte T, Rivas-Urbina A, Benítez S, Rotllan N, Crespo J, et al. Circulating lipoprotein-carried miRNome analysis reveals novel VLDL-enriched microRNAs that strongly correlate with the HDL-microRNA profile. Biomed Pharmacother 2023;162:114623. https://doi.org/10.1016/j.biopha.2023.114623.

[298] Conley A, Minciacchi VR, Lee DH, Knudsen BS, Karlan BY, Citrigno L, et al. High-throughput sequencing of two populations of extracellular vesicles provides an mRNA signature that can be detected in the circulation of breast cancer patients. RNA Biol 2017;14:305–16.

[299] Hisey CL, Tomek P, Nursalim YN, Chamley LW, Leung E, Kannan N, et al. Towards establishing extracellular vesicle-associated RNAs as biomarkers for HER2+ breast cancer [version 3; peer review: 3 approved] report report report 2020. https://doi.org/10.12688/f1000research.27393.1.

[300] Kumar SR, Kimchi ET, Manjunath Y, Gajagowni S, Stuckel AJ. RNA cargos in extracellular vesicles derived from blood serum in pancreas associated conditions. Sci Reports 2020 101 2020;10:1–10. https://doi.org/10.1038/s41598-020-59523-0.

[301] Riedmaier I, Bergmaier M, Pfaffl MW. Comparison of Two Available Platforms for Determination of RNA Quality. Http://McManuscriptcentralCom/Tbeq 2014;24:2154–9. https://doi.org/10.2478/V10133-010-0074-7.

[302] Kim KM, Abdelmohsen K, Mustapic M, Kapogiannis D, Gorospe M. RNA in extracellular vesicles. Wiley Interdiscip Rev RNA 2017;8:e1413. https://doi.org/10.1002/WRNA.1413.

[303] O'Brien K, Breyne K, Ughetto S, Laurent LC, Breakefield XO. RNA delivery by extracellular vesicles in mammalian cells and its applications. Nat Rev Mol Cell Biol 2020;21:585–606.

[304] Li YY, Zhao J, Yu S, Wang Z, He XX, Su Y, et al. Extracellular Vesicles Long RNA Sequencing Reveals Abundant mRNA, circRNA, and lncRNA in Human Blood as Potential Biomarkers for Cancer Diagnosis 2019;65:798–808. https://doi.org/10.1373/CLINCHEM.2018.301291.

[305] Guescini M, Genedani S, Stocchi V, Agnati LF. Astrocytes and Glioblastoma cells release exosomes carrying mtDNA. J Neural Transm 2009 1171 2009;117:1–4. https://doi.org/10.1007/S00702-009-0288-8.

[306] Belov L, Matic KJ, Hallal S, Best OG, Mulligan SP, Christopherson RI. Extensive

surface protein profiles of extracellular vesicles from cancer cells may provide diagnostic signatures from blood samples. J Extracell Vesicles 2016;5:25355. https://doi.org/10.3402/jev.v5.25355.

[307] Moon P. Molecules That Count® Molecules That Count® Translational Research – Gene Expression – miRNA Expression – Copy Number Variation nCounter® Expression Data Analysis Guide nCounter® Expression Data Analysis Guide 2011.

[308] nSolver TM 4.0 Quick Start Guide FOR RESEARCH USE ONLY. Not for use in diagnostic procedures 2017.

[309] Vandesompele J, De Preter K, Pattyn F, Poppe B, Van Roy N, De Paepe A, et al. Accurate normalization of real-time quantitative RT-PCR data by geometric averaging of multiple internal control genes. Genome Biol 2002;3:1–12. https://doi.org/10.1186/GB-2002-3-7-RESEARCH0034/COMMENTS.

[310] Urrutia A, Duffy D, Rouilly V, Posseme C, Djebali R, Illanes G, et al. Standardized Whole-Blood Transcriptional Profiling Enables the Deconvolution of Complex Induced Immune Responses. Cell Rep 2016;16:2777–91. https://doi.org/10.1016/J.CELREP.2016.08.011.

[311] Simonsen JB. What are we looking at? Extracellular vesicles, lipoproteins, or both? Circ Res 2017;121:920–2. https://doi.org/10.1161/CIRCRESAHA.117.311767.

[312] Otahal A, Kuten-Pella O, Kramer K, Neubauer M, Lacza Z, Nehrer S, et al. Functional repertoire of EV-associated miRNA profiles after lipoprotein depletion via ultracentrifugation and size exclusion chromatography from autologous blood products. Sci Reports 2021 111 2021;11:1–16. https://doi.org/10.1038/s41598-021-84234-5.

[313] Damavandi Z, Torkashvand S, Vasei M, Soltani BM, Tavallaei M, Mowla SJ. Aberrant Expression of Breast Development-Related MicroRNAs, miR-22, miR-132, and miR-212, in Breast Tumor Tissues. J Breast Cancer 2016;19:148. https://doi.org/10.4048/jbc.2016.19.2.148.

[314] Li X, Zou Z-Z, Wen M, Xie Y-Z, Peng K-J, Luo T, et al. ZLM-7 inhibits the occurrence and angiogenesis of breast cancer through miR-212-3p/Sp1/VEGFA signal axis. Mol Med 2020;26:109. https://doi.org/10.1186/s10020-020-00239-2.

[315] Li Z, Li Y, Wang X, Liang Y, Luo D, Han D, et al. LINC01977 Promotes Breast Cancer Progression and Chemoresistance to Doxorubicin by Targeting miR-212-3p/GOLM1 Axis. Front Oncol 2021;11:657094. https://doi.org/10.3389/fonc.2021.657094.

[316] Ding L, Xie Z. CircWHSC1 regulates malignancy and glycolysis by the miR-212-

5p/AKT3 pathway in triple-negative breast cancer. Exp Mol Pathol 2021;123:104704. https://doi.org/10.1016/j.yexmp.2021.104704.

[317] Xie M, Fu Z, Cao J, Liu Y, Wu J, Li Q, et al. MicroRNA-132 and microRNA-212 mediate doxorubicin resistance by down-regulating the PTEN-AKT/NF-κB signaling pathway in breast cancer. Biomed Pharmacother 2018;102:286–94. https://doi.org/10.1016/j.biopha.2018.03.088.

[318] Liao Y, Qiu Z, Bai L. miR-302d-3p regulates the viability, migration and apoptosis of breast cancer cells through regulating the TMBIM6-mediated ERK signaling pathway. Mol Med Rep 2021;24:853. https://doi.org/10.3892/mmr.2021.12493.

[319] Wang Y, Zhao L, Xiao Q, Jiang L, He M, Bai X, et al. miR-302a/b/c/d cooperatively inhibit BCRP expression to increase drug sensitivity in breast cancer cells. Gynecol Oncol 2016;141:592–601. https://doi.org/10.1016/j.ygyno.2015.11.034.

[320] Sun D, Zhong J, Wei W, Liu L, Liu J, Lin X. Long non-coding RNAs lnc-ANGPTL1-3:3 and lnc-GJA10-12:1 present as regulators of sentinel lymph node metastasis in breast cancer. Oncol Lett 2020;20:1–1. https://doi.org/10.3892/ol.2020.12050.

[321] CHEN D, YANG H. Integrated analysis of differentially expressed genes in breast cancer pathogenesis. Oncol Lett 2015;9:2560–6. https://doi.org/10.3892/ol.2015.3147.

[322] Khadka VS, Nasu M, Deng Y, Jijiwa M. Circulating microRNA Biomarker for Detecting Breast Cancer in High-Risk Benign Breast Tumors. Int J Mol Sci 2023;24:7553. https://doi.org/10.3390/ijms24087553.

[323] Zan X, Li W, Wang G, Yuan J, Ai Y, Huang J, et al. Circ-CSNK1G1 promotes cell proliferation, migration, invasion and glycolysis metabolism during triple-negative breast cancer progression by modulating the miR-28-5p/LDHA pathway. Reprod Biol Endocrinol 2022;20:138. https://doi.org/10.1186/s12958-022-00998-z.

[324] Afzali F, Salimi M. Unearthing Regulatory Axes of Breast Cancer circRNAs Networks to Find Novel Targets and Fathom Pivotal Mechanisms. Interdiscip Sci Comput Life Sci 2019;11:711–22. https://doi.org/10.1007/s12539-019-00339-6.

[325] Pordzik J, Pisarz K, De Rosa S, Jones AD, Eyileten C, Indolfi C, et al. The Potential Role of Platelet-Related microRNAs in the Development of Cardiovascular Events in High-Risk Populations, Including Diabetic Patients: A Review. Front Endocrinol (Lausanne) 2018;9:74. https://doi.org/10.3389/fendo.2018.00074.

[326] Sohel MH. Extracellular/Circulating MicroRNAs: Release Mechanisms, Functions and Challenges. Achiev Life Sci 2016;10:175–86. https://doi.org/10.1016/j.als.2016.11.007.

[327] Lambrechts Y, Garg A, Floris G, Punie K, Neven P, Nevelsteen I, et al. Relation between circulating biomarkers at diagnosis of early luminal-like breast cancer and subsequent risk of distant metastases. J Clin Oncol 2023;41:1077–1077. https://doi.org/10.1200/JCO.2023.41.16_suppl.1077.

[328] Zheng L, Li X, Gu Y, Lv X, Xi T. The 3′UTR of the pseudogene CYP4Z2P promotes tumor angiogenesis in breast cancer by acting as a ceRNA for CYP4Z1. Breast Cancer Res Treat 2015;150:105–18. https://doi.org/10.1007/s10549-015-3298-2.

[329] Wang T, Liu J, Zhong R, Zhang Y, Sun Z, Li J, et al. Bioinformatics Analysis Reveals the Related Role of miR-511-5p in the Progression of Breast Cancer. J Healthc Eng 2022;2022:1–8. https://doi.org/10.1155/2022/7146338.

[330] Kim J. Identification of MicroRNAs as Diagnostic Biomarkers for Breast Cancer Based on the Cancer Genome Atlas. Diagnostics 2021;11:107. https://doi.org/10.3390/diagnostics11010107.

[331] Bhome R, Del Vecchio F, Lee G-H, Bullock MD, Primrose JN, Sayan AE, et al. Exosomal microRNAs (exomiRs): Small molecules with a big role in cancer. Cancer Lett 2018;420:228–35. https://doi.org/10.1016/j.canlet.2018.02.002.

[332] Ni Q, Stevic I, Pan C, Müller V, Oliviera-Ferrer L, Pantel K, et al. Different signatures of miR-16, miR-30b and miR-93 in exosomes from breast cancer and DCIS patients. Sci Reports 2018 81 2018;8:1–10. https://doi.org/10.1038/s41598-018-31108-y.

[333] Jiang M, Zhang W, Zhang R, Liu P, Ye Y, Yu W, et al. Cancer exosome-derived miR-9 and miR-181a promote the development of early-stage MDSCs via interfering with SOCS3 and PIAS3 respectively in breast cancer. Oncogene 2020 3924 2020;39:4681–94. https://doi.org/10.1038/s41388-020-1322-4.

[334] Cava C, Colaprico A, Bertoli G, Bontempi G, Mauri G, Castiglioni I. How interacting pathways are regulated by miRNAs in breast cancer subtypes. BMC Bioinformatics 2016;17:348. https://doi.org/10.1186/s12859-016-1196-1.

[335] Lal M, Ansari AH, Agrawal A, Mukhopadhyay A. Diagnostic and Prognostic Potential of MiR-379/656 MicroRNA Cluster in Molecular Subtypes of Breast Cancer. J Clin Med 2021;10:4071. https://doi.org/10.3390/jcm10184071.

[336] McCarthy EC, Dwyer RM. Emerging Evidence of the Functional Impact of the miR379/miR656 Cluster (C14MC) in Breast Cancer. Biomedicines 2021;9:827. https://doi.org/10.3390/biomedicines9070827.

[337] Laddha S V, Nayak S, Paul D, Reddy R, Sharma C, Jha P, et al. Genome-wide analysis reveals downregulation of miR-379/miR-656 cluster in human cancers. Biol Direct 2013;8:10. https://doi.org/10.1186/1745-6150-8-10.

[338] Ghanbari R, Mosakhani N, Sarhadi VK, Armengol G, Nouraee N, Mohammadkhani A, et al. Simultaneous Underexpression of let-7a-5p and let-7f-5p microRNAs in Plasma and Stool Samples from Early Stage Colorectal Carcinoma. Biomark Cancer 2015;7s1:BIC.S25252. https://doi.org/10.4137/BIC.S25252.

[339] Fu C, Zhang Q, Wang A, Yang S, Jiang Y, Bai L, et al. EWI-2 controls nucleocytoplasmic shuttling of EGFR signaling molecules and miRNA sorting in exosomes to inhibit prostate cancer cell metastasis. Mol Oncol 2021;15:1543–65. https://doi.org/10.1002/1878-0261.12930.

[340] Ye Q, Raese RA, Luo D, Feng J, Xin W, Dong C, et al. MicroRNA-Based Discovery of Biomarkers, Therapeutic Targets, and Repositioning Drugs for Breast Cancer. Cells 2023;12:1917. https://doi.org/10.3390/cells12141917.

[341] Ali S, Almhanna K, Chen W, Philip PA, Sarkar FH. Differentially expressed miRNAs in the plasma may provide a molecular signature for aggressive pancreatic cancer. Am J Transl Res 2010;3:28–47.

[342] Nitusca D, Paunescu IA, Marcu A, Antonescu M, Cumpanas A, Bardan R, et al. PLASMA EXOSOMAL miRNA SCREENING FOR THE DISCOVERY OF NOVEL BIOMARKERS IN PROSTATE CANCER. A PILOT STUDY. Res Clin Med 2019;3:7–11.

[343] Rybarczyk A, Lehmann T, Iwańczyk-Skalska E, Juzwa W, Pławski A, Kopciuch K, et al. In silico and in vitro analysis of the impact of single substitutions within EXO-motifs on Hsa-MiR-1246 intercellular transfer in breast cancer cell. J Appl Genet 2023;64:105–24. https://doi.org/10.1007/s13353-022-00730-y.

[344] Khaliefa AK, Desouky EM, Hozayen WG, Shaaban SM, Hasona NA. miRNA-1246, HOTAIR, and IL-39 signature as potential diagnostic biomarkers in breast cancer. Non-Coding RNA Res 2023;8:205–10. https://doi.org/10.1016/j.ncrna.2023.02.002.

[345] Levati L, Bassi C, Mastroeni S, Lupini L, Antonini Cappellini GC, Bonmassar L, et al. Circulating miR-1246 and miR-485-3p as Promising Biomarkers of Clinical Response and Outcome in Melanoma Patients Treated with Targeted Therapy. Cancers (Basel) 2022;14:3706. https://doi.org/10.3390/cancers14153706.

[346] Hannafon BN, Trigoso YD, Calloway CL, Zhao YD, Lum DH, Welm AL, et al. Plasma exosome microRNAs are indicative of breast cancer. Breast Cancer Res 2016;18:90. https://doi.org/10.1186/s13058-016-0753-x.

[347] Zhai L-Y, Li M-X, Pan W-L, Chen Y, Li M-M, Pang J-X, et al. In Situ Detection of Plasma Exosomal MicroRNA-1246 for Breast Cancer Diagnostics by a Au Nanoflare Probe. ACS Appl Mater Interfaces 2018;10:39478–86. https://doi.org/10.1021/acsami.8b12725.

[348] Rezaei Z, Dastjerdi K, Allahyari A, ShahidSales S, Talebian S, Maharati A, et al. Plasma microRNA-195, −34c, and − 1246 as novel biomarkers for the diagnosis of trastuzumab-resistant HER2-positive breast cancer patients. Toxicol Appl Pharmacol 2023;475:116652. https://doi.org/10.1016/j.taap.2023.116652.

[349] Huynh KQ, Le AT, Phan TT, Ho TT, Pho SP, Nguyen HT, et al. The Diagnostic Power of Circulating miR-1246 in Screening Cancer: An Updated Meta-analysis. Oxid Med Cell Longev 2023;2023:1–13. https://doi.org/10.1155/2023/8379231.

[350] Li XJ, Ren ZJ, Tang JH, Yu Q. Exosomal MicroRNA MiR-1246 Promotes Cell Proliferation, Invasion and Drug Resistance by Targeting CCNG2 in Breast Cancer. Cell Physiol Biochem 2017;44:1741–8. https://doi.org/10.1159/000485780.

[351] Jang J, Kim Y, Kang K, Kim K, Park Y, Kim C. Multiple microRNAs as biomarkers for early breast cancer diagnosis. Mol Clin Oncol 2020;14:31. https://doi.org/10.3892/mco.2020.2193.

[352] Chen Y, Zhai L-Y, Zhang L-M, Ma X-S, Liu Z, Li M-M, et al. Breast cancer plasma biopsy by *in situ* determination of exosomal microRNA-1246 with a molecular beacon. Analyst 2021;146:2264–76. https://doi.org/10.1039/D0AN02224A.

[353] Zhang L-M, Gao Q-X, Chen J, Li B, Li M-M, Zheng L, et al. A universal catalytic hairpin assembly system for direct plasma biopsy of exosomal PIWI-interacting RNAs and microRNAs. Anal Chim Acta 2022;1192:339382. https://doi.org/10.1016/j.aca.2021.339382.

[354] Ma J, Zhou Z. Downregulation of miR-302b is associated with poor prognosis and tumor progression of breast cancer. Breast Cancer 2020;27:291–8. https://doi.org/10.1007/s12282-019-01022-w.

[355] Bahrami A, Aledavood A, Anvari K, Hassanian SM, Maftouh M, Yaghobzade A, et al. The prognostic and therapeutic application of microRNAs in breast cancer: Tissue and circulating microRNAs. J Cell Physiol 2018;233:774–86. https://doi.org/10.1002/jcp.25813.

[356] Van der Auwera I, Van Laere S, Limame R, Trinh X, Van Marck E, van Dam P, et al. A microRNA Expression Profile Consisting of 12 microRNAs Is Associated with Inflammatory Breast Cancer. Cancer Res 2009;69:6119–6119. https://doi.org/10.1158/0008-5472.SABCS-09-6119.

[357] Cataldo A, Cheung DG, Balsari A, Tagliabue E, Coppola V, Iorio M V., et al. miR-302b enhances breast cancer cell sensitivity to cisplatin by regulating E2F1 and the cellular DNA damage response. Oncotarget 2016;7:786–97. https://doi.org/10.18632/oncotarget.6381.

[358] Sevinc ED, Egeli U, Cecener G, Tezcan G, Tunca B, Gokgoz S, et al. Association of miR-1266 with Recurrence/Metastasis Potential in Estrogen Receptor Positive Breast Cancer Patients. Asian Pacific J Cancer Prev 2015;16:291–7. https://doi.org/10.7314/APJCP.2015.16.1.291.

[359] McFall TB. Abstract 1102: miRNAs are key mediators of crosstalk between estrogen and progesterone regulating breast cancer invasiveness. Cancer Res 2016;76:1102–1102. https://doi.org/10.1158/1538-7445.AM2016-1102.

[360] Almohaywi M, Sugita BM, Centa A, Fonseca AS, Antunes VC, Fadda P, et al. Deregulated miRNA Expression in Triple-Negative Breast Cancer of Ancestral Genomic-Characterized Latina Patients. Int J Mol Sci 2023;24:13046. https://doi.org/10.3390/ijms241713046.

[361] Tang H-H. MiR-640 and MiR-525-5p as Relapse-Associated MicroRNAs in Systematically Untreated Individuals with Low-Risk Primary Breast Cancer. Tohoku J Exp Med 2023;260:2023.J027. https://doi.org/10.1620/tjem.2023.J027.

[362] Xiao F, Jia H, Wu D, Zhang Z, Li S, Guo J. <scp>LINC01234</scp> aggravates cell growth and migration of triple-negative breast cancer by activating the Wnt pathway. Environ Toxicol 2021;36:1999–2012. https://doi.org/10.1002/tox.23318.

[363] Cordero F, Ferrero G, Polidoro S, Fiorito G, Campanella G, Sacerdote C, et al. Differentially methylated microRNAs in prediagnostic samples of subjects who developed breast cancer in the European Prospective Investigation into Nutrition and Cancer (EPIC-Italy) cohort. Carcinogenesis 2015;36:1144–53. https://doi.org/10.1093/carcin/bgv102.

[364] Pizzamiglio S, Ciniselli CM, De Azambuja E, Agbor-Tarh D, Moreno-Aspitia A, Suter T, et al. Circulating microRNAs for early detection of therapy-related cardiac events in HER2-positive breast cancer patients: an explorative analysis from NeoALTTO. Eur J Cancer 2022;175:S77–8. https://doi.org/10.1016/S0959-8049(22)01560-X.

[365] Liu X, Liu Y, Wang Q, Song S, Feng L, Shi C. The Alterations and Potential Roles of MCMs in Breast Cancer. J Oncol 2021;2021:1–17. https://doi.org/10.1155/2021/7928937.

[366] Zeng Z, Chen X, Zhu D, Luo Z, Yang M. Low Expression of Circulating MicroRNA-34c is Associated with Poor Prognosis in Triple-Negative Breast

Cancer. Yonsei Med J 2017;58:697. https://doi.org/10.3349/ymj.2017.58.4.697.

[367] Liu X, Feng J, Tang L, Liao L, Xu Q, Zhu S. The Regulation and Function of miR-21-FOXO3a-miR-34b/c Signaling in Breast Cancer. Int J Mol Sci 2015;16:3148–62. https://doi.org/10.3390/ijms16023148.

[368] Berber U, Yilmaz I, Narli G, Haholu A, Kucukodaci Z, Demirel D. miR-205 and miR-200c: Predictive Micro RNAs for Lymph Node Metastasis in Triple Negative Breast Cancer. J Breast Cancer 2014;17:143. https://doi.org/10.4048/jbc.2014.17.2.143.

[369] MotieGhader H, Masoudi-Sobhanzadeh Y, Ashtiani SH, Masoudi-Nejad A. mRNA and microRNA selection for breast cancer molecular subtype stratification using meta-heuristic based algorithms. Genomics 2020;112:3207–17. https://doi.org/10.1016/j.ygeno.2020.06.014.

[370] Icli B, Wu W, Ozdemir D, Li H, Cheng HS, Haemmig S, et al. MicroRNA-615-5p Regulates Angiogenesis and Tissue Repair by Targeting AKT/eNOS (Protein Kinase B/Endothelial Nitric Oxide Synthase) Signaling in Endothelial Cells. Arterioscler Thromb Vasc Biol 2019;39:1458–74. https://doi.org/10.1161/ATVBAHA.119.312726.

[371] Bellingham SA, Shambrook M, Hill AF. Quantitative Analysis of Exosomal miRNA via qPCR and Digital PCR, 2017, p. 55–70. https://doi.org/10.1007/978-1-4939-6728-5_5.

[372] Moldovan L, Batte K, Wang Y, Wisler J, Piper M. Analyzing the Circulating MicroRNAs in Exosomes/Extracellular Vesicles from Serum or Plasma by qRT-PCR, 2013, p. 129–45. https://doi.org/10.1007/978-1-62703-453-1_10.

[373] Wu M, Li Q, Wang H. Identification of Novel Biomarkers Associated With the Prognosis and Potential Pathogenesis of Breast Cancer via Integrated Bioinformatics Analysis. Technol Cancer Res Treat 2021;20:153303382199208. https://doi.org/10.1177/1533033821992081.

[374] Muti P, Donzelli S, Sacconi A, Hossain A, Ganci F, Frixa T, et al. MiRNA-513a-5p inhibits progesterone receptor expression and constitutes a risk factor for breast cancer: the hOrmone and Diet in the ETiology of breast cancer prospective study. Carcinogenesis 2018;39:98–108. https://doi.org/10.1093/carcin/bgx126.

[375] Wang H, Hu X, Yang F, Xiao H. miR-325-3p Promotes the Proliferation, Invasion, and EMT of Breast Cancer Cells by Directly Targeting S100A2. Oncol Res Featur Preclin Clin Cancer Ther 2021;28:731–44. https://doi.org/10.3727/096504020X16100888208039.

[376] Zhou Q, Guo J, Huang W, Yu X, Xu C, Long X. Linc-ROR promotes the

progression of breast cancer and decreases the sensitivity to rapamycin through miR-194-3p targeting MECP2. Mol Oncol 2020;14:2231–50. https://doi.org/10.1002/1878-0261.12700.

[377] van Schooneveld E, Wouters MC, Van der Auwera I, Peeters DJ, Wildiers H, Van Dam PA, et al. Expression profiling of cancerous and normal breast tissues identifies microRNAs that are differentially expressed in serum from patients with (metastatic) breast cancer and healthy volunteers. Breast Cancer Res 2012;14:R34. https://doi.org/10.1186/bcr3127.

[378] Huo D, Clayton WM, Yoshimatsu TF, Chen J, Olopade OI. Identification of a circulating MicroRNA signature to distinguish recurrence in breast cancer patients. Oncotarget 2016;7:55231–48. https://doi.org/10.18632/oncotarget.10485.

[379] Liu H, Xue L, Song C, Liu F, Jiang T, Yang X. Overexpression of circular RNA circ_001569 indicates poor prognosis in hepatocellular carcinoma and promotes cell growth and metastasis by sponging miR-411-5p and miR-432-5p. Biochem Biophys Res Commun 2018;503:2659–65. https://doi.org/10.1016/j.bbrc.2018.08.020.

[380] Zou M, Shen J, Wu Y, Zhong C, Fang L, Zhu F, et al. Dysregulation of miR-411 in cancer: Causative factor for pathogenesis, diagnosis and prognosis. Biomed Pharmacother 2022;149:112896. https://doi.org/10.1016/j.biopha.2022.112896.

[381] Miller AB, Wall C, Baines CJ, Sun P, To T, Narod SA. Twenty five year follow-up for breast cancer incidence and mortality of the Canadian National Breast Screening Study: randomised screening trial. BMJ 2014;348:g366–g366. https://doi.org/10.1136/bmj.g366.

[382] Fouladi N, Amani F, Harghi AS, Nayebyazdi N. Five year survival of women with breast cancer in Ardabil, north-west of Iran. Asian Pac J Cancer Prev 2011;12:1799–801.

[383] Fallahzadeh H, Momayyezi M, Akhundzardeini R, Zarezardeini S. Five Year Survival of Women with Breast Cancer in Yazd. Asian Pacific J Cancer Prev 2014;15:6597–601. https://doi.org/10.7314/APJCP.2014.15.16.6597.

[384] Dugo M, Huang X, Iorio M V., Cataldo A, Tagliabue E, Daidone MG, et al. MicroRNA co-expression patterns unravel the relevance of extra cellular matrix and immunity in breast cancer. The Breast 2018;39:46–52. https://doi.org/10.1016/j.breast.2018.03.008.

[385] Huang Y-W, Kuo C-T, Chen J-H, Goodfellow PJ, Huang TH-M, Rader JS, et al. Hypermethylation of miR-203 in endometrial carcinomas. Gynecol Oncol 2014;133:340–5. https://doi.org/10.1016/j.ygyno.2014.02.009.

[386] Cho NH. Cancer-associated fibroblasts regulate gene expression of breast cancer cells via exosomal microRNAs. yonsei university, 2015.

[387] Ding X, Zheng J, Cao M. Circ_0004771 Accelerates Cell Carcinogenic Phenotypes via Suppressing miR-1253-Mediated DDAH1 Inhibition in Breast Cancer. Cancer Manag Res 2020;13:1–11. https://doi.org/10.2147/CMAR.S273783.

[388] Pinto E. Blood pressure and ageing. Postgrad Med J 2007;83:109–14. https://doi.org/10.1136/pgmj.2006.048371.

[389] Narasimhan A, Ghosh S, Stretch C, Greiner R, Bathe OF, Baracos V, et al. Small RNAome profiling from human skeletal muscle: novel miRNAs and their targets associated with cancer cachexia. J Cachexia Sarcopenia Muscle 2017;8:405–16. https://doi.org/10.1002/jcsm.12168.

[390] Pescador N, Pérez-Barba M, Ibarra JM, Corbatón A, Martínez-Larrad MT, Serrano-Ríos M. Serum Circulating microRNA Profiling for Identification of Potential Type 2 Diabetes and Obesity Biomarkers. PLoS One 2013;8:e77251. https://doi.org/10.1371/journal.pone.0077251.

[391] Yang W, Wang J, Chen Z, Chen J, Meng Y, Chen L, et al. NFE2 Induces miR-423-5p to Promote Gluconeogenesis and Hyperglycemia by Repressing the Hepatic FAM3A-ATP-Akt Pathway. Diabetes 2017;66:1819–32. https://doi.org/10.2337/db16-1172.

[392] Balzano F, Deiana M, Dei Giudici S, Oggiano A, Baralla A, Pasella S, et al. miRNA Stability in Frozen Plasma Samples. Molecules 2015;20:19030–40. https://doi.org/10.3390/molecules201019030.

[393] Ge Q, Zhou Y, Lu J, Bai Y, Xie X, Lu Z. miRNA in Plasma Exosome is Stable under Different Storage Conditions. Molecules 2014;19:1568–75. https://doi.org/10.3390/molecules19021568.

[394] Agência Senado. Lei determina inclusão de dados sobre raça em documentos trabalhistas. Lei Determ Inclusão Dados Sobre Raça Em Doc Trab 2023. https://www12.senado.leg.br/noticias/materias/2023/04/24/lei-determina-inclusao-de-dados-sobre-raca-em-documentos-trabalhistas.

[395] Pena SDJ, Bastos-Rodrigues L, Pimenta JR, Bydlowski SP. DNA tests probe the genomic ancestry of Brazilians. Brazilian J Med Biol Res 2009;42:870–6. https://doi.org/10.1590/S0100-879X2009005000026.

[396] Souza AM de, Resende SS, Sousa TN de, Brito CFA de. A systematic scoping review of the genetic ancestry of the Brazilian population. Genet Mol Biol 2019;42:495–508. https://doi.org/10.1590/1678-4685-gmb-2018-0076.

[397] Lins TC, Vieira RG, Abreu BS, Grattapaglia D, Pereira RW. Genetic composition

of Brazilian population samples based on a set of twenty-eight ancestry informative SNPs. Am J Hum Biol 2009;22:187–92. https://doi.org/10.1002/ajhb.20976.

[398] da Costa Vieira RA, Sant'Anna D, Laus AC, Bacchi CE, Silva RJC, de Oliveira-Junior I, et al. Genetic Ancestry of 1127 Brazilian Breast Cancer Patients and Its Correlation With Molecular Subtype and Geographic Region. Clin Breast Cancer 2023;23:527–37. https://doi.org/10.1016/j.clbc.2023.04.001.

[399] Huo D, Hu H, Rhie SK, Gamazon ER, Cherniack AD, Liu J, et al. Comparison of Breast Cancer Molecular Features and Survival by African and European Ancestry in The Cancer Genome Atlas. JAMA Oncol 2017;3:1654. https://doi.org/10.1001/jamaoncol.2017.0595.

[400] Fejerman L, John EM, Huntsman S, Beckman K, Choudhry S, Perez-Stable E, et al. Genetic Ancestry and Risk of Breast Cancer among U.S. Latinas. Cancer Res 2008;68:9723–8. https://doi.org/10.1158/0008-5472.CAN-08-2039.

[401] Buleje J, Guevara-Fujita M, Acosta O, Huaman FDP, Danos P, Murillo A, et al. Mutational analysis of BRCA1 and BRCA2 genes in Peruvian families with hereditary breast and ovarian cancer. Mol Genet Genomic Med 2017;5:481–94. https://doi.org/10.1002/mgg3.301.

[402] Geeurickx E, Hendrix A. Targets, pitfalls and reference materials for liquid biopsy tests in cancer diagnostics. Mol Aspects Med 2020;72:100828. https://doi.org/10.1016/j.mam.2019.10.005.

[403] Witwer KW, Halushka MK. Toward the promise of microRNAs – Enhancing reproducibility and rigor in microRNA research. RNA Biol 2016;13:1103–16. https://doi.org/10.1080/15476286.2016.1236172.

[404] Moloney BM, Gilligan KE, Joyce DP, O'Neill CP, O'Brien KP, Khan S, et al. Investigating the Potential and Pitfalls of EV-Encapsulated MicroRNAs as Circulating Biomarkers of Breast Cancer. Cells 2020, Vol 9, Page 141 2020;9:141. https://doi.org/10.3390/CELLS9010141.

[405] Lakkisto P, Dalgaard LT, Belmonte T, Pinto-Sietsma S-J, Devaux Y, de Gonzalo-Calvo D. Development of circulating microRNA-based biomarkers for medical decision-making: a friendly reminder of what should NOT be done. Crit Rev Clin Lab Sci 2023;60:141–52. https://doi.org/10.1080/10408363.2022.2128030.

[406] Guo L, Yu J, Yu H, Zhao Y, Chen S, Xu C, et al. Evolutionary and Expression Analysis of miR-#-5p and miR-#-3p at the miRNAs/isomiRs Levels. Biomed Res Int 2015;2015:1–14. https://doi.org/10.1155/2015/168358.

[407] Hanahan D. Hallmarks of Cancer: New Dimensions. Cancer Discov 2022;12:31–

46. https://doi.org/10.1158/2159-8290.CD-21-1059.

[408] Da Cunha JPC, Galante PAF, De Souza JES, Pieprzyk M, Carraro DM, Old LJ, et al. The human cell surfaceome of breast tumors. Biomed Res Int 2013;2013:976816. https://doi.org/10.1155/2013/976816.

[409] Williams C, Royo F, Aizpurua-Olaizola O, Pazos R, Boons G-JJ, Reichardt N-CC, et al. Glycosylation of extracellular vesicles: current knowledge, tools and clinical perspectives. vol. 7. Taylor and Francis Ltd.; 2018. https://doi.org/10.1080/20013078.2018.1442985.

[410] ABEL PD, KEANE P, LEATHEM A, BUTT ST, WILLIAMS G. Change in Glycoconjugate for the Binding Site of the Lectin *Ulex europeus* 1 following Malignant Transformation of Prostatic Epithelium. Br J Urol 1989;63:183–5. https://doi.org/10.1111/j.1464-410X.1989.tb05161.x.

[411] Lim AW, Neves AA, Lam Shang Leen S, Lao-Sirieix P, Bird-Lieberman E, Singh N, et al. Lectins in Cervical Screening. Cancers (Basel) 2020;12:1928. https://doi.org/10.3390/cancers12071928.

[412] Hu Q, Su H, Li J, Lyon C, Tang W, Wan M, et al. Clinical applications of exosome membrane proteins. Precis Clin Med 2020;3:54–66. https://doi.org/10.1093/pcmedi/pbaa007.

[413] Kanehira K, Hu J, Pier T, Sebree L, Huang W. High endogenous avidin binding activity: an inexpensive and readily available marker for the differential diagnosis of kidney neoplasms. Int J Clin Exp Pathol 2008;1:435–9.

[414] Koliha N, Heider U, Ozimkowski T, Wiemann M, Bosio A, Wild S. Melanoma affects the composition of blood cell-derived extracellular vesicles. Front Immunol 2016;7:282. https://doi.org/10.3389/FIMMU.2016.00282/BIBTEX.

[415] Drake PM, Schilling B, Niles RK, Braten M, Johansen E, Liu H, et al. A lectin affinity workflow targeting glycosite-specific, cancer-related carbohydrate structures in trypsin-digested human plasma1. Anal Biochem 2011;408:71–85. https://doi.org/10.1016/j.ab.2010.08.010.

[416] Vykoukal J, Sun N, Aguilar-Bonavides C, Katayama H, Tanaka I, Fahrmann JF, et al. Plasma-derived extracellular vesicle proteins as a source of biomarkers for lung adenocarcinoma. Oncotarget 2017;8:95466–80. https://doi.org/10.18632/oncotarget.20748.

[417] Wu G, Yang G, Zhang R, Xu G, Zhang L, Wen W, et al. Altered microRNA Expression Profiles of Extracellular Vesicles in Nasal Mucus From Patients With Allergic Rhinitis. Allergy Asthma Immunol Res 2015;7:449. https://doi.org/10.4168/aair.2015.7.5.449.

[418] Wróblewska JP, Lach MS, Rucinski M, Piotrowski I, Galus L, Suchorska WM, et

al. MiRNAs from serum-derived extracellular vesicles as biomarkers for uveal melanoma progression. Front Cell Dev Biol 2022;10:1008901. https://doi.org/10.3389/fcell.2022.1008901.

[419] Kaddour H, Tranquille M, Okeoma CM. The Past, the Present, and the Future of the Size Exclusion Chromatography in Extracellular Vesicles Separation. Viruses 2021;13:2272. https://doi.org/10.3390/v13112272.

[420] Blans K, Hansen MS, Sørensen L V., Hvam ML, Howard KA, Möller A, et al. Pellet-free isolation of human and bovine milk extracellular vesicles by size-exclusion chromatography. J Extracell Vesicles 2017;6:1294340. https://doi.org/10.1080/20013078.2017.1294340.

[421] Sidhom K, Obi PO, Saleem A. A Review of Exosomal Isolation Methods: Is Size Exclusion Chromatography the Best Option? Int J Mol Sci 2020;21:6466. https://doi.org/10.3390/ijms21186466.

[422] Kim MW, Park S, Lee H, Gwak H, Hyun K-AA, Kim JY, et al. Multi-miRNA panel of tumor-derived extracellular vesicles as promising diagnostic biomarkers of early-stage breast cancer. Cancer Sci 2021;112:5078–87. https://doi.org/10.1111/CAS.15155.

[423] Arockia Jeyaprakash A, Jayashree G, Mahanta SK, Swaminathan CP, Sekar K, Surolia A, et al. Structural Basis for the Energetics of Jacalin–Sugar Interactions: Promiscuity Versus Specificity. J Mol Biol 2005;347:181–8. https://doi.org/10.1016/j.jmb.2005.01.015.

[424] Oliveira C, Felix W, Moreira RA, Teixeira JA, Domingues L. Expression of frutalin, an α-d-galactose-binding jacalin-related lectin, in the yeast Pichia pastoris. Protein Expr Purif 2008;60:188–93. https://doi.org/10.1016/j.pep.2008.04.008.

[425] Yoh KE, Lowe CJ, Mahajan S, Suttmann R, Nguy T, Reichelt M, et al. Enrichment of circulating tumor-derived extracellular vesicles from human plasma. J Immunol Methods 2021;490:112936. https://doi.org/10.1016/j.jim.2020.112936.

[426] Yamamoto M, Harada Y, Suzuki T, Fukushige T, Yamakuchi M, Kanekura T, et al. Application of high-mannose-type glycan-specific lectin from Oscillatoria Agardhii for affinity isolation of tumor-derived extracellular vesicles 2019;580:21–9.

[427] Royo F, Zuñiga-Garcia P, Sanchez-Mosquera P, Egia A, Perez A, Loizaga A, et al. Different EV enrichment methods suitable for clinical settings yield different subpopulations of urinary extracellular vesicles from human samples. J Extracell Vesicles 2016;5:29497. https://doi.org/10.3402/jev.v5.29497.

[428] Monguió-Tortajada M, Gálvez-Montón C, Bayes-Genis A, Roura S, Borràs FE. Extracellular vesicle isolation methods: rising impact of size-exclusion chromatography. Cell Mol Life Sci 2019;76:2369–82. https://doi.org/10.1007/s00018-019-03071-y.

[429] Manimala JC, Li Z, Jain A, VedBrat S, Gildersleeve JC. Carbohydrate Array Analysis of Anti-Tn Antibodies and Lectins Reveals Unexpected Specificities: Implications for Diagnostic and Vaccine Development. ChemBioChem 2005;6:2229–41. https://doi.org/10.1002/cbic.200500165.

[430] Bundle DR, Young NM. Carbohydrate-protein interactions in antibodies and lectins. Curr Opin Struct Biol 1992;2:666–73. https://doi.org/10.1016/0959-440X(92)90199-H.

[431] Echevarria J, Royo F, Pazos R, Salazar L, Falcon-Perez JM, Reichardt N-C. Microarray-Based Identification of Lectins for the Purification of Human Urinary Extracellular Vesicles Directly from Urine Samples. ChemBioChem 2014;15:1621–6. https://doi.org/10.1002/cbic.201402058.

[432] Dusoswa SA, Horrevorts SK, Ambrosini M, Kalay H, Paauw NJ, Nieuwland R, et al. Glycan modification of glioblastoma-derived extracellular vesicles enhances receptor-mediated targeting of dendritic cells. J Extracell Vesicles 2019;8:1648995. https://doi.org/10.1080/20013078.2019.1648995.

[433] Wu AM, Wu JH, Shen FS. Interaction of a Novel Tn (GalNAcα1→)Ser/Thr) Glycoprotein with Gal, GalNAc and GlcNAc Specific Lectins. Biochem Biophys Res Commun 1994;198:251–6. https://doi.org/10.1006/bbrc.1994.1035.

[434] Wu AM, Wu JH, Lin L-H, Lin S-H, Liu J-H. Binding profile of Artocarpus integrifolia agglutinin (Jacalin). Life Sci 2003;72:2285–302. https://doi.org/10.1016/S0024-3205(03)00116-4.

[435] Carnino JM, Ni K, Jin Y. Post-translational Modification Regulates Formation and Cargo-Loading of Extracellular Vesicles. Front Immunol 2020;11:948. https://doi.org/10.3389/fimmu.2020.00948.

[436] Zhang Y, Wu X, Tao WA. Characterization and applications of extracellular vesicle proteome with post-translational modifications. TrAC Trends Anal Chem 2018;107:21–30. https://doi.org/10.1016/j.trac.2018.07.014.

[437] Atukorala I, Mathivanan S. The Role of Post-Translational Modifications in Targeting Protein Cargo to Extracellular Vesicles. New Front. Extracell. Vesicles, vol. 97, Springer; 2021, p. 45–60. https://doi.org/10.1007/978-3-030-67171-6_3.

[438] Clancy JW, D'Souza-Schorey C. Tumor-Derived Extracellular Vesicles: Multifunctional Entities in the Tumor Microenvironment. Annu Rev Pathol Mech Dis 2023;18:205–29. https://doi.org/10.1146/annurev-pathmechdis-031521-

022116.

[439] Gold D V., Mattes J. Monoclonal Antibody B72.3 Reacts with a Core Region Structure of O-Linked Carbohydrates. Tumor Biol 1988;9:137–44. https://doi.org/10.1159/000217554.

[440] Persson N, Stuhr-Hansen N, Risinger C, Mereiter S, Polónia A, Polom K, et al. Epitope mapping of a new anti-Tn antibody detecting gastric cancer cells. Glycobiology 2017;27:635–45. https://doi.org/10.1093/glycob/cwx033.

APPENDICES

Appendix 1. Patient Characteristics of the Cohort A

Characteristic	Elderly HER2, N = 1[1]	Elderly Luminal A, N = 3[1]	Elderly Luminal B, N = 3[1]	Elderly Luminal HER2, N = 3[1]	Elderly TNBC, N = 6[1]	Young HER2, N = 2[1]	Young Luminal B, N = 3[1]	Young Luminal HER2, N = 3[1]	Young TNBC, N = 6[1]	p-value[2]
Current Age	57 (57-57)	64 (57-71)	62 (56-67)	63 (55-76)	66 (51-85)	32 (30-33)	31 (27-34)	36 (33-38)	35 (29-39)	**0.004***
Age at admission to the biobank	53 (53-53)	59 (50-69)	61 (54-66)	61 (53-74)	62 (48-79)	29 (27-31)	30 (26-32)	31 (25-36)	31 (29-34)	**0.004***
Age at blood collection	54 (54-54)	60 (51-71)	62 (55-67)	63 (54-75)	64 (50-81)	30 (28-32)	31 (27-33)	32 (26-36)	32 (30-34)	**0.004***
Age at diagnosis	54 (54-54)	60 (51-70)	61 (53-67)	62 (54-75)	63 (50-81)	30 (28-32)	30 (27-33)	32 (26-36)	32 (29-34)	**0.004***
Sex										
Female	1 / 1 (100%)	3 / 3 (100%)	3 / 3 (100%)	3 / 3 (100%)	6 / 6 (100%)	2 / 2 (100%)	3 / 3 (100%)	3 / 3 (100%)	6 / 6 (100%)	
Self-reported race										0.3
White	1 / 1 (100%)	2 / 3 (67%)	1 / 3 (33%)	0 / 3 (0%)	4 / 6 (67%)	0 / 2 (0%)	1 / 3 (33%)	0 / 3 (0%)	4 / 6 (67%)	
Black	0 / 1 (0%)	0 / 3 (0%)	1 / 3 (33%)	0 / 3 (0%)	1 / 6 (17%)	0 / 2 (0%)	0 / 3 (0%)	0 / 3 (0%)	0 / 6 (0%)	
Other	0 / 1 (0%)	0 / 3 (0%)	0 / 3 (0%)	0 / 3 (0%)	0 / 6 (0%)	0 / 2 (0%)	0 / 3 (0%)	1 / 3 (33%)	0 / 6 (0%)	
Brown	0 / 1 (0%)	1 / 3 (33%)	1 / 3 (33%)	3 / 3 (100%)	1 / 6 (17%)	2 / 2 (100%)	2 / 3 (67%)	2 / 3 (67%)	2 / 6 (33%)	
Education level										0.073
Complete High-school	0 / 1 (0%)	1 / 3 (33%)	2 / 3 (67%)	0 / 3 (0%)	2 / 6 (33%)	2 / 2 (100%)	3 / 3 (100%)	2 / 3 (67%)	1 / 6 (17%)	
Incomplete High-school	1 / 1 (100%)	0 / 3 (0%)	0 / 3 (0%)	0 / 3 (0%)	0 / 6 (0%)	0 / 2 (0%)	0 / 3 (0%)	0 / 3 (0%)	0 / 6 (0%)	
Incomplete Elementary School	0 / 1	2 / 3	0 / 3	1 / 3	3 / 6	0 / 2	0 / 3	0 / 3	0 / 6	

	(0%)	(67%)	(0%)	(33%)	(50%)	(0%)	(0%)	(0%)	(0%)	
Complete University-level	0 / 1 (0%)	0 / 3 (0%)	1 / 3 (33%)	2 / 3 (67%)	1 / 6 (17%)	0 / 2 (0%)	0 / 3 (0%)	1 / 3 (33%)	3 / 6 (50%)	
Incomplete University-level	0 / 1 (0%)	0 / 3 (0%)	0 / 3 (0%)	0 / 3 (0%)	0 / 6 (0%)	0 / 2 (0%)	0 / 3 (0%)	0 / 3 (0%)	2 / 6 (33%)	
Body-Mass Index (BMI)	35.5 (35.5-35.5)	25.1 (23.3-26.2)	30.7 (29.2-33.3)	28.9 (24.5-34.9)	25.6 (17.8-34.1)	27.8 (27.0-28.6)	29.8 (22.3-35.8)	27.5 (21.7-33.2)	28.4 (20.7-40.0)	0.7
Nutritional status										>0.9
Low weight	0 / 1 (0%)	0 / 3 (0%)	0 / 3 (0%)	0 / 3 (0%)	1 / 6 (17%)	0 / 2 (0%)	0 / 3 (0%)	0 / 3 (0%)	0 / 6 (0%)	
Eutrophic/Normal	0 / 1 (0%)	1 / 3 (33%)	0 / 3 (0%)	1 / 3 (33%)	2 / 6 (33%)	0 / 2 (0%)	1 / 3 (33%)	1 / 3 (33%)	2 / 6 (33%)	
Obese	1 / 1 (100%)	0 / 3 (0%)	0 / 3 (0%)	1 / 3 (33%)	1 / 6 (17%)	0 / 2 (0%)	1 / 3 (33%)	1 / 3 (33%)	1 / 6 (17%)	
Overweight	0 / 1 (0%)	2 / 3 (67%)	3 / 3 (100%)	1 / 3 (33%)	2 / 6 (33%)	2 / 2 (100%)	1 / 3 (33%)	1 / 3 (33%)	3 / 6 (50%)	
Physical activity										0.4
Do not practice	0 / 1 (0%)	3 / 3 (100%)	1 / 3 (33%)	2 / 3 (67%)	4 / 6 (67%)	1 / 2 (50%)	3 / 3 (100%)	2 / 3 (67%)	5 / 6 (83%)	
Pratice Sporadically	1 / 1 (100%)	0 / 3 (0%)	1 / 3 (33%)	1 / 3 (33%)	0 / 6 (0%)	1 / 2 (50%)	0 / 3 (0%)	0 / 3 (0%)	0 / 6 (0%)	
Pratice regularly	0 / 1 (0%)	0 / 3 (0%)	1 / 3 (33%)	0 / 3 (0%)	2 / 6 (33%)	0 / 2 (0%)	0 / 3 (0%)	1 / 3 (33%)	1 / 6 (17%)	
Drugs use										
No	0 / 0 (NA%)	2 / 2 (100%)	3 / 3 (100%)	1 / 1 (100%)	3 / 3 (100%)	2 / 2 (100%)	2 / 2 (100%)	2 / 2 (100%)	5 / 5 (100%)	
Unknown	1	1	0	2	3	0	1	1	1	
Smoking										0.057
Currently smoke	0 / 1 (0%)	2 / 3 (67%)	0 / 3 (0%)	1 / 3 (33%)	1 / 6 (17%)	0 / 2 (0%)	0 / 3 (0%)	0 / 3 (0%)	0 / 6 (0%)	
Smoked in the past	1 / 1 (100%)	1 / 3 (33%)	1 / 3 (33%)	1 / 3 (33%)	1 / 6 (17%)	0 / 2 (0%)	0 / 3 (0%)	0 / 3 (0%)	0 / 6 (0%)	
Never smoked	0 / 1 (0%)	0 / 3 (0%)	2 / 3 (67%)	1 / 3 (33%)	4 / 6 (67%)	2 / 2 (100%)	3 / 3 (100%)	3 / 3 (100%)	6 / 6 (100%)	

Alcohol use									0.5
Currently drunk	0 / 1 (0%)	0 / 3 (0%)	0 / 3 (0%)	0 / 3 (0%)	0 / 6 (0%)	0 / 2 (0%)	1 / 3 (33%)	0 / 3 (0%)	0 / 6 (0%)	
Drank in the past	0 / 1 (0%)	0 / 3 (0%)	0 / 3 (0%)	0 / 3 (0%)	0 / 6 (0%)	0 / 2 (0%)	0 / 3 (0%)	1 / 3 (33%)	2 / 6 (33%)	
Never drank	1 / 1 (100%)	3 / 3 (100%)	3 / 3 (100%)	3 / 3 (100%)	6 / 6 (100%)	2 / 2 (100%)	2 / 3 (67%)	2 / 3 (67%)	4 / 6 (67%)	
Other comorbidity	0 / 0 (NA%)	0 / 0 (NA%)	0 / 0 (NA%)	0 / 0 (NA%)	0 / 0 (NA%)	0 / 0 (NA%)	0 / 0 (NA%)	0 / 0 (NA%)	0 / 0 (NA%)	
Unknown	1	3	3	3	6	2	3	3	6	
Familiy history of cancer										**0.025***
No	1 / 1 (100%)	3 / 3 (100%)	3 / 3 (100%)	1 / 3 (33%)	1 / 6 (17%)	2 / 2 (100%)	2 / 3 (67%)	0 / 3 (0%)	2 / 6 (33%)	
Yes	0 / 1 (0%)	0 / 3 (0%)	0 / 3 (0%)	2 / 3 (67%)	5 / 6 (83%)	0 / 2 (0%)	1 / 3 (33%)	3 / 3 (100%)	4 / 6 (67%)	
Family history of cancer (first degree of kinship)										**0.033***
Yes	0 / 1 (0%)	0 / 3 (0%)	0 / 3 (0%)	1 / 3 (33%)	5 / 6 (83%)	0 / 2 (0%)	0 / 3 (0%)	0 / 3 (0%)	1 / 6 (17%)	
No	1 / 1 (100%)	3 / 3 (100%)	3 / 3 (100%)	2 / 3 (67%)	1 / 6 (17%)	2 / 2 (100%)	3 / 3 (100%)	3 / 3 (100%)	5 / 6 (83%)	
Family history of breast or ovarian cancer (first degree of kinship)	0 / 1 (0%)	0 / 3 (0%)	0 / 3 (0%)	0 / 3 (0%)	0 / 6 (0%)	0 / 2 (0%)	0 / 3 (0%)	0 / 3 (0%)	0 / 6 (0%)	
Previous breast-related surgeries										
No	1 / 1 (100%)	3 / 3 (100%)	3 / 3 (100%)	3 / 3 (100%)	6 / 6 (100%)	2 / 2 (100%)	3 / 3 (100%)	2 / 2 (100%)	6 / 6 (100%)	
Unknown	0	0	0	0	0	0	0	1	0	
Diabetes Mellitus										0.093
No	1 / 1 (100%)	2 / 3 (67%)	3 / 3 (100%)	1 / 3 (33%)	6 / 6 (100%)	2 / 2 (100%)	3 / 3 (100%)	3 / 3 (100%)	6 / 6 (100%)	
Yes	0 / 1 (0%)	1 / 3 (33%)	0 / 3 (0%)	2 / 3 (67%)	0 / 6 (0%)	0 / 2 (0%)	0 / 3 (0%)	0 / 3 (0%)	0 / 6 (0%)	
High Blood Pressure (HBP)										0.2

No	1 / 1 (100%)	2 / 3 (67%)	2 / 3 (67%)	0 / 3 (0%)	4 / 6 (67%)	2 / 2 (100%)	3 / 3 (100%)	3 / 3 (100%)	5 / 6 (83%)	
Yes	0 / 1 (0%)	1 / 3 (33%)	1 / 3 (33%)	3 / 3 (100%)	2 / 6 (33%)	0 / 2 (0%)	0 / 3 (0%)	0 / 3 (0%)	1 / 6 (17%)	
Chronic Obstructive Pulmonary Disease (COPD)										
No	1 / 1 (100%)	3 / 3 (100%)	3 / 3 (100%)	3 / 3 (100%)	6 / 6 (100%)	2 / 2 (100%)	3 / 3 (100%)	3 / 3 (100%)	6 / 6 (100%)	
Chronic Gastritis										0.6
No	1 / 1 (100%)	2 / 3 (67%)	3 / 3 (100%)	3 / 3 (100%)	6 / 6 (100%)	2 / 2 (100%)	3 / 3 (100%)	3 / 3 (100%)	6 / 6 (100%)	
Yes	0 / 1 (0%)	1 / 3 (33%)	0 / 3 (0%)	0 / 3 (0%)	0 / 6 (0%)	0 / 2 (0%)	0 / 3 (0%)	0 / 3 (0%)	0 / 6 (0%)	
Tubular Differentiation										0.12
2	0 / 1 (0%)	1 / 3 (33%)	2 / 3 (67%)	0 / 2 (0%)	0 / 6 (0%)	0 / 1 (0%)	0 / 3 (0%)	0 / 2 (0%)	0 / 5 (0%)	
3	1 / 1 (100%)	2 / 3 (67%)	1 / 3 (33%)	2 / 2 (100%)	6 / 6 (100%)	1 / 1 (100%)	3 / 3 (100%)	2 / 2 (100%)	5 / 5 (100%)	
Unknown	0	0	0	1	0	1	0	1	1	
Nuclear Grade										0.2
2	1 / 1 (100%)	2 / 3 (67%)	2 / 3 (67%)	1 / 2 (50%)	1 / 6 (17%)	0 / 2 (0%)	1 / 3 (33%)	0 / 2 (0%)	0 / 5 (0%)	
3	0 / 1 (0%)	1 / 3 (33%)	1 / 3 (33%)	1 / 2 (50%)	5 / 6 (83%)	2 / 2 (100%)	2 / 3 (67%)	2 / 2 (100%)	5 / 5 (100%)	
Unknown	0	0	0	1	0	0	0	1	1	
Mitotic Index										0.3
1	0 / 1 (0%)	3 / 3 (100%)	2 / 3 (67%)	1 / 1 (100%)	2 / 6 (33%)	2 / 2 (100%)	1 / 3 (33%)	1 / 2 (50%)	0 / 5 (0%)	
2	0 / 1 (0%)	0 / 3 (0%)	1 / 3 (33%)	0 / 1 (0%)	3 / 6 (50%)	0 / 2 (0%)	2 / 3 (67%)	1 / 2 (50%)	3 / 5 (60%)	
3	1 / 1 (100%)	0 / 3 (0%)	0 / 3 (0%)	0 / 1 (0%)	1 / 6 (17%)	0 / 2 (0%)	0 / 3 (0%)	0 / 2 (0%)	2 / 5 (40%)	
Unknown	0	0	0	2	0	0	0	1	1	
Histologic Grade										**0.049***
1	0 / 1	1 / 3	1 / 3	0 / 1	0 / 6	0 / 1	0 / 3	0 / 2	0 / 5	

	(0%)	(33%)	(33%)	(0%)	(0%)	(0%)	(0%)	(0%)	(0%)	
2	0 / 1 (0%)	2 / 3 (67%)	2 / 3 (67%)	1 / 1 (100%)	2 / 6 (33%)	1 / 1 (100%)	2 / 3 (67%)	1 / 2 (50%)	0 / 5 (0%)	
3	1 / 1 (100%)	0 / 3 (0%)	0 / 3 (0%)	0 / 1 (0%)	4 / 6 (67%)	0 / 1 (0%)	1 / 3 (33%)	1 / 2 (50%)	5 / 5 (100%)	
Unknown	0	0	0	2	0	1	0	1	1	
Estrogen Receptor										**<0.001***
Negative	1 / 1 (100%)	0 / 3 (0%)	0 / 3 (0%)	1 / 3 (33%)	6 / 6 (100%)	2 / 2 (100%)	0 / 3 (0%)	0 / 3 (0%)	6 / 6 (100%)	
Positive	0 / 1 (0%)	3 / 3 (100%)	3 / 3 (100%)	2 / 3 (67%)	0 / 6 (0%)	0 / 2 (0%)	3 / 3 (100%)	3 / 3 (100%)	0 / 6 (0%)	
Progesterone Receptor										**<0.001***
Inconclusive	0 / 1 (0%)	0 / 3 (0%)	0 / 3 (0%)	1 / 3 (33%)	0 / 6 (0%)	0 / 2 (0%)	0 / 3 (0%)	0 / 3 (0%)	0 / 6 (0%)	
Negative	1 / 1 (100%)	0 / 3 (0%)	0 / 3 (0%)	0 / 3 (0%)	6 / 6 (100%)	2 / 2 (100%)	0 / 3 (0%)	0 / 3 (0%)	6 / 6 (100%)	
Positive	0 / 1 (0%)	3 / 3 (100%)	3 / 3 (100%)	2 / 3 (67%)	0 / 6 (0%)	0 / 2 (0%)	3 / 3 (100%)	3 / 3 (100%)	0 / 6 (0%)	
HER2 (IHC)										**<0.001***
+ (negative)	0 / 1 (0%)	0 / 3 (0%)	2 / 3 (67%)	0 / 3 (0%)	0 / 6 (0%)	0 / 2 (0%)	1 / 3 (33%)	0 / 3 (0%)	0 / 6 (0%)	
++ (suspicious)	0 / 1 (0%)	0 / 3 (0%)	0 / 3 (0%)	1 / 3 (33%)	1 / 6 (17%)	0 / 2 (0%)	2 / 3 (67%)	0 / 3 (0%)	0 / 6 (0%)	
+++ (positive)	1 / 1 (100%)	0 / 3 (0%)	0 / 3 (0%)	1 / 3 (33%)	0 / 6 (0%)	2 / 2 (100%)	0 / 3 (0%)	3 / 3 (100%)	0 / 6 (0%)	
0 (negative)	0 / 1 (0%)	3 / 3 (100%)	1 / 3 (33%)	1 / 3 (33%)	5 / 6 (83%)	0 / 2 (0%)	0 / 3 (0%)	0 / 3 (0%)	6 / 6 (100%)	
HER2 (FISH)										**0.025***
Amplified	1 / 1 (100%)	0 / 3 (0%)	0 / 3 (0%)	2 / 2 (100%)	0 / 6 (0%)	0 / 2 (0%)	0 / 1 (0%)	1 / 2 (50%)	0 / 3 (0%)	
Suspicious	0 / 1 (0%)	0 / 3 (0%)	0 / 3 (0%)	0 / 2 (0%)	0 / 6 (0%)	0 / 2 (0%)	1 / 1 (100%)	0 / 2 (0%)	0 / 3 (0%)	
Not evaluated	0 / 1 (0%)	2 / 3 (67%)	3 / 3 (100%)	0 / 2 (0%)	5 / 6 (83%)	2 / 2 (100%)	0 / 1 (0%)	1 / 2 (50%)	3 / 3 (100%)	
Not amplified	0 / 1	1 / 3	0 / 3	0 / 2	1 / 6	0 / 2	0 / 1	0 / 2	0 / 3	

	(0%)	(33%)	(0%)	(0%)	(17%)	(0%)	(0%)	(0%)	(0%)	
Unknown	0	0	0	1	0	0	2	1	3	
Ki67	70 (70-70)	9 (8-10)	38 (25-60)	35 (15-70)	67 (50-90)	35 (30-40)	43 (30-70)	53 (40-80)	83 (50-95)	**0.014***
T										0.6
T1	1 / 1 (100%)	2 / 3 (67%)	0 / 3 (0%)	0 / 2 (0%)	0 / 6 (0%)	1 / 2 (50%)	0 / 3 (0%)	0 / 3 (0%)	0 / 5 (0%)	
T2	0 / 1 (0%)	0 / 3 (0%)	2 / 3 (67%)	1 / 2 (50%)	2 / 6 (33%)	0 / 2 (0%)	1 / 3 (33%)	1 / 3 (33%)	1 / 5 (20%)	
T3	0 / 1 (0%)	0 / 3 (0%)	0 / 3 (0%)	0 / 2 (0%)	3 / 6 (50%)	1 / 2 (50%)	1 / 3 (33%)	1 / 3 (33%)	2 / 5 (40%)	
T4	0 / 1 (0%)	1 / 3 (33%)	1 / 3 (33%)	0 / 2 (0%)	1 / 6 (17%)	0 / 2 (0%)	1 / 3 (33%)	0 / 3 (0%)	1 / 5 (20%)	
T4d	0 / 1 (0%)	0 / 3 (0%)	0 / 3 (0%)	0 / 2 (0%)	0 / 6 (0%)	0 / 2 (0%)	0 / 3 (0%)	1 / 3 (33%)	1 / 5 (20%)	
Tis	0 / 1 (0%)	0 / 3 (0%)	0 / 3 (0%)	1 / 2 (50%)	0 / 6 (0%)	0 / 2 (0%)	0 / 3 (0%)	0 / 3 (0%)	0 / 5 (0%)	
Unknown	0	0	0	1	0	0	0	0	1	
N										0.5
N0	1 / 1 (100%)	0 / 3 (0%)	2 / 3 (67%)	1 / 2 (50%)	2 / 6 (33%)	1 / 2 (50%)	0 / 3 (0%)	0 / 3 (0%)	1 / 5 (20%)	
N1	0 / 1 (0%)	3 / 3 (100%)	1 / 3 (33%)	0 / 2 (0%)	2 / 6 (33%)	1 / 2 (50%)	2 / 3 (67%)	2 / 3 (67%)	3 / 5 (60%)	
N2	0 / 1 (0%)	0 / 3 (0%)	0 / 3 (0%)	1 / 2 (50%)	0 / 6 (0%)	0 / 2 (0%)	1 / 3 (33%)	1 / 3 (33%)	0 / 5 (0%)	
N3	0 / 1 (0%)	0 / 3 (0%)	0 / 3 (0%)	0 / 2 (0%)	2 / 6 (33%)	0 / 2 (0%)	0 / 3 (0%)	0 / 3 (0%)	0 / 5 (0%)	
N3c	0 / 1 (0%)	0 / 3 (0%)	0 / 3 (0%)	0 / 2 (0%)	0 / 6 (0%)	0 / 2 (0%)	0 / 3 (0%)	0 / 3 (0%)	1 / 5 (20%)	
Unknown	0	0	0	1	0	0	0	0	1	
M										0.7
M0	1 / 1 (100%)	3 / 3 (100%)	3 / 3 (100%)	2 / 2 (100%)	6 / 6 (100%)	2 / 2 (100%)	3 / 3 (100%)	2 / 3 (67%)	3 / 4 (75%)	
M1	0 / 1 (0%)	0 / 3 (0%)	0 / 3 (0%)	0 / 2 (0%)	0 / 6 (0%)	0 / 2 (0%)	0 / 3 (0%)	1 / 3 (33%)	1 / 4 (25%)	

Unknown	0	0	0	1	0	0	0	0	2	
Immunohistochemical Subtype										**<0.001***
HER2	1 / 1 (100%)	0 / 3 (0%)	0 / 3 (0%)	0 / 3 (0%)	0 / 6 (0%)	2 / 2 (100%)	0 / 3 (0%)	0 / 3 (0%)	0 / 6 (0%)	
Luminal A	0 / 1 (0%)	3 / 3 (100%)	0 / 3 (0%)	0 / 3 (0%)	0 / 6 (0%)	0 / 2 (0%)	0 / 3 (0%)	0 / 3 (0%)	0 / 6 (0%)	
Luminal B	0 / 1 (0%)	0 / 3 (0%)	3 / 3 (100%)	0 / 3 (0%)	0 / 6 (0%)	0 / 2 (0%)	3 / 3 (100%)	0 / 3 (0%)	0 / 6 (0%)	
Luminal HER2	0 / 1 (0%)	0 / 3 (0%)	0 / 3 (0%)	3 / 3 (100%)	0 / 6 (0%)	0 / 2 (0%)	0 / 3 (0%)	3 / 3 (100%)	0 / 6 (0%)	
TNBC	0 / 1 (0%)	0 / 3 (0%)	0 / 3 (0%)	0 / 3 (0%)	6 / 6 (100%)	0 / 2 (0%)	0 / 3 (0%)	0 / 3 (0%)	6 / 6 (100%)	
International Classification of Diseases (ICD)										
C50 (Malignant neoplasm of breast)	1 / 1 (100%)	3 / 3 (100%)	3 / 3 (100%)	3 / 3 (100%)	6 / 6 (100%)	2 / 2 (100%)	3 / 3 (100%)	3 / 3 (100%)	6 / 6 (100%)	
Clinical Stage FOSP										0.3
I	1 / 1 (100%)	1 / 2 (50%)	0 / 1 (0%)	0 / 0 (NA%)	0 / 5 (0%)	0 / 1 (0%)	0 / 1 (0%)	0 / 2 (0%)	0 / 3 (0%)	
II	0 / 1 (0%)	1 / 2 (50%)	0 / 1 (0%)	0 / 0 (NA%)	2 / 5 (40%)	0 / 1 (0%)	0 / 1 (0%)	1 / 2 (50%)	2 / 3 (67%)	
III	0 / 1 (0%)	0 / 2 (0%)	1 / 1 (100%)	0 / 0 (NA%)	3 / 5 (60%)	1 / 1 (100%)	1 / 1 (100%)	0 / 2 (0%)	0 / 3 (0%)	
IV	0 / 1 (0%)	0 / 2 (0%)	0 / 1 (0%)	0 / 0 (NA%)	0 / 5 (0%)	0 / 1 (0%)	0 / 1 (0%)	1 / 2 (50%)	1 / 3 (33%)	
Unknown	0	1	2	3	1	1	2	1	3	
Clinical T stage										0.5
1C	1 / 1 (100%)	2 / 2 (100%)	0 / 1 (0%)	0 / 0 (NA%)	0 / 5 (0%)	0 / 1 (0%)	0 / 1 (0%)	0 / 2 (0%)	0 / 3 (0%)	
2	0 / 1 (0%)	0 / 2 (0%)	0 / 1 (0%)	0 / 0 (NA%)	2 / 5 (40%)	0 / 1 (0%)	0 / 1 (0%)	1 / 2 (50%)	2 / 3 (67%)	
3	0 / 1 (0%)	0 / 2 (0%)	1 / 1 (100%)	0 / 0 (NA%)	1 / 5 (20%)	1 / 1 (100%)	1 / 1 (100%)	0 / 2 (0%)	0 / 3 (0%)	
4B	0 / 1	0 / 2	0 / 1	0 / 0	1 / 5	0 / 1	0 / 1	0 / 2	0 / 3	

	(0%)	(0%)	(0%)	(NA%)	(20%)	(0%)	(0%)	(0%)	(0%)	
4D	0 / 1 (0%)	0 / 2 (0%)	0 / 1 (0%)	0 / 0 (NA%)	1 / 5 (20%)	0 / 1 (0%)	0 / 1 (0%)	1 / 2 (50%)	1 / 3 (33%)	
Unknown	0	1	2	3	1	1	2	1	3	
Clinical N stage										0.5
0	1 / 1 (100%)	0 / 2 (0%)	0 / 1 (0%)	0 / 0 (NA%)	2 / 5 (40%)	0 / 1 (0%)	0 / 1 (0%)	0 / 2 (0%)	0 / 3 (0%)	
1	0 / 1 (0%)	2 / 2 (100%)	1 / 1 (100%)	0 / 0 (NA%)	3 / 5 (60%)	0 / 1 (0%)	1 / 1 (100%)	1 / 2 (50%)	2 / 3 (67%)	
2	0 / 1 (0%)	0 / 2 (0%)	0 / 1 (0%)	0 / 0 (NA%)	0 / 5 (0%)	0 / 1 (0%)	0 / 1 (0%)	1 / 2 (50%)	0 / 3 (0%)	
2A	0 / 1 (0%)	0 / 2 (0%)	0 / 1 (0%)	0 / 0 (NA%)	0 / 5 (0%)	1 / 1 (100%)	0 / 1 (0%)	0 / 2 (0%)	0 / 3 (0%)	
3	0 / 1 (0%)	0 / 2 (0%)	0 / 1 (0%)	0 / 0 (NA%)	0 / 5 (0%)	0 / 1 (0%)	0 / 1 (0%)	0 / 2 (0%)	1 / 3 (33%)	
Unknown	0	1	2	3	1	1	2	1	3	
Clinical M stage	0 / 1 (0%)	0 / 2 (0%)	0 / 1 (0%)	0 / 0 (NA%)	0 / 5 (0%)	0 / 1 (0%)	0 / 1 (0%)	1 / 2 (50%)	1 / 3 (33%)	0.6
Unknown	0	1	2	3	1	1	2	1	3	
Tumor relapse										0.4
No	1 / 1 (100%)	3 / 3 (100%)	0 / 1 (0%)	2 / 2 (100%)	4 / 5 (80%)	2 / 2 (100%)	0 / 0 (NA%)	1 / 2 (50%)	1 / 3 (33%)	
Yes	0 / 1 (0%)	0 / 3 (0%)	1 / 1 (100%)	0 / 2 (0%)	1 / 5 (20%)	0 / 2 (0%)	0 / 0 (NA%)	1 / 2 (50%)	2 / 3 (67%)	
Unknown	0	0	2	1	1	0	3	1	3	
Treatment before blood collection										
No	1 / 1 (100%)	3 / 3 (100%)	3 / 3 (100%)	3 / 3 (100%)	6 / 6 (100%)	2 / 2 (100%)	3 / 3 (100%)	3 / 3 (100%)	6 / 6 (100%)	

[1] n / N (%); Mean (Minimum-Maximum)
[2] Kruskal-Wallis rank sum test; Fisher's exact test

IHC: Immunohistochemistry, FISH: Fluorescence In situ Hybridization, FOSP: Fundação Oncocentro de São Paulo, TNM Classification 8th edition.

Appendix 2. Patient Characteristics of the Cohort B

Characteristic	Elderly TNBC, N = 6[1]	Young Luminal A, N = 4[1]	Young Luminal B, N = 6[1]	Young Luminal HER2, N = 4[1]	Young TNBC, N = 4[1]	p-value[2]
Current Age	66 (62-70)	40 (33-46)	37 (29-41)	36 (30-40)	39 (35-43)	**0.019***
Age at admission to the biobank	60 (55-67)	32 (27-39)	32 (26-36)	32 (26-35)	35 (31-38)	**0.006***
Age at blood collection	61 (56-68)	33 (27-40)	33 (26-37)	31 (27-33)	36 (32-39)	**0.004***
Age at diagnosis	61 (56-68)	33 (27-40)	33 (26-37)	31 (27-33)	36 (32-39)	**0.004***
Sex						
Female	6 / 6 (100%)	4 / 4 (100%)	6 / 6 (100%)	4 / 4 (100%)	4 / 4 (100%)	
Self-reported race						0.2
Black	2 / 6 (33%)	4 / 4 (100%)	1 / 6 (17%)	0 / 4 (0%)	3 / 4 (75%)	
Other	3 / 6 (50%)	0 / 4 (0%)	2 / 6 (33%)	1 / 4 (25%)	0 / 4 (0%)	
Brown	0 / 6 (0%)	0 / 4 (0%)	1 / 6 (17%)	1 / 4 (25%)	0 / 4 (0%)	
Education level						**0.043***
Complete High-school	2 / 6 (33%)	3 / 4 (75%)	4 / 6 (67%)	4 / 4 (100%)	1 / 4 (25%)	
Complete Elementary School	1 / 6 (17%)	0 / 4 (0%)	0 / 6 (0%)	0 / 4 (0%)	0 / 4 (0%)	
Incomplete Elementary School	3 / 6 (50%)	0 / 4 (0%)	0 / 6 (0%)	0 / 4 (0%)	1 / 4 (25%)	
Complete University-level	0 / 6 (0%)	0 / 4 (0%)	0 / 6 (0%)	0 / 4 (0%)	2 / 4 (50%)	
Incomplete University-level	0 / 6 (0%)	1 / 4 (25%)	2 / 6 (33%)	0 / 4 (0%)	0 / 4 (0%)	

Body-Mass Index (BMI)	46 (25-64)	42 (23-75)	42 (22-80)	25 (19-34)	29 (26-34)	0.4
Nutritional status						0.7
Eutrophic/Normal	2 / 6 (33%)	1 / 4 (25%)	3 / 6 (50%)	3 / 4 (75%)	1 / 4 (25%)	
Obese	2 / 6 (33%)	0 / 4 (0%)	2 / 6 (33%)	1 / 4 (25%)	1 / 4 (25%)	
Overweight	2 / 6 (33%)	3 / 4 (75%)	1 / 6 (17%)	0 / 4 (0%)	2 / 4 (50%)	
Physical activity						0.7
Do not practice	5 / 6 (83%)	4 / 4 (100%)	3 / 6 (50%)	3 / 4 (75%)	3 / 4 (75%)	
Pratice Sporadically	1 / 6 (17%)	0 / 4 (0%)	0 / 6 (0%)	0 / 4 (0%)	0 / 4 (0%)	
Pratice regularly	0 / 6 (0%)	0 / 4 (0%)	1 / 6 (17%)	0 / 4 (0%)	0 / 4 (0%)	
Drugs use						
No	1 / 1 (100%)	3 / 3 (100%)	4 / 4 (100%)	4 / 4 (100%)	4 / 4 (100%)	
Unknown	5	1	2	0	0	
Smoking						0.5
Currently smoke	2 / 6 (33%)	1 / 4 (25%)	0 / 6 (0%)	0 / 4 (0%)	0 / 4 (0%)	
Smoked in the past	1 / 6 (17%)	1 / 4 (25%)	3 / 6 (50%)	1 / 4 (25%)	0 / 4 (0%)	
Never smoked	3 / 6 (50%)	2 / 4 (50%)	3 / 6 (50%)	3 / 4 (75%)	4 / 4 (100%)	
Alcohol use						0.9
Currently drunk	0 / 6 (0%)	0 / 4 (0%)	1 / 6 (17%)	0 / 4 (0%)	0 / 4 (0%)	
Drank in the past	1 / 6 (17%)	0 / 4 (0%)	2 / 6 (33%)	1 / 4 (25%)	1 / 4 (25%)	
Never drank	5 / 6 (83%)	4 / 4 (100%)	3 / 6 (50%)	3 / 4 (75%)	3 / 4 (75%)	
Other comorbidity	0 / 0	0 / 0	0 / 0	0 / 0	0 / 0	

	(NA%)	(NA%)	(NA%)	(NA%)	(NA%)	
Unknown	6	4	6	4	4	
Familiy history of cancer						0.9
No	2 / 6 (33%)	1 / 4 (25%)	1 / 6 (17%)	2 / 4 (50%)	2 / 4 (50%)	
Yes	4 / 6 (67%)	3 / 4 (75%)	5 / 6 (83%)	2 / 4 (50%)	2 / 4 (50%)	
Family history of cancer (first degree of kinship)						0.3
Yes	4 / 6 (67%)	1 / 4 (25%)	1 / 6 (17%)	0 / 4 (0%)	1 / 4 (25%)	
No	2 / 6 (33%)	3 / 4 (75%)	5 / 6 (83%)	4 / 4 (100%)	3 / 4 (75%)	
Family history of breast or ovarian cancer (first degree of kinship)	1 / 6 (17%)	1 / 4 (25%)	1 / 6 (17%)	0 / 4 (0%)	0 / 4 (0%)	
Previous breast-related surgeries						0.3
No	6 / 6 (100%)	4 / 4 (100%)	5 / 6 (83%)	2 / 4 (50%)	3 / 4 (75%)	
Yes	0 / 6 (0%)	0 / 4 (0%)	1 / 6 (17%)	2 / 4 (50%)	1 / 4 (25%)	
Diabetes Mellitus						0.2
No	4 / 6 (67%)	4 / 4 (100%)	6 / 6 (100%)	4 / 4 (100%)	4 / 4 (100%)	
Yes	2 / 6 (33%)	0 / 4 (0%)	0 / 6 (0%)	0 / 4 (0%)	0 / 4 (0%)	
High Blood Pressure (HBP)						0.081
No	3 / 6 (50%)	4 / 4 (100%)	6 / 6 (100%)	3 / 4 (75%)	4 / 4 (100%)	
Yes	3 / 6 (50%)	0 / 4 (0%)	0 / 6 (0%)	1 / 4 (25%)	0 / 4 (0%)	
Chronic Obstructive Pulmonary Disease (COPD)						0.9
No	5 / 6 (83%)	4 / 4 (100%)	6 / 6 (100%)	4 / 4 (100%)	3 / 4 (75%)	
Yes	1 / 6 (17%)	0 / 4 (0%)	0 / 6 (0%)	0 / 4 (0%)	1 / 4 (25%)	
Chronic Gastritis						>0.9

No	5 / 6 (83%)	4 / 4 (100%)	6 / 6 (100%)	4 / 4 (100%)	4 / 4 (100%)	
Yes	1 / 6 (17%)	0 / 4 (0%)	0 / 6 (0%)	0 / 4 (0%)	0 / 4 (0%)	
Tubular Differentiation						0.4
2	1 / 6 (17%)	2 / 4 (50%)	1 / 6 (17%)	0 / 4 (0%)	0 / 4 (0%)	
3	5 / 6 (83%)	2 / 4 (50%)	5 / 6 (83%)	4 / 4 (100%)	4 / 4 (100%)	
Nuclear Grade						>0.9
2	1 / 6 (17%)	1 / 4 (25%)	2 / 6 (33%)	1 / 4 (25%)	0 / 4 (0%)	
3	5 / 6 (83%)	3 / 4 (75%)	4 / 6 (67%)	3 / 4 (75%)	4 / 4 (100%)	
Mitotic Index						0.8
1	3 / 6 (50%)	4 / 4 (100%)	5 / 6 (83%)	2 / 4 (50%)	2 / 4 (50%)	
2	1 / 6 (17%)	0 / 4 (0%)	0 / 6 (0%)	1 / 4 (25%)	1 / 4 (25%)	
3	2 / 6 (33%)	0 / 4 (0%)	1 / 6 (17%)	1 / 4 (25%)	1 / 4 (25%)	
Histologic Grade						0.5
1	0 / 6 (0%)	0 / 4 (0%)	1 / 6 (17%)	0 / 4 (0%)	0 / 4 (0%)	
2	3 / 6 (50%)	4 / 4 (100%)	4 / 6 (67%)	2 / 4 (50%)	2 / 4 (50%)	
3	3 / 6 (50%)	0 / 4 (0%)	1 / 6 (17%)	2 / 4 (50%)	2 / 4 (50%)	
Estrogen Receptor						**<0.001***
Negative	6 / 6 (100%)	0 / 4 (0%)	0 / 6 (0%)	0 / 4 (0%)	4 / 4 (100%)	
Positive	0 / 6 (0%)	4 / 4 (100%)	6 / 6 (100%)	4 / 4 (100%)	0 / 4 (0%)	
Progesterone Receptor						**<0.001**
Negative	6 / 6	0 / 4	1 / 6	1 / 4	4 / 4	

	(100%)	(0%)	(17%)	(25%)	(100%)	
Positive	0 / 6 (0%)	4 / 4 (100%)	5 / 6 (83%)	3 / 4 (75%)	0 / 4 (0%)	
HER2 (IHC)						
0 (negative)	5 / 5 (100%)	4 / 4 (100%)	4 / 4 (100%)	0 / 0 (NA%)	4 / 4 (100%)	
Unknown	1	0	2	4	0	
HER2 (FISH)						**0.002***
Amplified	0 / 6 (0%)	0 / 4 (0%)	0 / 6 (0%)	4 / 4 (100%)	0 / 4 (0%)	
Suspicious	0 / 6 (0%)	0 / 4 (0%)	1 / 6 (17%)	0 / 4 (0%)	0 / 4 (0%)	
Not evaluated	3 / 6 (50%)	4 / 4 (100%)	4 / 6 (67%)	0 / 4 (0%)	3 / 4 (75%)	
Not amplified	3 / 6 (50%)	0 / 4 (0%)	1 / 6 (17%)	0 / 4 (0%)	1 / 4 (25%)	
Ki67	38 (25-60)	10 (5-13)	50 (30-90)	50 (30-70)	91 (80-100)	**0.003***
T						0.3
T1	2 / 5 (40%)	0 / 3 (0%)	2 / 6 (33%)	1 / 4 (25%)	0 / 4 (0%)	
T2	2 / 5 (40%)	3 / 3 (100%)	0 / 6 (0%)	1 / 4 (25%)	2 / 4 (50%)	
T3	1 / 5 (20%)	0 / 3 (0%)	3 / 6 (50%)	1 / 4 (25%)	2 / 4 (50%)	
T4	0 / 5 (0%)	0 / 3 (0%)	1 / 6 (17%)	0 / 4 (0%)	0 / 4 (0%)	
Tis	0 / 5 (0%)	0 / 3 (0%)	0 / 6 (0%)	1 / 4 (25%)	0 / 4 (0%)	
Unknown	1	1	0	0	0	
N						0.6
N0	2 / 5 (40%)	2 / 3 (67%)	2 / 6 (33%)	3 / 4 (75%)	2 / 4 (50%)	
N1	2 / 5 (40%)	0 / 3 (0%)	1 / 6 (17%)	1 / 4 (25%)	2 / 4 (50%)	

N2	1 / 5 (20%)	0 / 3 (0%)	3 / 6 (50%)	0 / 4 (0%)	0 / 4 (0%)	
N3	0 / 5 (0%)	1 / 3 (33%)	0 / 6 (0%)	0 / 4 (0%)	0 / 4 (0%)	
Unknown	1	1	0	0	0	
M						0.2
M0	5 / 5 (100%)	2 / 3 (67%)	6 / 6 (100%)	3 / 4 (75%)	4 / 4 (100%)	
M1	0 / 5 (0%)	1 / 3 (33%)	0 / 6 (0%)	1 / 4 (25%)	0 / 4 (0%)	
Unknown	1	1	0	0	0	
Immunohistochemical Subtype						**<0.001***
Luminal A	0 / 6 (0%)	4 / 4 (100%)	0 / 6 (0%)	0 / 4 (0%)	0 / 4 (0%)	
Luminal B	0 / 6 (0%)	0 / 4 (0%)	6 / 6 (100%)	0 / 4 (0%)	0 / 4 (0%)	
Luminal HER2	0 / 6 (0%)	0 / 4 (0%)	0 / 6 (0%)	4 / 4 (100%)	0 / 4 (0%)	
TNBC	6 / 6 (100%)	0 / 4 (0%)	0 / 6 (0%)	0 / 4 (0%)	4 / 4 (100%)	
International Classification of Diseases (ICD)						
C50 (Malignant neoplasm of breast)	6 / 6 (100%)	4 / 4 (100%)	6 / 6 (100%)	4 / 4 (100%)	4 / 4 (100%)	
Clinical Stage FOSP						0.3
I	3 / 6 (50%)	0 / 4 (0%)	1 / 6 (17%)	0 / 4 (0%)	1 / 4 (25%)	
II	1 / 6 (17%)	3 / 4 (75%)	1 / 6 (17%)	2 / 4 (50%)	1 / 4 (25%)	
III	2 / 6 (33%)	0 / 4 (0%)	4 / 6 (67%)	1 / 4 (25%)	2 / 4 (50%)	
IV	0 / 6 (0%)	1 / 4 (25%)	0 / 6 (0%)	1 / 4 (25%)	0 / 4 (0%)	
Clinical T stage						0.069
1A	1 / 6	0 / 4	0 / 6	0 / 4	0 / 4	

	(17%)	(0%)	(0%)	(0%)	(0%)	
1B	0 / 6 (0%)	0 / 4 (0%)	1 / 6 (17%)	0 / 4 (0%)	0 / 4 (0%)	
1C	2 / 6 (33%)	0 / 4 (0%)	1 / 6 (17%)	0 / 4 (0%)	0 / 4 (0%)	
2	2 / 6 (33%)	4 / 4 (100%)	0 / 6 (0%)	3 / 4 (75%)	1 / 4 (25%)	
3	1 / 6 (17%)	0 / 4 (0%)	3 / 6 (50%)	0 / 4 (0%)	2 / 4 (50%)	
4B	0 / 6 (0%)	0 / 4 (0%)	1 / 6 (17%)	1 / 4 (25%)	0 / 4 (0%)	
4D	0 / 6 (0%)	0 / 4 (0%)	0 / 6 (0%)	0 / 4 (0%)	1 / 4 (25%)	
Clinical N stage						0.5
0	3 / 6 (50%)	2 / 4 (50%)	1 / 6 (17%)	1 / 4 (25%)	2 / 4 (50%)	
1	2 / 6 (33%)	1 / 4 (25%)	2 / 6 (33%)	3 / 4 (75%)	1 / 4 (25%)	
2	0 / 6 (0%)	0 / 4 (0%)	3 / 6 (50%)	0 / 4 (0%)	0 / 4 (0%)	
2A	1 / 6 (17%)	0 / 4 (0%)	0 / 6 (0%)	0 / 4 (0%)	1 / 4 (25%)	
3A	0 / 6 (0%)	1 / 4 (25%)	0 / 6 (0%)	0 / 4 (0%)	0 / 4 (0%)	
Clinical M stage	0 / 6 (0%)	1 / 4 (25%)	0 / 6 (0%)	1 / 4 (25%)	0 / 4 (0%)	0.3
Tumor relapse						>0.9
No	5 / 6 (83%)	3 / 4 (75%)	5 / 6 (83%)	3 / 4 (75%)	4 / 4 (100%)	
Yes	1 / 6 (17%)	1 / 4 (25%)	1 / 6 (17%)	1 / 4 (25%)	0 / 4 (0%)	
Treatment before blood collection						0.7
Yes	2 / 4 (50%)	0 / 3 (0%)	3 / 6 (50%)	2 / 4 (50%)	1 / 4 (25%)	
No	2 / 4	3 / 3	3 / 6	2 / 4	3 / 4	

	(50%)	(100%)	(50%)	(50%)	(75%)
Unknown	2	1	0	0	0

[1] n / N (%); Mean (Minimum-Maximum)
[2] Kruskal-Wallis rank sum test; Fisher's exact test

IHC: Immunohistochemistry, FISH: Fluorescence In situ Hybridization, FOSP: Fundação Oncocentro de São Paulo, TNM Classification 8th edition.

Appendix 3. Gene Expression Omnibus accession GSE240872 with data of cf-miRNA from Brazilian breast cancer patients (n=12, pooling strategy)

NCBI

Gene Expression Omnibus

HOME | SEARCH | SITE MAP | GEO Publications | FAQ | MIAME | Email GEO

NCBI > GEO > **Accession Display**

Not logged in | Login

Scope: Self Format: HTML Amount: Quick GEO accession: GSE240872 GO

Series GSE240872 Query DataSets for GSE240872

Status	Public on Sep 25, 2023
Title	Expression of cell-free miRNAs from plasma of Brazilian breast cancer patients
Organism	Homo sapiens
Experiment type	Non-coding RNA profiling by array
Summary	in this study, we aimed to determine the cell-free miRNA (cf-miRNA) profile between five cohorts of BC patients according to main molecular subtypes. These samples were classified according to their age at diagnosis in two groups: Young (diagnosed before 40 years old) and Elderly (diagnosed after 40 years old). We isolated total miRNA from the plasma of these patients and then assessed their miRNA levels using a high-throughput and high-resolution technique based on digital barcode hybridization.
Overall design	We collected plasma samples of breast cancer patients diagnosed at Hospital das Clinicas, Medicine School (Universidade de São Paulo). Using 200 uL of this plasma, we isolated cell-free miRNA (cf-miRNA) following the instructions of the miRNeasy Serum/plasma kit (cat. 217184, Qiagen). Then, we quantified the cf-miRNA by spectrophotometry and used 40 or 120 µL of each sample were concentrated up to 4 µL using the Eppendorf® 5301 concentrator for 20 or 35 minutes at 45 °C following the manufacturer's recommendations. After concentration, 0.5 µL of each sample was loaded into the NanoDrop™ 8000 Spectrophotometer (ThermoFisher) to verify the miRNA mass. Then, ~25 ng of cf-miRNA were hybridized for 16.5 hours with molecular barcoding for 827 experimentally validated human miRNAs (from miRBase v21) using the nCounter Master Mix (NanoString® Technologies, cat. NAA-AKIT-012). Subsequently, miRNAv3 NanoString® cartridges (NanoString® Technologies, cat. CSO-MIR3-12) were loaded with the mix per sample, sealed, and transferred to an nCounter® Digital Analyzer device (NanoString® Technologies) for data collection. miRNA expression data were analyzed in the nSolver™ Data Analysis v.4.0 software (NanoString® Tech.) with the default protocol by the manufacturer. For cf-miRNA, we normalize the expression of human miRNAs by the geometric mean of all negative (negative normalization) and positive (positive normalization) probes. Then, we used the top 15 more stable regions (up to 15% of the coefficient of variation) to normalize the content set data. Data were exported in comma-separated value (*.csv) format for further analysis.
Contributor(s)	Carrasco AG, Andrade LN, Chammas R

Appendix 4. Gene Expression Omnibus accession GSE241784 with data of vesicular miRNA from Brazilian breast cancer patients (n=12, pooling strategy)

NCBI

Gene Expression Omnibus

HOME | SEARCH | SITE MAP | GEO Publications | FAQ | MIAME | Email GEO

NCBI > GEO > **Accession Display**

Not logged in | Login

Scope: Self Format: HTML Amount: Quick GEO accession: GSE241784 GO

Series GSE241784 Query DataSets for GSE241784

Status	Public on Sep 25, 2023
Title	Expression of vesicular miRNAs from plasma of Brazilian breast cancer patients
Organism	Homo sapiens
Experiment type	Non-coding RNA profiling by array
Summary	in this study, we aimed to determine the vesicular miRNA profile between five cohorts of BC patients according to main molecular subtypes. These samples were classified according to their age at diagnosis in two groups: Young (diagnosed before 40 years old) and Elderly (diagnosed after 40 years old). We isolated vesicular miRNA from the plasma of these patients and then assessed their miRNA levels using a high-throughput and high-resolution technique based on digital barcode hybridization.
Overall design	We collected plasma samples of breast cancer patients diagnosed at Hospital das Clinicas, Medicine School (Universidade de São Paulo). Using 200 uL of this plasma, we isolated extracellular vesicles (EVs) using the qEV original size-exclusion chromatography (SEC) columns. Then, we treated EVs with proteinase K and RNAse before isolating vesicular miRNA by following the instructions of the miRNeasy Serum/plasma kit (cat. 217184, Qiagen). Next, we quantified the vesicular miRNA by spectrophotometry and used 40 or 120 µL of each sample to concentrate up to 4 µL using the Eppendorf® 5301 concentrator for 20 or 35 minutes at 45 °C following the manufacturer's recommendations. After concentration, 0.5 µL of each sample was loaded into the NanoDrop™ 8000 Spectrophotometer (ThermoFisher) to verify the miRNA mass. Then, ~65 ng of vesicular miRNA were hybridized for 16.5 hours with molecular barcoding for 827 experimentally validated human miRNAs (from miRBase v21) using the nCounter Master Mix (NanoString® Technologies, cat. NAA-AKIT-012). Subsequently, miRNAv3 NanoString® cartridges (NanoString® Technologies, cat. CSO-MIR3-12) were loaded with the mix per sample, sealed, and transferred to a nCounter® Digital Analyzer device (NanoString® Technologies) for data collection. miRNA expression data were analyzed in the nSolver™ Data Analysis v.4.0 software (NanoString® Tech.) with the default protocol by the manufacturer. For vesicular miRNA, we normalize the expression of human miRNAs by the geometric mean of all negative (negative normalization) and positive (positive normalization) probes. Then, we used the top 15 more stable regions to normalize the content set data. Data were exported in comma-separated value (*.csv) format for further analysis.
Contributor(s)	Murillo Carrasco AG, Andrade LS, Chammas R

Appendix 5. Gene Expression Omnibus accession GSE241785 with data of vesicular miRNA from Brazilian breast cancer patients (n=24, individual samples)

NCBI

Gene Expression Omnibus

HOME | SEARCH | SITE MAP | GEO Publications | FAQ | MIAME | Email GEO

NCBI > GEO > **Accession Display** Not logged in | Login

GEO help: Mouse over screen elements for information.

Scope: Self Format: HTML Amount: Quick GEO accession: GSE241785 GO

Series GSE241785 Query DataSets for GSE241785

Status	Public on Sep 25, 2023
Title	Expression of vesicular miRNAs from plasma of Brazilian breast cancer patients diagnosed before 40 years old
Organism	Homo sapiens
Experiment type	Non-coding RNA profiling by array
Summary	in this study, we aimed to determine the vesicular miRNA profile between four cohorts of BC patients according to main molecular subtypes. These samples were classified according to their age at diagnosis in two groups: Young (diagnosed before 40 years old) and Elderly (diagnosed after 40 years old). We isolated vesicular miRNA from the plasma of these patients and then assessed their miRNA levels using a high-throughput and high-resolution technique based on digital barcode hybridization.
Overall design	We collected plasma samples of breast cancer patients diagnosed at Hospital das Clinicas, Medicine School (Universidade de São Paulo). Using 1mL of this plasma, we isolated extracellular vesicles (EVs) using the qEV original size-exclusion chromatography (SEC) columns. Then, we treated EVs with proteinase K and RNAse before isolating vesicular miRNA by following the instructions of the miRNeasy Serum/plasma kit (cat. 217184, Qiagen). Next, we quantified the vesicular miRNA by spectrophotometry and used 20 µL of each sample were concentrated up to 4 µL using the Eppendorf® 5301 concentrator for 20 minutes at 45 °C following the manufacturer's recommendations. After concentration, 0.5 µL of each sample was loaded into the NanoDrop™ 8000 Spectrophotometer (ThermoFisher) to verify the miRNA mass. Then, all vesicular miRNA were hybridized for 16.5 hours with molecular barcoding for 827 experimentally validated human miRNAs (from miRBase v21) using the nCounter Master Mix (NanoString® Technologies, cat. NAA-AKIT-012). Subsequently, miRNAv3 NanoString® cartridges (NanoString® Technologies, cat. CSO-MIR3-12) were loaded with the mix per sample, sealed, and transferred to an nCounter® Digital Analyzer device (NanoString® Technologies) for data collection. miRNA expression data were analyzed in the nSolver™ Data Analysis v.4.0 software (NanoString® Tech.) with the default protocol by the manufacturer. For vesicular miRNA, we normalize the expression of human miRNAs by the geometric mean of all negative (negative normalization) and positive (positive normalization) probes. Then, we used the top 15 more stable regions to normalize the content set data. Data were exported in comma-separated value (*.csv) format for further analysis.
Contributor(s)	Murillo Carrasco AG, Andrade LS, Chammas R

Appendix 6. Checklist of the ESMO Guidance for Reporting Oncology real-World evidence (GROW).

ESMO-GROW Checklist for Authors and Reviewers

This checklist integrates all ESMO-GROW recommendation and could be used by authors and reviewers when assessing the reporting standards of a real-world evidence study in Oncology.

For the the ESMO-GROW checklist, the following criteria are considered:
"Yes, fully reported" – The recommendation is adequately considered.
"Yes, partially reported" – The recommendation is considered, but some important details are missing.
"Not reported" – The recommendation is applicable for the case, but it was not considered.
"Not applicable" – The recommendation is not applicable for this study.

Name of Author/Reviewer: **Date:** **Title of Manuscript or Identifier:** **Recommendations**	Yes, fully reported	Yes, partially reported	Not reported	Not applicable
1. Title				
1.1: Concisely include relevant key terms referring to the study type, study population, objectives, data sources and outcomes, depending on the study. Consider including the terms 'real-world' or 'observational'	◉	○	○	○
2. Introduction				
2.1: Explain the scientific rationale for the research question(s), providing concise background information on previous core evidence from systematic reviews, meta-analyses, clinical trials and/or real-world evidence studies	◉	○	○	○
2.2: Identify the gaps in evidence and explain why and how they can be suitably addressed by real-world evidence research. Specify the new evidence that is expected from the current study	◉	○	○	○
2.3: Briefly introduce the aim(s) of the study	◉	○	○	○
3. Methods				
Study objective(s), design, data sources and variables				
3.1: Provide the study research question(s) including a description of the patients or the object under study and the target outcome(s)	◉	○	○	○
3.2: Provide the study objective(s) and consider classifying the type of research as descriptive and/or analytical (explanatory or predictive)	◉	○	○	○
3.3: Provide relevant information to describe and classify the study design used to address the research question	◉	○	○	○
3.4: Give a clear definition of the eligibility criteria used to select the patients or objects under study, particularly regarding cancer-related aspects	◉	○	○	○
3.5: Report the specific type and purpose of real-world data source(s) used, providing a detailed description and the reason(s) why the source was considered appropriate for the study objectives	◉	○	○	○
3.6: When multiple real-world data sources are used, provide details on interoperability, including identification of duplicated cases or data linkage from separate databases	○	○	○	◉
3.7: Provide details and timings of source and study data management. Consider specifying methods of raw data collection, updates and completeness, data extraction, cleaning and/or quality controls and validation	◉	○	○	○
3.8: Provide core details on database and/or study registration, governance, ownership, metadata and full data accessibility in the main text or supplementary material	◉	○	○	○
3.9: Identify the data source of each core variable, its definition, if the variable was derived or coded, and describe how the derivation or coding was conducted and validated.	◉	○	○	○
3.10: Specify the time points of core variables in relation to the cancer disease trajectory	◉	○	○	○
3.11: Provide a complete list of core variables included in the study. Variables can be grouped as baseline characteristics, exposure and outcomes or endpoints	◉	○	○	○
3.12: For biomarker-related studies, provide details on biomarker description, timing, and methods of assessment and analytical validation	◉	○	○	○
Statistical analysis and artificial intelligence methods				
3.13: Summarise the main aspects of the statistical analysis	◉	○	○	○
3.14: When applicable, provide details on the pre-planned sample size requirements and power of the study	○	○	○	◉
3.15: Specify the pre-planned strategies to identify and mitigate the main sources of bias	◉	○	○	○
3.16: Clearly distinguish prespecified from *post hoc* analyses, especially for subgroup analyses	○	○	○	◉
3.17: Provide information on internal and external validity, as well as any sensitivity analyses	○	○	○	◉
3.18: For analytical studies, the full version of the statistical analysis plan should be provided in the supplementary material, including a brief explanation of any amendments	◉	○	○	○
3.19: When applicable, specify which machine learning, deep learning or alternative artificial intelligence method has been used	○	○	○	◉
3.20: When reporting real-world data analysis with artificial intelligence (e.g. machine learning and deep learning) algorithms, include comprehensive aspects on data pre-processing techniques, feature engineering strategies and model development	○	○	○	◉
3.21: Address the artificial intelligence model explainability and interpretability, and present the plan for integration into clinical practice, if applicable	○	○	○	◉
3.22: When applicable, briefly describe the multidisciplinary team required for the study and explain how these needs were met	◉	○	○	○

ESMO GOOD SCIENCE BETTER MEDICINE BEST PRACTICE

ESMO Guidance for Reporting Oncology real-World evidence (GROW)

ESMO-GROW Checklist for Authors and Reviewers

Recommendations	Yes, fully reported	Yes, partially reported	Not reported	Not applicable
4. Results				
4.1: Provide number of cases excluded or nonparticipating and reasons at each stage of sample selection, as well as numbers lost to follow-up. Compare the cases excluded with those included in the analyses. Illustrate this with a flowchart	○	○	○	◉
4.2: Describe the baseline characteristics of the cases included (e.g. clinico-demographic and tumour characteristics). The baseline characteristics of different groups under analysis should be compared, if applicable	◉	○	○	○
4.3: Report the results of the primary analysis of study outcomes. Briefly describe the results of exploratory analyses if relevant (prespecified and/or *post hoc*). Provide details of how readers can access the full results	◉	○	○	○
5. Discussion and conclusions				
Discussion				
5.1: Summarise the core results that address the primary research question(s) and objectively discuss the data in relation to the best available evidence on the topic. Avoid a convenient selection of literature to support a point	◉	○	○	○
5.2: Discuss the strengths and limitations of the current study, including the main biases, how the strategies applied contributed to bias avoidance or mitigation, and, if applicable, in which direction the authors estimate that residual bias may influence the core results of the study	◉	○	○	○
5.3: Discuss the generalisability of the study results and their potential implications for clinical practice, health policies or public health and for the generation of hypotheses for future research	◉	○	○	○
Conclusions				
5.4: Provide a balanced summary of core results relating to the primary research question and the main implications for clinical practice, health policies and/or public health. Suggest further research considering the remaining unmet needs and limitations from the reported study	◉	○	○	○
6. Final considerations				
6.1: Specify all relevant study sponsorship(s) as well as direct and/or indirect or in-kind funding	◉	○	○	○
6.2: Specify all relevant acknowledgements, author disclosures, individual contributions and other final considerations as per journal regulations	◉	○	○	○

Notes:

To access full manuscripts and for citations, please consider the following references and links:

- Castelo-Branco L et al. "ESMO Guidance for Reporting Oncology real-World evidence (GROW)". Ann Oncol 2023; 34: 10.1016/j.annonc.2023.10.001
- Castelo-Branco L et al. "ESMO Guidance for Reporting Oncology real-World evidence (GROW)". ESMO Real World Data & Digital Oncol 2023; 1: 10.1016/j.esmorw.2023.10.001

ESMO GOOD SCIENCE BETTER MEDICINE BEST PRACTICE

Appendix 7. Standardized Reporting Tool for Blood EV Research (MIBlood-EV).

INTERNATIONAL SOCIETY for EXTRACELLULAR VESICLES

MIBlood-EV

Standardized Reporting Tool for Blood EV Research (Human)

STUDY INFORMATION

1.0 **Manuscript title**	Breast cancer-related heterogeneity reflected on circulating and vesicular miRNAs: high-throughput results and proof-of-concept for selecting tumor-derived extracellular vesicles				
1.1 **Corresponding author (Name and Email)**	Alexis Murillo (agmurilloc@gmail.com)				
1.2 **Institution name**	Instituto do Câncer do Estado de São Paulo (ICESP)				
1.3 **Time period of experiment (years)**	5	1.4 **Number of samples**	54		
1.5 **Cargo of interest**	✔ Vesicles	☐ Protein	✔ RNA	☐ DNA	☐ Other:
1.6 **Biospecimen type**	✔ Plasma	☐ Serum	1.7 **Biospecimen state**	Frozen	
1.8 **Source of frozen specimens**	Obtained from biobank	1.9 **Years of collection (range)**	4		

BLOOD COLLECTION AND PROCESSING

2.0 **Patient fasting status**	Uncertain	2.1 **Fasting length (e.g. hours/days)**			
2.2 **Anatomical access site**		2.3 **Needle diameter (e.g. gauge)**			
2.4 **Blood volume collected (mL)**	18				
2.5 **Plasma anticoagulant**	✔ EDTA	☐ Citrate	☐ Heparin	☐ Other:	
2.6 **Serum tube type**		2.7 **Serum clotting time (minutes)**			
2.8 **Time between collection and first centrifugation (range in hours)**	0.5-1.7				
2.9 **Transport temperature**	4°C	2.10 **Transport condition of tubes**	Vertical		
2.11 **Centrifuge brand and model**	Thermo Scientific™ Sorvall™ Legend™ XT/XF				
2.12 **Bucket rotor type**	Fixed	2.13 **Number of centrifugation cycles**	Two		
2.14 **1st Centrifugation speed (RCF in x g)**	800	2.15 **1st Rotor brake**	Slow		
2.16 **1st Centrifugation temperature**	4°C	2.17 **2nd Centrifugation speed (RCF in x g)**	11 000		
2.18 **2nd Rotor brake**	Slow	2.19 **2nd Centrifugation temperature**	4°C		
2.20 **Additional processing steps (e.g. filtration)**	NA				
2.21 **Storage tubes (brand, type, source, catalog number)**	Cryovials Corning				
2.22 **Storage temperature**	-80°C	2.23 **Length of storage (range in years)**	0.5-3		

PLASMA/SERUM QUALITY CONTROL

3.0 **Number of freeze-thaw cycles (range)**	1-2		
3.1 **Thawing temperature**	on ice	3.2 **Thawing duration (minutes)**	30

Hemolysis

3.3 **Presence of hemolysis**	Not tested	3.4 **Number of samples affected (e.g. <25%, 25-50%)**	NA	
3.5 **Method used**		3.6 **RBC count (Median, 95% CI, N)**	NA	
3.7 **RBC counter brand and type**	NA			
3.8 **Spectrophotometry hemoglobin concentration (g/L)**	NA			
3.9 **Spectrophotometer brand, model and wavelength measured (e.g. 414 nm)**	NA			
3.10 **Hemolized samples were discarded**	No			

INTERNATIONAL SOCIETY for EXTRACELLULAR VESICLES

Platelets

3.11 **Presence of platelets**	Not Tested	3.12 **Method used (e.g. Flow Cytometry)**	
3.13 **Marker(s) used (e.g. CD61, CD41)**	NA		
3.14 **Concentration (median, 95% CI, N)**	NA		
3.15 **Platelet counter instrument brand and type**	NA		
3.16 **Flow cytometer brand and type**	NA		
3.17 **Flow cytometry size and fluorescence ranges of detection in nanometers and MESF, respectively**	NA		

Lipoproteins

3.18 **Presence of lipoproteins**	No	3.19 **Method used (WB, ELISA, FC)**	Western-blot
3.20 **Spectrophotometry L-index**	Not Determined		
3.21 **Spectrophotometer brand, model and wavelength measured (e.g. 700 nm)**			
3.22 **WB Marker(s) used (e.g. Apo B)**	Apo AI		
3.23 **Western blot images provided in manuscript?**	Yes		
3.24 **Flow cytometry marker(s) used (e.g. ApoB)**	NA		
3.25 **Flow cytometry concentration (median, 95% CI, N)**	NA		
3.26 **Flow cytometer brand and type**	NA		
3.27 **Flow cytometry size and fluorescence ranges of detection in nanometers and MESF, respectively**	NA		

ATTACHMENTS

Attachment 1. Ethical approval for performing this study (last version: 11, October 2022)

USP - HOSPITAL DAS CLÍNICAS DA FACULDADE DE MEDICINA DA UNIVERSIDADE DE SÃO PAULO - HCFMUSP

PARECER CONSUBSTANCIADO DO CEP

DADOS DA EMENDA

Título da Pesquisa: Retratos da Mama
Pesquisador: Roger Chammas
Área Temática:
Versão: 11
CAAE: 99542818.0.0000.0065
Instituição Proponente: FUNDACAO FACULDADE DE MEDICINA
Patrocinador Principal: Ministério da Saúde

DADOS DO PARECER

Número do Parecer: 5.688.046

Apresentação do Projeto:
Novas Emendas foram submtidas

Objetivo da Pesquisa:
Referem-se à exclusão e inclusão de colaboradores no projeto

Avaliação dos Riscos e Benefícios:
Sem alterações

Comentários e Considerações sobre a Pesquisa:
As modificações propostas são pertinentes e se justificam

Considerações sobre os Termos de apresentação obrigatória:
O TCLE dos delegados que responderão ao questionário foi atualizado

Recomendações:
Não há

Conclusões ou Pendências e Lista de Inadequações:
Não há pendências

Considerações Finais a critério do CEP:

Endereço: Rua Ovídio Pires de Campos, 225 5º andar
Bairro: Cerqueira Cesar **CEP:** 05.403-010
UF: SP **Município:** SAO PAULO
Telefone: (11)2661-7585 **Fax:** (11)2661-7585 **E-mail:** cappesq.adm@hc.fm.usp.br

Continuação do Parecer: 5.688.046

Este parecer foi elaborado baseado nos documentos abaixo relacionados:

Tipo Documento	Arquivo	Postagem	Autor	Situação
Informações Básicas do Projeto	PB_INFORMAÇÕES_BÁSICAS_2025998_E9.pdf	28/09/2022 18:25:18		Aceito
Outros	Delegados_TCLEs_Questionarios_Pronon_Retratos_da_mama_atualizado_27092022.pdf	28/09/2022 18:21:41	Miyuki Uno	Aceito
Outros	Delegados_TCLEs_Questionarios_Pronon_Retratos_da_mama_atualizado_27092022.docx	28/09/2022 18:21:14	Miyuki Uno	Aceito
Outros	EMENDA_INCLUSAO_ANA_STINA_EXCLUSAO_COLABORADORES280920222.pdf	28/09/2022 18:20:32	Miyuki Uno	Aceito
Outros	EMENDA_INCLUSAO_ANA_STINA_EXCLUSAO_COLABORADORES280920222.doc	28/09/2022 18:19:57	Miyuki Uno	Aceito
Outros	EMENDA_INCLUSAOCOLABORADORES.pdf	22/07/2022 18:30:56	Miyuki Uno	Aceito
Outros	EMENDA_NOVO_COLABORADOR.pdf	23/05/2022 19:06:31	Miyuki Uno	Aceito
Projeto Detalhado / Brochura Investigador	Proj_Retratos_da_Mama_adendo5.doc	11/12/2020 19:32:37	Miyuki Uno	Aceito
Projeto Detalhado / Brochura Investigador	Proj_Retratos_da_Mama_adendo5.pdf	11/12/2020 19:31:19	Miyuki Uno	Aceito
Outros	FORMULARIO_ENCAMINHAMENTO_EMENDAS.pdf	11/12/2020 19:30:31	Miyuki Uno	Aceito
TCLE / Termos de Assentimento / Justificativa de Ausência	TCLE_Retratos_Mama_adendo6_com_destaque.pdf	30/11/2020 15:36:09	Miyuki Uno	Aceito
Outros	Memorando_Adendo6.pdf	30/11/2020 15:32:22	Miyuki Uno	Aceito
Outros	FORMULARIO_SUBMISSAO_EMENDAS.pdf	24/06/2020 12:42:31	Miyuki Uno	Aceito
Outros	Proj_Retratos_da_Mama_adendo5_destaque.pdf	19/05/2020 17:39:26	Miyuki Uno	Aceito
Outros	Memorando_Desvio.pdf	19/05/2020 17:38:40	Miyuki Uno	Aceito
Outros	Memorando_Adendo5.pdf	19/05/2020 17:38:07	Miyuki Uno	Aceito
Outros	memorando_adendo4.pdf	21/11/2019 11:26:39	Lara Zimmermann	Aceito
Projeto Detalhado / Brochura	Proj_Retratos_da_Mama_adendo4_destaque.pdf	21/11/2019 11:24:44	Lara Zimmermann	Aceito

Endereço: Rua Ovídio Pires de Campos, 225 5º andar
Bairro: Cerqueira Cesar **CEP:** 05.403-010
UF: SP **Município:** SAO PAULO
Telefone: (11)2661-7585 **Fax:** (11)2661-7585 **E-mail:** cappesq.adm@hc.fm.usp.br

Continuação do Parecer: 5.688.046

Investigador	Proj_Retratos_da_Mama_adendo4_destaque.pdf	21/11/2019 11:24:44	Lara Zimmermann	Aceito
Projeto Detalhado / Brochura Investigador	Proj_Retratos_da_Mama_adendo4.pdf	21/11/2019 11:24:01	Lara Zimmermann	Aceito
TCLE / Termos de Assentimento / Justificativa de Ausência	TCLE_Retratos_Mama_adendo4.pdf	21/11/2019 11:23:03	Lara Zimmermann	Aceito
TCLE / Termos de Assentimento / Justificativa de Ausência	TCLE_Retratos_Mama_adendo4_destaque.pdf	21/11/2019 11:22:21	Lara Zimmermann	Aceito
Outros	Memorando_adendo_3.pdf	25/10/2019 16:03:00	Lara Zimmermann	Aceito
TCLE / Termos de Assentimento / Justificativa de Ausência	TCLE_Retratos_da_mama_versao2.pdf	16/09/2019 12:04:23	Lara Zimmermann	Aceito
Outros	Adendo_Retratos_da_Mama2019.pdf	25/06/2019 19:21:10	Lara Zimmermann	Aceito
TCLE / Termos de Assentimento / Justificativa de Ausência	TCLE_Retratos_da_Mama2019.pdf	25/06/2019 19:12:58	Lara Zimmermann	Aceito
Projeto Detalhado / Brochura Investigador	Proj_Retratos_da_Mama_adendo_cep2019.pdf	25/06/2019 19:12:30	Lara Zimmermann	Aceito
Folha de Rosto	folha_de_rosto.pdf	17/09/2018 15:03:01	Lara Zimmermann	Aceito
Outros	anuencia_InRad.pdf	17/09/2018 15:02:15	Lara Zimmermann	Aceito
Outros	cadastro_HC.pdf	17/09/2018 15:01:08	Lara Zimmermann	Aceito
Outros	Anuencia_Biobanco.pdf	14/09/2018 15:59:40	Lara Zimmermann	Aceito
Outros	quest_epidemiologico.pdf	13/09/2018 14:17:18	Lara Zimmermann	Aceito
TCLE / Termos de Assentimento / Justificativa de Ausência	TCLE.pdf	13/09/2018 12:47:36	Lara Zimmermann	Aceito
Cronograma	Cronograma_Atividades.pdf	13/09/2018 12:47:25	Lara Zimmermann	Aceito
Projeto Detalhado / Brochura Investigador	Projeto_Retratos_da_Mama.pdf	13/09/2018 12:47:14	Lara Zimmermann	Aceito

Endereço: Rua Ovídio Pires de Campos, 225 5º andar
Bairro: Cerqueira Cesar **CEP:** 05.403-010
UF: SP **Município:** SAO PAULO
Telefone: (11)2661-7585 **Fax:** (11)2661-7585 **E-mail:** cappesq.adm@hc.fm.usp.br

Continuação do Parecer: 5.688.046

Situação do Parecer:
Aprovado

Necessita Apreciação da CONEP:
Não

SAO PAULO, 06 de Outubro de 2022

Assinado por:
ALFREDO JOSE MANSUR
(Coordenador(a))

Endereço: Rua Ovídio Pires de Campos, 225 5º andar
Bairro: Cerqueira Cesar **CEP:** 05.403-010
UF: SP **Município:** SAO PAULO
Telefone: (11)2661-7585 **Fax:** (11)2661-7585 **E-mail:** cappesq.adm@hc.fm.usp.br

Attachment 2. Written informed consent for the "Retratos da Mama" project

INSTITUTO DO CANCER DO ESTADO DE SÃO PAULO
Octávio Frias de Oliveira
Secretaria de Estado da Saúde
Faculdade de Medicina da Universidade de São Paulo
TERMO DE CONSENTIMENTO LIVRE E ESCLARECIDO

I - DADOS DE IDENTIFICAÇÃO DO SUJEITO DA PESQUISA OU RESPONSÁVEL LEGAL

1. NOME:.....
DOCUMENTO DE IDENTIDADE Nº : ..... SEXO: .M □ F □
DATA NASCIMENTO: ...../...../.....
ENDEREÇO ..... Nº ..... APTO: .....
BAIRRO: ..... CIDADE .....
CEP:..... TELEFONE: DDD (.....) .....

2. RESPONSÁVEL LEGAL .....
NATUREZA (grau de parentesco, tutor, curador etc.) .....
DOCUMENTO DE IDENTIDADE Nº : ..... SEXO: .M □ F □
DATA NASCIMENTO: ...../...../.....
ENDEREÇO ..... Nº ..... APTO: .....
BAIRRO: ..... CIDADE .....
CEP:..... TELEFONE: DDD (.....) .....

II - DADOS SOBRE A PESQUISA CIENTÍFICA

1. TÍTULO DO PROTOCOLO DE PESQUISA: Retratos da mama
PESQUISADOR: Roger Chammas
CARGO/FUNÇÃO: Professor **INSCRIÇÃO CONSELHO REGIONAL Nº** CRM 63307
UNIDADE DO HCFMUSP: Departamento de Radiologia e Oncologia

2. **AVALIAÇÃO DO RISCO DA PESQUISA:**

RISCO MÍNIMO	RISCO MÉDIO X
RISCO BAIXO	RISCO MAIOR

3.DURAÇÃO DA PESQUISA : 36 meses

A senhora esta sendo convidada a participar de um estudo e para decidir se aceita ou não participar desta pesquisa, a senhora precisa entender o suficiente sobre os riscos e benefícios para que possa fazer o julgamento consciente. Este processo é chamado de Consentimento Livre e Esclarecido.

Este formulário de consentimento contém informações sobre a pesquisa em estudo e será discutido com seu médico. Uma vez compreendido o estudo e havendo seu interesse em participar do mesmo, será solicitada a sua assinatura neste termo. A senhora receberá uma copia para o seu arquivo. Se a senhora julgar necessário, consulte outros profissionais (médicos ou não) antes de assinar este documento.

Rubrica do Pesquisador Rubrica Paciente Impressão Digital

INSTITUTO DO CANCER DO ESTADO DE SÃO PAULO
Octávio Frias de Oliveira
Secretaria de Estado da Saúde
Faculdade de Medicina da Universidade de São Paulo

O projeto de pesquisa "Retratos da Mama" pretende estudar alterações genéticas (alterações no DNA) presentes em mulheres jovens diagnosticadas com câncer de mama, subtipo triplo negativo. Essas alterações serão estudas e relacionadas com os dados clínicos coletados durante o tratamento.

III - REGISTRO DAS EXPLICAÇÕES DO PESQUISADOR AO PACIENTE OU SEU REPRESENTANTE LEGAL SOBRE A PESQUISA, CONSIGNANDO

1 – Objetivo:

O objetivo desta pesquisa será o de identificar possíveis alterações no DNA, que tenham valor clínico para mulheres com idade abaixo de 40 anos, com câncer de mama triplo negativo. O projeto também busca a padronização de metodologia pouco invasiva para análise de possíveis marcadores tumorais no plasma em amostras de sangue. A qualidade de vida será avaliada durante o decorrer dos tratamentos utilizando entrevista por questionários específicos.

2 – Procedimentos:

Como parte do seu tratamento poderá ser solicitado exames de imagem, exames de sangue, procedimentos como biopsias e clipagem e cirurgias para remoção de tumor. Durante o processo de biopsia e/ou a remoção do tumor primário em cirurgia existe a coleta de tecido tumoral, que será encaminhado para análise para que o diagnóstico final seja realizado. Ainda durante a cirurgia para remoção do tumor, ocorre também dentro do protocolo já estabelecido a remoção de tecido normal (sem a presença de células malignas) como forma de segurança do procedimento. Após todas as análises necessárias para diagnostico, o tecido restante é descartado.

Convidamos você a participar desse estudo, doando material biológico, tecido tumoral, tecido normal e sangue para análise de possíveis alterações no seu DNA. Estas determinações serão realizadas apenas se o tumor for subtipo triplo negativo. Se o tumor da Senhora não for triplo negativo, este material será armazenado no Biobanco, localizado no Centro de Investigação Translacional em Oncologia - ICESP e pediremos para que seja assinado outro Termo de Consentimento Livre Esclarecido.

O tecido tumoral poderá ser coletado no momento da realização da biópsia ou da cirurgia para a remoção do tumor. Serão retirados fragmentos do tecido tumoral, sendo que esses fragmentos serão enviados para análise para o diagnóstico. Após o diagnostico, os fragmentos excedentes serão utilizados no projeto. Caso você já tenha realizado a biopsia em outro serviço e não tiver orientação médica para realizar uma cirurgia primária, gostaríamos de convidá-la a realizar uma nova biopsia em nossa instituição. Durante o procedimento da biopsia, será coletado tecido tumoral para o projeto e para a realização de um novo exame de anatomopatológico. Juntamente com o procedimento de biopsia, será realizado o procedimento de clipagem, que tem por objetivo determinar os limites do tumor, permitindo ao médico acompanhar a resposta do tumor frente ao tratamento que será adotado. O processo de biópsia e clipagem é feito sob anestesia e apresentam riscos reduzidos, incluindo hematomas, dor temporária no local da punção e edema.

O tecido normal poderá ser coletado no momento da realização da cirurgia primária ou da clipagem, caso haja indicação. Como o protocolo da cirurgia primária prevê a retirada de tecido normal, fragmentos desse tecido serão encaminhados ao Biobanco para o projeto. O protocolo de clipagem acontecerá caso você concorde com uma nova biopsia, o que permitirá realizar o mesmo processo de obtenção de tecido tumoral para o tecido normal.

As amostras de sangue serão coletas adicionais de 15ml (1 colher de sopa). O projeto prevê coletas seriadas, em que parte coincidirá com coletas de sangue necessárias durante o tratamento, sendo assim será realizada coleta conjunta e parte das coletas será necessária somente para o estudo, não estando relacionada com o tratamento. Caso você concorde com as coletas não relacionadas ao tratamento, neste caso haverá uma quantia pré-fixada de ajuda de custo relacionado aos gastos com transporte e alimentação.

Rubrica do Pesquisador Rubrica Paciente Impressão Digital

INSTITUTO DO CANCER DO ESTADO DE SÃO PAULO
Octávio Frias de Oliveira
Secretaria de Estado da Saúde
Faculdade de Medicina da Universidade de São Paulo

Com a sua permissão será aplicado questionários a respeito do seu histórico pessoal e familiar relacionados a fatores de risco para o câncer de mama e sobre sua qualidade de vida. Estes questionários serão aplicados por enfermeiros e pesquisadores envolvidos no estudo, sempre que possível no dia de uma de suas consultas e dias de coleta de monitoramento habituais ao hospital ou excepcionalmente por telefone para sua maior segurança e conforto. No caso de sua concordância em responder o questionário por telefone, será agendado dia e horário e você será informado da duração aproximada do tempo que será necessário para responder o questionário.

Ainda com a sua permissão, dados referentes à doença atual ou pregressa e tratamentos realizados serão obtidos do seu prontuário médico para ser utilizado, de forma anônima, na pesquisa.

Para possibilitar uma melhor compreensão, segue esquema detalhando os passos do projeto, que poderá variar de acordo com o tratamento adotado pela equipe médica:

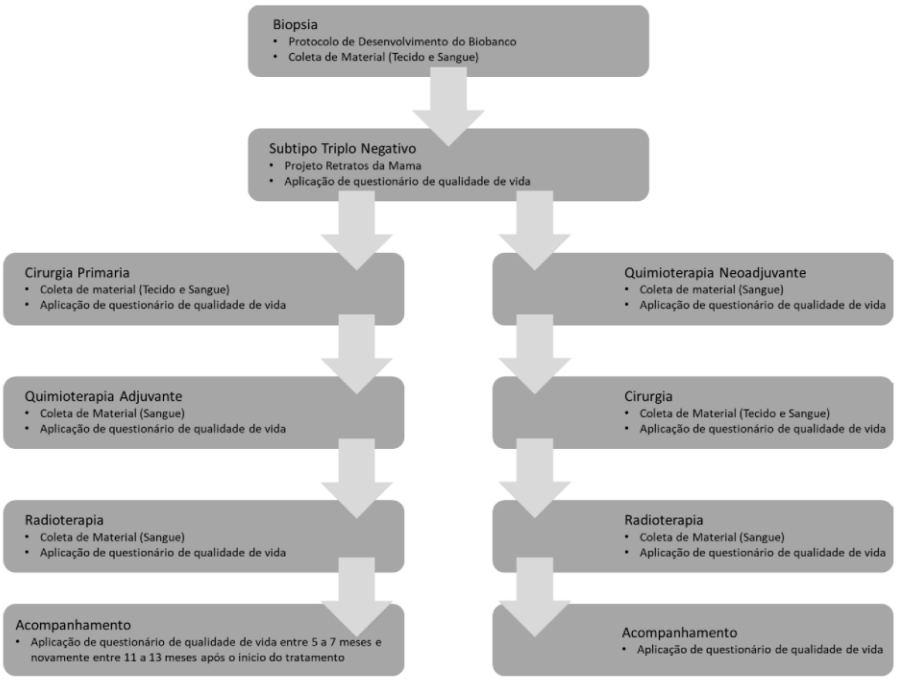

Posteriormente serão realizadas técnicas de biologia celular e molecular a fim de avaliar possíveis alterações em suas células e em seu DNA que possam estar relacionadas ao câncer de mama. Toda amostra colhida para este projeto será processada, analisada e armazenada, pelo tempo indeterminado, no Biobanco, localizado Centro de Investigação Translacional em Oncologia - ICESP.

Rubrica do Pesquisador Rubrica Paciente Impressão Digital

INSTITUTO DO CANCER DO ESTADO DE SÃO PAULO
Octávio Frias de Oliveira
Secretaria de Estado da Saúde
Faculdade de Medicina da Universidade de São Paulo

Antes de decidir, leia este documento e faça quantas perguntas achar necessário e, se for preciso, leve para casa e discuta com seus amigos e familiares. Tenha certeza que entendeu todo o texto.

3 – Descrição dos desconfortos e riscos esperados nos procedimentos do ítem 2:

O procedimento não apresenta nenhum risco adicional ao seu tratamento. O tratamento será o de rotina, sem qualquer interferência por parte dos pesquisadores. Pode ser que, no local de coleta do sangue, apareça um pequeno hematoma. Caso você seja submetida a uma nova biopsia seguida de clipagem, os riscos desse procedimento são reduzidos, podendo apresentar hematomas, dor temporária no local da punção e edema.

4 – Benefícios para o participante:

Este estudo não proporcionará benefício direto para a senhora. No entanto, a melhor compreensão das causas e comportamento da doença poderá beneficiar outras pacientes futuramente. A senhora tem direito em buscar indenização por danos decorrentes do estudo Os dados referentes às alterações no DNA poderão trazer informações herdadas de seus pais, podem ser transmitidas para os descendentes e podem ser importantes para os demais membros da sua família. A senhora poderá optar por ser informada ou não do resultado da análise de seu DNA. Caso opte pela informação e seja detectada alguma alteração do DNA que implique em aconselhamento genético, este será realizado nesta instituição pela equipe médica do instituto.

A senhora gostaria de ser informada a respeito do resultado da análise de seu DNA?
( ) Sim ( ) Não

5 – Relação de procedimentos alternativos que possam ser vantajosos, pelos quais o paciente pode optar:

Não há procedimentos alternativos.

IV - ESCLARECIMENTOS DADOS PELO PESQUISADOR SOBRE GARANTIAS DO SUJEITO DA PESQUISA:

1 – Garantia de acesso: Em qualquer etapa do estudo, você terá acesso aos profissionais responsáveis pela pesquisa para esclarecimento de eventuais dúvidas.

2 – É garantida a liberdade da retirada de consentimento a qualquer momento e deixar de participar do estudo, sem qualquer prejuízo à continuidade de seu tratamento na Instituição.

3 – Direito de confidencialidade: As informações obtidas serão analisadas em conjunto com outros pacientes, não sendo divulgada a identificação de nenhum paciente. Os resultados serão apresentados em relatórios científicos, congressos nacionais e internacionais, revistas Internacionais a fim de divulgar os novos achados e as alterações do DNA serão depositadas em bancos de dados nacionais e internacionais.

4 – Direito de ser mantido atualizado sobre os resultados parciais das pesquisas, quando em estudos abertos, ou de resultados que sejam do conhecimento dos pesquisadores.

5 – Despesas e compensações: Com a concordância da Senhora, caso seja necessário o ressarcimento pela necessidade de coleta de amostra em situação fora do tratamento, a Senhora terá ressarcimento de gastos com transporte e alimentação. Não há compensação financeira relacionada à sua participação.

Rubrica do Pesquisador Rubrica Paciente Impressão Digital

INSTITUTO DO CANCER DO ESTADO DE SÃO PAULO
Octávio Frias de Oliveira
Secretaria de Estado da Saúde
Faculdade de Medicina da Universidade de São Paulo

V. INFORMAÇÕES DE NOMES, ENDEREÇOS E TELEFONES DOS RESPONSÁVEIS PELO ACOMPANHAMENTO DA PESQUISA, PARA CONTATO EM CASO DE INTERCORRÊNCIAS CLÍNICAS E REAÇÕES ADVERSAS

O investigador responsável é o Prof. Dr. Roger Chammas, que pode ser encontrado no endereço Av. Dr. Arnaldo, 251 - 8oandar – Cerqueira César – São Paulo – SP – CEP: 01246-000 Telefone(s) (11) 38932000.

Se você tiver alguma consideração ou dúvida sobre a ética da pesquisa, entre em contato com a Comissão de Ética para Análise de Projetos de Pesquisa (CAPPesp) do Hospital das Clínicas da Faculdade de Medicina da Universidade de São Paulo (HCFMUSP).

A CAPPesq é um órgão de natureza técnico-cientifica permanente, que tem por finalidade avaliar a pesquisa em seres humanos, realizadas no HCFMUSP. Para tanto o CAPPesq zela, nos projetos de pesquisa, pelos aspectos: técnicos-científicos; éticos; enquadramento nas legislações vigentes; financiamento e origem dos recursos; adequação as diretrizes das políticas institucionais; integração com as demais ações setoriais; interesse e conveniência para o setor público. O projeto de pesquisa "Retratos da mama" foi avaliado e aprovado pelo CEP.

Se você tiver alguma consideração ou duvida sobre a ética de pesquisa, entre em contato com o Comissão de Ética para Análise de Projetos de Pesquisa (CAPPesp) do HCFMUSP – Rua Ovídio Pires de Campos, 225 – 5º andar – Prédio da Administração. Tel: (11) 2661-7585 – 2661-1548 e 2661-1549. Email: cappesq.adm@hc.fm.usp.br

---

VI. OBSERVAÇÕES COMPLEMENTARES

Nenhuma informação envolvendo seu nome será fornecida a qualquer pessoa, à exceção dos pesquisadores participantes do estudo. Você não será identificado pessoalmente em qualquer relatório deste estudo. Seus dados serão computadorizados e anonimamente utilizados em um relatório final sobre os resultados obtidos. Poderão ser controlados de acordo com os regulamentos atualmente em vigência.

VII – CONSENTIMENTO

Acredito ter sido suficientemente informado a respeito das informações que li ou que foram lidas para mim, descrevendo o estudo: "Retratos da mama". Ficaram claros para mim quais são os propósitos do estudo, os procedimentos a serem realizados, seus desconfortos e riscos, as garantias de confidencialidade e de esclarecimentos permanentes. Ficou claro também que minha participação é isenta de despesas e que tenho garantia do acesso a tratamento hospitalar quando necessário. Concordo voluntariamente em participar deste estudo e poderei retirar o meu consentimento a qualquer momento, antes ou durante o mesmo, sem penalidades ou prejuízo ou perda de qualquer benefício que eu possa ter adquirido, ou no meu atendimento neste Serviço.

Rubrica do Pesquisador Rubrica Paciente Impressão Digital

INSTITUTO DO CANCER DO ESTADO DE SÃO PAULO
Octávio Frias de Oliveira
Secretaria de Estado da Saúde
Faculdade de Medicina da Universidade de São Paulo

_____ _____

Assinatura do paciente/responsável legal Data
__/__/__

Assinatura da testemunha Data __/__/__

(Somente para o responsavel ao projeto)

Declaro que obtive de forma apropriada e voluntária o Consentimento Livre e Esclarecido deste paciente ou representante legal para a participação neste estudo.

Data / /

Rubrica do Pesquisador Rubrica Paciente Impressão Digital

Attachment 3. Written informed consent for the Academic Biobank of Research on Cancer

INSTITUTO DO CANCER DO ESTADO DE SÃO PAULO
Octávio Frias de Oliveira
Secretaria de Estado da Saúde
Faculdade de Medicina da Universidade de São Paulo

FUNDAÇÃO FACULDADE DE MEDICINA

TERMO DE CONSENTIMENTO LIVRE E ESCLARECIDO

DADOS DE IDENTIFICAÇÃO DO PARTICIPANTE DA PESQUISA OU RESPONSÁVEL LEGAL

1.NOME: .....
DOCUMENTO DE IDENTIDADE Nº: ..... SEXO: .M □ F □
DATA NASCIMENTO: ...../...../.....
ENDEREÇO: ..... Nº ..... APTO: .....
BAIRRO: ..... CIDADE: .....
CEP:..... TELEFONE: DDD (.....) .....

2.RESPONSÁVEL LEGAL: .....
NATUREZA (grau de parentesco, tutor, curador etc.): .....
DOCUMENTO DE IDENTIDADE: ..... SEXO: M □ F □
DATA NASCIMENTO.: ...../...../.....
ENDEREÇO: ..... Nº ..... APTO: .....
BAIRRO: ..... CIDADE: .....
CEP:..... TELEFONE: DDD: (.....) .....

DADOS SOBRE A PESQUISA

1. TÍTULO: **Protocolo de Desenvolvimento de Biobanco**

2. LOCAL: **Instituto do Câncer do Estado de São Paulo**

3.. AVALIAÇÃO DO RISCO DA PESQUISA:

RISCO MÍNIMO	x	RISCO MÉDIO	□
RISCO BAIXO	□	RISCO MAIOR	□

Rubrica Participante_____ Rubrica responsável pelo Consentimento_____

Você foi admitido(a) neste hospital para o tratamento de sua doença. Como parte deste tratamento, poderão ser solicitados exames de sangue e biópsias e até mesmo a realização de cirurgia para retirada do tumor. O tecido tumoral coletado nas biópsias ou retirado na cirurgia são encaminhados para análise para que seu diagnóstico seja finalizado. Nestes casos pode ser que sobre um pouco deste material, que depois é descartado.

Você está sendo convidado(a) a fornecer este material que será descartado, amostra(s) de sangue adicional, de aproximadamente 15ml cada e, eventualmente, uma amostra de urina de 50ml ou de saliva de 5ml também poderão ser solicitadas. Antes de decidir, leia este documento que se chama Termo de Consentimento Livre e Esclarecido - TCLE. Faça quantas perguntas achar necessário e, se for preciso, leve para casa e discuta com seus amigos e familiares. Tenha certeza que entendeu todo o texto.

Objetivos – Porque fornecer o material?
É importante conhecer melhor a sua doença e os pesquisadores (médicos de diversas áreas) vão fazer testes com estas amostras. Os resultados encontrados poderão ajudar a desenvolver novas possibilidades de diagnóstico e tratamento para o tipo de câncer que você tem.

Riscos de sua participação:
Não existem riscos adicionais relacionados ao processo de armazenamento das amostras.
Os riscos para coleta de sangue são os mesmos existentes para as outras coletas que já tenha realizado. São eles: dor e sangramento, e em alguns casos mais raros, infecção. Você pode sentir-se tonto e, às vezes, até mesmo desmaiar. A coleta do tecido tumoral no ato operatório ou da biópsia não implica na mudança de plano cirúrgico ou da biópsia originais. Assim, não há riscos adicionais nesses casos além dos já previstos para estes procedimentos. Para eventuais coletas de urina ou saliva não há riscos adicionais.
Você estará nos cedendo o direito de armazenar e de usar o material para diferentes projetos de pesquisa sobre o câncer, sempre em busca de conhecermos mais sobre esta doença, sua prevenção e tratamento. Sempre que quiser, você poderá ter acesso às informações que obtivermos que podem indicar se você ou seus familiares tem ou não risco de desenvolver alguma outra doença, por exemplo. Nossa equipe estará pronta para orientá-lo sobre o que precisa ser feito, no momento que você quiser.
Este protocolo de nada vai interferir com o seu tratamento. Todos os procedimentos serão realizados por profissionais treinados e qualificados para minimizar os potenciais riscos e desconfortos que possam acontecer ao participante deste protocolo.

Coleta do material:
As amostras de tecido tumoral serão coletadas a partir do material que sobrar dos procedimentos de biópsia e/ou cirurgia. Serão coletados tubos extras de sangue, aproximadamente 15ml. As eventuais coletas de urina 50ml ou saliva 5ml acontecerão durante seu atendimento ambulatorial ou internação. Não será exigido que você faça consultas extras ou tome medicações a mais.

Depósito do material:
O material coletado será processado, congelado e/ou feito cultura de células e as informações ficarão guardadas em um Banco que é chamado de **Biobanco.** Este Biobanco é de responsabilidade do Instituto do Câncer do Estado de São Paulo - ICESP. O ICESP garante que seu material será guardado em segurança e utilizado somente com a autorização da comissão do Biobanco. Tanto os pesquisadores quanto o ICESP garantem e são responsáveis pela conservação do material que você forneceu.

Caso o material seja perdido, destruído, ou alterado de alguma forma, você será comunicado o mais rápido possível. Se houver transferência do Biobanco ou caso o Biobanco seja fechado, você também será comunicado. Se houver necessidade de descartar as suas amostras, você será consultado antes que isto ocorra.
O Biobanco irá armazenar seu material, bem como suas informações clínicas e todos os resultados provenientes das pesquisas realizadas.

Utilização do material: Proteção dos seus direitos e de sua confidencialidade.
Todo o material se usado para pesquisa será identificado no laboratório por um código formado por números e letras. Assim seu nome não vai ser divulgado e sua privacidade e identidade serão preservadas. Os resultados da pesquisa, quando publicados, irão manter o seu anonimato e poderão ser utilizados em pesquisas futuras. As amostras serão liberadas para pesquisa somente com a aprovação da comissão do Biobanco e do Comitê de Ética em Pesquisa. As informações obtidas serão analisadas em conjunto com outros participantes, não sendo divulgada a identificação de nenhum participante individualmente.

Direitos de informação:
Você tem o direito de ser mantido informado sobre os resultados das pesquisas que utilizarem sua amostra. Este direito é assegurado e você pode solicitar a qualquer momento. Os resultados disponíveis poderão ser explicados para você, incluindo dados genéticos (resultados de exames do seu DNA). Se for necessário, você poderá receber um aconselhamento genético. Esta é uma consulta sobre possíveis riscos de doenças que podem afetar membros de sua família.

Pagamentos, despesas e benefícios:
Se você concordar que os pesquisadores usem o material fornecido do modo explicado aqui, você não receberá pagamentos por isso. Se a pesquisa gerar resultados com este material, você também não terá direito a pagamentos por isso. Os resultados das pesquisas com seu material podem, futuramente, ajudar e beneficiar outras pessoas com câncer, melhorando o diagnóstico da doença e/ou seu tratamento. Não há despesas pessoais para o voluntário e nem ajuda de custo. Havendo qualquer despesa decorrente da sua participação, a mesma será ressarcida pelo Biobanco.

Autonomia:
Sua decisão de fornecer o material é totalmente voluntária. Se você não concordar em permitir o uso do seu material para futuras pesquisas, sua decisão não afetará em nenhum modo o seu tratamento. Você pode também decidir não querer mais participar do protocolo a qualquer momento. Esta decisão será respeitada sem qualquer problema a você ou seu atendimento na instituição. Caso isso ocorra, você ou seu representante legal deverá assinar um documento escrito que confirme e registre sua decisão. Após a manifestação escrita o material será separado pelo Biobanco e entregue a você ou ao seu representante legal.

Por favor, leia com atenção e assinale as opções que você concorda. Estas serão as condições que iremos tratar o material que você fornecerá.

1) Você concorda em fornecer o material para pesquisa e concorda com a guarda no Biobanco de todas as informações?
   ( ) Sim ( ) Não

   Se sim, você autoriza a utilização do material em diversas pesquisas?
   ( ) Sim, pode usar em todas ( ) Não

   Se sim, você quer ser notificado e autorizar a cada pesquisa?
   ( ) Sim ( ) Não é necessário

   Caso você não consiga autorizar o uso do material, você indicaria uma ou mais pessoas para autorizar por você?
   ( ) Sim ( ) Não, não quero indicar outras pessoas ( ) Não se aplica

   Se sim, qual(is) o(s) nome(s) da(s) pessoa(s), grau de parentesco e forma de contato?
   _____
   _____
   _____

2) Eventualmente, poderá ser necessário realizar coletas adicionais de material biológico ao longo de seu tratamento, você está de acordo?

-Sangue (15mL)	( ) Sim	( ) Não	( ) Não se aplica
-Urina	( ) Sim	( ) Não	( ) Não se aplica
-Saliva	( ) Sim	( ) Não	( ) Não se aplica
-Tecido (cirurgia/biópsia)	( ) Sim	( ) Não	( ) Não se aplica

3) Você autoriza que seja aplicado um questionário de qualidade de vida?
   ( ) Sim ( ) Não
   Em caso afirmativo, você autoriza a utilização dos dados para fins de pesquisa?
   ( ) Sim ( ) Não

Sempre que você quiser conversar sobre algum resultado de pesquisa de seu material, ou quiser obter informações de qualquer tipo, ou tirar qualquer dúvida, você deve procurar a um dos responsáveis pelo Protocolo de Desenvolvimentodo Biobanco (11-38932000).
O investigador responsável é o Prof. Dr. Roger Chammas, que pode ser encontrado no endereço Av. Dr. Arnaldo, 251 - 8ºandar – Cerqueira César – São Paulo – SP – CEP: 01246-000, Telefone: (11) 38932000.
Se você tiver alguma consideração ou dúvida sobre a ética da pesquisa, entre em contato com o Comitê de Ética para Análise de Projetos de Pesquisa (CAPPesq) do Hospital das Clínicas da Faculdade de Medicina da Universidade de São Paulo (HC-FMUSP).
A Coordenadoria de Ética em Pesquisa do HC-FMUSP é um órgão de natureza técnico-cientifica permanente, que tem por finalidade avaliar a pesquisa em seres humanos, realizadas no complexo HC-FMUSP. Para tanto o CAPPesq zela, nos projetos de pesquisa, pelos aspectos: técnicos-cientificos; éticos; enquadramento nas legislações vigentes; financiamento e origem dos recursos; adequação as diretrizes das políticas institucionais; integração com as demais ações setoriais; interesse e conveniência para o setor público. O "Protocolo de Desenvolvimento de Biobanco" foi avaliado e aprovado pelos Comitês de Ética em Pesquisa da FMUSP (CEP-FMUSP) e Comitê de Ética Nacional em Pesquisa (CONEP). Todos os futuros projetos de pesquisa envolvendo as amostras armazenadas pelo Biobanco serão avaliados e aprovados pelo Comitê de Ética em pesquisa.

O CAPPesq-HC-FMUSP pode ser encontrado na Rua Ovídio Pires de Campos, 225 – 5º andar – Prédio da Administração– Telefones: (11) 26617585 ou 26611548 ou 26611549
E-mail: cappesq.adm@hc.fm.usp.br. Horário de funcionamento das 7h00 as 16h00.

Acredito ter sido suficientemente informado a respeito das informações que li ou que foram lidas para mim, descrevendo "Protocolo de Desenvolvimento de Biobanco"
Eu discuti com _____ sobre a minha decisão em participar nesse protocolo. Ficaram claros para mim quais são os propósitos, os procedimentos a serem realizados, seus desconfortos e riscos, as garantias de confidencialidade e de esclarecimentos permanentes. Ficou claro também que minha participação é isenta de despesas e que tenho garantia do acesso a tratamento hospitalar quando necessário. Concordo voluntariamente em participar deste protocolo e poderei retirar o meu consentimento a qualquer momento, antes ou durante o mesmo, sem penalidades ou prejuízo ou perda de qualquer benefício que eu possa ter adquirido, ou no meu atendimento neste Serviço.

Este TCLE, elaborado em duas vias, deverá ser obrigatoriamente rubricado em todas as paginas por você ou pelo seu representante legal e pelo pesquisador responsável.

Rubrica Participante_____ Rubrica responsável pelo Consentimento_____

Página de assinaturas:

Nome do Participante/Representante legal

Assinatura do Participante/Representante legal Data ____/____/____

Nome da Testemunha

Assinatura da testemunha Data ____/____/____

Para casos de participantes, analfabetos, semi-analfabetos ou portadores de deficiência auditiva ou visual.

(Somente para o responsável do projeto)

Declaro que obtive de forma apropriada e voluntária o Consentimento Livre e Esclarecido deste participante ou representante legal para a participação neste estudo.

Nome do Investigador

Assinatura do Investigador do Biobanco Data ____/____/____

Attachment 4. Curriculum vitae of the candidate

ALEXIS GERMÁN MURILLO CARRASCO

EDUCATION

2018-2023 **Doctorate program in Oncology**

Universidade de São Paulo (São Paulo, Brazil)

2011-2015 **Genetics and Biotechnology**

Universidad Nacional Mayor de San Marcos (Lima, Peru)

RESEARCH ARTICLES (2018-2023)

- Evaluación del estado secretor en una muestra de estudiantes universitarios de Lima. Luis Rodriguez, **Alexis Murillo**, Jorge Rua, Carla Bernal, Juana Quispe, Henry Mallqui, Erasmo Colona, Libertad Alzamora, Ela Contreras. Ágora;4(1):21-5. https://revistaagora.com/index.php/cieUMA/article/view/60

- LungCARD–Report on worldwide research and clinical practices related to lung cancer. Radmila Jankovic, Helena J Goncalves, Milena Cavic, Carla Clemente, Michael Lind**,** Alexis Murillo Carrasco, Selama Nadifi, Meriem Khyatti, Tumininu Adebambo, Dilshod Egamberdiev. J BUON. 2019 Jan-Feb;24(1):11-19. https://www.jbuon.com/archive/24-1-11.pdf

- Novel mutation in ENG gene causing Hereditary Hemorrhagic Telangiectasia in a Peruvian family. Alejandro Zevallos-Morales, Alexis Murillo, Milagros M Dueñas-Roque, Ana Prötzel, Luis Venegas-Tresierra, Verónica Ángeles-Villalba, Miguel Guevara-Cruz, Ada Chávez-Gil, Ricardo Fujita, Maria L Guevara-Fujita. Genet. Mol. Biol. 43 (01) • 2020. http://dx.doi.org/10.1590/1678-4685-gmb-2019-0126

- Simultaneous silencing of lysophosphatidylcholine acyltransferases 1-4 by nucleic acid nanoparticles (NANPs) improves radiation response of melanoma cells. Renata F Saito, Maria Cristina Rangel, Justin R Halman, Morgan Chandler, Luciana Nogueira de Sousa Andrade, Silvina Odete-Bustos, Tatiane Katsue Furuya, **Alexis Germán Murillo Carrasco**, Adriano B Chaves-Filho, Marcos Y Yoshinaga, Sayuri Miyamoto, Kirill A Afonin & **Roger**

Chammas. Nanomedicine. 2021 Aug;36:102418; https://doi.org/10.1016/j.nano.2021.102418

- PUM1 and RNase P genes as potential cell-free DNA markers in breast cancer. **Alexis Murillo Carrasco**, Oscar Acosta,Jaime Ponce, José Cotrina,Alfredo Aguilar, Jhajaira Araujo,Pamela Rebaza, Joseph A. Pinto, Ricardo Fujita, José Buleje. J Clin Lab Anal. 2021 Apr;35(4):e23720; https://doi.org/10.1002/jcla.23720

- Disruption of miRNA-mRNA Networks Defines Novel Molecular Signatures for Penile Carcinogenesis. Tatiane Katsue Furuya, Claudio Bovolenta Murta, **Alexis Germán Murillo Carrasco**, Miyuki Uno, Laura Sichero, Luisa Lina Villa, Leonardo Cardilli, Rafael Ferreira Coelho, Giuliano Betoni Guglielmetti, Mauricio Dener Cordeiro, Katia Ramos Moreira Leite, William Carlos Nahas, **Roger Chammas** & José Pontes, Jr. Cancers 2021, 13(19), 4745; https://doi.org/10.3390/cancers13194745

- miRNA and mRNA Expression Profiles Associated with Lymph Node Metastasis and Prognosis in Penile Carcinoma. Claudio B Murta, Tatiane K Furuya, **Alexis GM Carrasco**, Miyuki Uno, Laura Sichero, Luisa L Villa, Sheila F Faraj, Rafael F Coelho, Giuliano B Guglielmetti, Mauricio D Cordeiro, Katia RM Leite, William C Nahas, **Roger Chammas**, José Pontes Jr. Int. J. Mol. Sci. 2022, 23(13), 7103; https://doi.org/10.3390/ijms23137103

- Allergic sensitization and exposure to ambient air pollution beginning early in life lead to a COPD-like phenotype in young adult mice. Natália de Souza Xavier Costa, Aila Mirtes Teles, Jôse Mára de Brito, Thaís de Barros Mendes Lopes, Renata Calciolari Rossi, Fernanda Magalhães Arantes Costa, Beatriz Mangueira Saraiva-Romanholo, Adenir Perini, Tatiane Katsue Furuya, **Alexis Germán Murillo Carrasco**, Mariana Matera Veras, Paulo Hilário Nascimento Saldiva, **Roger Chammas**, Thais M. Ecotoxicology and Environmental Safety; 241, August 2022, 113821. https://doi.org/10.1016/j.ecoenv.2022.113821

- Chip-based digital Polymerase Chain Reaction as quantitative technique for the detection of PIK3CA mutations in breast cancer patients. Stefano Giannoni-Luza, Oscar Acosta, **Alexis Germán Murillo Carrasco**, Pierina Danos, José Manuel Cotrina Concha, Henry Guerra Miller, Joseph A Pinto, Alfredo Aguilar, Jhajaira M Araujo, Ricardo Fujita, Jose Buleje. Heliyon. Vol 8, Issue 11, November 2022, e11396. https://doi.org/10.1016/j.heliyon.2022.e11396

- Impact of mini-driver genes in the prognosis and tumor features of colorectal cancer samples: a novel perspective to support current biomarkers. Anthony Vladimir Campos Segura, Mariana Belén Velásquez Sotomayor, Ana Isabel Flor Gutiérrez Román, César Alexander Ortiz Rojas, **Alexis Germán Murillo Carrasco**. PeerJ 11:e15410 https://doi.org/10.7717/peerj.15410

- Insights from a Computational-Based Approach for Analyzing Autophagy Genes across Human Cancers. **Alexis Germán Murillo Carrasco**, Guilherme Giovanini, Alexandre Ferreira Ramos, **Roger Chammas**, Silvina Odete Bustos. Genes 2023, 14(8), 1550; https://doi.org/10.3390/genes14081550

- Promoter hypermethylation of RARB and GSTP1 genes in plasma cell-free DNA as breast cancer biomarkers in Peruvian women. Pierina Danos, Stefano Giannoni-Luza, **Alexis Germán Murillo Carrasco**, Oscar Acosta, Maria Luisa Guevara-Fujita, José Manuel Cotrina Concha, Henry Guerra Miller, Joseph Pinto Oblitas, Alfredo Aguilar Cartagena, Jhahaira Araujo Soria, Ricardo Fujita, José Luis Buleje Sono. Mol Genet Genomic Med. 2023;00:e2260. https://doi.org/10.1002/mgg3.2260

- Deciphering the Functional Status of Breast Cancers through the Analysis of Their Extracellular Vesicles. **Alexis Germán Murillo Carrasco**, Andreia Hanada Otake, Janaina Macedo-da-Silva, Veronica Feijoli Santiago, Giuseppe Palmisano, Luciana Nogueira de Sousa Andrade, **Roger Chammas**. Int. J. Mol. Sci. 2023, 24(16), 13022; https://doi.org/10.3390/ijms241613022

- Establishment of a 7-gene expression panel to improve the prognosis classification of gastric cancer patients. Mariana Belén Velásquez Sotomayor, Anthony Vladimir Campos Segura, Ricardo José Asurza Montalva, Obert Marín-Sánchez, **Alexis Germán Murillo Carrasco**, César Alexander Ortiz Rojas. Frontiers in Genetics, v. 14, p. 1206609; https://doi.org/10.3389/fgene.2023.1206609

BOOK CHAPTERS (2018-2023)

- Evaluation of plasma miRNAs for early diagnosis of breast cancer. In: Conceitos Básicos da Genética.1 ed.: Atena Editora, 2019, p. 128-138. **Carrasco, Alexis Germán Murillo**; Luza, Stefano Giannoni; Conchucos, Oscar Acosta; Concha, José Manuel Cotrina; Cartagena, Alfredo Aguilar; Vásquez,

Lia Pamela Rebaza; Alarcón, Ricardo Miguel Fujita; Sono, José Luis Buleje. http://dx.doi.org/10.22533/at.ed.21419210612

- Chapter 21: Biomarcadores. In Oncologia Da Molécula à Clínica. Authors: **Alexis Murillo Carrasco** & Miyuki Uno. Editors: **Roger Chammas**, Luisa Villa & Maria Aparecida Koike. https://www.editoradoseditores.com.br/oncologia-clinica/oncologia-da-molecula-a-clinica

PRESENTATIONS IN ACADEMIC EVENTS (2018-2023)

- Biopsias líquidas en Cáncer de mama: Estado del arte y futuros desafíos en el Perú. **Alexis Murillo.** V International Congress of Bioscience Research. Hamutay. January 15-17, 2020. Lima, Peru. http://hamutay.org/v-jcib/

- Evaluation of mirna-145 levels in plasma by digital PCR and *in silico* analysis. Implications in cancer. Motta Angelo; Acosta Oscar; Buleje Jose; **Murillo Alexis**; Danos Pierina; Fujita Ricardo. XX Curso de Verão: Genoma, Proteoma e o Universo Celular - Oncologia, Células-tronco e Terapia Celular. February 3-14, 2020. Ribeirão Preto, SP.

- Vacuna en contra de COVID-19: Progreso y perspectiva en las Américas y el Caribe**. Alexis Murillo.** International conferences for Spanish speakers, Public Health Literacy. 30 April 2021.

- Uso de nanopartículas para sensibilizar células tumorales a través de silenciamiento génico. **Alexis Murillo**. Perú: Biociencias e Investigación en el Bicentenario. 28-29 August 2021.

- Evaluación de los niveles de miRNA-145 circulante en plasma de mujeres peruanas y análisis in silico en cáncer. Motta Pardo A, O. Acosta Conchucos, J. Buleje Sono, **A. Murillo Carrasco**, R. Fujita Alarcon, P. Danos Diaz, M.L. Guevara Gil, A. Salazar Eusebio. Latin American Congress of Genetics, ALAG 2021. 5-8 October 2021.

- Análisis del gen FMO3 en pacientes peruanos con traza de trimetilaminuria. Laymito Chumbimuni L.R, **A. Murillo-Carrasco**, A. Zevallos-Morales, R. Sanchez M., R. Fujita, M.L. Guevara-Fujita. Latin American Congress of Genetics, ALAG 2021. 5-8 October 2021.

- COVID-19, las vacunas y sus implicaciones en la Población Latinoamericana**. Alexis Murillo.** International conferences for Spanish speakers, Public Health Literacy. 30 September 2021.

- Uso de nanopartículas para sensibilizar células tumorales a través de silenciamiento génico. **Alexis Murillo.** International Congress of technologic development and innovation, Peru. 6-10 December 2021.

- Enriquecimento das vesículas extracelulares derivadas de tumor a partir do seu padrão de glicosilação (antígenos Tn/Stn) para caracterizar o conteúdo de miRNA em pacientes com câncer de mama. **Alexis Murillo** & **Roger Chammas**. Annual presentations of the Postgraduate Course in Oncology at the Faculty of Medicine of the University of São Paulo (FMUSP). 10-11 December 2020.

- Compreensão dos mecanismos de resistência a tratamentos: uma plataforma para inovação diagnóstica e terapêutica em Oncologia. **Alexis Murillo**, Nathalia Leal, Silvina Bustos & **Roger Chammas**. I Symposium "Desafios em Oncologia Molecular" held at the Faculty of Medicine of the University of São Paulo. 06 March 2021.

- Biomarkers. **Alexis Murillo**. VI Course of Molecular Oncology held at the Faculty of Medicine of the University of São Paulo. 19-27 July 2021.

- Expresión concomitante de genes como herramienta para evaluar la hipótesis de los mini impulsores en cáncer colorectal. Anthony Vladimir Campos Segura & **Alexis Germán Murillo Carrasco**. International Scientific Congress of Biosciences “Hamutay”. 15-17 December 2021. Lima-Peru.

- Análisis de reproducibilidad en datos de expresión génica medida por microarrays en muestras de cáncer colorrectal. Anthony Vladimir Campos Segura & **Alexis Germán Murillo Carrasco**. International Scientific Congress of Biosciences “Hamutay”. 15-17 December 2021. Lima-Peru.

- Análisis transcriptómico en pacientes con cáncer gástrico propone 7 genes para predecir el pronóstico con alta performance. Mariana Velásquez Sotomayor, Ricardo Asurza Montalva, **Alexis Murillo Carrasco**, Obert Marín Sánchez & Cesar Ortiz Rojas. International Scientific Congress of Biosciences “Hamutay”. 15-17 December 2021. Lima-Peru.

- Age-related vesicular miRNA comparison proposes potential biomarkers for triple-negative young breast cancer in a Brazilian cohort. **Alexis Germán Murillo Carrasco**, Silvina Odete Bustos, Tainara Francini Felix, Patricia Pintor Dos Reis, Luciana Nogueira de Sousa Andrade & **Roger Chammas**. 11th

International Society for Extracellular Vesicles Annual Meeting (ISEV2022). 25-29 May 2022. Lyon- France.

- Análisis bioinformático para explorar el impacto de las mutaciones somáticas en los genes SAMHD1, GNL1, POLE, MRE11 y ASXL2 como potenciales mini impulsores en Cáncer Colorrectal. Anthony Vladimir Campos Segura & **Alexis Germán Murillo Carrasco**. Simposio de Estudiantes Hispanohablantes de Bioinformática y Biología Computacional (SEH2Bioinfo). 2-3 June 2022. Online event: https://seh2bioinfo.netlify.app/

- Transcriptome-based analysis identifies ASXL1 and MAP4K4 as prognostic markers in microsatellite instability gastric cáncer. Álvaro de Jesús Huamani Ortiz, Anthony Vladimir Campos Segura, Kevin Jorge Magano Bocanegra, Obert Marín Sánchez, **Alexis Germán Murillo Carrasco** & César Alexander Ortiz Rojas. Simposio de Estudiantes Hispanohablantes de Bioinformática y Biología Computacional (SEH2Bioinfo). 2-3 June 2022. Online event: https://seh2bioinfo.netlify.app/

- Influencia de la etnicidad latina y no latina en la asociación entre niveles de mutaciones y expresiones genéticas en pacientes con cáncer de mama Uriel S. Capcha-Jimenez, Jesus F. Pasache Juarez & **Alexis Germán Murillo Carrasco**. Simposio de Estudiantes Hispanohablantes de Bioinformática y Biología Computacional (SEH2Bioinfo). 2-3 June 2022. Online event: https://seh2bioinfo.netlify.app/

- Enriquecimento das vesículas extracelulares derivadas de tumor a partir do seu padrão de glicosilação (antígenos Tn/Stn) para caracterizar o conteúdo de miRNA em pacientes com câncer de mama. **Alexis Murillo** & **Roger Chammas.** Annual presentations of the Postgraduate Course in Oncology at the Faculty of Medicine of the University of São Paulo (FMUSP). 24-25 March 2022.

- Correlation of the expression of microRNA and their predicted targets with prognosis and mortality of penile squamous cell carcinoma Murta C.B. , Furuya T.K. , Uno M. , **Carrasco A.G.M.** , Sichero L. , Villa L.L. , Faraj S.F. , Coelho R.F., Guglielmetti G.B. , Cordeiro M.D. , Leite K.R.M. , Nahas W.C. , **Chammas R.** , Pontes Jr J. European Association of Urology Meeting - EAU22, 1-4 July 2022

- Vesicular miRNAs allow characterizing Triple-negative subtype among young-diagnosed Brazilian breast cancer patients. **Alexis Germán Murillo Carrasco**, Silvina Odete Bustos, Tainara Francini Felix, Patricia Pintor Dos Reis, Luciana Nogueira de Sousa Andrade & **Roger Chammas**. SNEV2023 International Virtual Conference. 13-14 July 2023. https://snevresearch.wordpress.com

- Avaliação por rt-pcr de marcadores gênicos tumorais no sangue periférico de pacientes com câncer gástrico. Gabriel Da Silva Kawakami; Márcia Saldanha Kubrusly; Marina Alessandra Pereira; **Alexis Germán Murillo Carrasco**; Ulysses Ribeiro Júnior. GASTRÃO 50 ANOS 28-30 June 2023.

- Medicina de precisão em Oncologia. Bootcamp "INNOVACIÓN BIOTECNOLÓGICA Y SU IMPACTO EN SALUD". July 2022. Online event.

- JRDapp: a criação de um aplicativo para análise de dados single-cell. CTO Seminars. August 2022. Hybrid event.

- Age-related vesicular miRNA comparison proposes potential biomarkers for triple-negative young breast cancer in a Brazilian cohort. **Alexis Germán Murillo Carrasco**, Silvina Odete Bustos, Tainara Francini Felix, Patricia Pintor Dos Reis, Luciana Nogueira de Sousa Andrade & **Roger Chammas**. At the Young Investigator Symposium, Satellite event of the ISEV Workshop QuantitatEVs: Multiscale analyses, from bulk to single vesicle at CNR Centro Congressi, Milano, Italy on February 3rd 2023

AWARDS (2018-2023)

- Fellowship to join the Escuela de Doctorado UC. 2019. Pontificia Universidad Católica de Chile, PUCC, Santiago, Chile

- Fellowship to join the course “Herramientas básicas de bioinformática con aplicaciones en Metagenómica”. 2019. Universidad Mayor San Andrés. La Paz, Bolivia. Sponsored by Instituto Pasteur Montevideo, Montevideo, Uruguay.

- Award Maria Mitzi Brentani for the best presentation in the Annual event of the Postgraduate Course in Oncology at the Faculty of Medicine of the University of São Paulo (FMUSP). 10-11 December 2020.

- Award Maria Mitzi Brentani for the best presentation in the Annual event of the Postgraduate Course in Oncology at the Faculty of Medicine of the University of São Paulo (FMUSP). 24-25 March 2022.

- Registration fee waiver and acceptance to attend the ISEV Workshop QuantitatEVs: Multiscale analyses, from bulk to single vesicle at CNR Centro Congressi, Milano, Italy on February 3rd 2023
- Fellowship to join the course “WCS GT: Single Cell Genomics”. 2023. Instituto do Câncer. Rio de Janeiro, Brazil. Sponsored by Wellcome Connecting Science.
- Award Maria Mitzi Brentani for the best presentation in the Annual event of the Postgraduate Course in Oncology at the Faculty of Medicine of the University of São Paulo (FMUSP). 24 November 2023.

For more information about participations as scientific reviewer, participation in projects, mentor programs, and others access the following links:

- DINA Concytec: https://ctivitae.concytec.gob.pe/appDirectorioCTI/VerDatosInvestigador.do?id_investigador=21143
- CNPq Lattes: http://lattes.cnpq.br/7039519059605148
- Biblioteca Virtual FAPESP: https://bv.fapesp.br/pt/pesquisador/707491/alexis-german-murillo-carrasco/
- ORCiD: https://orcid.org/0000-0002-7372-2608
- Web of Science (WoS) profile: https://www.webofscience.com/wos/author/record/Q-5255-2017

Attachment 5. Published manuscript related to the project

International Journal of *Molecular Sciences*

IMPACT FACTOR 5.6 | Indexed in: PubMed | CITESCORE 7.8

Review

Deciphering the Functional Status of Breast Cancers through the Analysis of Their Extracellular Vesicles

Alexis Germán Murillo Carrasco, Andreia Hanada Otake, Janaina Macedo-da-Silva, Veronica Feijoli Santiago, Giuseppe Palmisano, Luciana Nogueira de Sousa Andrade and Roger Chammas

Special Issue
State-of-the-Art Molecular Oncology in Brazil 2.0
Edited by
Dr. Tiago Rodrigues and Prof. Dr. Roger Chammas

MDPI

https://doi.org/10.3390/ijms241613022

International Journal of
Molecular Sciences

MDPI

Review

Deciphering the Functional Status of Breast Cancers through the Analysis of Their Extracellular Vesicles

Alexis Germán Murillo Carrasco [1,2], Andreia Hanada Otake [1,2], Janaina Macedo-da-Silva [3], Veronica Feijoli Santiago [3], Giuseppe Palmisano [3,4], Luciana Nogueira de Sousa Andrade [1,2] and Roger Chammas [1,2,*]

[1] Center for Translational Research in Oncology (LIM24), Instituto do Cancer do Estado de Sao Paulo (ICESP), Hospital das Clinicas da Faculdade de Medicina da Universidade de Sao Paulo (HCFMUSP), São Paulo 01246-000, Brazil; agmurilloc@usp.br (A.G.M.C.); andreia.otake@hc.fm.usp.br (A.H.O.); lnsa@usp.br (L.N.d.S.A.)
[2] Comprehensive Center for Precision Oncology, Universidade de São Paulo, São Paulo 01246-000, Brazil
[3] Departamento de Parasitologia, Instituto de Ciências Biomédicas, Universidade de São Paulo, São Paulo 05508-000, Brazil; janaina.macedo.silva@usp.br (J.M.-d.-S.); veronicafeijoli@gmail.com (V.F.S.); palmisano.gp@usp.br (G.P.)
[4] School of Natural Sciences, Macquarie University, Macquarie Park, NSW 2109, Australia
* Correspondence: rchammas@usp.br

Abstract: Breast cancer (BC) accounts for the highest incidence of tumor-related mortality among women worldwide, justifying the growing search for molecular tools for the early diagnosis and follow-up of BC patients under treatment. Circulating extracellular vesicles (EVs) are membranous nanocompartments produced by all human cells, including tumor cells. Since minimally invasive methods collect EVs, which represent reservoirs of signals for cell communication, these particles have attracted the interest of many researchers aiming to improve BC screening and treatment. Here, we analyzed the cargoes of BC-derived EVs, both proteins and nucleic acids, which yielded a comprehensive list of potential markers divided into four distinct categories, namely, (i) modulation of aggressiveness and growth; (ii) preparation of the pre-metastatic niche; (iii) epithelial-to-mesenchymal transition; and (iv) drug resistance phenotype, further classified according to their specificity and sensitivity as vesicular BC biomarkers. We discuss the therapeutic potential of and barriers to the clinical implementation of EV-based tests, including the heterogeneity of EVs and the available technologies for analyzing their content, to present a consistent, reproducible, and affordable set of markers for further evaluation.

Keywords: extracellular vesicles; breast cancer; omics; theranostics; nanomedicine

Citation: Murillo Carrasco, A.G.; Otake, A.H.; Macedo-da-Silva, J.; Feijoli Santiago, V.; Palmisano, G.; Andrade, L.N.d.S.; Chammas, R. Deciphering the Functional Status of Breast Cancers through the Analysis of Their Extracellular Vesicles. *Int. J. Mol. Sci.* **2023**, *24*, 13022. https://doi.org/10.3390/ijms241613022

Academic Editor: Chiara Laezza

Received: 30 June 2023
Revised: 10 August 2023
Accepted: 18 August 2023
Published: 21 August 2023

1. Introduction

Breast cancer (BC) is currently the most commonly diagnosed type of cancer in the world. In 2020, this disease accounted for 25.5% of new cases among women, and it was responsible for 15.5% of the cases of death via cancer among women [1]. Due to these rates, it is important to continue searching for screening and therapeutic options. Cancer is a disease produced by specific tissue cells with uncontrolled growth. Tumor cells use cell-to-cell communication to spread through diverse strategies, invading lymph nodes or distant organs, evading growth suppressors, or inducing tumor-supporting angiogenesis [2].

Extracellular vesicles (EVs) represent one form of cell-to-cell communication through a range of different types of membranous nano- and microparticles (ranging from 30 nm to 5 µm in size), each with a specific biogenesis, cargo, and function [3]. EVs are involved in several biological processes such as cell signaling, cell proliferation, immune system modulation [4–6], and the production of amphisomes as a consequence of their fusion with autophagosomes [7]. EV proteins are markers for early diagnosis and are prognostic

in several types of solid tumors. In lung cancer, EV leucine-rich alpha-2-glycoprotein 1 was reported to be up-regulated in urinary and lung tissue [8]. Moreover, ovarian cancer EVs are enriched in integrin, PI3 kinase, p53, Ras, and other proteins related to cancer development [9,10]. In gastrointestinal system cancers, the amount of exosome is increased in patients with colorectal cancer, and it is correlated with carcinoembryogenic antigen [11]. EVs also participate in cancer progression processes such as tumor invasion, growth, and metastasis [12,13]. For example, several studies have shown that EV protein content is associated with breast cancer cells, demonstrating its modulation during oncogenesis and tumor progression. EVs support cancer progression, signaling recipient cells' motility and growth [14]. In breast cancer, increased EV biogenesis has been related to the activation of protease-activated receptor 2 (PAR2), which is induced by different factors, including coagulation factor-FVIIa and trypsin [15]. PAR2 is cleaved by trypsin, which triggers PIK3-dependent AKT phosphorylation. AKT's phosphorylation induces Rab5a activation, resulting in actin polymerization, which contributes to microvesicle budding, cell migration, and invasion [16]. Moreover, three different signaling cascades contribute to EV production via PAR2: (1) actin polymerization via the sequential activation of P38, MK2, and HSP27; (2) ERK1/2 activation, which stimulates MLC2 via MLCK; and (3) MLC2 activation via ROCK-II independently of ERK1/2 activation. The activation of MLC2 and HSP27 is essential to actomyosin rearrangement and EV production [15].

The versatility attributed to EVs is due to their heterogeneity. EVs include at least three main groups of membranous particles: exosomes, ectosomes, and apoptotic bodies [3]. Exosomes (30–150 nm in size) are initially packaged by a cell membrane bud called a multivesicular body (MVB), whereas ectosomes (200 nm–5 µm in size) are produced by protrusions of the cell membrane shed by the cell. On the other hand, apoptotic bodies are formed via cell fragmentation during programmed cell death [3]. Therefore, these particles are classified according to their sizes and the expression of a signature of surface proteins, a consequence of their different biogenesis processes. Nevertheless, the classification of these EV subtypes neglects a fourth group of EVs with no expression of the minimal set of markers described for any of the three first groups. This group includes particles whose functions and surface proteins are still being discovered, for example, migrasomes [17]. Extracellular vesicle biology is a highly dynamic and relatively recent research field. The International Society of Extracellular Vesicles (ISEV) seeks to harmonize the studies in the field, and it continuously updates the markers, mechanisms, and technologies for classifying these EVs in documents published as Minimal Information for Studies of EVs (MISEV) [18]. As researchers are still adopting the newest edition of MISEV, which includes recommendations for characterizing EV subtypes, for this review, we did not focus on specific EV subgroups, except when the authors have defined their particles as belonging to one of these subgroups.

Furthermore, EVs have arisen as a growing field of research due to their main characteristics, namely, (i) a wide of sizes from nano- to microscale (30 nm–5 µm) enabling their classification into groups (small or large EVs) [18–20]; (ii) a great diversity of proteins present on the surface of their lipid bilayer membranes, generally related to the molecular signature of the cell of origin [20,21]; and (iii) rhe mixed composition of their lumen or cargo, consisting of messenger RNA (mRNA) [22], microRNA (miRNA) [23], long non-coding RNA (lncRNA), circular RNA (circRNA) [24], double-stranded DNA (dsDNA) [25], mitochondrial DNA (mtDNA) [26], and proteins [27].

These characteristics allow EVs to be present in human fluids such as blood, urine, or saliva as a relevant form of cell-free circulating material helping to provide special protection for their luminal cargo, increasing the latter's stability and half-life [28]. Furthermore, there is currently a need to understand more about the biology behind these vesicles and their potential applications, stimulating the creation of new EV-related databases [29–31]. These databases aim to organize the information on EV profiling being continuously produced worldwide despite the technical challenges surrounding their isolation and characterization [32].

Since EVs are collected through minimally invasive methods and carry different types of information, these particles represent a suitable source of information that may lead to the improvement of breast cancer screening and treatment. However, we still face challenges related to (i) the requirement for the proper identification and quantification of EVs; (ii) the identification of breast-cancer-related markers in EVs; and (iii) strategies for taking advantage of these breast-cancer-related EVs to create new therapeutic options, among others (Figure 1).

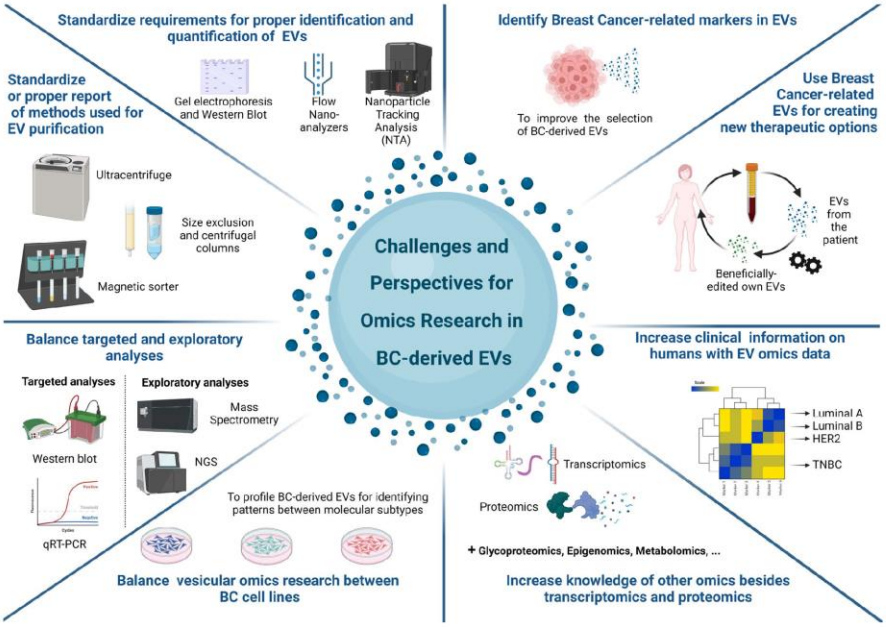

Figure 1. Challenges and perspectives regarding omics research on BC-derived EVs. This review presents the current state of the art of the most-studied omics topics on EVs from BC, namely, transcriptomics and proteomics. However, we must fill omics-related gaps before proposing reliable EV-based tools for this disease. Here, we cited some challenges for future research. As vesicles are heterogeneous in terms of size, biogenesis, and cargo, authors must standardize the reporting of methods for the isolation, quantification, characterization, and profiling of EVs. Furthermore, consistent findings in relation to EVs are characterized by their ability to be replicated. Nevertheless, many studies use targeted analysis approaches, which can bias observations. In addition, such replicability must be related to characterizing different individuals of the same subgroup or cell lines of the same subtype. To evaluate this correctly, it is necessary to increase the number of studies comparing less-studied BC cell lines and include a translational approach between tumor cell markers and their vesicular pairs. Regarding associations with the subtype of BC patients, there are gaps produced by the lack of available information about the molecular or clinical profiles of these patients, which can complicate future secondary analysis. After conquering this challenge, we can promisingly combine data from different omics studies of BC-derived EVs and select potentially tumor-derived EVs via liquid biopsies from patients to debug or edit these vesicles and induce a beneficial effect in BC patients. Image created on BioRender.com.

Transcriptomic approaches are usually performed on EVs secreted by cell lines in vitro and also in body fluid samples, which could be used to select targets for regulation in tumors. Meanwhile, since exploratory proteomic approaches are conventionally performed using cell lines, we can use this approach to characterize EVs from a single cell type from a classic perspective and propose tools for recognizing tumor-derived EVs. Therefore, this review aims to support the development of strategies for overcoming these challenges by compiling proteomic and transcriptomic information previously described in relation to breast cancer-derived EVs.

2. Transcriptomic and Genomics of BC-Related EVs

In addition to proteins, nucleic acids are another important component of EVs. The nucleic acid profile of Evs is primarily characterized by RNA types such as mRNA [24,33–35], miRNA [36–39], circRNA [24,40], rRNA [41,42], siRNA [41], and lncRNA [24,43]. However, mtDNA [33,44] and viral DNA [45] were also described in EVs from breast cancer samples. Herein, we explored the transcriptomic and genomic profiles of BC-related EVs to search for common markers and specific signatures associated with breast tumor features.

2.1. miRNA Profile in BC-Related EVs

Extracellular RNA (exRNA) is found in body fluids and can be protected from RNases through binding to circulating proteins like Ago2 and being sorted into extracellular vesicles (EVs) [23,46]. Since it is known that cancer cells secrete heterogeneous populations of EVs and that these EVs indeed contain diverse species of functional RNAs [47], the concept of accessing tumor RNA using circulating EVs is gaining great attention in the oncological field.

Among all vesicular nucleic acids, miRNAs represent the largest (and most analyzed) group. So far, at least 128 vesicular miRNAs are being studied for breast cancer (Supplementary Table S1 [36,38,39,48–123]). These studies comprise analyses conducted to characterize breast tumors as well as understand the tumorigenic process and propose candidate vesicular biomarkers for diagnosis and prognosis.

Despite the high diversity described for this type of RNA, EVs from breast cancer culture supernatants (Supplementary Table S1, Figure 2A) and liquid biopsies (Supplementary Table S1, Figure 2B) have been shown to have three miRNAs in common that can be potential markers of this tumor: hsa-miR-21, hsa-miR-122, and hsa-miR-1246.

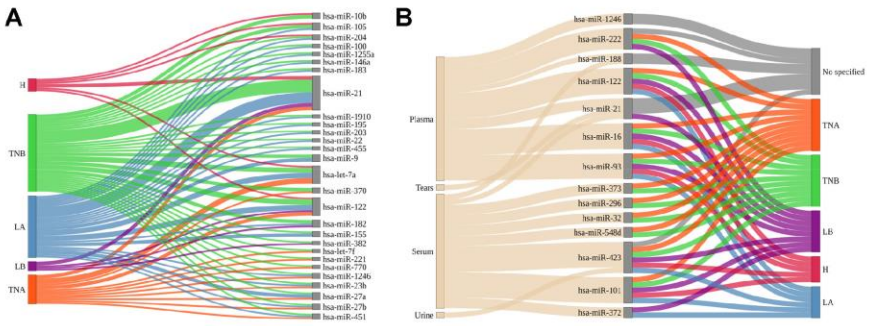

Figure 2. Extracellular vesicle (EV) miRNAs in breast-cancer-related studies. Sankey plots show the number of studies mentioning each relevant vesicular miRNA from cell supernatant (**A**) or human bodily fluids (**B**). The cell lines in which the EV cargo was analyzed are classified into the main BC subtypes following the criteria given in Dai et al.'s (2017) study [124]. For studies on EVs collected from BC patients, the subtype information was retrieved from each study. H: Her2, TNA: Triple-Negative A, TNB: Triple-Negative B, LA: Luminal A, and LB: Luminal B.

Interestingly, the miRNAs hsa-miR-21 and hsa-miR-122 were found in EVs from cell lines belonging to all the main subtypes of breast cancer following the classification provided by Dai et al. (2017) [124]. Nevertheless, it is essential to note that this review includes studies presenting both exploratory (RNA-seq, microarray, barcoding hybridization, etc.) and targeted (qRT-PCR) experiments analyzing samples from different countries/ancestral groups. Targeted analyses have broadly described oncomiRs, e.g., hsa-miR-21 [125,126] (Figure 3). Subsequently, this miRNA was extensively tested in extracellular vesicles, with the results confirming their role as an inductor of tumor processes [36–38,65,72,110] despite the existence of a minority of studies with divergent results [90]. In addition, Arisan et al., 2021 demonstrated that vesicular hsa-miR-21 facilitates the expansion of breast cancer cells favoring the epithelial–mesenchymal transition (EMT) by targeting Wnt-11 [66]. Moreover, this miRNA can support bone metastasis via the inhibition of PDCD4 [36,110] and cancer-related thrombosis by blocking IL6R in endothelial progenitor cells [65]. Regarding their involvement in the tumor microenvironment, Donnarumma et al. (2017) suggested that hsa-miR-21 could be transferred from cancer-associated fibroblasts (CAFs) to breast cancer cells via exosomes [127]. The horizontal transfer from this miRNA creates a self-regulating cycle that drives the presence of hsa-miR-21 in tumor cells.

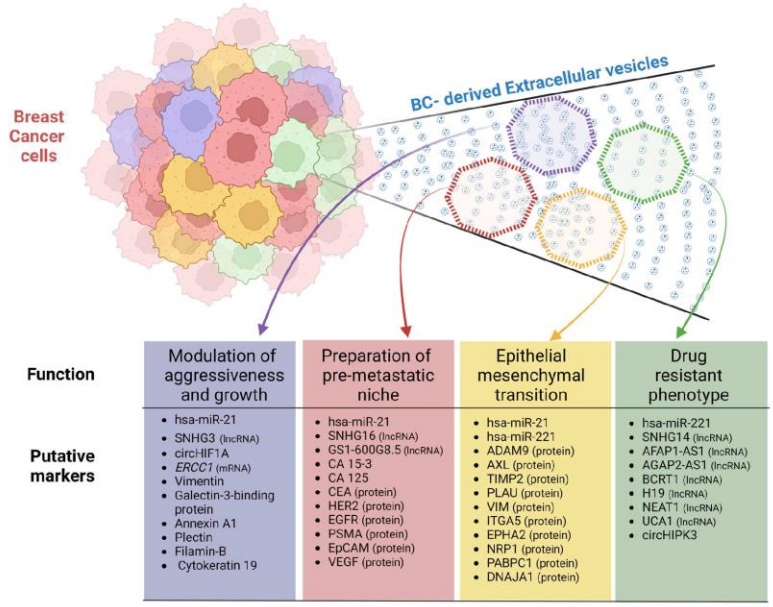

Figure 3. Relevant putative markers in BC-derived EVs. Breast cancer cells produce a great diversity of EVs. These EVs can be classified into subpopulations based on their proteomic and transcriptomic cargo. In this review, we associate some BC-derived EV subpopulations with tumor-related functions. In addition, we include putative markers related to their types (miRNA, lncRNA, mRNA, circRNA, or protein) for each subpopulation. Image created on BioRender.com.

On the other hand, other microRNAs like hsa-let-7f, hsa-miR-221, and hsa-miR-770 have consistently been found in EVs from Triple-Negative BC (TNBC) cells (TNA and TNB groups, Figure 2A). Interestingly, Wei et al. (2014) showed that vesicular hsa-miR-221 induced tamoxifen resistance in MCF7 cells (Luminal A subtype) by repressing the

expression of p27 and ERα [76]. However, if an estrogen-receptor-positive BC cell receives hsa-miR-221 from an estrogen-receptor-negative cell through EVs, it induces the repression of the receptor via the MAPK pathway [128] (Figure 3). In TNBC, this vesicular miRNA will induce an EMT by targeting PTEN while also stimulating the expression of mesenchymal markers such as Snail, Slug, N-cadherin, and vimentin [75]. These findings support the hypothesis that specific components of vesicular cargo can modulate the aggressiveness of cell lines.

Nevertheless, one should keep in mind that these findings raise some concerns about the similarity of cargoes between EVs produced by pure cell lines and those captured via liquid biopsies that are secreted by multiple and heterogeneous types of cells, including breast tumors and non-malignant cells such as platelets. Among all the vesicular miRNAs observed in body fluids (Figure 2B), there is still a notable difference between miRNAs found in EVs from plasma and serum. Although these sources can be separated from blood, they have been reported to include different EV-related compositions [129,130] and, according to this review, varied cargoes as well. Intriguingly, hsa-miR-21 and hsa-miR-188 were consistently found in EVs from the plasma and serum of BC patients (Figure 2B). In addition, the study conducted by Inubushi et al. (2020) described the presence of hsa-miR-21 in the tears of BC patients [118]. Since cancer research is moving toward analyzing liquid biopsy sources, these efforts are intended to improve the screening and selection of candidates who will undergo solid biopsies (which are highly invasive). More recently, the scientific community has been interested in classifying studies using systemic liquid biopsy sources (blood, plasma, or serum) and local liquid biopsies (tears or urine), with the latter group guaranteeing completely noninvasive tests. Therefore, further research in this field of study is warranted in order to assess its feasibility.

A frequently encountered difficulty in characterizing EVs from body fluids concerns the specific tumor subtype of each patient cohort (Figure 1). In our review, we identified hsa-miR-373, hsa-miR-296, hsa-miR-32, and hsa-miR-548d that were exclusively expressed in EVs from the serum of TNBC patients. In addition, hsa-miR-373 was found in the EVs of luminal BC patients [113]. A few years later, hsa-miR-27a/b, hsa-miR-335, hsa-miR-365, hsa-miR-376c, hsa-miR-382, hsa-miR-422a, hsa-miR-433, and hsa-miR-628 were found to be differentially expressed in plasma small vesicles (classified by the authors as exosomes) from either TNBC or HER2+ patients compared to healthy individuals. Moreover, the authors found that a specific set of microRNAs composed of hsa-miR-16, hsa-miR-328, and hsa-miR-660 was associated with lymph node status among HER2+ patients, indicating that vesicular microRNA can also be associated with clinicopathological characteristics [131]. Interestingly, based on the increased abundance of hsa-miR-150-5p, hsa-miR-576-3p, and hsa-miR-4665-5p in exosomes from the plasma of BC patients, Wu et al. (2020) were able to distinguish patients with recurrence from patients without disease recurrence [132]. Finally, in this review, we identified the following vesicular miRNAs present in patients from all BC subtypes: hsa-miR-122, hsa-miR-16, hsa-miR-93, hsa-miR-423, and hsa-miR-101. Tissue-specific alterations are associated with different expression profiles such as HER-2 overexpression [121], TNBC [91,133], or the stem-like profile among basal-like ductal carcinoma in situ (DCIS) tumors [134], demonstrating the possibility of modifying levels of vesicular miRNAs. Once these findings have been consistently reported by studies performed on different BC cohorts, we believe these miRNAs deserve further attention as potential BC biomarkers in EVs.

In addition, short non-coding RNAs, including miRNA and siRNA, are potential therapeutic options. In this case, it is possible to transfect nucleic acids in extracellular vesicles to induce transcriptional changes in recipient cells. For example, the suppressor miRNA hsa-let-7a was used to design anti-tumor extracellular vesicles for targeting EGFR [68] and c-Myc [79] to repress tumor growth. Subsequently, Bose et al. (2018) suggested editing tumor-derived EVs from SKBR3 BC cells so that they included Cy5-anti-miR-21 in their cargo. This technique allowed for the inhibition of the oncogenic hsa-miR-21 and the tracking of the biodistribution of these tumor-derived EVs [135]. Afterward, the same group

developed an engineered version of Evs coated on polymeric nanocarriers and loaded with anti-miR-21 and anti-miR-10b [70]. The prototype was tested in an in vivo model of TNBC that demonstrated an improved biodistribution to the tumor and the ability to exert a synergic effect with doxorubicin to control tumor growth.

Following this concept, Taghikhani et al., 2018 modified the cargo of tumor-derived extracellular vesicles so that they included higher concentrations of hsa-miR-155, hsa-miR-142, and hsa-let-7i for the further treatment of immature dendritic cells [136]. Their results showed that vesicular hsa-let-7i, enhanced by hsa-miR-155 and hsa-miR-142, acted as a cell-free vaccine for cancer treatment by inducing the maturation of dendritic cells. Using this characteristic, some studies have proposed the modification of autologous BC-derived EVs including siS100A4 [137] and ASO-1537S [138]. siS100A4 targets S100A4, a previously reported gene for the EMT in cancer [139], whereas ASO-1537S is an antisense oligonucleotide against 1537S, a non-coding mitochondrial RNA identified in oncogenic processes [138]. After these insertions, modified EVs prevented metastasis in an in vivo model for BC, providing a non-immunogenic method of transferring information and controlling cancer.

On the other hand, research on suppressor miRNA that is lowly expressed in tumor-derived EVs also opens a new window for therapy development. According to Zhou et al., (2021), BC cells treated with EVs carrying hsa-miR-424-5p, a suppressor miRNA, inhibited their growth though the miRNA-driven repression of PD-L1 [140].

Amalgamating these precedents, researchers have proposed new tools for cell editing using EVs (Figure 1). The main idea is to select (or develop) specific subpopulations of EVs that we can use to target cancer cells or change their environments. Nevertheless, although the use of vesicular microRNAs for diagnosis and prognosis seems promising, no panels of EV microRNAs are available for BC diagnosis in a clinical setting due to a lack of standardization and reproducibility concerning EV isolation and microRNA identification, as discussed in the final section (Figure 1).

2.2. Other Regulatory Non-Coding RNAs in BC-Related EVs

As described above, vesicular miRNAs can inhibit mRNA expression in their target cell. Then, oncomiRs repress tumor suppressors, and suppressor miRNAs inhibit the expression of tumor promoters. Nevertheless, exploratory techniques such as RNA-seq have supported the discovery of competing endogenous RNA (ceRNA) in BC-derived EVs [24,43]. This type of RNA can attract miRNAs by competing with their mRNA targets, thereby adding a new level of EV-based expression regulation. Herein, a ceRNA can inhibit a suppressor miRNA in order to induce the overexpression of the mRNA target, which stimulates tumor growth.

Some lncRNAs, a type of ceRNA, have been reported to be overexpressed in EVs from BC tissues, cells, and human fluids. For example, the lncRNAs SNHG16 [141,142], HOTAIR [143], H19 [144], SNHG14 [145], AFAP1-AS1 [146], AGAP2-AS1 [147,148], BCRT1 [149], UCA1 [150], GS1-600G8.5 [151], and NEAT1 [152] were found to be overexpressed in BC-derived EVs (Figure 3). Moreover, they have demonstrated their ability to induce new features in recipient cells.

SNHG14, AFAP1-AS1, AGAP2-AS1, and BCRT1 have been proven to be carried by tumor-derived EVs in order to induce trastuzumab resistance in BC cells (Figure 3). Interestingly, they achieve the same outcome in different ways. SNHG14 affects the Bcl-2 apoptosis pathway [145]; AFAP1-AS1 stimulates the overproduction of HER2, leading to treatment ineffectiveness [146]; AGAP2-AS1 is packaged in vesicles by hnRNPA2B1 [148] to link ELAVL1 in the receptor cell in order to modulate autophagy activity via the transcription of ATG10 [147]; and BCRT1 inhibits hsa-miR-1303 in order to induce the expression of PTBP3, a tumor promoter and target of hsa-miR-1303 [149]. Moreover, other studies have shown that vesicular H19, NEAT1, and UCA1 lncRNAs induce resistance to doxorubicin [144], cisplatin/paclitaxel [152], and tamoxifen [150], respectively. In all cases, it is possible to revert treatment resistance by silencing the respective lncRNA.

Tumor growth and metastatic expansion are processes that involve many molecular regulations. Accordingly, the mRNA–miRNA–lncRNA axis is analyzed to understand cancer biology. This reseaerch explains how tumor-derived EVs help to disseminate a competitive advantage among cancer cells. However, in some cases, they can "educate" neighboring epithelial and immune cells in terms of facilitating tumor expansion. For example, vesicular SNHG16 lncRNA induces metastasis by blocking hsa-miR-892 in BC cells; this action naturally represses PPAPDC1A, a metastasis promoter [142]. But the same lncRNA is able to block hsa-miR-16-5p in γδT1 lymphocytes in order to induce SMAD5 expression, which upregulates CD73 at the membrane of these tumor-infiltrating lymphocytes [141]. Vesicular BCRT1 induces M2 polarization in macrophages, thereby boosting BC progression [149]. Also, the presence of vesicular GS1-600G8.5 was associated with the destruction of the blood–brain barrier, thus facilitating brain metastases in BC patients [151].

In the same way that vesicular lncRNA from BC cells can modify the metabolism of other cell types, EVs produced in other cell types affect tumor growth. As an example, BC-modulating vesicular HISLA and SNHG3 lncRNAs are expressed in tumor-associated macrophages (TAM) and cancer-associated fibroblasts (CAF), respectively. HISLA obstructs the interaction between PHD2 and HIF-1α that leads to the accumulation of HIF-1α, which regulates glycolytic metabolism in the tumor cell [153]. SNHG3 sponges hsa-miR-330-5p in tumor cells that positively regulate PKM, thereby increasing tumor growth [154]. However, the transcriptome from BC-derived EVs also includes suppressor lncRNAs such as XIST, whose repression promotes brain metastasis in BC patients [155]. The absence of XIST induces an accumulation of hsa-miR-503, which triggers M1-M2 polarization, thereby suppressing T-cell proliferation and, in turn, facilitating tumor expansion.

For the time being, we have limited information regarding circRNAs. Some descriptive studies have described circHIPK3 [156], circHIF1A [157], hsa-circRNA-000615 [158], hsa-circRNA-0005795, and hsa-circRNA-0088088 [159] as being overexpressed in BC-derived EVs playing vital roles in BC development (Figure 3). Interestingly, circHIPK3 was associated with trastuzumab resistance [156]. Moreover, circHIF1A was identified as an oncogenic RNA because it downregulates hsa-miR-149-5p levels [157]. Subsequently, low levels of hsa-miR-149-5p induce overexpression of NFIB, an oncogenic promoter that functions via p21 inhibition.

2.3. Messenger RNA (mRNA) in BC-Related EVs

Besides regulating RNA, some studies have shown that mRNA is present in EVs derived from or targeting BC cells. A few years ago, Conley and co-authors identified an mRNA signature of this disease in EVs from breast cancer patients at advanced stages [34]. Under the same context, Rodríguez et al. (2015) found elevated levels of eight metastasis-related mRNAs and 27 stemness-related mRNAs in exosomes from breast cancer patients with poor prognosis, suggesting that exo-mRNA can be used as a prognostic marker for BC patients [160].

Andreeva et al., 2021 have demonstrated that *PIK3CA* mutations can be transferred between BC cell lines via their EVs [33]. Using RNA and DNA sequencing, this study described the presence of mutated versions of the PIK3CA gene in EVs from BC cell lines. BC-derived EVs have been observed overexpressing some mRNAs. According to Rodríguez et al. (2015), vesicular levels of *HTR7*, *NEUROD1*, and *HOXC6* mRNA are related to disease-free survival among BC patients ($p < 0.05$), while *NANOG*, *HTR7*, *NEUROD1*, and *HOXC6* mRNA levels are associated with overall survival ($p < 0.05$) [160]. Moreover, vesicular *ERCC1* mRNA could be indicative of tumor progression (Figure 3) via their association with metastatic BC ($p = 0.03$) [161]. Furthermore, mRNA transcripts packaged inside tumor-derived EVs can be used as a disease indicator through liquid biopsy as proposed by Hu et al. (2023) [162]. To achieve this, the authors propose isolating different subsets of EVs using mAbs targeting tumor epitopes. Subsequently, they demonstrated that the mRNA profiling results from PAM50 genes of specific subtypes of vesicles from breast cancer

patients were 100% in accordance with the tumor tissue and could be used to predict BC subtypes using minimally invasive methods.

On the other hand, different cell types can transmit growth signals to BC cells via EVs. Yao et al., 2019 demonstrated that platelets from BC patients overexpress *TPM3* mRNA and transfer it via EVs to BC cells in order to promote their growth [163].

However, it should be mentioned that these studies face challenges relating to the low abundance of vesicular RNAs and the lack of housekeeping RNA species with which to make comparisons between different samples. Indeed, these important issues push scientists in the field to discuss the standardization of and guidelines for EV RNA analysis (Figure 1). Within this context, Gorji-Bahri et al., 2021 have proposed using the *YWHAZ* gene alone or in combination with *GAPDH* and *UBC* as stable values for vesicular RNA quantification [164].

2.4. DNA Profiles in Breast Cancer-Derived EVs

Interestingly, besides the presence of PIK3CA mRNA in BC-derived EVs, Andreeva and co-authors also found fragments of mutated DNA in these nanocompartments [33]. Accordingly, one might assume that EVs can contribute to the discarding or transmission of pathogenic variants present in one cell to another. Ruhen et al. (2021) also demonstrated that tumors export Copy Number Variations (CNVs) through EVs. Although the transference of somatic mutations has been reported before in the form of circulating tumor DNA (ctDNA), some of these mutated copies are sheltered by EVs that allow for their direct detection using highly sensitive technologies [44].

Moreover, some studies have described the presence of mtDNA in BC-derived EVs. Fragments of mtDNA in BC-derived EVs are associated with invasiveness via the activation of Toll-like receptor 9 [165], chemoresistance in TNBC cells [166], and escape from metabolic quiescence in hormone-therapy-resistant BC via estrogen-receptor-independent oxidative phosphorylation [167]. As it has been shown, this is a hitherto unexplored field that needs more research, mainly to determine the genes responsible for mtDNA transmission that can serve as candidates for gene therapy (Figure 1). Although the *PINK1* gene was identified as a driver of mtDNA-carrying EVs [165], there are likely other drivers of this feature.

In addition, non-human DNA was also reported in BC-derived EVs. This is the case of HPV-positive EVs isolated from the serum of BC patients [45]. There is an important finding that could extend liquid biopsy features for the determination of viral subtypes in EV from patients as demonstrated by De Carolis et al., 2019 [45]. Although vesicular RNA has shown better information delivery characteristics than DNA [168], EVs serve as important tools for cellular communication that evades immune control. Therefore, EVs, their molecular topography, and their cargo deserve further attention.

Overall, the nucleic acid composition of BC-derived vesicles is highly diverse. Furthermore, some of these components are related to tumor processes such as the modulation of aggressiveness, the EMT, the preparation of the metastatic niche, and treatment resistance. Although EVs cannot deliver many nucleic acids per particle [22] (Figure 1), we present an overview of the relevant nucleic-acid-based markers in Figure 3.

3. Proteome of EVs in Breast Cancer

3.1. Analysis of BC-Related EV Proteomes Using High-Throughput Technologies

In order to elucidate the role of EV-related proteins during breast cancer pathogenesis, we reviewed the literature to determine the proteomes of EVs associated with breast cancer. A total of 21 studies [14,169–188] that analyzed EVs from human breast cancer cell lines and biofluids using high-throughput and exploratory technologies were selected. A total of 8312 proteins were reported. The proteins were divided into core level 1 (protein identification in 50–100% of studies), core level 2 (protein identification in 40–50% of the studies), and core level 3 (protein identification in less than 40% of the studies), and they are reported in Supplementary Table S2 [14,169–188]. Six and twenty-six proteins were assigned to cores 1 and 2, respectively. Although these data indicate high variability in

the qualitative proteome content of EVs associated with breast cancer (Figure 1), we selected a few studies that evaluated methodological strategies for isolating EVs from breast cancer cells and biofluids and characterized their protein content. As many proteomic results were produced using BC cell lines, we used the classification system developed by Dai et al. (2017) to standardize the nomenclature and disease subtypes potentially represented by these cell lines [124].

Harris et al., 2015 investigated the subcellular localization of proteins found in the EVs of three BC cell lines with different types of metastatic profiles, namely, MDA-MB-231 (Triple-negative B subtype), MCF-7 overexpressing Rab27b, and MCF-7 (Luminal A subtype), and found several cellular localizations (the majority were from cytoplasm/cytoskeleton and integral/peripheral membrane proteins) and a minor proportion of EV proteins from the Golgi apparatus, ER, or mitochondria [14].

Regarding the molecular functions of the EV proteins, the majority displayed a protein-binding function and hydrolase activity. Comparing the EV protein expression between the three cell lines, 85 proteins were differentially expressed, with the non-invasive breast cancer cell line (MCF-7, Luminal A subtype) containing several up-regulated proteins with a tumor suppression function. Among the up-regulated proteins in MCF-7 compared to MDA-MB-231 were Tetraspanin (CD63, CD81, CD9, and Tetraspanin-14), Adhesion proteins (Neural cell adhesion molecule 2, Integrin alpha-V, Integrin beta-5, Epithelial cell adhesion molecule, Alpha-Parvin, Claudin-3, Cadherin-1, CD99, CD276, and Clusterin), stress response proteins (Heat shock protein beta-1), Small GTPase superfamily proteins (Rho-related GTP-binding protein RhoB, GTPase NRas, Ras-related protein Rap-2c, and RacGTPase-activating protein 1), and Endosome Trafficking/Transport proteins (Multivesicular body subunit 12B, Vacuolar protein sorting-associated protein 28 homolog, Vacuolar protein sorting-associated protein 37B, and Multivesicular body subunit 12A) [14]. The up-regulated proteins in MDA-MB-231 and MCF-7 overexpressing Rab27b compared to wild-type MCF-7 were adhesion/motility/cytoskeleton proteins (Vimentin, Galectin-3-binding protein, Annexin A1, Plectin, and Filamin-B), cell-surface receptor proteins (Ephrin type-A receptor 2), and stress response proteins (Protein NDRG1, Stress-70 protein, mitochondrial, and heat shock protein HSP 90-beta). Many of these proteins that were dysregulated in both cell lines are associated with tumorigenesis and metastasis [14] (Figure 3). Another protein of the Rab family, Rab5a, was associated with high migration and invasion rates in MDA-MB-231 cells along with the promotion of high rates of vesicle shedding. Interestingly, this process could be externally regulated by activating protease-activated receptor 2 (PAR2), using trypsin or coagulation factor-FVIIa to promote the accumulation of Rab5a [15,16].

Kruger et al., 2014 performed a molecular characterization of EVs from MCF-7 and MDA-MB-231 BC cells [188]. Using sucrose gradient ultracentrifugation and LC-MS/MS, the authors identified 59 and 88 proteins in MCF-7 and MDA-MB-231 EVs, respectively. The identified proteins were grouped based on molecular functions, such as catalytic activity, protein transport, adhesion, and extracellular matrix activity. Both EVs isolated from MCF-7 and MDA-MB-231 supernatants presented differences in their protein content. The MCF-7-derived EVs showed a greater abundance of biomolecule-binding and protein transport activity, while the MDA-MB-231-derived EVs contained proteins with catalytic activity. Moreover, 24% of the EV proteins of MDA-MB-231 were extracellular matrix proteins. These findings can be correlated with the higher metastatic potential of MDA-MB-231 (Triple-negative B subtype) compared to MCF-7 cells (Luminal A subtype) [188].

This study reported several proteins identified in both MDA-MB-231 and MCF-7 EVs, such as proteins from the Annexin family (Figure 3), Histone H4, and Calmodulin. Furthermore, the common EV proteins participate in cellular growth, signaling pathways, epigenomic alterations, DNA and histone methyltransferase, and Akt pathway regulation [189]. Moreover, these processes can be related to the malignancy of cancer cells and the poor prognosis of breast cancer [190]. Heinemann et al., 2014 used the MDA-MB-231 breast cancer cell line to develop a simple and efficient method for purifying cancer exo-

somes [183]. A three-step filtration method was implemented as the first step of a normal flow prefiltration using a 0.1 µm filter to remove larger constituents such as intact cells and cell debris. In the second step, tangential flow filtration using a 500kDa membrane filter was performed in order to remove proteins, and the retentate was passed to the third step, namely, track-etch filtration, where low pressure is applied using a 0.1 µm filter to isolate exosomes and remove microvesicles. A total of 60 unique proteins were identified sequential filtration, including the exosome marker CD63. In the exosome content, membrane trafficking proteins and proteins associated with transcription regulation, signal transduction, and the epigenetic modulation of nucleic acids were identified [183]. Regarding the heterogeneity of the vesicle entities, it is important to mention that filter-based techniques usually require the use of an automatized mechanism in order to avoid user interference during vesicle collection (Figure 1). Nevertheless, these techniques seem to support a relevant volume of EV proteomic data, so their application to EVs from different cell lines is recommended.

Smyth et al., 2014 examined the exosome proteomes from MCF-7 and PC3, cell lines of mammary gland/breast, and prostate cancers [185]. The identified exosome-delivered MCF-7 proteins were Heat Shock Proteins 70, 90, and 27; CD9; Ras-related protein 13 (RAB-13 and others); Annexins 1, 2, 5, and 7; Pyruvate kinase (PKM); Alpha-enolase (ENO1); Glyceraldehyde-3-phosphate dehydrogenase (GAPDH); Glucose-6-phosphate 1-dehydrogenase (G6PD); and actin. The functions of the exosomal proteins were related to amino acid transport, protease inhibition, the cytoskeleton, GTPase, ATPase, transcription regulation, transduction, adhesion, and chaperoning. Regarding subcellular localization, most of the proteins were in the membrane and cytoplasm; however, proteins localized in the Golgi and nucleus were also identified in MCF-7 exosomes. Moreover, it was found that the exosomal lipid composition also contributes to facilitating adherence/internalization in recipient cells [185]. The current stage of analytical methods, together with the optimization of pre-analytical factors and computational strategies, allowed for a better understanding of the EVs lipid compositions [191]. A comparison of the lipid compositions between EVs and cells of origin [192] has shown that, in vitro, EVs are more enriched in cholesterol, sphingomyelin, glycosphingolipids, and phosphatidylserine compared to their origin cells, while phosphatidylcholine and phosphatidylinositol are more enriched in cells compared to exosomes. Quantitative analyses of oxysterols in exosomes released from breast cancer cells revealed that levels of 27-Hydroxycholesterol were higher in exosomes from MCF-7 cells compared to MDA-MB-231 and non-cancerous cells, showing a dependence of the levels of this exosomal lipid on the ER status of the cell of origin [193]. Another study compared the lipid profiles of EVs isolated from TNBC cell lines, namely, D3H2LN and D3H1, with high and low metastatic potential, respectively [194]. The exosomal levels of unsaturated diacylglycerols isolated from the highly metastatic cells were higher and stimulated angiogenesis through the protein kinase D signaling pathway.

The EVs isolated from the MCF10 and MDA-MB231 cell lines shared proteins such as regulators of cell death, membrane components, adhesion, and cell motility proteins. The EVs from MDA-MB-231 were enriched in proteins associated with transcriptional regulation, proteolysis, EV formation (annexin, LAMP-1), cell cycle (NUMA1), and adherence to extracellular matrices (EDIL3, collagen, vitronectin). These results showed differences in the EV protein content of invasive and non-invasive breast cancer cells, which can contribute to the metastatic process [171].

The EV proteomes of two tumorigenic breast cancer cell lines, invasive (SKBR3, Her2 subtype) and non-invasive (MCF-7), were compared to non-tumorigenic MCF-10a. In this study, the authors used a synthetic peptide (Vn96) with a high affinity for heat shock proteins (highly expressed in cancer cells) to isolate EVs. Heat shock proteins are present on the exosome surface, binding to Vn96 and facilitating EV recovery [195]. In total, 392 (SKBR3) and 301 (MCF-7) exosomal proteins were identified, and they were associated with membranes (19%) and the cell surface (12%). The functions of EV proteins from SKBR3 are related to metabolism (enolase, fatty acid synthase, phosphoglycerate kinase,

fructose bisphosphatase 1, GAPDH, malate dehydrogenase, L-lactate dehydrogenase, aldehyde dehydrogenase, aldolase, triosephosphate isomerase, and glucosidase 2 subunit beta), binding (Selenium-binding protein 1, 60 kDa heat shock protein, Protein disulfide-isomerase, Lamin A/C, and Tumor protein D52), and assembly (Myosin-9, alpha-Actinin-4, Cytokeratin 16, Cytokeratin 18, Cytokeratin 8, and Cytokeratin 19). Although MCF-7 EV protein content displayed the same molecular function as SKBR3, different proteins were identified, namely, Aldolase, Pyruvate kinase, Tryptophan-tRNA ligase, Cathepsin D, Kynureninase, TER ATPase, Lactoferroxin-C, and Hexokinase-1, which are involved in metabolism, and HSP90-a, Agrin, and protein SET are related to binding. Cytokeratin 19, which was identified in both SKBR3 and MCF-7 EVs, has been suggested to be involved in more aggressive tumor proliferation, metastasis, and invasion [196] (Figure 3). Cytokeratin 8 and 18 were reported to be secreted cancer biomarkers when detected in the serum of breast cancer patients [197]. EV proteins from SKBR3 (Her2 subtype) and MCF-7 (Luminal A subtype) cells are involved in lipogenesis, glycolysis/gluconeogenesis, and tricarboxylic acid, corroborating the important role of altered metabolism in cancer. Moreover, glycolytic enzymes can protect cancer cells from stress by inhibiting apoptosis [198]. Taken together, these data show that EV cargo is associated with the progression, proliferation, metabolic control, and malignancy of breast cancer (Figure 3).

Koh et al., 2021 analyzed the modulation of the plasma EV proteome of breast cancer patients with and without cognitive impairment following anthracycline-based treatment [187]. Plasma from the early-stage breast cancer patients was collected longitudinally at three different time points (before the start of chemotherapy, 3 weeks after cycle 2 of chemotherapy, and 3 weeks of the last cycle of chemotherapy) from two groups (cognitive non-impaired and impaired). Circulating EVs were isolated through ultracentrifugation and analyzed using Tandem-Mass-Tag (TMT)-based quantitative proteomics. A total of 517 regulated proteins were identified in the cognitive impairment group, which was compared to a non-impairment group at three time points. Among these regulated proteins were EV markers, such as CD9, TSPAN14, and CD5L. Moreover, a down-regulation of galactosylceramidase from the plasma EV protein content was observed in the cognitive non-impaired group at timepoint T3 compared to T1. On the other hand, p2X purinoceptor and cofilin-1 were up-regulated at timepoint 3 compared to T1. In contrast, the EV content of the cognitive impairment group displayed a down-regulation of p2X purinoceptor, cofilin-1, nexilin, and ADAM10 at T3 compared to T1 [187]. In this study, the authors also analyzed N-glycosylation sites in the EV content from plasma samples. However, none of the regulated proteins were identified in the N-glycosylation analysis. However, CD5L, which is an EV marker, displayed two glycosylation sites in both groups (non-impaired and impaired). An altered N-glycosylation profile was identified in CD5L peptides, which presented decreased glycosylation in the non-impaired group. These findings contribute to our understanding of how different omics characteristics interact between EVs, their cells of origin, and their destination. Nevertheless, due to the heterogeneity of the tumor itself as well as the intra and interpatient heterogeneity (Figure 1), further studies would need to include more available information about the clinical statuses of these patients (age at diagnosis, molecular subtype, immunohistochemical profiles, etc.) in order to find patterns in the EV-related markers using large-scale cohort analyses.

The EVs released from cancer cells can regulate specific biological processes in recipient cells and modulate the central nervous system, thereby impairing the cognitive abilities of breast cancer patients [187]. Jordan et al., analyzed the differences in the protein cargo of EVs isolated from breast cancer cell lines and the plasma of breast cancer patients and healthy donors to identify the structural features that contribute to altered functional activities [171]. EVs from peripheral plasma samples of patients presented an increased degree of invasion of non-invasive breast cancer cells. Breast cancer plasma EVs displayed a unique proteome profile, with typical EV markers, such as CD9, CD81, CD63, and HSP70; Rab proteins; and clathrin. Moreover, the data were used in a comparison between the gene expression of MCF-10 treated with EVs obtained from breast cancer plasma patients,

healthy donors, MDA-MB-231 cells, and untreated cells. The results displayed altered gene expression associated with angiogenesis, cell adhesion, and proliferation. In particular, it was confirmed that EVs released from aggressive breast cancer cells could stimulate the invasive behavior of non-invasive breast cancer cells. Moreover, the EV content from breast cancer patients can be used as a biomarker once these EVs contain a specific set of proteins [171].

3.2. Protein Markers in EVs Associated with Breast Cancer Features

Cancer-delivered EVs are a potential source of markers due to the fact that the cargo of EVs is enriched with molecules associated with tumor progression, metastasis, and invasion [199–201]. Rontogianni et al., analyzed the proteome content of EVs to discriminate cancer types and subtypes [176]. For this analysis, the authors used ten BC cell lines to identify a protein signature in EVs for use as a biomarker for breast cancer monitoring, diagnosis, and subtyping. Among the 4676 identified proteins, 14-3-3 proteins, integrins, annexin proteins, and cytoskeletal proteins, which are required for intermediate EV formation, were identified in all ten cancer cell lines. To discriminate the breast cancer subtypes, a total of 64 proteins were differentially expressed in TNBC compared to HER2+; these proteins are involved in angiogenesis (PLAU, ADAM9, and EPHA2), integrin-binding (ITGA5 and TIMP2), and cell motility (VIM and AXL). HER2+ EVs presented proteins associated with translation (EIFs), axon guidance (DNM2 and PIK3R1), and ERBB signaling (GRB7 and SHC1). Periostin, an extracellular matrix component, was described as a metastatic breast cancer biomarker identified in exosomes. It was observed that this protein was up-regulated in both murine and human cancer cell lines. Periostin has been reported to be highly expressed in several cancer types, including breast cancer [202], and it has been associated with osteoblast adhesion and cancer cell migration and is also involved in tumor angiogenesis [203]. Increased abundance of the Transient Receptor Potential Channel 5 (TrpC5) in EVs was observed in adriamycin-resistant human breast cancer cells (MCF-7/ADM) and was correlated with EV formation; additionally, adriamycin was found in EVs. The transference of TrpC5 to recipient cells mediated by EVs allows recipient cells to acquire TrpC5 and to P-glycoprotein multidrug transporter expression, conferring chemoresistance to non-resistance cells [204]. Considering the relevance of studies involving several BC cell lines, there are two main factors that must be considered. First, previous studies on tumor-derived EVs have determined that culture conditions can affect the omics components of EV cargo [205]. Second, despite the above, it is necessary to have a reliable collection of vesicular omics data from BC cell lines to find consistent markers for further research (Figure 1).

Regarding the use of liquid biopsies in relation to metastatic breast cancer, in one study, EV proteins were monitored to identify potential biomarkers for prognostics using a thermophoretic aptasensor. A total of 286 plasma samples from metastatic patients, non-metastatic patients, and healthy donors were submitted to a thermophoretic aptasensor to obtain a profile of eight EV markers (Figure 3): CA 15-3, CA 125, carcinoembryonic antigen (CEA), human epidermal growth factor receptor 2 (HER2), epidermal growth factor receptor (EGFR), prostate-specific membrane antigen (PSMA), epithelial cell adhesion molecule (EpCAM), and vascular endothelial growth factor (VEGF). These markers are involved in survival and migration, cell proliferation, metastasis, invasion, cell stemness, vascular permeability, and angiogenesis [200]. In an independent study, sera-derived exosomes from breast cancer patients were used to characterize CD24 and EpCAM as markers for exosomes (Figure 3). Western-blotting analysis was performed to identify exosomal markers in breast cancer samples. EpCAM and CD24 were identified in exosomes isolated from ascites ovarian cancer patients. However, only CD24 was detected in the EVs isolated from the serum of breast cancer patients. The absence of EpCAM in the serum-derived exosomes from breast cancer can be explained by the cleavage of EpCAM by serum metalloproteinases and the fact that both CD24 and EpCAM are not present in the same EV populations, which was confirmed in this study after the immunoaffinity purification of exosomes using anti-

EpCAM beads [206]. Taken together, these studies show the importance of EV proteins as breast cancer markers for clinical use in order to diagnose, stratify, and monitor breast cancer progression.

3.3. EV Protein Glycosylation in Breast Cancer

Glycoconjugates such as glycoproteins functionally decorate the cell surface and are released in the extracellular milieu, playing an essential role in cell communication with the extracellular environment in several pathophysiological conditions, including cancer [207,208]. Any alteration in glycosylation levels due to the variation in the expression of glycosyltransferases and glycosidases [209], the dysregulation of chaperone activity [210], different levels of substrates, and alterations in nucleotide sugar transporter levels are diagnostic signs in cancer [211]. Aberrant glycosylation in tumor cells influences angiogenesis, cell proliferation, invasion, and metastatic processes [212–215]. The surface of an EV is enriched with glycoproteins, such as the Tetraspanin CD63, which is known to regulate cancer malignancy, and glycolipids [216]. EV glycosylation has been reported in several cancer types, including breast cancer. A list of 15 studies on EV glycosylation in breast cancer was reported by Macedo-Silva et al. (2021) [217], which is provided herein in Supplementary Table S3 [169,170,172,182–185,190,218–224].

Nishida-Aoki et al. (2020) developed an EV glycosylation profile from breast cancer cells with brain metastasis tropism (BMD2a) comparing lymph node-metastatic (MDA-MB-231-luc-D3H2LN) and primary tumor-derived TNBC cell lines (MDA-MB-231-luc-D3H1) using lectin blotting [225]. The data showed a reduced level of sialic acid and a specific glycosylation pattern associated with galactose, GalNAc, lactose, and GalNAcα1−3GalNAc in BMD2a EVs. This study concluded that the glycosylation of EVs exerted an inhibitory effect on EV uptake [225]. This evidence shows that EV uptake depends on glycosylation profiles, as the authors showed that the cessation of O-glycosylation increases tumor EV accumulation in the lungs; meanwhile, N-glycosylation inhibition does not alter tumor EV biodistribution. It appears that the specific glycosylation profile in tumor EVs highlights their importance in breast cancer aggressiveness. For instance, EVs secreted by TNBC cells present higher levels of sialylation when compared to parental cells [226], and this process could interfere with EVs uptake. Sialic acid is negatively charged; its removal from the surfaces of EVs can promote the interaction of EVs and recipient cells through the uncovering of carbohydrate ligands that bind to lectins and promote the uptake of EV by recipient cells. Additionally, EV cargo contains glycosylated proteins that can interfere with EV–cell interaction. Cytokines binding to surface glycosaminoglycan side chains of proteoglycans decorate EVs isolated from breast cancer patients, altering EV biodistribution and leading to a higher metastatic burden [227]. The structure of bisecting GlcNAc glycan (β1,4-linked GlcNAc at the β-mannose residue core) on target proteins (EGFR and integrins) plays a role in cell metastasis and adhesion. The role of bisecting GlcNAc of EVs in breast cancer cells was described by Tan et al. (2020) [228]. Some proteins were described as being markers of EVs from tumor cells in breast cancer, such as extracellular matrix metalloproteinase inducer (EMMPRIN). A higher abundance of glycosylated EMMPRIN was identified in EVs from metastatic breast cancer patients. PNGase F treatment resulted in EVs' deglycosylation and inhibited EV-induced invasion [222]. Somehow, glycans being components of EV cargo seems to dictate cell function. ST6Gal1-mediated sialylation modulates cell surface receptor function, promoting cell proliferation and invasion. Hait et al., showed that ST6Gal1 RNA transcripts and protein expression were variable and heterogeneous in a panel of TNBC and ER+ cell lines. However, EVs containing ST6Gal1 potentiate aggressive cancer cell growth, proliferation, and invasion in cells containing low amounts of endogenous ST6Gal1 [229]. In a heterogeneous tumor microenvironment, EVs act as important mediators of tumor progression, dictating EV organ tropism and metastasis. CA15-3/CA27.29 epitopes from Mucin 1 were reported to be tumor markers for breast cancer diagnosis. Additionally, alterations in Mucin 1 glycosylation profiles were observed in several cancer types, including human breast cancer, and in exosomes

derived from luminal A breast carcinoma cells MCF-7 [170,230]. Extracellular matrix protein nephronectin (NPNT) could be present in a truncated or a glycosylated form in EVs secreted by mouse breast carcinoma cells [231]. N-glycosylation sites in integrin β1 modulate cell migration and the adhesion of MCF7 cells (luminal A), activating focal adhesion kinase (FAK) signaling, and these sites are crucial to integrin activity in EVs [232]. Additionally, exosomes released by MCF-7 cells after irradiation (luminal A type) increase concentrations of the enzyme GalNAc-T6, which is important for promoting epithelial–mesenchymal transition [233]. Furthermore, there is still a gap concerning whether alterations in EV glycosylation are due to changes in glycoprotein levels or changes in the expression/activity levels of glycan-modifying enzymes (Figure 1).

3.4. EV Proteome during the Metastatic Process in Breast Cancer

A screening of the literature regarding EV proteins identified in human and other species' breast cancer cells, tissues, and biofluids, focusing on the TNBC and metastatic cases, allowed us to retrieve 22 studies and a total of 7265 proteins [14,170,171,173,175–179,181,184,186–188,221,234–240] (Supplementary Table S4). Interestingly, we observed that one set of proteins was identified more frequently (Figure 4A), with HLA-A, HLA-B, A2M, ACTB, ALDOA, ANXA2, and FN1 identified in at least 13 of 22 studies that explored the vesicular proteome in breast cancer.

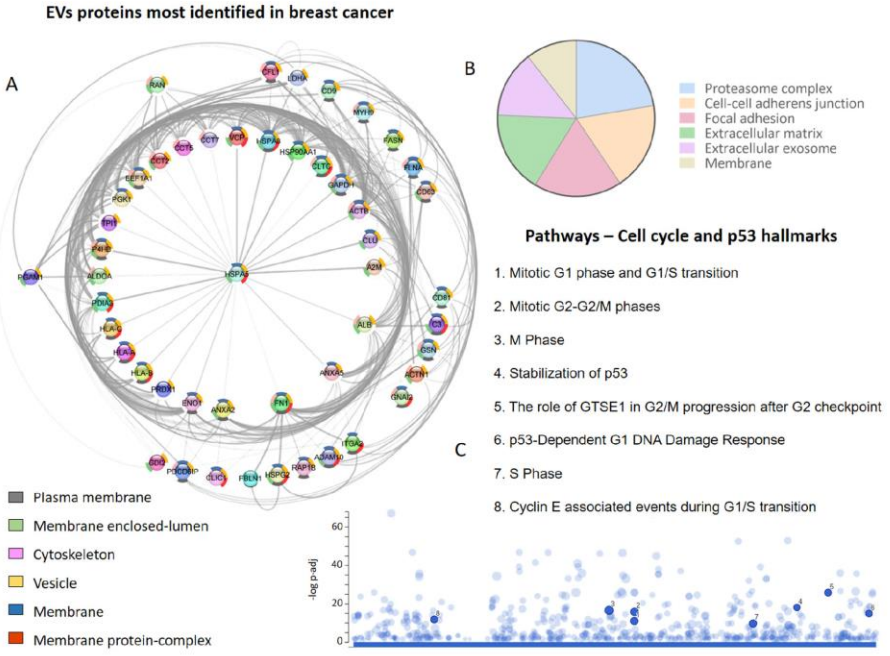

Figure 4. Extracellular vesicle (EVs) proteins in breast cancer proteome studies. (**A**) The most frequently identified proteins in the evaluated studies. The donut graph shows the corresponding subcellular locations. (**B**) Subcellular localization of proteins identified in EVs in at least two studies. (**C**) Cell-cycle-related and p53 pathways in which EV proteins participate.

Among the most frequent proteins, those located in membranes (plasma and organellar) and the cytoskeleton were particularly prominent (Figure 4A). On the other hand, after evaluating the subcellular localization of all the proteins identified at least twice in the EVs derived from breast cancer cells, it was determined that the proteasome complex, cell–cell adhesion junctions, focal adhesions, extracellular matrix, extracellular exosome, and membranes were also relevant (Figure 4B). It is possible to identify vesicular proteins that are involved in different phases of the cell cycle and the p53-linked response (Figure 4C), reinforcing the role of EVs in metastatic processes and breast cancer progression.

In fact, studies have demonstrated the crucial role of EVs in pro-metastatic processes, wherein a cancer cell's communication with its local environment is necessary to initiate growth and invasion through the transfer of molecules, which include mRNAs, microRNAs, and proteins [235]. Different studies have revealed the vesicular proteins associated with metastatic events (Table 1), and among those listed, ADAM10 (four studies), VIM (three studies), and ANXA6 (two studies) stand out. An important finding was that exosomes expressing these proteins play important roles in TNBC (Figure 3).

Table 1. Protein clusters found in EVs derived from cell lines and bodily fluids from humans with breast cancer.

Protein Clusters	Highlight	BC-Related Subtype [1] (Cell Lines) or Type of Sample (Bodily Fluids)	Reference
PDIA1, PDIA3, SUSD2, LGALS3BP, PRKCSH	The SKBR3 cell line presents a higher number of peptide spectral matches with invasion-related proteins compared to MCF7 and MCF10.	Her2 and Luminal A	[186]
FZD6, DVL1, PK1, VANGL1	Inhibition of Fzd6, Dvl1, Pk1, and Vangl1 (PCP pathway) reduced tumor cell motility.	Triple-Negative B	[238]
VIM, LGALS3BP, ANXA1, EDIL3, FLNB, TGM2, CTSD, PLAU, PRSS23, SERPINE1, CLIC1, EPHA2, NDRG1, HSPA9, HSP90AB1, SRP68	There are relatively few proteins that are differentially expressed in exosomes from MDA-MB-231 cells (invasive/metastatic) and MCF-7 cells (non-invasive/non-metastatic). However, the identified proteins that were upregulated at MDA-MB-231 have known functions in migration.	Luminal A and Triple-Negative B	[14]
C4B, EDIL3, VTN, ANXA6, NUMA1, FLNC, TXNRD1, COL5A1, PSMB4, FLNA, EEA1, ENPP1, PSMA1, ILF2, RPL12, ISG15, PSMB7, PON1, PSMD6, LAMP1, FTL, PSMC5, RPL27	EVs from young women breast cancer patients drive increased invasion of non-malignant cells via the Focal Adhesion Kinase pathway. These results suggest that the protein content of EVs from MDA-MB231 and MCF10DCIS.com cells reflects the biologic differences between these invasive and non-invasive breast cancer cells.	Triple-Negative B	[171]
ZEB1, SNAI1	EVs from metastatic cells can affect the behavior of less-aggressive neighboring cells.	Luminal A and Triple-Negative B	[237]
ADAM10	Exosomal ADAM10 increases aldehyde dehydrogenase expression in breast cancer cells through Notch receptor activation and enhances motility through the GTPase RhoA.	Triple-Negative B	[239]

Table 1. *Cont.*

Protein Clusters	Highlight	BC-Related Subtype [1] (Cell Lines) or Type of Sample (Bodily Fluids)	Reference
ADAM10	ADAM-10 expression levels are increased in exosomes from luminal cancer subtype blood in comparison with healthy patients.	Blood	[173]
PEPD, NCL, PARP1, ACTA2, ACTG2, TBCA, TTYH3, MATR3, KPNB1, KRT16, RANBP2, CCT6A	The application of protein signatures to discriminate breast cancer patients with or without metastasis yielded a sensitivity of 81% and a specificity of 81%.	Serum	[241]
CD151	CD151 levels in serum exosomes derived from TNBC were significantly higher than the levels of exosomes from healthy individuals. This protein facilitates the secretion of ribosomal proteins via exosomes while inhibiting the secretion of complement proteins. CD151-deleted exosomes significantly decreased cell migration and invasion.	Serum	[175]
ADAM9, AXL, TIMP2, PLAU, VIM, ITGA5, EPHA2, NRP1, PABPC1, DNAJA1	TNBC-specific signature proteins featured prominently in angiogenesis, cell motility and cell migration, and integrin binding.	All main subtypes	[176]
A1BG, ACSM3, ADAM10, AHSG, AMBP, APOA1, APPBP2, BANF1, BMP7, C3, CLK3, ELL2, GTSE1, HIG1AN, HMOX1, IGF2R, ITIH4, KRT1, KRT6A, KRT6B, MBD4, PCNT, PIBF1, PPM1A, SERPINA1, SERPINB7	Exosomal proteins from the blood of breast cancer patients are associated with crucial steps of tumor progression and metastasis.	Blood	[177]
ANXA5, ANXA6, VIM, CD44, EIF4A1, ITGA2, CD147, ENO1, ITGB1, FLNB, FLNA, EGFR	It was observed that the metastatic proteins ENO1 and ITGB3 were upregulated in all biological replicates of MDA-MB-231 EVs.	Luminal A and Triple-Negative B	[179]
GLUT-1, ADAM10, GPC-1	GPC-1, ADAM10, and GLUT-1 proteins may be novel potential biomarkers for breast cancer detection and prognosis.	Luminal A and Triple-Negative B	[181]

[1] Cell lines were classified into subtypes using the data reported in study conducted by Dai et al. (2017) [124].

It has been identified that the levels of the CD151 protein are increased in serum exosomes from TNBC patients, and this protein has been shown to promote proliferation, migration, and invasion by modulating the activities of laminin-binding integrins α3β1, α6β4, and α6β1 [175]. An increase in CD151 abundance was also verified in a TNBC cell model (MDA-MB-231) [181]. These results indicate that exosomal CD151 can be used as a biomarker to distinguish TNBC patients from healthy individuals.

The data gathered in Table 1 reveal the importance of other vesicular proteins in TNBC, such as VIM (three studies) and ANXA6, EDIL3, EPHA2, FLNA, FLNB, and PLAU (two studies). It has been observed that the VIM protein and its gene play important roles in controlling migration and invasion in different types of cancer [242,243]; here, it is highlighted that its location in EVs can be associated with the aggressiveness of cancer. Based on the collected data, it is possible to select possible markers of EVs in breast cancer. In addition to conventional markers such as CD9, CD81, and CD83, the proteins HLA-A,

HLA-B, HSPA5, A2M, ACTB, ALDOA, ANXA2, FN1, ANXA5, GSN, MYH9, PGK1, and ACTN1 are also often identified in EVs in cells and breast cancer patients at different stages. Therefore, these markers could be used to purify EVs potentially related to highly aggressive tumor subpopulations and study them separately (Figure 1).

4. Current Status of BC-Related Biomarkers in EVs

EVs are natural sources of cancer biomarkers. In Table 2, we summarize potential markers described as vesicular cargo.

Table 2. Features of vesicular cargo conducive to their use as potential biomarkers for breast cancer.

Markers	RNA Type	Marker Type	Comparison (Group 1 vs. Group 2)	Source	Method for EV Isolation	Total or Specific Group of EVs	Method for Vesicular RNA Isolation	Method for Vesicular RNA Quantification	Area under the Curve	Ref.
hsa-let-7a-5p and hsa-miR-222-3p	miRNA	Classification	Inflammatory BC (n = 23) vs Non-Inflammatory BC (n = 34)	Plasma	Combination of methods	Total	Organic extraction method	qRT-PCR	0.973	[100]
hsa-miR-142-5p	miRNA	Classification	TNBC (n = 15) vs. Luminal A (n = 16)	Serum	Precipitation using chemical reagent	Total	Organic extraction method	qRT-PCR	0.921	[244]
hsa-miR-4448, hsa-miR-2392, hsa-miR-2467-3p and hsa-miR-4800-3p	miRNA	Classification	recurrent TNBC (n = 12) vs. Non recurrent TNBC (n = 12)	Serum	Precipitation using chemical reagent	Total	Organic extraction method	qRT-PCR	0.765	[245]
HLA-DRB1, HAVCR1, ENPEP, TIMP1, CD36, MARCKS, DAB2, and *CXCL14*	mRNA	Diagnosis	BC patients (n = 101) vs. Healthy individuals or those with benign breast disease (n = 81)	Plasma	Affinity-based binding to spin columns	Total	Organic extraction method	qRT-PCR	0.77	[246]
PGR, ERBB2	mRNA	Diagnosis	BC patients (n = 63) vs. Healthy individuals (n = 20)	Plasma	Ultracentrifugation	Total	Affinity-based binding to spin columns	ddPCR	0.93	[35]
hsa-miR-424, hsa-miR-423, hsa-miR-660, and hsa-let-7i	miRNA	Diagnosis	BC patients (n = 69) vs. Healthy individuals (n = 40)	Urine	Size-exclusion filter	Total	Silicon-carbide-based method	qRT-PCR	0.995	[119]
hsa-miR-21	miRNA	Diagnosis	BC patients (n = 30) vs. Healthy individuals or other tumors (n = 54)	Plasma	Ultracentrifugation	Total	Organic extraction method	qRT-PCR	0.961	[39]
hsa-miR-16, hsa-miR-21, hsa-miR-429, and hsa-miR-9	miRNA	Diagnosis	BC patients (n = 62) vs. Healthy individuals (n = 20)	Plasma	Microfluidic device	CD49f and EpCAM-positive EVs	Organic extraction method	qRT-PCR	0.880	[106]

Table 2. *Cont.*

Markers	RNA Type	Marker Type	Comparison (Group 1 vs. Group 2)	Source	Method for EV Isolation	Total or Specific Group of EVs	Method for Vesicular RNA Isolation	Method for Vesicular RNA Quantification	Area under the Curve	Ref.
hsa-miR-142-5p, hsa-miR-320a, and hsa-miR-4433b-5p	miRNA	Diagnosis	BC patients (n = 31) vs. Healthy individuals (n = 16)	Serum	Precipitation using chemical reagent	Total	Organic extraction method	qRT-PCR	0.839	[244]
hsa-miR-421	miRNA	Diagnosis	BC patients (n = 20) vs. Healthy individuals (n = 10)	Plasma	Ultracentrifugation	Total	Organic extraction method	qRT-PCR	0.835	[115]
hsa-miR-421	miRNA	Diagnosis	stage I BC patients (n = 13) vs. Healthy individuals (n = 10)	Plasma	Ultracentrifugation	Total	Organic extraction method	qRT-PCR	0.809	[115]
hsa-miR-375, hsa-miR-655-3p, hsa-miR-548b-5p, and hsa-miR-24-2-5p	miRNA	Diagnosis	stage I BC patients (n = 12) vs. Healthy individuals (n = 10)	Plasma	Precipitation using chemical reagent	Total	Organic extraction method	RNA-seq	0.808	[104]
hsa-miR-17-5p	miRNA	Diagnosis	BC patients (n = 83) vs. Healthy individuals (n = 34)	Serum	NA	NA	NA	qRT-PCR	0.784	[247]
hsa-miR-1246 and hsa-miR-21	miRNA	Diagnosis	BC patients (n = 16) vs. Healthy individuals (n = 16)	Plasma	Combination of methods	Total	Organic extraction method	RNA-seq	0.727	[38]
BEX2, AC104843.1, AL136981.2, KRT19, NPM1P25, CTSC, CBR3, HOXB7, AL691447.3, RNA5SP141, and circRNA chr13_42953948_42970670_-	lncRNA/cir-cRNA	Diagnosis	stages I-II BC patients (n = 63) vs. Healthy individuals or those with benign breast disease (n = 60)	Plasma	Affinity-based binding to spin columns	Total	Organic extraction method	RNA-seq	0.940	[248]
HOTAIR	lncRNA	Diagnosis	BC patients (n = 15) vs. Healthy individuals (n = 15)	Serum	Combination of methods	Total	Affinity-based binding to spin columns	qRT-PCR	0.918	[249]
H19	lncRNA	Diagnosis	BC patients (n = 50) vs. Healthy individuals or those with benign breast disease (n = 100)	Serum	Precipitation using chemical reagent	Total	Organic extraction method	qRT-PCR	0.870	[250]
hsa-miR-150-5p	miRNA	Prognosis	Recurrent BC (n = 12) vs. non-recurrent BC (n = 15)	Plasma	Precipitation using chemical reagent	Total	Organic extraction method	RNA-seq	0.705	[132]

Table 2. *Cont.*

Markers	RNA Type	Marker Type	Comparison (Group 1 vs. Group 2)	Source	Method for EV Isolation	Total or Specific Group of EVs	Method for Vesicular RNA Isolation	Method for Vesicular RNA Quantification	Area under the Curve	Ref.
hsa-miR-1246 and hsa-miR-155	miRNA	Treatment Response Prediction	Tratuzumab-resistant (n = 32) vs. Trastuzumab-sensitive BC patients (n = 36)	Plasma	Precipitation using chemical reagent	Total	Magnetic-beads-based method	qRT-PCR	0.898	[98]
MSMO1	lncRNA	Treatment Response Prediction	Patients with PCR (n = 24) vs patients with no-PCR after treatment with NACT (n = 34)	Plasma	Affinity-based binding to spin columns	Total	Organic extraction method	RNA-seq	0.79	[248]

Ref.: Reference; BC: Breast Cancer; TNBC: Triple-Negative Breast Cancer; EV: Extracellular Vesicle; PCR: pathological complete response; NACT: neoadjuvant chemotherapy; NA: Not Available.

Considering that miRNAs are the most-studied components in the vesicular context, most putative markers for BC-related EVs depend on these non-coding RNA sequences. Herein, we found potential biomarkers for diagnosis, classification, prognosis, and the prediction of treatment response in relation to BC. Despite differences in the methods used for EV isolation and target selection, all area-under-the-curve (AUC) values shown for the diagnosis of BC were higher than 0.7.

Notably, vesicular hsa-miR-21 was identified as a relevant candidate for diagnosing BC patients in different cohorts [38,39,106]. According to some studies, its performance could be improved by estimating multi-miRNA scores [106] or by combining the levels of this miRNA with MMP1/CD63 protein quantification [37]. In addition, vesicular hsa-miR-421 levels demonstrated the potential to discriminate BC patients from healthy individuals, even those with early stages of the disease [115]. Furthermore, the analysis of vesicular miRNA levels revealed a dual function of some miRNAs. For example, hsa-miR-1246 [38,98] and hsa-miR-142-5p [244] allow for the diagnosis of BC patients and contribute to estimating the treatment response or classifying BC patients, respectively.

Moreover, other kinds of RNA markers (lncRNA, mRNAs, and circRNA) are currently being studied to characterize their features in EVs from BC patients (Table 2) and accumulate evidence to improve current classification systems. It is important to note that classification features can be enhanced if we specially analyze tumor-derived EVs. Although we still lack an exclusive tumor-cell-derived BC marker for EVs, some tumor markers, such as CD49f or the epithelial cell-specific marker (EpCAM), have shown promising results in this regard [106].

5. EVs in Oncological Precision Medicine and Treatment: Promising Avenues and Open Questions

There is no doubt that EVs are an important component of the tumor microenvironment, and a great deal of advancement has been made in understanding how these subcellular nanocompartments affect tumor progression and dissemination. Since tumor-derived EVs can be found in all biological fluids and EV cargo contains genetic information from parental cells, they have been considered potential candidates for liquid biopsies. One approach for specifically investigating circulating EVs derived from tumor cells is based on tumor surface markers that are present in EV membranes. In this context, glycoconjugates have recently attracted attention. Specific antibodies or lectins that recognize the aberrant glycosylation patterns of tumors serve as potential tools that can be used to isolate circulating-tumor-derived-EVs, allowing for the investigation of vesicular components such as RNA and proteins with clinical significance as biomarkers.

Nevertheless, despite EVs' promising applicability and the advances in their use as a liquid biopsy tool, there are still some pitfalls that should be addressed by researchers. Technical challenges concerning effective and selective EV isolation, as well as EV nomenclature, still require better standardization to allow for the comparison of data between different groups. Additionally, we should certainly consider additional factors or biases that affect the collection of EVs from biological fluids like handling, storage, the use of anticoagulants, the volume of blood drawn, age, sex, ancestry groups, disease state (in addition to other comorbidities), medication, circadian rhythm, body mass index, hydration, and dietary status. Indeed, all these issues should be considered when data are interpreted. In addition, another layer of complexity can be added with respect to the methods for the quantitative analysis of EV cargo. First, the quantification of small amounts of RNA and, to a certain extent, protein are non-trivial. In particular, the required input of RNA often does not match the minimal amount recommended for different downstream procedures, leading to a poor signal-to-background ratio. Furthermore, the lack of normalization methods for the quantitative analysis of nucleic acids, proteins, and other biological molecules constitutes yet another gap in the field. Therefore, the scientific community is engaging in extensive discussions and research to establish pipelines to fill these gaps.

Despite the many issues mentioned above, better biomarkers for early detection and predicting therapeutic response are still needed in order to provide a more favorable clinical outcome. As for any new, growing field in science, some technical obstacles, such as those mentioned above, are still a reality; however, due to the number of circulating EVs and their nature as intrinsic sources of biological molecules for modulating cell phenotypes, we believe that circulating EVs hold a great deal of potential in the clinical setting since they represent a method for tracking cancer-associated changes in a personalized manner. Moreover, as the field advances toward overcoming these limitations, the information gleaned from EVs will certainly represent an interesting approach not only to understanding the clinical evolution of BC but also to revealing new routes for clinical intervention.

From the perspective of therapy, EVs have been considered as an important tool with which to improve cancer treatment. Since EVs are natural carriers, some strategies focus on loading EVs with therapeutic components such as chemotherapeutic drugs, siRNAs, peptides, and proteins, presenting significantly enhanced anti-tumor effects [251]. Different methods can be used for EV loading, including electroporation, extrusion, sonication, freeze–thawing, the use of pH gradients, ultrasound, the use of streptomycin O, and hybridization. Another alternative that has been used is the anchorage of a drug on an EV's surface, which can be achieved via click chemistry, to modify the surface of EVs (reviewed in [252]).

Another approach of EV engineering is more indirect and involves the manipulation of the cellular EV source. In this approach, producing cells are incubated with therapeutic agents to increase the loading of these drugs into EVs. Furthermore, the producing cells can be transfected or infected with plasmids or viral vectors to overexpress specific molecules in secreted EVs. The presence of these biomolecules on an EV's surface can be a promising strategy for tumor targeting and specific delivery, thereby improving therapeutic efficacy and reducing toxicity [253]. Nevertheless, it should be mentioned that there is not a gold-standard method for modifying EVs, and each one has its own advantages and disadvantages. Nonetheless, there are a few ongoing clinical trials using engineered EVs for cancer treatment (Clinical Trials, NCT03608631 and NCT01294072).

6. Conclusions

EVs play a substantial role in BC initiation and progression, impacting the natural history of the disease. Tumor-derived EVs are biological nanostructures that carry important genetic information from tumor cells and can be found in all biological fluids, representing a natural source of diagnostic and prognostic biomarkers in cancer. Within this context, finding a set of biomarkers in circulating EVs able to (1) discriminate between healthy individuals and BC patients, (2) discriminate between different molecular subtypes of BC,

and (3) determine the probability of disease recurrence would represent a game changer in the field that could pave the way for precision oncology medicine. In addition, in the therapeutic setting, EV engineering can greatly improve the specificity and effectiveness of tumor therapy, as demonstrated in pre-clinical studies. However, further efforts are still necessary to better standardize technical procedures for EVs' isolation and cargo identification along with the establishment of reliable assays with which to evaluate the therapeutic potential of EVs in clinical practice.

Supplementary Materials: The following supporting information can be downloaded at: https://www.mdpi.com/article/10.3390/ijms241613022/s1.

Author Contributions: Conceptualization, A.G.M.C., A.H.O., L.N.d.S.A. and R.C.; investigation, A.G.M.C., A.H.O., J.M.-d.-S., V.F.S., G.P., L.N.d.S.A. and R.C.; writing—original draft preparation, A.G.M.C., A.H.O., J.M.-d.-S., V.F.S., G.P., L.N.d.S.A. and R.C.; writing—review and editing, A.G.M.C., A.H.O., J.M.-d.-S., V.F.S., G.P., L.N.d.S.A. and R.C.; supervision, A.H.O., G.P., L.N.d.S.A. and R.C.; funding acquisition, R.C. All authors have read and agreed to the published version of the manuscript.

Funding: This research was funded by grants #2019/05583-0 (A.G.M.C. and R.C.), #2021/00140-3 (J.M.-d.-S.), #2018/18257-1 (G.P.), #2018/15549-1 (G.P.), and #2020/04923-0 (G.P.) from the São Paulo Research Foundation (FAPESP); CNPq grant #870219/1997-9 (V.F.) and grant #305239/2022-8 (R.C.); and the Coordenação de Aperfeiçoamento de Pessoal de Nível Superior–Brasil (CAPES)–Finance Code 001 (A.G.M.C. and R.C.).

Institutional Review Board Statement: Not applicable.

Informed Consent Statement: Not applicable.

Data Availability Statement: No new data were created or analyzed in this study. Data sharing is not applicable to this article.

Conflicts of Interest: The authors declare no conflict of interest.

References

1. Sung, H.; Ferlay, J.; Siegel, R.L.; Laversanne, M.; Soerjomataram, I.; Jemal, A.; Bray, F. Global Cancer Statistics 2020: GLOBOCAN Estimates of Incidence and Mortality Worldwide for 36 Cancers in 185 Countries. *CA Cancer J. Clin.* **2021**, *71*, 209–249. [CrossRef] [PubMed]
2. Hanahan, D.; Weinberg, R.A. Hallmarks of cancer: The next generation. *Cell* **2011**, *144*, 646–674. [CrossRef] [PubMed]
3. Dixson, A.C.; Dawson, T.R.; Di Vizio, D.; Weaver, A.M. Context-specific regulation of extracellular vesicle biogenesis and cargo selection. *Nat. Rev. Mol. Cell Biol.* **2023**, *24*, 454–476. [CrossRef] [PubMed]
4. Bobrie, A.; Colombo, M.; Raposo, G.; Théry, C. Exosome Secretion: Molecular Mechanisms and Roles in Immune Responses. *Traffic* **2011**, *12*, 1659–1668. [CrossRef] [PubMed]
5. Mathivanan, S.; Ji, H.; Simpson, R.J. Exosomes: Extracellular organelles important in intercellular communication. *J. Proteom.* **2010**, *73*, 1907–1920. [CrossRef]
6. Théry, C. Exosomes: Secreted vesicles and intercellular communications. *F1000 Biol. Rep.* **2011**, *3*, 15. [CrossRef]
7. Gross, J.C.; Parbin, S. Crossroads of the endosomal machinery: Multivesicular bodies, small extracellular vesicles and autophagy. *Trillium. Exctracellular. Vesicles* **2020**, *2*, 48–53. [CrossRef]
8. Li, Y.; Zhang, Y.; Qiu, F.; Qiu, Z. Proteomic identification of exosomal LRG1: A potential urinary biomarker for detecting NSCLC. *Electrophoresis* **2011**, *32*, 1976–1983. [CrossRef]
9. Liang, B.; Peng, P.; Chen, S.; Li, L.; Zhang, M.; Cao, D.; Yang, J.; Li, H.; Gui, T.; Li, X.; et al. Characterization and proteomic analysis of ovarian cancer-derived exosomes. *J. Proteom.* **2013**, *80*, 171–182. [CrossRef]
10. Sinha, A.; Ignatchenko, V.; Ignatchenko, A.; Mejia-Guerrero, S.; Kislinger, T. In-depth proteomic analyses of ovarian cancer cell line exosomes reveals differential enrichment of functional categories compared to the NCI 60 proteome. *Biochem. Biophys. Res. Commun.* **2014**, *445*, 694–701. [CrossRef]
11. Silva, J.; Garcia, V.; Rodriguez, M.; Compte, M.; Cisneros, E.; Veguillas, P.; Garcia, J.M.; Dominguez, G.; Campos-Martin, Y.; Cuevas, J.; et al. Analysis of exosome release and its prognostic value in human colorectal cancer. *Genes Chromosom. Cancer* **2012**, *51*, 409–418. [CrossRef] [PubMed]
12. Park, J.E.; Sen Tan, H.; Datta, A.; Lai, R.C.; Zhang, H.; Meng, W.; Lim, S.K.; Sze, S.K. Hypoxic tumor cell modulates its microenvironment to enhance angiogenic and metastatic potential by secretion of proteins and exosomes. *Mol. Cell. Proteom.* **2010**, *9*, 1085–1099. [CrossRef] [PubMed]
13. Zhang, X.; Yuan, X.; Shi, H.; Wu, L.; Qian, H.; Xu, W. Exosomes in cancer: Small particle, big player. *J. Hematol. Oncol.* **2015**, *8*, 83. [CrossRef] [PubMed]

14. Harris, D.A.; Patel, S.H.; Gucek, M.; Hendrix, A.; Westbroek, W.; Taraska, J.W. Exosomes Released from Breast Cancer Carcinomas Stimulate Cell Movement. *PLoS ONE* **2015**, *10*, e0117495. [CrossRef] [PubMed]
15. Das, K.; Prasad, R.; Singh, A.; Bhattacharya, A.; Roy, A.; Mallik, S.; Mukherjee, A.; Sen, P. Protease-activated receptor 2 promotes actomyosin dependent transforming microvesicles generation from human breast cancer. *Mol. Carcinog.* **2018**, *57*, 1707–1722. [CrossRef]
16. Das, K.; Prasad, R.; Roy, S.; Mukherjee, A.; Sen, P. The Protease Activated Receptor2 Promotes Rab5a Mediated Generation of Pro-metastatic Microvesicles. *Sci. Rep.* **2018**, *8*, 7357. [CrossRef]
17. Ma, L.; Li, Y.; Peng, J.; Wu, D.; Zhao, X.; Cui, Y.; Chen, L.; Yan, X.; Du, Y.; Yu, L. Discovery of the migrasome, an organelle mediating release of cytoplasmic contents during cell migration. *Cell Res.* **2015**, *25*, 24–38. [CrossRef]
18. Théry, C.; Witwer, K.W.; Aikawa, E.; Alcaraz, M.J.; Anderson, J.D.; Andriantsitohaina, R.; Antoniou, A.; Arab, T.; Archer, F.; Atkin-Smith, G.K.; et al. Minimal information for studies of extracellular vesicles 2018 (MISEV2018): A position statement of the International Society for Extracellular Vesicles and update of the MISEV2014 guidelines. *J. Extracell. Vesicles* **2018**, *7*, 1535750. [CrossRef]
19. Alberro, A.; Iparraguirre, L.; Fernandes, A.; Otaegui, D. Extracellular Vesicles in Blood: Sources, Effects, and Applications. *Int. J. Mol. Sci.* **2021**, *22*, 8163. [CrossRef]
20. Martins, Á.M.; Ramos, C.C.; Freitas, D.; Reis, C.A. Glycosylation of Cancer Extracellular Vesicles: Capture Strategies, Functional Roles and Potential Clinical Applications. *Cells* **2021**, *10*, 109. [CrossRef]
21. Li, Y.; He, X.; Li, Q.; Lai, H.; Zhang, H.; Hu, Z.; Li, Y.; Huang, S. EV-origin: Enumerating the tissue-cellular origin of circulating extracellular vesicles using exLR profile. *Comput. Struct. Biotechnol. J.* **2020**, *18*, 2851–2859. [CrossRef] [PubMed]
22. O'Brien, K.; Breyne, K.; Ughetto, S.; Laurent, L.C.; Breakefield, X.O. RNA delivery by extracellular vesicles in mammalian cells and its applications. *Nat. Rev. Mol. Cell Biol.* **2020**, *21*, 585–606. [CrossRef] [PubMed]
23. Valadi, H.; Ekström, K.; Bossios, A.; Sjöstrand, M.; Lee, J.J.; Lötvall, J.O. Exosome-mediated transfer of mRNAs and microRNAs is a novel mechanism of genetic exchange between cells. *Nat. Cell Biol.* **2007**, *9*, 654–659. [CrossRef] [PubMed]
24. Li, Y.; Zhao, J.; Yu, S.; Wang, Z.; He, X.; Su, Y.; Guo, T.; Sheng, H.; Chen, J.; Zheng, Q.; et al. Extracellular Vesicles Long RNA Sequencing Reveals Abundant mRNA, circRNA, and lncRNA in Human Blood as Potential Biomarkers for Cancer Diagnosis. *Clin. Chem.* **2019**, *65*, 798–808. [CrossRef]
25. Thakur, B.K.; Zhang, H.; Becker, A.; Matei, I.; Huang, Y.; Costa-Silva, B.; Zheng, Y.; Hoshino, A.; Brazier, H.; Xiang, J.; et al. Double-stranded DNA in exosomes: A novel biomarker in cancer detection. *Cell Res.* **2014**, *24*, 766–769. [CrossRef]
26. Guescini, M.; Genedani, S.; Stocchi, V.; Agnati, L.F. Astrocytes and Glioblastoma cells release exosomes carrying mtDNA. *J. Neural Transm.* **2009**, *117*, 1–4. [CrossRef]
27. Belov, L.; Matic, K.J.; Hallal, S.; Best, O.G.; Mulligan, S.P.; Christopherson, R.I. Extensive surface protein profiles of extracellular vesicles from cancer cells may provide diagnostic signatures from blood samples. *J. Extracell. Vesicles* **2016**, *5*, 25355. [CrossRef]
28. Boukouris, S.; Mathivanan, S. Exosomes in bodily fluids are a highly stable resource of disease biomarkers. *Proteom.—Clin. Appl.* **2015**, *9*, 358–367. [CrossRef]
29. Li, S.; Li, Y.; Chen, B.; Zhao, J.; Yu, S.; Tang, Y.; Zheng, Q.; Li, Y.; Wang, P.; He, X.; et al. exoRBase: A database of circRNA, lncRNA and mRNA in human blood exosomes. *Nucleic Acids Res.* **2018**, *46*, D106–D112. [CrossRef] [PubMed]
30. Liu, C.-J.; Xie, G.-Y.; Miao, Y.-R.; Xia, M.; Wang, Y.; Lei, Q.; Zhang, Q.; Guo, A.-Y. EVAtlas: A comprehensive database for ncRNA expression in human extracellular vesicles. *Nucleic Acids Res.* **2022**, *50*, D111–D117. [CrossRef] [PubMed]
31. Liu, T.; Zhang, Q.; Zhang, J.; Li, C.; Miao, Y.R.; Lei, Q.; Li, Q.; Guo, A.Y. EVmiRNA: A database of miRNA profiling in extracellular vesicles. *Nucleic Acids Res.* **2019**, *47*, D89–D93. [CrossRef] [PubMed]
32. Melling, G.E.; Carollo, E.; Conlon, R.; Simpson, J.C.; Carter, D.R.F. The Challenges and Possibilities of Extracellular Vesicles as Therapeutic Vehicles. *Eur. J. Pharm. Biopharm.* **2019**, *144*, 50–56. [CrossRef] [PubMed]
33. Andreeva, O.E.; Shchegolev, Y.Y.; Scherbakov, A.M.; Mikhaevich, E.I.; Sorokin, D.V.; Gudkova, M.V.; Bure, I.V.; Kuznetsova, E.B.; Mikhaylenko, D.S.; Nemtsova, M.V.; et al. Secretion of Mutant DNA and mRNA by the Exosomes of Breast Cancer Cells. *Molecules* **2021**, *26*, 2499. [CrossRef] [PubMed]
34. Conley, A.; Minciacchi, V.R.; Lee, D.H.; Knudsen, B.S.; Karlan, B.Y.; Citrigno, L.; Viglietto, G.; Tewari, M.; Freeman, M.R.; Demichelis, F.; et al. High-throughput sequencing of two populations of extracellular vesicles provides an mRNA signature that can be detected in the circulation of breast cancer patients. *RNA Biol.* **2017**, *14*, 305–316. [CrossRef]
35. Liu, C.; Li, B.; Lin, H.; Yang, C.; Guo, J.; Cui, B.; Pan, W.; Feng, J.; Luo, T.; Chu, F.; et al. Multiplexed analysis of small extracellular vesicle-derived mRNAs by droplet digital PCR and machine learning improves breast cancer diagnosis. *Biosens. Bioelectron.* **2021**, *194*, 113615. [CrossRef]
36. Abdulhussain, M.M.; Hasan, N.A.; Hussain, A.G. Interrelation of the Circulating and Tissue MicroRNA-21 with Tissue PDCD4 Expression and the Invasiveness of Iraqi Female Breast Tumors. *Indian J. Clin. Biochem.* **2017**, *34*, 26–38. [CrossRef]
37. Ando, W.; Kikuchi, K.; Uematsu, T.; Yokomori, H.; Takaki, T.; Sogabe, M.; Kohgo, Y.; Otori, K.; Ishikawa, S.; Okazaki, I. Novel breast cancer screening: Combined expression of miR-21 and MMP-1 in urinary exosomes detects 95% of breast cancer without metastasis. *Sci. Rep.* **2019**, *9*, 13595. [CrossRef]
38. Hannafon, B.N.; Trigoso, Y.D.; Calloway, C.L.; Zhao, Y.D.; Lum, D.H.; Welm, A.L.; Zhao, Z.J.; Blick, K.E.; Dooley, W.C.; Ding, W.Q. Plasma exosome microRNAs are indicative of breast cancer. *Breast Cancer Res.* **2016**, *18*, 90. [CrossRef]

39. Liu, M.; Mo, F.; Song, X.; He, Y.; Yuan, Y.; Yan, J.; Yang, Y.; Huang, J.; Zhang, S. Exosomal hsa-miR-21-5p is a biomarker for breast cancer diagnosis. *PeerJ* **2021**, *9*, e12147. [CrossRef]
40. Wang, J.; Zhang, Q.; Zhou, S.; Xu, H.; Wang, D.; Feng, J.; Zhao, J.; Zhong, S. Circular RNA expression in exosomes derived from breast cancer cells and patients. *Epigenomics* **2019**, *11*, 411–421. [CrossRef]
41. Fiskaa, T.; Knutsen, E.; Nikolaisen, M.A.; Jørgensen, T.E.; Johansen, S.D.; Perander, M.; Seternes, O.M. Distinct Small RNA Signatures in Extracellular Vesicles Derived from Breast Cancer Cell Lines. *PLoS ONE* **2016**, *11*, e0161824. [CrossRef] [PubMed]
42. Jenjaroenpun, P.; Kremenska, Y.; Nair, V.M.; Kremenskoy, M.; Joseph, B.; Kurochkin, I.V. Characterization of RNA in exosomes secreted by human breast cancer cell lines using next-generation sequencing. *PeerJ* **2013**, *2013*, e201. [CrossRef] [PubMed]
43. Feng, T.; Zhang, P.; Sun, Y.; Wang, Y.; Tong, J.; Dai, H.; Hua, Z. High throughput sequencing identifies breast cancer-secreted exosomal LncRNAs initiating pulmonary pre-metastatic niche formation. *Gene* **2019**, *710*, 258–264. [CrossRef]
44. Ruhen, O.; Mirzai, B.; Clark, M.E.; Nguyen, B.; Salomon, C.; Erber, W.; Meehan, K. Comparison of Circulating Tumour DNA and Extracellular Vesicle DNA by Low-Pass Whole-Genome Sequencing Reveals Molecular Drivers of Disease in a Breast Cancer Patient. *Biomedicines* **2020**, *9*, 14. [CrossRef]
45. De Carolis, S.; Storci, G.; Ceccarelli, C.; Savini, C.; Gallucci, L.; Sansone, P.; Santini, D.; Seracchioli, R.; Taffurelli, M.; Fabbri, F.; et al. HPV DNA Associates with Breast Cancer Malignancy and It Is Transferred to Breast Cancer Stromal Cells by Extracellular Vesicles. *Front. Oncol.* **2019**, *9*, 860. [CrossRef] [PubMed]
46. Arroyo, J.D.; Chevillet, J.R.; Kroh, E.M.; Ruf, I.K.; Pritchard, C.C.; Gibson, D.F.; Mitchell, P.S.; Bennett, C.F.; Pogosova-Agadjanyan, E.L.; Stirewalt, D.L.; et al. Argonaute2 complexes carry a population of circulating microRNAs independent of vesicles in human plasma. *Proc. Natl. Acad. Sci. USA* **2011**, *108*, 5003–5008. [CrossRef]
47. Crescitelli, R.; Lässer, C.; Szabó, T.G.; Kittel, A.; Eldh, M.; Dianzani, I.; Buzás, E.I.; Lötvall, J. Distinct RNA profiles in subpopulations of extracellular vesicles: Apoptotic bodies, microvesicles and exosomes. *J. Extracell. Vesicles* **2013**, *2*, 20677. [CrossRef]
48. Uen, Y.; Wang, J.-W.; Wang, C.; Jhang, Y.; Chung, J.-Y.; Tseng, T.; Sheu, M.; Lee, S. Mining of potential microRNAs with clinical correlation—Regulation of syndecan-1 expression by miR-122-5p altered mobility of breast cancer cells and possible correlation with liver injury. *Oncotarget* **2018**, *9*, 28165–28175. [CrossRef]
49. Fong, M.Y.; Zhou, W.; Liu, L.; Alontaga, A.Y.; Chandra, M.; Ashby, J.; Chow, A.; O'Connor, S.T.F.; Li, S.; Chin, A.R.; et al. Breast-cancer-secreted miR-122 reprograms glucose metabolism in premetastatic niche to promote metastasis. *Nat. Cell Biol.* **2015**, *17*, 183–194. [CrossRef]
50. Xun, J.; Du, L.; Gao, R.; Shen, L.; Wang, D.; Kang, L.; Chen, C.A.; Zhang, Z.; Zhang, Y.; Yue, S.; et al. Cancer-derived exosomal miR-138-5p modulates polarization of tumor-Associated macrophages through inhibition of KDM6B. *Theranostics* **2021**, *11*, 6847–6859. [CrossRef]
51. Yang, S.S.; Ma, S.; Dou, H.; Liu, F.; Zhang, S.Y.; Jiang, C.; Xiao, M.; Huang, Y.X. Breast cancer-derived exosomes regulate cell invasion and metastasis in breast cancer via miR-146a to activate cancer associated fibroblasts in tumor microenvironment. *Exp. Cell Res.* **2020**, *391*, 111983. [CrossRef] [PubMed]
52. Cereghetti, D.; Lee, P. Tumor-Derived Exosomes Contain microRNAs with Immunological Function: Implications for a Novel Immunosuppression Mechanism. *MicroRNA* **2014**, *2*, 194–204. [CrossRef] [PubMed]
53. Santos, J.C.; Lima, N.D.S.; Sarian, L.O.; Matheu, A.; Ribeiro, M.L.; Derchain, S.F.M. Exosome-mediated breast cancer chemoresistance via miR-155 transfer. *Sci. Rep.* **2018**, *8*, 829. [CrossRef] [PubMed]
54. Andreeva, O.E.; Sorokin, D.V.; Mikhaevich, E.I.; Bure, I.V.; Shchegolev, Y.Y.; Nemtsova, M.V.; Gudkova, M.V.; Scherbakov, A.M.; Krasil'nikov, M.A. Towards Unravelling the Role of ERα-Targeting miRNAs in the Exosome-Mediated Transferring of the Hormone Resistance. *Molecules* **2021**, *26*, 6661. [CrossRef]
55. Lu, C.; Zhao, Y.; Wang, J.; Shi, W.; Dong, F.; Xin, Y.; Zhao, X.; Liu, C. Breast cancer cell-derived extracellular vesicles transfer miR-182-5p and promote breast carcinogenesis via the CMTM7/EGFR/AKT axis. *Mol. Med.* **2021**, *27*, 78. [CrossRef] [PubMed]
56. Mihelich, B.L.; Dambal, S.; Lin, S.; Nonn, L. miR-182, of the miR-183 cluster family, is packaged in exosomes and is detected in human exosomes from serum, breast cells and prostate cells. *Oncol. Lett.* **2016**, *12*, 1197–1203. [CrossRef]
57. Li, X.J.; Ren, Z.J.; Tang, J.H.; Yu, Q. Exosomal MicroRNA MiR-1246 Promotes Cell Proliferation, Invasion and Drug Resistance by Targeting CCNG2 in Breast Cancer. *Cell. Physiol. Biochem.* **2017**, *44*, 1741–1748. [CrossRef]
58. Wang, M.; Zhang, H.; Yang, F.; Qiu, R.; Zhao, X.; Gong, Z.; Yu, W.; Zhou, B.; Shen, B.; Zhu, W. miR-188-5p suppresses cellular proliferation and migration via IL6ST: A potential noninvasive diagnostic biomarker for breast cancer. *J. Cell. Physiol.* **2020**, *235*, 4890–4901. [CrossRef]
59. Wang, B.; Mao, J.H.; Wang, B.Y.; Wang, L.X.; Wen, H.Y.; Xu, L.J.; Fu, J.X.; Yang, H. Exosomal miR-1910-3p promotes proliferation, metastasis, and autophagy of breast cancer cells by targeting MTMR3 and activating the NF-κB signaling pathway. *Cancer Lett.* **2020**, *489*, 87–99. [CrossRef]
60. Wu, K.; Feng, J.; Lyu, F.; Xing, F.; Sharma, S.; Liu, Y.; Wu, S.Y.; Zhao, D.; Tyagi, A.; Deshpande, R.P.; et al. Exosomal miR-19a and IBSP cooperate to induce osteolytic bone metastasis of estrogen receptor-positive breast cancer. *Nat. Commun.* **2021**, *12*, 5196. [CrossRef]
61. Le, M.T.N.; Hamar, P.; Guo, C.; Basar, E.; Perdigão-Henriques, R.; Balaj, L.; Lieberman, J. miR-200–containing extracellular vesicles promote breast cancer cell metastasis. *J. Clin. Investig.* **2014**, *124*, 5109–5128. [CrossRef]

62. Buschmann, D.; González, R.; Kirchner, B.; Mazzone, C.; Pfaffl, M.W.; Schelling, G.; Steinlein, O.; Reithmair, M. Glucocorticoid receptor overexpression slightly shifts microRNA expression patterns in triple-negative breast cancer. *Int. J. Oncol.* **2018**, *52*, 1765–1776. [CrossRef] [PubMed]
63. Zhao, Y.; Jin, L.J.; Zhang, X.Y. Exosomal miRNA-205 promotes breast cancer chemoresistance and tumorigenesis through E2F1. *Aging* **2021**, *13*, 18498–18514. [CrossRef] [PubMed]
64. Guo, L.; Zhu, Y.; Li, L.; Zhou, S.; Yin, G.; Yu, G.; Cui, H. Breast cancer cell-derived exosomal miR-20a-5p promotes the proliferation and differentiation of osteoclasts by targeting SRCIN1. *Cancer Med.* **2019**, *8*, 5687–5701. [CrossRef] [PubMed]
65. Wang, W.; Yuan, X.; Xu, A.; Zhu, X.; Zhan, Y.; Wang, S.; Liu, M. Human cancer cells suppress behaviors of endothelial progenitor cells through miR-21 targeting IL6R. *Microvasc. Res.* **2018**, *120*, 21–28. [CrossRef]
66. Arisan, E.D.; Rencuzogullari, O.; Cieza-borrella, C.; Miralles Arenas, F.; Dwek, M.; Lange, S.; Uysal-onganer, P. MiR-21 is Required for the Epithelial–Mesenchymal Transition in MDA-MB-231 Breast Cancer Cells. *Int. J. Mol. Sci.* **2021**, *22*, 1557. [CrossRef]
67. Lee, J.H.; Kim, J.A.; Kwon, M.H.; Kang, J.Y.; Rhee, W.J. In situ single step detection of exosome microRNA using molecular beacon. *Biomaterials* **2015**, *54*, 116–125. [CrossRef]
68. Ohno, S.; Takanashi, M.; Sudo, K.; Ueda, S.; Ishikawa, A.; Matsuyama, N.; Fujita, K.; Mizutani, T.; Ohgi, T.; Ochiya, T.; et al. Systemically Injected Exosomes Targeted to EGFR Deliver Antitumor MicroRNA to Breast Cancer Cells. *Mol. Ther.* **2013**, *21*, 185–191. [CrossRef]
69. Guzman, N.; Agarwal, K.; Asthagiri, D.; Yu, L.; Saji, M.; Ringel, M.D.; Paulaitis, M.E. Breast Cancer–Specific miR Signature Unique to Extracellular Vesicles Includes "microRNA-like" tRNA Fragments. *Mol. Cancer Res.* **2015**, *13*, 891–901. [CrossRef]
70. Bose, R.J.; Kumar, U.S.; Garcia-Marques, F.; Zeng, Y.; Habte, F.; McCarthy, J.R.; Pitteri, S.; Massoud, T.F.; Paulmurugan, R. Engineered Cell-Derived Vesicles Displaying Targeting Peptide and Functionalized with Nanocarriers for Therapeutic microRNA Delivery to Triple-Negative Breast Cancer in Mice. *Adv. Healthc. Mater.* **2021**, *11*, 2101387. [CrossRef]
71. Wang, Z.; Zong, S.; Liu, Y.; Qian, Z.; Zhu, K.; Yang, Z.; Wang, Z.; Cui, Y. Simultaneous detection of multiple exosomal microRNAs for exosome screening based on rolling circle amplification. *Nanotechnology* **2020**, *32*, 085504. [CrossRef] [PubMed]
72. Wang, H.; He, D.; Wan, K.; Sheng, X.; Cheng, H.; Huang, J.; Zhou, X.; He, X.; Wang, K. In situ multiplex detection of serum exosomal microRNAs using an all-in-one biosensor for breast cancer diagnosis. *Analyst* **2020**, *145*, 3289–3296. [CrossRef] [PubMed]
73. Aslan, C.; Maralbashi, S.; Kahroba, H.; Asadi, M.; Soltani-Zangbar, M.S.; Javadian, M.; Shanehbandi, D.; Baradaran, B.; Darabi, M.; Kazemi, T. Docosahexaenoic acid (DHA) inhibits pro-angiogenic effects of breast cancer cells via down-regulating cellular and exosomal expression of angiogenic genes and microRNAs. *Life Sci.* **2020**, *258*, 118094. [CrossRef] [PubMed]
74. Feng, Y.; Wang, L.; Wang, T.; Li, Y.; Xun, Q.; Zhang, R.; Liu, L.; Li, L.; Wang, W.; Tian, Y.; et al. Tumor cell-secreted exosomal miR-22-3p inhibits transgelin and induces vascular abnormalization to promote tumor budding. *Mol. Ther.* **2021**, *29*, 2151–2166. [CrossRef]
75. Das, K.; Paul, S.; Singh, A.; Ghosh, A.; Roy, A.; Ansari, S.A.; Prasad, R.; Mukherjee, A.; Sen, P. Triple-negative breast cancer-derived microvesicles transfer microRNA221 to the recipient cells and thereby promote epithelial-to-mesenchymal transition. *J. Biol. Chem.* **2019**, *294*, 13681–13696. [CrossRef]
76. Wei, Y.; Lai, X.; Yu, S.; Chen, S.; Ma, Y.; Zhang, Y.; Li, H.; Zhu, X.; Yao, L.; Zhang, J. Exosomal miR-221/222 enhances tamoxifen resistance in recipient ER-positive breast cancer cells. *Breast Cancer Res. Treat.* **2014**, *147*, 423–431. [CrossRef]
77. Dan Yu, D.; Wu, Y.; Zhang, X.H.; Lv, M.M.; Chen, W.X.; Chen, X.; Yang, S.J.; Shen, H.; Zhong, S.L.; Tang, J.H.; et al. Exosomes from adriamycin-resistant breast cancer cells transmit drug resistance partly by delivering miR-222. *Tumour Biol.* **2016**, *37*, 3227–3235. [CrossRef]
78. Chen, W.X.; Wang, D.D.; Zhu, B.; Zhu, Y.Z.; Zheng, L.; Feng, Z.Q.; Qin, X.H. Exosomal miR-222 from adriamycin-resistant MCF-7 breast cancer cells promote macrophages M2 polarization via PTEN/Akt to induce tumor progression. *Aging* **2021**, *13*, 10415–10430. [CrossRef]
79. Du, J.; Fan, J.J.; Dong, C.; Li, H.T.; Ma, B.L. Inhibition effect of exosomes-mediated Let-7a on the development and metastasis of Triple negative breast cancer by down-regulating the expression of c-Myc. *Eur. Rev. Med. Pharmacol. Sci.* **2019**, *23*, 5301–5314. [CrossRef]
80. Ding, J.; Xu, Z.; Zhang, Y.; Tan, C.; Hu, W.; Wang, M.; Xu, Y.; Tang, J. Exosome-mediated miR-222 transferring: An insight into NF-κB-mediated breast cancer metastasis. *Exp. Cell Res.* **2018**, *369*, 129–138. [CrossRef]
81. Morad, G.; Daisy, C.C.; Otu, H.H.; Libermann, T.A.; Dillon, S.T.; Moses, M.A. Cdc42-Dependent Transfer of mir301 from Breast Cancer-Derived Extracellular Vesicles Regulates the Matrix Modulating Ability of Astrocytes at the Blood–Brain Barrier. *Int. J. Mol. Sci.* **2020**, *21*, 3851. [CrossRef] [PubMed]
82. Ren, Z.; Lv, M.; Yu, Q.; Bao, J.; Lou, K.; Li, X. MicroRNA-370-3p shuttled by breast cancer cell-derived extracellular vesicles induces fibroblast activation through the CYLD/Nf-κB axis to promote breast cancer progression. *FASEB J.* **2021**, *35*, e21383. [CrossRef] [PubMed]
83. Wang, B.; Zhang, Y.; Ye, M.; Wu, J.; Ma, L.; Chen, H. Cisplatin-resistant MDA-MB-231 Cell-derived Exosomes Increase the Resistance of Recipient Cells in an Exosomal miR-423-5p-dependent Manner. *Curr. Drug Metab.* **2019**, *20*, 804–814. [CrossRef] [PubMed]
84. Wang, J.; Zhang, Q.; Wang, D.; Yang, S.; Zhou, S.; Xu, H.; Zhang, H.; Zhong, S.; Feng, J. Microenvironment-induced TIMP2 loss by cancer-secreted exosomal miR-4443 promotes liver metastasis of breast cancer. *J. Cell. Physiol.* **2020**, *235*, 5722–5735. [CrossRef]

85. Moloney, B.M.; Gilligan, K.E.; Joyce, D.P.; O'Neill, C.P.; O'Brien, K.P.; Khan, S.; Glynn, C.L.; Waldron, R.M.; Maguire, C.M.; Holian, E.; et al. Investigating the Potential and Pitfalls of EV-Encapsulated MicroRNAs as Circulating Biomarkers of Breast Cancer. *Cells* **2020**, *9*, 141. [CrossRef]
86. Xin, Y.; Wang, X.; Meng, K.; Ni, C.; Lv, Z.; Guan, D. Identification of exosomal miR-455-5p and miR-1255a as therapeutic targets for breast cancer. *Biosci. Rep.* **2020**, *40*, 20190303. [CrossRef]
87. Shen, S.; Song, Y.; Zhao, B.; Xu, Y.; Ren, X.; Zhou, Y.; Sun, Q. Cancer-derived exosomal miR-7641 promotes breast cancer progression and metastasis. *Cell Commun. Signal.* **2021**, *19*, 20. [CrossRef]
88. Li, Y.; Liang, Y.; Sang, Y.; Song, X.; Zhang, H.; Liu, Y.; Jiang, L.; Yang, Q. MiR-770 suppresses the chemo-resistance and metastasis of triple negative breast cancer via direct targeting of STMN1. *Cell Death Dis.* **2018**, *9*, 14. [CrossRef]
89. Liu, J.; Zhu, S.; Tang, W.; Huang, Q.; Mei, Y.; Yang, H. Exosomes from tamoxifen-resistant breast cancer cells transmit drug resistance partly by delivering miR-9-5p. *Cancer Cell Int.* **2021**, *21*, 55. [CrossRef]
90. Hannafon, B.N.; Carpenter, K.J.; Berry, W.L.; Janknecht, R.; Dooley, W.C.; Ding, W.Q. Exosome-mediated microRNA signaling from breast cancer cells is altered by the anti-angiogenesis agent docosahexaenoic acid (DHA). *Mol. Cancer* **2015**, *14*, 133. [CrossRef]
91. Kia, V.; Paryan, M.; Mortazavi, Y.; Biglari, A.; Mohammadi-Yeganeh, S. Evaluation of exosomal miR-9 and miR-155 targeting PTEN and DUSP14 in highly metastatic breast cancer and their effect on low metastatic cells. *J. Cell. Biochem.* **2019**, *120*, 5666–5676. [CrossRef] [PubMed]
92. Shen, M.; Dong, C.; Ruan, X.; Yan, W.; Cao, M.; Pizzo, D.; Wu, X.; Yang, L.; Liu, L.; Ren, X.; et al. Chemotherapy-Induced Extracellular Vesicle miRNAs Promote Breast Cancer Stemness by Targeting ONECUT2. *Cancer Res.* **2019**, *79*, 3608–3621. [CrossRef] [PubMed]
93. Wang, B.; Wang, Y.; Wang, X.; Gu, J.; Wu, W.; Wu, H.; Wang, Q.; Zhou, D. Extracellular Vesicles Carrying miR-887-3p Promote Breast Cancer Cell Drug Resistance by Targeting BTBD7 and Activating the Notch1/Hes1 Signaling Pathway. *Dis. Markers* **2022**, *2022*, 5762686. [CrossRef]
94. Zhang, W.; Liu, H.; Jiang, J.; Yang, Y.; Wang, W.; Jia, Z. CircRNA circFOXK2 facilitates oncogenesis in breast cancer via IGF2BP3/miR-370 axis. *Aging* **2021**, *13*, 18978. [CrossRef] [PubMed]
95. Li, M.; Zou, X.; Xia, T.; Wang, T.; Liu, P.; Zhou, X.; Wang, S.; Zhu, W. A five-miRNA panel in plasma was identified for breast cancer diagnosis. *Cancer Med.* **2019**, *8*, 7006–7017. [CrossRef]
96. Chen, Y.; Zhai, L.-Y.; Zhang, L.-M.; Ma, X.-S.; Liu, Z.; Li, M.-M.; Chen, J.-X.; Duan, W.-J. Breast cancer plasma biopsy by *in situ* determination of exosomal microRNA-1246 with a molecular beacon. *Analyst* **2021**, *146*, 2264–2276. [CrossRef]
97. Zhai, L.-Y.; Li, M.-X.; Pan, W.-L.; Chen, Y.; Li, M.-M.; Pang, J.-X.; Zheng, L.; Chen, J.-X.; Duan, W.-J. In Situ Detection of Plasma Exosomal MicroRNA-1246 for Breast Cancer Diagnostics by a Au Nanoflare Probe. *ACS Appl. Mater. Interfaces* **2018**, *10*, 39478–39486. [CrossRef]
98. Zhang, Z.; Zhang, L.; Yu, G.; Sun, Z.; Wang, T.; Tian, X.; Duan, X.; Zhang, C. Exosomal miR-1246 and miR-155 as predictive and prognostic biomarkers for trastuzumab-based therapy resistance in HER2-positive breast cancer. *Cancer Chemother. Pharmacol.* **2020**, *86*, 761–772. [CrossRef]
99. Ni, Q.; Stevic, I.; Pan, C.; Müller, V.; Oliviera-Ferrer, L.; Pantel, K.; Schwarzenbach, H. Different signatures of miR-16, miR-30b and miR-93 in exosomes from breast cancer and DCIS patients. *Sci. Rep.* **2018**, *8*, 12974. [CrossRef]
100. Ahmed, S.H.; Espinoza-Sánchez, N.A.; El-Damen, A.; Fahim, S.A.; Badawy, M.A.; Greve, B.; El-Shinawi, M.; Götte, M.; Ibrahim, S.A. Small extracellular vesicle-encapsulated miR-181b-5p, miR-222-3p and let-7a-5p: Next generation plasma biopsy-based diagnostic biomarkers for inflammatory breast cancer. *PLoS ONE* **2021**, *16*, e0250642. [CrossRef]
101. Chen, W.; Liu, X.; Lv, M.; Chen, L.; Zhao, J.; Zhong, S.; Ji, M.; Hu, Q.; Luo, Z.; Wu, J.; et al. Exosomes from Drug-Resistant Breast Cancer Cells Transmit Chemoresistance by a Horizontal Transfer of MicroRNAs. *PLoS ONE* **2014**, *9*, e95240. [CrossRef] [PubMed]
102. Rodríguez-Martínez, A.; De Miguel-Pérez, D.; Ortega, F.G.; García-Puche, J.L.; Robles-Fernández, I.; Exposito, J.; Martorell-Marugan, J.; Carmona-Sáez, P.; Garrido-Navas, M.D.C.; Rolfo, C.; et al. Exosomal miRNA profile as complementary tool in the diagnostic and prediction of treatment response in localized breast cancer under neoadjuvant chemotherapy. *Breast Cancer Res.* **2019**, *2019*, 21. [CrossRef] [PubMed]
103. Yoshikawa, M.; Iinuma, H.; Umemoto, Y.; Yanagisawa, T.; Matsumoto, A.; Jinno, H. Exosome-encapsulated microRNA-223-3p as a minimally invasive biomarker for the early detection of invasive breast cancer. *Oncol. Lett.* **2018**, *15*, 9584–9592. [CrossRef]
104. Yan, C.; Hu, J.; Yang, Y.; Hu, H.; Zhou, D.; Ma, M.; Xu, N. Plasma extracellular vesicle-packaged microRNAs as candidate diagnostic biomarkers for early-stage breast cancer. *Mol. Med. Rep.* **2019**, *20*, 3991–4002. [CrossRef] [PubMed]
105. Zou, X.; Li, M.; Huang, Z.; Zhou, X.; Liu, Q.; Xia, T.; Zhu, W. Circulating miR-532-502 cluster derived from chromosome X as biomarkers for diagnosis of breast cancer. *Gene* **2020**, *722*, 144104. [CrossRef]
106. Kim, M.W.; Park, S.; Lee, H.; Gwak, H.; Hyun, K.A.; Kim, J.Y.; Jung, H.I.; Il Kim, S. Multi-miRNA panel of tumor-derived extracellular vesicles as promising diagnostic biomarkers of early-stage breast cancer. *Cancer Sci.* **2021**, *112*, 5078–5087. [CrossRef] [PubMed]
107. Wang, X.; Qian, T.; Bao, S.; Zhao, H.; Chen, H.; Xing, Z.; Li, Y.; Zhang, M.; Meng, X.; Wang, C.; et al. Circulating exosomal miR-363-5p inhibits lymph node metastasis by downregulating PDGFB and serves as a potential noninvasive biomarker for breast cancer. *Mol. Oncol.* **2021**, *15*, 2466–2479. [CrossRef]

108. Gonzalez-Villasana, V.; Rashed, M.H.; Gonzalez-Cantú, Y.; Bayraktar, R.; Menchaca-Arredondo, J.L.; Vazquez-Guillen, J.M.; Rodriguez-Padilla, C.; Lopez-Berestein, G.; Resendez-Perez, D. Presence of Circulating miR-145, miR-155, and miR-382 in Exosomes Isolated from Serum of Breast Cancer Patients and Healthy Donors. *Dis. Markers* **2019**, *2019*, 6852917. [CrossRef]
109. Li, D.; Wang, J.; Ma, L.J.; Yang, H.B.; Jing, J.F.; Jia, M.M.; Zhang, X.J.; Guo, F.; Gao, J.N. Identification of serum exosomal miR-148a as a novel prognostic biomarker for breast cancer. *Eur. Rev. Med. Pharmacol. Sci.* **2020**, *24*, 7303–7309. [CrossRef]
110. Yuan, X.; Qian, N.; Ling, S.; Li, Y.; Sun, W.; Li, J.; Du, R.; Zhong, G.; Liu, C.; Yu, G.; et al. Breast cancer exosomes contribute to pre-metastatic niche formation and promote bone metastasis of tumor cells. *Theranostics* **2021**, *11*, 1429–1445. [CrossRef]
111. Li, S.; Zhang, M.; Xu, F.; Wang, Y.; Leng, D. Detection significance of miR-3662, miR-146a, and miR-1290 in serum exosomes of breast cancer patients. *J. Cancer Res. Ther.* **2021**, *17*, 749–755. [CrossRef] [PubMed]
112. Yan, W.; Wu, X.; Zhou, W.; Fong, M.Y.; Cao, M.; Liu, J.; Liu, X.; Chen, C.-H.; Fadare, O.; Pizzo, D.P.; et al. Cancer-cell-secreted exosomal miR-105 promotes tumour growth through the MYC-dependent metabolic reprogramming of stromal cells. *Nat. Cell Biol.* **2018**, *20*, 597–609. [CrossRef] [PubMed]
113. Eichelser, C.; Stückrath, I.; Müller, V.; Milde-Langosch, K.; Wikman, H.; Pantel, K.; Schwarzenbach, H.; Eichelser, C.; Stückrath, I.; Müller, V.; et al. Increased serum levels of circulating exosomal microRNA-373 in receptor-negative breast cancer patients. *Oncotarget* **2014**, *5*, 9650–9663. [CrossRef]
114. Yang, Q.; Zhao, S.; Shi, Z.; Cao, L.; Liu, J.; Pan, T.; Zhou, D.; Zhang, J. Chemotherapy-elicited exosomal miR-378a-3p and miR-378d promote breast cancer stemness and chemoresistance via the activation of EZH2/STAT3 signaling. *J. Exp. Clin. Cancer Res.* **2021**, *40*, 120. [CrossRef] [PubMed]
115. Bao, S.; Hu, T.; Liu, J.; Su, J.; Sun, J.; Ming, Y.; Li, J.; Wu, N.; Chen, H.; Zhou, M. Genomic instability-derived plasma extracellular vesicle-microRNA signature as a minimally invasive predictor of risk and unfavorable prognosis in breast cancer. *J. Nanobiotechnol.* **2021**, *19*, 22. [CrossRef] [PubMed]
116. Curtaz, C.J.; Reifschläger, L.; Strähle, L.; Feldheim, J.; Feldheim, J.J.; Schmitt, C.; Kiesel, M.; Herbert, S.-L.; Wöckel, A.; Meybohm, P.; et al. Analysis of microRNAs in Exosomes of Breast Cancer Patients in Search of Molecular Prognostic Factors in Brain Metastases. *Int. J. Mol. Sci.* **2022**, *23*, 3683. [CrossRef]
117. Liu, D.; Li, B.; Shi, X.; Zhang, J.; Chen, A.M.; Xu, J.; Wang, W.; Huang, K.; Gao, J.; Zheng, Z.; et al. Cross-platform genomic identification and clinical validation of breast cancer diagnostic biomarkers. *Aging* **2021**, *13*, 4258–4273. [CrossRef]
118. Inubushi, S.; Kawaguchi, H.; Mizumoto, S.; Kunihisa, T.; Baba, M.; Kitayama, Y.; Takeuchi, T.; Hoffman, R.M.; Sasaki, R. Oncogenic miRNAs Identified in Tear Exosomes from Metastatic Breast Cancer Patients. *Anticancer Res.* **2020**, *40*, 3091–3096. [CrossRef]
119. Hirschfeld, M.; Rücker, G.; Weiß, D.; Berner, K.; Ritter, A.; Jäger, M.; Erbes, T. Urinary Exosomal MicroRNAs as Potential Non-invasive Biomarkers in Breast Cancer Detection. *Mol. Diagn. Ther.* **2020**, *24*, 215–232. [CrossRef]
120. Koi, Y.; Tsutani, Y.; Nishiyama, Y.; Ueda, D.; Ibuki, Y.; Sasada, S.; Akita, T.; Masumoto, N.; Kadoya, T.; Yamamoto, Y.; et al. Predicting the presence of breast cancer using circulating small RNAs, including those in the extracellular vesicles. *Cancer Sci.* **2020**, *111*, 2104–2115. [CrossRef]
121. Galli De Amorim, M.; Branco, G.; Valieris, R.; Tarcitano, E.; Tojal Da Silva, I.; Ferreira De Araújo, L.; Noronha Nunes, D.; Dias-Neto, E. The impact of HER2 overexpression on the miRNA and circRNA transcriptomes in two breast cell lines and their vesicles. *Pharmacogenomics* **2019**, *20*, 493–502. [CrossRef] [PubMed]
122. Fong, M.Y.; Yan, W.; Ghassemian, M.; Wu, X.; Zhou, X.; Cao, M.; Jiang, L.; Wang, J.; Liu, X.; Zhang, J.; et al. Cancer-secreted miRNAs regulate amino-acid-induced mTORC1 signaling and fibroblast protein synthesis. *EMBO Rep.* **2021**, *22*, e51239. [CrossRef] [PubMed]
123. Singh, R.; Pochampally, R.; Watabe, K.; Lu, Z.; Mo, Y.-Y. Exosome-mediated transfer of miR-10b promotes cell invasion in breast cancer. *Mol. Cancer* **2014**, *13*, 256. [CrossRef] [PubMed]
124. Dai, X.; Cheng, H.; Bai, Z.; Li, J. Breast Cancer Cell Line Classification and Its Relevance with Breast Tumor Subtyping. *J. Cancer* **2017**, *8*, 3131–3141. [CrossRef]
125. Petrović, N. miR-21 Might be Involved in Breast Cancer Promotion and Invasion Rather than in Initial Events of Breast Cancer Development. *Mol. Diagn. Ther.* **2016**, *20*, 97–110. [CrossRef]
126. Yan, L.-X.; Huang, X.-F.; Shao, Q.; Huang, M.-Y.; Deng, L.; Wu, Q.-L.; Zeng, Y.-X.; Shao, J.-Y. MicroRNA miR-21 overexpression in human breast cancer is associated with advanced clinical stage, lymph node metastasis and patient poor prognosis. *RNA* **2008**, *14*, 2348–2360. [CrossRef]
127. Donnarumma, E.; Fiore, D.; Nappa, M.; Roscigno, G.; Adamo, A.; Iaboni, M.; Russo, V.; Affinito, A.; Puoti, I.; Quintavalle, C.; et al. Cancer-associated fibroblasts release exosomal microRNAs that dictate an aggressive phenotype in breast cancer. *Oncotarget* **2017**, *8*, 19592–19608. [CrossRef]
128. Shah, S.H.; Miller, P.; Garcia-Contreras, M.; Ao, Z.; Machlin, L.; Issa, E.; El-Ashry, D. Hierarchical paracrine interaction of breast cancer associated fibroblasts with cancer cells via hMAPK-microRNAs to drive ER-negative breast cancer phenotype. *Cancer Biol. Ther.* **2015**, *16*, 1671–1681. [CrossRef]
129. Palviainen, M.; Saraswat, M.; Varga, Z.; Kitka, D.; Neuvonen, M.; Puhka, M.; Joenväärä, S.; Renkonen, R.; Nieuwland, R.; Takatalo, M.; et al. Extracellular vesicles from human plasma and serum are carriers of extravesicular cargo—Implications for biomarker discovery. *PLoS ONE* **2020**, *15*, e0236439. [CrossRef]
130. Sun, Y.; Saito, K.; Saito, Y. Lipid Profile Characterization and Lipoprotein Comparison of Extracellular Vesicles from Human Plasma and Serum. *Metabolites* **2019**, *9*, 259. [CrossRef]

131. Stevic, I.; Müller, V.; Weber, K.; Fasching, P.A.; Karn, T.; Marmé, F.; Schem, C.; Stickeler, E.; Denkert, C.; van Mackelenbergh, M.; et al. Specific microRNA signatures in exosomes of triple-negative and HER2-positive breast cancer patients undergoing neoadjuvant therapy within the GeparSixto trial. *BMC Med.* **2018**, *16*, 179. [CrossRef] [PubMed]
132. Wu, H.; Wang, Q.; Zhong, H.; Li, L.; Zhang, Q.; Huang, Q.; Yu, Z. Differentially expressed microRNAs in exosomes of patients with breast cancer revealed by next-generation sequencing. *Oncol. Rep.* **2020**, *43*, 240–250. [CrossRef] [PubMed]
133. Baroni, S.; Romero-Cordoba, S.; Plantamura, I.; Dugo, M.; D'Ippolito, E.; Cataldo, A.; Cosentino, G.; Angeloni, V.; Rossini, A.; Daidone, M.G.; et al. Exosome-mediated delivery of miR-9 induces cancer-associated fibroblast-like properties in human breast fibroblasts. *Cell Death Dis.* **2016**, *7*, e2312. [CrossRef] [PubMed]
134. Li, Q.; Eades, G.; Yao, Y.; Zhang, Y.; Zhou, Q. Characterization of a Stem-like Subpopulation in Basal-like Ductal Carcinoma in Situ (DCIS) Lesions *. *J. Biol. Chem.* **2014**, *289*, 1303–1312. [CrossRef] [PubMed]
135. Jc Bose, R.; Uday Kumar, S.; Zeng, Y.; Afjei, R.; Robinson, E.; Lau, K.; Bermudez, A.; Habte, F.; Pitteri, S.J.; Sinclair, R.; et al. Tumor Cell-Derived Extracellular Vesicle-Coated Nanocarriers: An Efficient Theranostic Platform for the Cancer-Specific Delivery of Anti-miR-21 and Imaging Agents. *ACS Nano* **2018**, *12*, 10817–10832. [CrossRef] [PubMed]
136. Taghikhani, A.; Hassan, Z.M.; Ebrahimi, M.; Moazzeni, S.M. microRNA modified tumor-derived exosomes as novel tools for maturation of dendritic cells. *J. Cell. Physiol.* **2019**, *234*, 9417–9427. [CrossRef]
137. Zhao, L.; Gu, C.; Gan, Y.; Shao, L.; Chen, H.; Zhu, H. Exosome-mediated siRNA delivery to suppress postoperative breast cancer metastasis. *J. Control. Release* **2020**, *318*, 1–15. [CrossRef]
138. Lobos-González, L.; Bustos, R.; Campos, A.; Silva, V.; Silva, V.; Jeldes, E.; Salomon, C.; Varas-Godoy, M.; Cáceres-Verschae, A.; Duran, E.; et al. Exosomes released upon mitochondrial ASncmtRNA knockdown reduce tumorigenic properties of malignant breast cancer cells. *Sci. Rep.* **2020**, *10*, 343. [CrossRef]
139. Xu, X.; Su, B.; Xie, C.; Wei, S.; Zhou, Y.; Liu, H.; Dai, W.; Cheng, P.; Wang, F.; Xu, X.; et al. Sonic Hedgehog-Gli1 Signaling Pathway Regulates the Epithelial Mesenchymal Transition (EMT) by Mediating a New Target Gene, S100A4, in Pancreatic Cancer Cells. *PLoS ONE* **2014**, *9*, e96441. [CrossRef]
140. Zhou, Y.; Yamamoto, Y.; Takeshita, F.; Yamamoto, T.; Xiao, Z.; Ochiya, T. Delivery of miR-424-5p via Extracellular Vesicles Promotes the Apoptosis of MDA-MB-231 TNBC Cells in the Tumor Microenvironment. *Int. J. Mol. Sci.* **2021**, *22*, 844. [CrossRef]
141. Ni, C.; Fang, Q.Q.; Chen, W.Z.; Jiang, J.X.; Jiang, Z.; Ye, J.; Zhang, T.; Yang, L.; Meng, F.B.; Xia, W.J.; et al. Breast cancer-derived exosomes transmit lncRNA SNHG16 to induce CD73+γδ1 Treg cells. *Signal Transduct. Target. Ther.* **2020**, *5*, 1–14. [CrossRef]
142. Xia, W.; Liu, Y.; Cheng, T.; Xu, T.; Dong, M.; Hu, X. Extracellular Vesicles Carry lncRNA SNHG16 to Promote Metastasis of Breast Cancer Cells via the miR-892b/PPAPDC1A Axis. *Front. Cell Dev. Biol.* **2021**, *9*, 1319. [CrossRef] [PubMed]
143. Wang, Y.L.; Liu, L.C.; Hung, Y.; Chen, C.J.; Lin, Y.Z.; Wu, W.R.; Wang, S.C. Long non-coding RNA HOTAIR in circulatory exosomes is correlated with ErbB2/HER2 positivity in breast cancer. *Breast* **2019**, *46*, 64–69. [CrossRef] [PubMed]
144. Wang, X.; Pei, X.; Guo, G.; Qian, X.; Dou, D.; Zhang, Z.; Xu, X.; Duan, X. Exosome-mediated transfer of long noncoding RNA H19 induces doxorubicin resistance in breast cancer. *J. Cell. Physiol.* **2020**, *235*, 6896–6904. [CrossRef]
145. Dong, H.; Wang, W.; Chen, R.; Zhang, Y.; Zou, K.; Ye, M.; He, X.; Zhang, F.; Han, J. Exosome-mediated transfer of lncRNA-SNHG14 promotes trastuzumab chemoresistance in breast cancer. *Int. J. Oncol.* **2018**, *53*, 1013–1026. [CrossRef]
146. Han, M.; Gu, Y.; Lu, P.; Li, J.; Cao, H.; Li, X.; Qian, X.; Yu, C.; Yang, Y.; Yang, X.; et al. Exosome-mediated lncRNA AFAP1-AS1 promotes trastuzumab resistance through binding with AUF1 and activating ERBB2 translation. *Mol. Cancer* **2020**, *19*, 1–18. [CrossRef]
147. Qian, X.; Qu, H.; Zhang, F.; Peng, S.; Dou, D.; Yang, Y.; Ding, Y.; Xie, M.; Dong, H.; Liao, Y.; et al. Exosomal long noncoding RNA AGAP2-AS1 regulates trastuzumab resistance via inducing autophagy in breast cancer. *Am. J. Cancer Res.* **2021**, *11*, 1962. [CrossRef]
148. Zheng, Z.; Chen, M.; Xing, P.; Yan, X.; Xie, B. Increased Expression of Exosomal AGAP2-AS1 (AGAP2 Antisense RNA 1) In Breast Cancer Cells Inhibits Trastuzumab-Induced Cell Cytotoxicity. *Med. Sci. Monit.* **2019**, *25*, 2211–2220. [CrossRef]
149. Liang, Y.; Song, X.; Li, Y.; Chen, B.; Zhao, W.; Wang, L.; Zhang, H.; Liu, Y.; Han, D.; Zhang, N.; et al. LncRNA BCRT1 promotes breast cancer progression by targeting miR-1303/PTBP3 axis. *Mol. Cancer* **2020**, *19*, 85. [CrossRef]
150. Xu, C.G.; Yang, M.F.; Ren, Y.Q.; Wu, C.H.; Wang, L.Q. Exosomes mediated transfer of lncRNA UCA1 results in increased tamoxifen resistance in breast cancer cells. *Eur. Rev. Med. Pharmacol. Sci.* **2016**, *20*, 4362–4368.
151. Lu, Y.; Chen, L.; Li, L.; Cao, Y. Exosomes Derived from Brain Metastatic Breast Cancer Cells Destroy the Blood-Brain Barrier by Carrying lncRNA GS1-600G8.5. *Biomed. Res. Int.* **2020**, *2020*, 7461727. [CrossRef] [PubMed]
152. Zhou, D.P.; Gu, J.; Wang, Y.P.; Wu, H.G.; Cheng, W.; Wang, Q.P.; Zheng, G.P.; Wang, X.D. Long non-coding RNA NEAT1 transported by extracellular vesicles contributes to breast cancer development by sponging microRNA-141-3p and regulating KLF12. *Cell Biosci.* **2021**, *11*, 68. [CrossRef] [PubMed]
153. Chen, F.; Chen, J.; Yang, L.; Liu, J.; Zhang, X.; Zhang, Y.; Tu, Q.; Yin, D.; Lin, D.; Wong, P.P.; et al. Extracellular vesicle-packaged HIF-1α-stabilizing lncRNA from tumour-associated macrophages regulates aerobic glycolysis of breast cancer cells. *Nat. Cell Biol.* **2019**, *21*, 498–510. [CrossRef] [PubMed]
154. Li, Y.; Zhao, Z.; Liu, W.; Li, X. SNHG3 Functions as miRNA Sponge to Promote Breast Cancer Cells Growth Through the Metabolic Reprogramming. *Appl. Biochem. Biotechnol.* **2020**, *191*, 1084–1099. [CrossRef] [PubMed]

155. Xing, F.; Liu, Y.; Wu, S.Y.; Wu, K.; Sharma, S.; Mo, Y.Y.; Feng, J.; Sanders, S.; Jin, G.; Singh, R.; et al. Loss of XIST in Breast Cancer Activates MSN-c-Met and Reprograms Microglia via Exosomal miRNA to Promote Brain Metastasis. *Cancer Res.* **2018**, *78*, 4316–4330. [CrossRef]
156. Zhang, H.; Yan, C.; Wang, Y. Exosome-mediated transfer of circHIPK3 promotes trastuzumab chemoresistance in breast cancer. *J. Drug Target.* **2021**, *29*, 1004–1015. [CrossRef] [PubMed]
157. Chen, T.; Wang, X.; Li, C.; Zhang, H.; Liu, Y.; Han, D.; Li, Y.; Li, Z.; Luo, D.; Zhang, N.; et al. CircHIF1A regulated by FUS accelerates triple-negative breast cancer progression by modulating NFIB expression and translocation. *Oncogene* **2021**, *40*, 2756–2771. [CrossRef]
158. Liu, J.; Peng, X.; Liu, Y.; Hao, R.; Zhao, R.; Zhang, L.; Zhao, F.; Liu, Q.; Liu, Y.; Qi, Y. The Diagnostic Value of Serum Exosomal Has_circ_0000615 for Breast Cancer Patients. *Int. J. Gen. Med.* **2021**, *14*, 4545–4554. [CrossRef]
159. Yang, S.J.; Wang, D.D.; Zhou, S.Y.; Zhang, Q.; Wang, J.Y.; Zhong, S.L.; Da Zhang, H.; Wang, X.Y.; Xia, X.; Chen, W.; et al. Identification of circRNA–miRNA networks for exploring an underlying prognosis strategy for breast cancer. *Epigenomics* **2020**, *12*, 101–125. [CrossRef]
160. Rodríguez, M.; Silva, J.; Herrera, A.; Herrera, M.; Peña, C.; Martín, P.; Gil-Calderón, B.; Larriba, M.J.; Coronado, M.J.; Soldevilla, B.; et al. Exosomes enriched in stemness/metastatic-related mRNAS promote oncogenic potential in breast cancer. *Oncotarget* **2015**, *6*, 40575–40587. [CrossRef]
161. Keup, C.; Suryaprakash, V.; Storbeck, M.; Hoffmann, O.; Kimmig, R.; Kasimir-bauer, S. Longitudinal Multi-Parametric Liquid Biopsy Approach Identifies Unique Features of Circulating Tumor Cell, Extracellular Vesicle, and Cell-Free DNA Characterization for Disease Monitoring in Metastatic Breast Cancer Patients. *Cells* **2021**, *10*, 212. [CrossRef] [PubMed]
162. Hu, M.; Brown, V.; Jackson, J.M.; Wijerathne, H.; Pathak, H.; Koestler, D.C.; Nissen, E.; Hupert, M.L.; Muller, R.; Godwin, A.K.; et al. Assessing Breast Cancer Molecular Subtypes Using Extracellular Vesicles' mRNA. *Anal. Chem.* **2023**, *95*, 7665–7675. [CrossRef] [PubMed]
163. Yao, B.; Qu, S.; Hu, R.; Gao, W.; Jin, S.; Ju, J.; Zhao, Q. Delivery of platelet TPM3 mRNA into breast cancer cells via microvesicles enhances metastasis. *FEBS Open Biol.* **2019**, *9*, 2159–2169. [CrossRef] [PubMed]
164. Gorji-Bahri, G.; Moradtabrizi, N.; Vakhshiteh, F.; Hashemi, A. Validation of common reference genes stability in exosomal mRNA-isolated from liver and breast cancer cell lines. *Cell Biol. Int.* **2021**, *45*, 1098–1110. [CrossRef]
165. Rabas, N.; Palmer, S.; Mitchell, L.; Ismail, S.; Gohlke, A.; Riley, J.S.; Tait, S.W.G.; Gammage, P.; Soares, L.L.; Macpherson, I.R.; et al. Pink1 drives production of mtDNA-containing extracellular vesicles to promote invasiveness. *J. Cell Biol.* **2021**, *220*, e202006049. [CrossRef]
166. Abad, E.; Lyakhovich, A. Movement of Mitochondria with Mutant DNA through Extracellular Vesicles Helps Cancer Cells Acquire Chemoresistance. *ChemMedChem* **2021**, *17*, e202100642. [CrossRef]
167. Sansone, P.; Savini, C.; Kurelac, I.; Chang, Q.; Amato, L.B.; Strillacci, A.; Stepanova, A.; Iommarini, L.; Mastroleo, C.; Daly, L.; et al. Packaging and transfer of mitochondrial DNA via exosomes regulate escape from dormancy in hormonal therapy-resistant breast cancer. *Proc. Natl. Acad. Sci. USA* **2017**, *114*, E9066–E9075. [CrossRef]
168. Wang, J.H.; Forterre, A.V.; Zhao, J.; Frimannsson, D.O.; Delcayre, A.; Antes, T.J.; Efron, B.; Jeffrey, S.S.; Pegram, M.D.; Matin, A.C. Anti-HER2 scFv-Directed Extracellular Vesicle-Mediated mRNA-Based Gene Delivery Inhibits Growth of HER2-Positive Human Breast Tumor Xenografts by Prodrug Activation. *Mol. Cancer Ther.* **2018**, *17*, 1133–1142. [CrossRef]
169. Hurwitz, S.N.; Rider, M.A.; Bundy, J.L.; Liu, X.; Singh, R.K.; Meckes, D.G., Jr. Proteomic profiling of NCI-60 extracellular vesicles uncovers common protein cargo and cancer type-specific biomarkers. *Oncotarget* **2016**, *7*, 86999–87015. [CrossRef]
170. Staubach, S.; Razawi, H.; Hanisch, F.G. Proteomics of MUC1-containing lipid rafts from plasma membranes and exosomes of human breast carcinoma cells MCF-7. *Proteomics* **2009**, *9*, 2820–2835. [CrossRef]
171. Jordan, K.R.; Hall, J.K.; Schedin, T.; Borakove, M.; Xian, J.J.; Dzieciatkowska, M.; Lyons, T.R.; Schedin, P.; Hansen, K.C.; Borges, V.F. Extracellular vesicles from young women's breast cancer patients drive increased invasion of non-malignant cells via the Focal Adhesion Kinase pathway: A proteomic approach. *Breast Cancer Res.* **2020**, *22*, 128. [CrossRef] [PubMed]
172. Antonyak, M.A.; Li, B.; Boroughs, L.K.; Johnson, J.L.; Druso, J.E.; Bryant, K.L.; Holowka, D.A.; Cerione, R.A. Cancer cell-derived microvesicles induce transformation by transferring tissue transglutaminase and fibronectin to recipient cells. *Proc. Natl. Acad. Sci. USA* **2011**, *108*, 4852–4857. [CrossRef]
173. Tutanov, O.; Orlova, E.; Proskura, K.; Grigor'eva, A.; Yunusova, N.; Tsentalovich, Y.; Alexandrova, A.; Tamkovich, S. Proteomic Analysis of Blood Exosomes from Healthy Females and Breast Cancer Patients Reveals an Association between Different Exosomal Bioactivity on Non-tumorigenic Epithelial Cell and Breast Cancer Cell Migration in Vitro. *Biomolecules* **2020**, *10*, 495. [CrossRef] [PubMed]
174. Vinik, Y.; Ortega, F.G.; Mills, G.B.; Lu, Y.; Jurkowicz, M.; Halperin, S.; Aharoni, M.; Gutman, M.; Lev, S. Proteomic analysis of circulating extracellular vesicles identifies potential markers of breast cancer progression, recurrence, and response. *Sci. Adv.* **2020**, *6*, eaba5714. [CrossRef] [PubMed]
175. Li, S.; Li, X.; Yang, S.; Pi, H.; Li, Z.; Yao, P.; Zhang, Q.; Wang, Q.; Shen, P.; Li, X.; et al. Proteomic landscape of exosomes reveals the functional contributions of CD151 in triple-negative breast cancer. *Mol. Cell. Proteom.* **2021**, *20*, 100121. [CrossRef] [PubMed]
176. Rontogianni, S.; Synadaki, E.; Li, B.; Liefaard, M.C.; Lips, E.H.; Wesseling, J.; Wu, W.; Altelaar, M. Proteomic profiling of extracellular vesicles allows for human breast cancer subtyping. *Commun. Biol.* **2019**, *2*, 325. [CrossRef]

177. Tutanov, O.; Proskura, K.; Kamyshinsky, R.; Shtam, T.; Tsentalovich, Y.; Tamkovich, S. Proteomic Profiling of Plasma and Total Blood Exosomes in Breast Cancer: A Potential Role in Tumor Progression, Diagnosis, and Prognosis. *Front. Oncol.* **2020**, *10*, 2173. [CrossRef]
178. Martínez-Greene, J.A.; Hernández-Ortega, K.; Quiroz-Baez, R.; Resendis-Antonio, O.; Pichardo-Casas, I.; Sinclair, D.A.; Budnik, B.; Hidalgo-Miranda, A.; Uribe-Querol, E.; del Pilar Ramos-Godínez, M.; et al. Quantitative proteomic analysis of extracellular vesicle subgroups isolated by an optimized method combining polymer-based precipitation and size exclusion chromatography. *J. Extracell. Vesicles* **2021**, *10*, e12087. [CrossRef]
179. Dalla, P.V.; Santos, J.; Milthorpe, B.K.; Padula, M.P. Selectively-Packaged Proteins in Breast Cancer Extracellular Vesicles Involved in Metastasis. *Int. J. Mol. Sci.* **2020**, *21*, 4990. [CrossRef]
180. Vardaki, I.; Ceder, S.; Rutishauser, D.; Baltatzis, G.; Foukakis, T.; Panaretakis, T.; Vardaki, I.; Ceder, S.; Rutishauser, D.; Baltatzis, G.; et al. Periostin is identified as a putative metastatic marker in breast cancer-derived exosomes. *Oncotarget* **2016**, *7*, 74966–74978. [CrossRef]
181. Risha, Y.; Minic, Z.; Ghobadloo, S.M.; Berezovski, M.V. The proteomic analysis of breast cell line exosomes reveals disease patterns and potential biomarkers. *Sci. Rep.* **2020**, *10*, 13572. [CrossRef] [PubMed]
182. Palazzolo, G.; Albanese, N.N.; Di Cara, G.; Gygax, D.; Vittorelli, M.L.; Pucci-Minafra, I. Proteomic analysis of exosome-like vesicles derived from breast cancer cells. *Anticancer Res.* **2012**, *32*, 847–860. [PubMed]
183. Heinemann, M.L.; Ilmer, M.; Silva, L.P.; Hawke, D.H.; Recio, A.; Vorontsova, M.A.; Alt, E.; Vykoukal, J. Benchtop isolation and characterization of functional exosomes by sequential filtration. *J. Chromatogr. A* **2014**, *1371*, 125–135. [CrossRef]
184. Clark, D.J.; Fondrie, W.E.; Liao, Z.; Hanson, P.I.; Fulton, A.; Mao, L.; Yang, A.J. Redefining the Breast Cancer Exosome Proteome by Tandem Mass Tag Quantitative Proteomics and Multivariate Cluster Analysis. *Anal. Chem.* **2015**, *87*, 10462–10469. [CrossRef] [PubMed]
185. Smyth, T.J.; Redzic, J.S.; Graner, M.W.; Anchordoquy, T.J. Examination of the specificity of tumor cell derived exosomes with tumor cells in vitro. *Biochim. Biophys. Acta-Biomembr.* **2014**, *1838*, 2954–2965. [CrossRef]
186. Griffiths, S.G.; Cormier, M.T.; Clayton, A.; Doucette, A.A. Differential Proteome Analysis of Extracellular Vesicles from Breast Cancer Cell Lines by Chaperone Affinity Enrichment. *Proteomes* **2017**, *5*, 25. [CrossRef]
187. Koh, Y.Q.; Ng, D.Q.; Ng, C.C.; Boey, A.; Wei, M.; Sze, S.K.; Ho, H.K.; Acharya, M.; Limoli, C.L.; Chan, A. Extracellular Vesicle Proteome of Breast Cancer Patients with and without Cognitive Impairment Following Anthracycline-based Chemotherapy: An Exploratory Study. *Biomark. Insights* **2021**, *16*, 11772719211018204. [CrossRef]
188. Kruger, S.; Elmageed, Z.Y.A.; Hawke, D.H.; Wörner, P.M.; Jansen, D.A.; Abdel-Mageed, A.B.; Alt, E.U.; Izadpanah, R. Molecular characterization of exosome-like vesicles from breast cancer cells. *BMC Cancer* **2014**, *14*, 1–10. [CrossRef]
189. Tryndyak, V.P.; Kovalchuk, O.; Pogribny, I.P. Loss of DNA methylation and histone H4 lysine 20 trimethylation in human breast cancer cells is associated with aberrant expression of DNA methyltransferase 1, Suv4-20h2 histone methyltransferase and methyl-binding proteins. *Cancer Biol. Ther.* **2006**, *5*, 65–70. [CrossRef]
190. Coticchia, C.M.; Revankar, C.M.; Deb, T.B.; Dickson, R.B.; Johnson, M.D. Calmodulin modulates Akt activity in human breast cancer cell lines. *Breast Cancer Res. Treat.* **2008**, *115*, 545–560. [CrossRef]
191. Skotland, T.; Sagini, K.; Sandvig, K.; Llorente, A. An emerging focus on lipids in extracellular vesicles. *Adv. Drug Deliv. Rev.* **2020**, *159*, 308–321. [CrossRef] [PubMed]
192. Skotland, T.; Hessvik, N.P.; Sandvig, K.; Llorente, A. Exosomal lipid composition and the role of ether lipids and phosphoinositides in exosome biology. *J. Lipid Res.* **2019**, *60*, 9–18. [CrossRef] [PubMed]
193. Roberg-Larsen, H.; Lund, K.; Seterdal, K.E.; Solheim, S.; Vehus, T.; Solberg, N.; Krauss, S.; Lundanes, E.; Wilson, S.R. Mass spectrometric detection of 27-hydroxycholesterol in breast cancer exosomes. *J. Steroid Biochem. Mol. Biol.* **2017**, *169*, 22–28. [CrossRef] [PubMed]
194. Nishida-Aoki, N.; Izumi, Y.; Takeda, H.; Takahashi, M.; Ochiya, T.; Bamba, T. Lipidomic Analysis of Cells and Extracellular Vesicles from High- and Low-Metastatic Triple-Negative Breast Cancer. *Metabolites* **2020**, *10*, 67. [CrossRef]
195. Góss Santos, T.; Regina Martins, V.; Noeli Maroso Hajj, G.; Di Sansebastiano, G.-P.; Gaballo, A. Unconventional Secretion of Heat Shock Proteins in Cancer. *Int. J. Mol. Sci.* **2017**, *18*, 946. [CrossRef]
196. Zhang, D.H.; Tai, L.K.; Wong, L.L.; Sethi, S.K.; Koay, E.S.C. Proteomics of breast cancer: Enhanced expression of cytokeratin19 in human epidermal growth factor receptor type 2 positive breast tumors. *Proteomics* **2005**, *5*, 1797–1805. [CrossRef]
197. Olofsson, M.H.; Ueno, T.; Pan, Y.; Xu, R.; Cai, F.; Van Der Kuip, H.; Muerdter, T.E.; Sonnenberg, M.; Aulitzky, W.E.; Schwarz, S.; et al. Cytokeratin-18 Is a Useful Serum Biomarker for Early Determination of Response of Breast Carcinomas to Chemotherapy. *Clin. Cancer Res.* **2007**, *13*, 3198–3206. [CrossRef]
198. Muñoz-Pinedo, C.; El Mjiyad, N.; Ricci, J.E. Cancer metabolism: Current perspectives and future directions. *Cell Death Dis.* **2012**, *3*, e248. [CrossRef]
199. Becker, A.; Thakur, B.K.; Weiss, J.M.; Kim, H.S.; Peinado, H.; Lyden, D. Extracellular Vesicles in Cancer: Cell-to-Cell Mediators of Metastasis. *Cancer Cell* **2016**, *30*, 836–848. [CrossRef]
200. Tian, F.; Zhang, S.; Liu, C.; Han, Z.; Liu, Y.; Deng, J.; Li, Y.; Wu, X.; Cai, L.; Qin, L.; et al. Protein analysis of extracellular vesicles to monitor and predict therapeutic response in metastatic breast cancer. *Nat. Commun.* **2021**, *12*, 2536. [CrossRef]
201. Tkach, M.; Théry, C. Communication by Extracellular Vesicles: Where We Are and Where We Need to Go. *Cell* **2016**, *164*, 1226–1232. [CrossRef] [PubMed]

202. Horiuchi, K.; Amizuka, N.; Takeshita, S.; Takamatsu, H.; Katsuura, M.; Ozawa, H.; Toyama, Y.; Bonewald, L.F.; Kudo, A. Identification and Characterization of a Novel Protein, Periostin, with Restricted Expression to Periosteum and Periodontal Ligament and Increased Expression by Transforming Growth Factor β. *J. Bone Miner. Res.* **1999**, *14*, 1239–1249. [CrossRef] [PubMed]
203. Shao, R.; Bao, S.; Bai, X.; Blanchette, C.; Anderson, R.M.; Dang, T.; Gishizky, M.L.; Marks, J.R.; Wang, X.-F. Acquired Expression of Periostin by Human Breast Cancers Promotes Tumor Angiogenesis through Up-Regulation of Vascular Endothelial Growth Factor Receptor 2 Expression. *Mol. Cell. Biol.* **2004**, *24*, 3992–4003. [CrossRef]
204. Ma, X.; Chen, Z.; Hua, D.; He, D.; Wang, L.; Zhang, P.; Wang, J.; Cai, Y.; Gao, C.; Zhang, X.; et al. Essential role for TrpC5-containing extracellular vesicles in breast cancer with chemotherapeutic resistance. *Proc. Natl. Acad. Sci. USA* **2014**, *111*, 6389–6394. [CrossRef] [PubMed]
205. Palviainen, M.; Saari, H.; Kärkkäinen, O.; Pekkinen, J.; Auriola, S.; Yliperttula, M.; Puhka, M.; Hanhineva, K.; Siljander, P.R.-M. Metabolic signature of extracellular vesicles depends on the cell culture conditions. *J. Extracell. Vesicles* **2019**, *8*, 1596669. [CrossRef] [PubMed]
206. Rupp, A.K.; Rupp, C.; Keller, S.; Brase, J.C.; Ehehalt, R.; Fogel, M.; Moldenhauer, G.; Marmé, F.; Sültmann, H.; Altevogt, P. Loss of EpCAM expression in breast cancer derived serum exosomes: Role of proteolytic cleavage. *Gynecol. Oncol.* **2011**, *122*, 437–446. [CrossRef] [PubMed]
207. Ilver, D.; Johansson, P.; Miller-Podraza, H.; Nyholm, P.G.; Teneberg, S.; Karlsson, K.A. Bacterium–Host Protein–Carbohydrate Interactions. *Methods Enzymol.* **2003**, *363*, 134–157. [CrossRef]
208. Pinho, S.S.; Reis, C.A. Glycosylation in cancer: Mechanisms and clinical implications. *Nat. Rev. Cancer* **2015**, *15*, 540–555. [CrossRef]
209. Marcos, N.T.; Bennett, E.P.; Gomes, J.; Magalhaes, A.; Gomes, C.; David, L.; Dar, I.; Jeanneau, C.; DeFrees, S.; Krustrup, D.; et al. ST6GalNAc-I controls expression of sialyl-Tn antigen in gastrointestinal tissues. *Front. Biosci.-Elit.* **2011**, *3*, 1443–1455. [CrossRef]
210. Wang, Y.; Ju, T.; Ding, X.; Xia, B.; Wang, W.; Xia, L.; He, M.; Cummings, R.D. Cosmc is an essential chaperone for correct protein O-glycosylation. *Proc. Natl. Acad. Sci. USA* **2010**, *107*, 9228–9233. [CrossRef]
211. Kumamoto, K.; Goto, Y.; Sekikawa, K.; Takenoshita, S.; Ishida, N.; Kawakita, M.; Kannagi, R. Increased Expression of UDP-Galactose Transporter Messenger RNA in Human Colon Cancer Tissues and Its Implication in Synthesis of Thomsen-Friedenreich Antigen and Sialyl Lewis A/X Determinants1. *Cancer Res.* **2001**, *61*, 4620–4627. [PubMed]
212. Croci, D.O.; Cerliani, J.P.; Pinto, N.A.; GMorosi, L.; Rabinovich, G.A. Regulatory role of glycans in the control of hypoxia-driven angiogenesis and sensitivity to anti-angiogenic treatment. *Glycobiology* **2014**, *24*, 1283–1290. [CrossRef] [PubMed]
213. Freitas, D.; Campos, D.; Gomes, J.; Pinto, F.; Macedo, J.A.; Matos, R.; Mereiter, S.; Pinto, M.T.; Polónia, A.; Gartner, F.; et al. O-glycans truncation modulates gastric cancer cell signaling and transcription leading to a more aggressive phenotype. *EBioMedicine* **2019**, *40*, 349–362. [CrossRef] [PubMed]
214. Häuselmann, I.; Borsig, L. Altered tumor-cell glycosylation promotes metastasis. *Front. Oncol.* **2014**, *4*, 28. [CrossRef]
215. Lau, K.S.; Partridge, E.A.; Grigorian, A.; Silvescu, C.I.; Reinhold, V.N.; Demetriou, M.; Dennis, J.W. Complex N-Glycan Number and Degree of Branching Cooperate to Regulate Cell Proliferation and Differentiation. *Cell* **2007**, *129*, 123–134. [CrossRef]
216. Tominaga, N.; Hagiwara, K.; Kosaka, N.; Honma, K.; Nakagama, H.; Ochiya, T. RPN2-mediated glycosylation of tetraspanin CD63 regulates breast cancer cell malignancy. *Mol. Cancer* **2014**, *13*, 134. [CrossRef]
217. Macedo-da-Silva, J.; Santiago, V.F.; Rosa-Fernandes, L.; Marinho, C.R.F.; Palmisano, G. Protein glycosylation in extracellular vesicles: Structural characterization and biological functions. *Mol. Immunol.* **2021**, *135*, 226–246. [CrossRef]
218. Battke, C.; Ruiss, R.; Welsch, U.; Wimberger, P.; Lang, S.; Jochum, S.; Zeidler, R. Tumour exosomes inhibit binding of tumour-reactive antibodies to tumour cells and reduce ADCC. *Cancer Immunol. Immunother.* **2011**, *60*, 639–648. [CrossRef]
219. Pigati, L.; Yaddanapudi, S.C.S.; Iyengar, R.; Kim, D.J.; Hearn, S.A.; Danforth, D.; Hastings, M.L.; Duelli, D.M. Selective release of microRNA species from normal and malignant mammary epithelial cells. *PLoS ONE* **2010**, *5*, e13515. [CrossRef]
220. Smyth, T.; Petrova, K.; Payton, N.M.; Persaud, I.; Redzic, J.S.; Graner, M.W.; Smith-Jones, P.; Anchordoquy, T.J. Surface functionalization of exosomes using click chemistry. *Bioconjug. Chem.* **2014**, *25*, 1777–1784. [CrossRef]
221. Gangoda, L.; Liem, M.; Ang, C.S.; Keerthikumar, S.; Adda, C.G.; Parker, B.S.; Mathivanan, S. Proteomic Profiling of Exosomes Secreted by Breast Cancer Cells with Varying Metastatic Potential. *Proteomics* **2017**, *17*, 1600370. [CrossRef] [PubMed]
222. Menck, K.; Scharf, C.; Bleckmann, A.; Dyck, L.; Rost, U.; Wenzel, D.; Dhople, V.M.; Siam, L.; Pukrop, T.; Binder, C.; et al. Tumor-derived microvesicles mediate human breast cancer invasion through differentially glycosylated EMMPRIN. *J. Mol. Cell Biol.* **2015**, *7*, 143–153. [CrossRef] [PubMed]
223. Koga, K.; Matsumoto, K.; Akiyoshi, T.; Kubo, M.; Yamanaka, N.; Tasaki, A.; Nakashima, H.; Nakamura, M.; Kuroki, S.; Tanaka, M.; et al. Purification, Characterization and Biological Significance of Tumor-derived Exosomes. *Anticancer Res.* **2005**, *25*, 3703–3707. [PubMed]
224. Wolfers, J.; Lozier, A.; Raposo, G.; Regnault, A.; Théry, C.; Masurier, C.; Flament, C.; Pouzieux, S.; Faure, F.; Tursz, T.; et al. Tumor-derived exosomes are a source of shared tumor rejection antigens for CTL cross-priming. *Nat. Med.* **2001**, *7*, 297–303. [CrossRef] [PubMed]
225. Nishida-Aoki, N.; Tominaga, N.; Kosaka, N.; Ochiya, T. Altered biodistribution of deglycosylated extracellular vesicles through enhanced cellular uptake. *J. Extracell. Vesicles* **2020**, *9*, 1713527. [CrossRef]

226. Kavanagh, E.L.; Halasz, M.; Dowling, P.; Withers, J.; Lindsay, S.; Higgins, M.J.; Irwin, J.A.; Rudd, P.M.; Saldova, R.; McCann, A. *N* -Linked glycosylation profiles of therapeutic induced senescent (TIS) triple negative breast cancer cells (TNBC) and their extracellular vesicle (EV) progeny. *Mol. Omics* **2021**, *17*, 72–85. [CrossRef]
227. Lima, L.G.; Ham, S.; Shin, H.; Chai, E.P.Z.; Lek, E.S.H.; Lobb, R.J.; Müller, A.F.; Mathivanan, S.; Yeo, B.; Choi, Y.; et al. Tumor microenvironmental cytokines bound to cancer exosomes determine uptake by cytokine receptor-expressing cells and biodistribution. *Nat. Commun.* **2021**, *12*, 3543. [CrossRef]
228. Tan, Z.; Cao, L.; Wu, Y.; Wang, B.; Song, Z.; Yang, J.; Cheng, L.; Yang, X.; Zhou, X.; Dai, Z. Bisecting GlcNAc modification diminishes the pro-metastatic functions of small extracellular vesicles from breast cancer cells. *J. Extracell. Vesicles* **2020**, *10*, e12005. [CrossRef]
229. Hait, N.C.; Maiti, A.; Wu, R.; Andersen, V.L.; Hsu, C.-C.; Wu, Y.; Chapla, D.G.; Takabe, K.; Rusiniak, M.E.; Bshara, W.; et al. Extracellular sialyltransferase st6gal1 in breast tumor cell growth and invasiveness. *Cancer Gene Ther.* **2022**, *29*, 1662–1675. [CrossRef]
230. Stowell, S.R.; Ju, T.; Cummings, R.D. Protein glycosylation in cancer. *Annu. Rev. Pathol.* **2015**, *10*, 473–510. [CrossRef]
231. Toraskar, J.; Magnussen, S.N.; Hagen, L.; Sharma, A.; Hoang, L.; Bjørkøy, G.; Svineng, G.; Steigedal, T.S. A novel truncated form of nephronectin is present in small extracellular vesicles isolated from 66cl4 cells. *J. Proteome Res.* **2019**, *18*, 1237–1247. [CrossRef]
232. Cao, L.; Wu, Y.; Wang, X.; Li, X.; Tan, Z.; Guan, F. Role of Site-Specific Glycosylation in the I-Like Domain of Integrin β1 in Small Extracellular Vesicle-Mediated Malignant Behavior and FAK Activation. *Int. J. Mol. Sci.* **2021**, *22*, 1770. [CrossRef]
233. AL-Abedi, R.; Tuncay Cagatay, S.; Mayah, A.; Brooks, S.A.; Kadhim, M. Ionising Radiation Promotes Invasive Potential of Breast Cancer Cells: The Role of Exosomes in the Process. *Int. J. Mol. Sci.* **2021**, *22*, 11570. [CrossRef]
234. Bard, M.P.; Hegmans, J.P.; Hemmes, A.; Luider, T.M.; Willemsen, R.; Severijnen, L.A.A.; Van Meerbeeck, J.P.; Burgers, S.A.; Hoogsteden, H.C.; Lambrecht, B.N. Proteomic analysis of exosomes isolated from human malignant pleural effusions. *Am. J. Respir. Cell Mol. Biol.* **2004**, *31*, 114–121. [CrossRef] [PubMed]
235. Keklikoglou, I.; Cianciaruso, C.; Güç, E.; Squadrito, M.L.; Spring, L.M.; Tazzyman, S.; Lambein, L.; Poissonnier, A.; Ferraro, G.B.; Baer, C.; et al. Chemotherapy elicits pro-metastatic extracellular vesicles in breast cancer models. *Nat. Cell Biol.* **2018**, *21*, 190–202. [CrossRef] [PubMed]
236. Vergauwen, G.; Tulkens, J.; Pinheiro, C.; Avila Cobos, F.; Dedeyne, S.; De Scheerder, M.A.; Vandekerckhove, L.; Impens, F.; Miinalainen, I.; Braems, G.; et al. Robust sequential biophysical fractionation of blood plasma to study variations in the biomolecular landscape of systemically circulating extracellular vesicles across clinical conditions. *J. Extracell. Vesicles* **2021**, *10*, e12122. [CrossRef]
237. Gonzalez, E.; Piva, M.; Rodriguez-Suarez, E.; Gil, D.; Royo, F.; Elortza, F.; Falcon-Perez, J.M.; Vivanco, M.D.M. Human Mammospheres Secrete Hormone-Regulated Active Extracellular Vesicles. *PLoS ONE* **2014**, *9*, e83955. [CrossRef]
238. Luga, V.; Zhang, L.; Viloria-Petit, A.M.; Ogunjimi, A.A.; Inanlou, M.R.; Chiu, E.; Buchanan, M.; Hosein, A.N.; Basik, M.; Wrana, J.L. Exosomes mediate stromal mobilization of autocrine Wnt-PCP signaling in breast cancer cell migration. *Cell* **2012**, *151*, 1542–1556. [CrossRef]
239. Shimoda, M.; Principe, S.; Jackson, H.W.; Luga, V.; Fang, H.; Molyneux, S.D.; Shao, Y.W.; Aiken, A.; Waterhouse, P.D.; Karamboulas, C.; et al. Loss of the Timp gene family is sufficient for the acquisition of the CAF-like cell state. *Nat. Cell Biol.* **2014**, *16*, 889–901. [CrossRef]
240. Moon, P.G.; Lee, J.E.; Cho, Y.E.; Lee, S.J.; Jung, J.H.; Chae, Y.S.; Bae, H.I.; Kim, Y.B.; Kim, I.S.; Park, H.Y.; et al. Identification of Developmental Endothelial Locus-1 on Circulating Extracellular Vesicles as a Novel Biomarker for Early Breast Cancer Detection. *Clin. Cancer Res.* **2016**, *22*, 1757–1766. [CrossRef]
241. Xu, G.; Huang, W.; Du, S.; Huang, M.; Lyu, J.; Zhou, F.; Zhu, R.; Cao, Y.; Xv, J.; Li, N.; et al. Proteomic Characterization of Serum Small Extracellular Vesicles in Human Breast Cancer. *bioRxiv* **2021**, bioRxiv:11.26.470104. [CrossRef]
242. SUN, J.G.; LI, X.B.; YIN, R.H.; LI, X.F. lncRNA VIM-AS1 promotes cell proliferation, metastasis and epithelial–mesenchymal transition by activating the Wnt/β-catenin pathway in gastric cancer. *Mol. Med. Rep.* **2020**, *22*, 4567–4578. [CrossRef] [PubMed]
243. Wu, S.; Du, Y.; Beckford, J.; Alachkar, H. Upregulation of the EMT marker vimentin is associated with poor clinical outcome in acute myeloid leukemia. *J. Transl. Med.* **2018**, *16*, 170. [CrossRef] [PubMed]
244. Ozawa, P.M.M.; Vieira, E.; Lemos, D.S.; Souza, I.L.M.; Zanata, S.M.; Pankievicz, V.C.; Tuleski, T.R.; Souza, E.M.; Wowk, P.F.; Urban, C.D.A.; et al. Identification of miRNAs Enriched in Extracellular Vesicles Derived from Serum Samples of Breast Cancer Patients. *Biomolecules* **2020**, *10*, 150. [CrossRef] [PubMed]
245. Sueta, A.; Fujiki, Y.; Goto-Yamaguchi, L.; Tomiguchi, M.; Yamamoto-Ibusuki, M.; Iwase, H.; Yamamoto, Y. Exosomal miRNA profiles of triple-negative breast cancer in neoadjuvant treatment. *Oncol. Lett.* **2021**, *22*, 819. [CrossRef]
246. Cai, G.X.; Lin, L.; Zhai, X.M.; Guo, Z.W.; Wu, Y.S.; Ye, G.L.; Liu, Q.; Chen, L.S.; Xing, G.Y.; Zhao, Q.H.; et al. A plasma-derived extracellular vesicle mRNA classifier for the detection of breast cancer. *Gland Surg.* **2021**, *10*, 2002009. [CrossRef]
247. Lv, S.; Wang, Y.; Xu, W.; Dong, X. Serum Exosomal miR-17-5p as a Promising Biomarker Diagnostic Biomarker for Breast Cancer. *Clin. Lab.* **2020**, *66*, 1823–1834. [CrossRef]
248. Su, Y.; Li, Y.; Guo, R.; Zhao, J.; Chi, W.; Lai, H.; Wang, J.; Wang, Z.; Li, L.; Sang, Y.; et al. Plasma extracellular vesicle long RNA profiles in the diagnosis and prediction of treatment response for breast cancer. *NPJ Breast Cancer* **2021**, *7*, 154. [CrossRef]
249. Tang, S.; Zheng, K.; Tang, Y.; Li, Z.; Zou, T.; Liu, D. Overexpression of serum exosomal HOTAIR is correlated with poor survival and poor response to chemotherapy in breast cancer patients. *J. Biosci.* **2019**, *44*, 37. [CrossRef]

250. Zhong, G.; Wang, K.; Li, J.; Xiao, S.; Wei, W.; Liu, J. Determination of Serum Exosomal H19 as a Noninvasive Biomarker for Breast Cancer Diagnosis. *Onco. Targets Ther.* **2020**, *13*, 2563–2571. [CrossRef]
251. Wu, M.; Wang, M.; Jia, H.; Wu, P. Extracellular vesicles: Emerging anti-cancer drugs and advanced functionalization platforms for cancer therapy. *Drug Deliv.* **2022**, *29*, 2513–2538. [CrossRef] [PubMed]
252. Liu, C.; Wang, Y.; Li, L.; He, D.; Chi, J.; Li, Q.; Wu, Y.; Zhao, Y.; Zhang, S.; Wang, L.; et al. Engineered extracellular vesicles and their mimetics for cancer immunotherapy. *J. Control. Release* **2022**, *349*, 679–698. [CrossRef] [PubMed]
253. Ahmadi, M.; Hassanpour, M.; Rezaie, J. Engineered extracellular vesicles: A novel platform for cancer combination therapy and cancer immunotherapy. *Life Sci.* **2022**, *308*, 120935. [CrossRef] [PubMed]